The functional significance of the sodium-potassium pump in motor control and movement disorders

Francesca Leigh Sorrell

A thesis submitted for the degree of PhD
at the
University of St Andrews

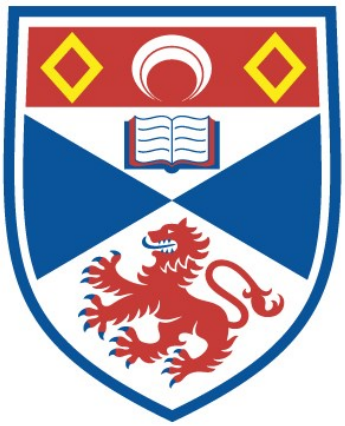

2022

Full metadata for this item is available in
St Andrews Research Repository
at:
https://research-repository.st-andrews.ac.uk/

Identifier to use to cite or link to this thesis:

DOI: https://doi.org/10.17630/sta/313

This item is protected by original copyright

Candidate's declaration

I, Francesca Leigh Sorrell, do hereby certify that this thesis, submitted for the degree of PhD, which is approximately 40,000 words in length, has been written by me, and that it is the record of work carried out by me, or principally by myself in collaboration with others as acknowledged, and that it has not been submitted in any previous application for any degree. I confirm that any appendices included in my thesis contain only material permitted by the 'Assessment of Postgraduate Research Students' policy.

I was admitted as a research student at the University of St Andrews in September 2017.

I received funding from an organisation or institution and have acknowledged the funder(s) in the full text of my thesis.

Date 18/10/2022 Signature of candidate

Supervisor's declaration

I hereby certify that the candidate has fulfilled the conditions of the Resolution and Regulations appropriate for the degree of PhD in the University of St Andrews and that the candidate is qualified to submit this thesis in application for that degree. I confirm that any appendices included in the thesis contain only material permitted by the 'Assessment of Postgraduate Research Students' policy.

Date 18/10/2022 Signature of supervisor

Permission for publication

In submitting this thesis to the University of St Andrews we understand that we are giving permission for it to be made available for use in accordance with the regulations of the University Library for the time being in force, subject to any copyright vested in the work not being affected thereby. We also understand, unless exempt by an award of an embargo as requested below, that the title and the abstract will be published, and that a copy of the work may be made and supplied to any bona fide library or research worker, that this thesis will be electronically accessible for personal or research use and that the library has the right to migrate this thesis into new electronic forms as required to ensure continued access to the thesis.

I, Francesca Leigh Sorrell, confirm that my thesis does not contain any third-party material that requires copyright clearance.

The following is an agreed request by candidate and supervisor regarding the publication of this thesis:

Printed copy

No embargo on print copy.

Electronic copy

Embargo on all of electronic copy for a period of 2 years on the following ground(s):

- Publication would preclude future publication

Supporting statement for electronic embargo request

Parts of this thesis are included in a manuscript currently being prepared for submission to an academic journal.

Title and Abstract

- I agree to the title and abstract being published.

Date 18/10/2022 Signature of candidate

Date 18/10/2022 Signature of supervisor

Underpinning Research Data or Digital Outputs

Candidate's declaration

I, Francesca Leigh Sorrell, hereby certify that no requirements to deposit original research data or digital outputs apply to this thesis and that, where appropriate, secondary data used have been referenced in the full text of my thesis.

Date 18/10/2022 Signature of candidate

Acknowledgements

First and foremost, I would like to thank my primary supervisor Professor Gareth Miles for his support during my PhD. More than just mentorship and guidance, thanks for always making time for me when I know you had very little, for always being a good laugh, for all the games of darts, the barbecues, the bonfires, and for making coming to work rarely feel like work at all. The saddest part of finishing this degree will be leaving the Miles Lab.

My thanks go to Professor Keith Sillar whose kindness and sincerity will have a lasting effect on me always. Thank you for your support from the very beginning of my research journey whether it be academic or pastoral – there was never a problem I did not feel I could come to you with. Thank you for fostering an environment that meant I couldn't bear to leave the School of Psychology and Neuroscience after the end of my undergraduate degree.

My thanks to all the past and present members of the Miles and Sillar labs but especially: Laurence for his patience with me when I was just a tadpole growing legs; Matt and Filip for showing me the ropes; and Sarah, Simon, Calum, Lamia, and Gina for their camaraderie throughout. A special thanks to the Friday Night Pub Crew for keeping me sane (you know who you are!).

Thank you to Trevor Hawkey, Shaun Wilson, Laura Fordyce, and Sandy Gardner for all your animal support and great chats – I genuinely couldn't have done it without you guys. A special thanks to John Macintyre for all his technical support over the years also.

Thank you to my examiners, Dr. David Hughes and Dr. Wenchang Li. for their thoughtful comments and insight with regards to this thesis. Furthermore, this thesis would not have been possible were it not for the generous funding provided by the Wellcome Trust.

Most of all these acknowledgements are for my parents: Rosemary and John. Thank you for your unconditional support with all things, no challenge feels too great with you in my corner. I hope this makes you proud.

Finally, thank you to the University of St Andrews and all its students and staff I have come to know along the way – you have made this wee seaside town my home.

Abstract

The sodium-potassium pump (NKA) is a ubiquitously expressed membrane protein. Mammalian neurons express two isoforms of the NKA's catalytic α-subunit, the ubiquitous α1, and the neuron-specific α3. Mutations in the α3-NKA encoding protein *ATP1A3* result in a spectrum of neurological disorders with pronounced motor deficits, including Rapid-Onset Dystonia Parkinsonism (RDP). The NKA has also been shown to facilitate activity-dependent changes in spinal motor networks via an ultra-slow afterhyperpolarisation (usAHP) which is thought to be an α3-NKA mediated current.

First, we provide a comprehensive characterisation of a novel mouse model of RDP harbouring the T613M mutation of *ATP1A3* most commonly found in patients. We show that T613M animals are hyperactive and hyperambulatory. We show involvement of spinal motor circuit pathology in this behaviour via a complete lack of usAHPs in T613M-affected motor neurons, and a reduced capacity for isolated spinal cords to regulate rhythmic motor output in response to large increases of intracellular sodium. We show that this deficiency is likely caused by a reduced capacity for T613M-affected α3-NKA to extrude sodium and therefore maintain sodium homeostasis.

Next, we characterised post-discharge activity more generally in motor neurons from wildtype mice. We show that usAHPs are more commonly observed in the second postnatal week which may be due to an upregulation of α3-NKA protein expression in motor neurons alongside the development of weight-bearing locomotion. While the heterogenous distribution of usAHPs amongst populations of neurons was previously thought to be due to mosaicism of α3-NKA expression, we show that all lumbar motor neurons express α3-NKA. We present an alternative to this hypothesis, showing that usAHPs can be masked by competing conductances. Finally, we show that the post-discharge activity of a neuron can be modulated by extrinsic and intrinsic modulators to enhance or unmask certain post-discharge activity subtypes.

Collaboration Statement

Parts of this research were performed in collaboration with Evgeny Akkuratov, Simon Sharples, and Gina Gnanasampanthan. All collaborations are detailed at the beginning of each chapter including details of author contributions.

General Introduction

The Sodium-Potassium Pump

The evolution of the sodium-potassium pump and the birth of movement

To fully explain the essential nature of the sodium-potassium pump to life as we know it, it is easiest to start at the beginning. Eukaryotic cells diverged from prokaryotic cells approximately 2.7 billion years ago (Cooper, 2000). With this evolution, several morphological changes occurred, such as the emergence of the nucleus, membrane-bound organelles, and the cytoskeleton. But as time passed, certain features preserved from prokaryotic ancestors for aeons were lost, giving rise to a new cell type: the 'animal' cell.

Plant cells and bacteria cells are surrounded by a cell wall which grants structural support and protection. The wall allows the cells that possess it to maintain their high osmotic pressure easily but condemn them to a life of sessility in the process: a life without movement. There is a significant advantage to being without a cell wall, mainly that wall-less cells can change the shape of their plasma membrane when required. For Protista, the early single-celled 'animals', this allowed them to engulf other cells via phagocytosis. With a newfound hunger for stored energy, a flexible membrane, and a cytoskeleton, cells began to 'move'.

Like living with a cell wall, living without one also comes at an expense. Without the wall to contain the cell's osmotic pressure, 'animal' cells are in constant osmotic equilibrium with their environment. Since the plasma membrane is permeable, the ions within the cell will reach an osmotic equilibrium with the extracellular environment. This would be survivable were it not for the many non-permeable metabolites within the cell (nucleic acids, proteins, etc.), which would leave an osmotic burden within the cell when unable to equilibrate. August Krogh was the first to point out this risk of 'death-by-flooding' (Krogh, 1945). To explain how 'animal' cells managed to escape this flooding, Krogh postulates on the possible existence of a membrane-bound structure, found in 'animal' cells but not

plant cells, that would remove intracellular sodium[1] to compensate for the absence of the cell wall. The sodium-potassium pump immobilises one of the major ions, sodium, externally. A lack of intracellular sodium compensates for impermeable metabolites, and osmotic equilibrium is achieved. As I will explain in this introduction, the mechanism is simple yet profound and allows cells to accomplish much more than volume control.

The structure and function of the sodium pump

The sodium pump is a heterodimer composed of two dimer subunits (α and β) and a smaller gamma subunit (Fig. 1). The α subunit contains the binding sites for all ligands currently known to associate with the protein (Farley *et al.*, 1984; Walderhaug *et al.*, 1985), including the binding site for ATP, which, once bound, facilitates the function of the pump. Once ATP has bound to the intracellular α site, three intracellular sodium ions also bind to the pump. The ATP is hydrolysed, causing phosphorylation of the pump and release of ADP. The subsequent conformational change exposes the bound sodium ions to the extracellular space, and they are released. The pump then binds two extracellular potassium ions, causing dephosphorylation of the pump. Thus, the pump returns to its previous conformational state, transporting the two bound potassium ions into the cell as it does so. In its original conformational state, the sodium pump has a higher affinity for sodium ions so that the process may begin again. Through this mechanism, many functions are achieved, such as osmotic regulation, ionic homeostasis, cell cycle regulation, and cellular metabolism regulation (Boldyrev, 1993). There is even a role for the sodium pump in regulating the endosomal pH (Cain, Sipe and Murphy, 1989; Fuchs, Schmid and Mellman, 1989). However, of most interest to this review is the unique role of the sodium pump in neurons. Through the exchange of monovalent cations resulting in a more negative intracellular

[1] While the existence of an active pump that transported sodium and potassium across the membrane had been postulated for many years, the formal discovery of the mechanism was achieved by Jens Christian Skou in 1957, for which he was awarded the Nobel Prize in Chemistry in 1997.

environment compared to the extracellular environment, the sodium pump creates and maintains the electrochemical gradient that is the basis of excitation in these cells.

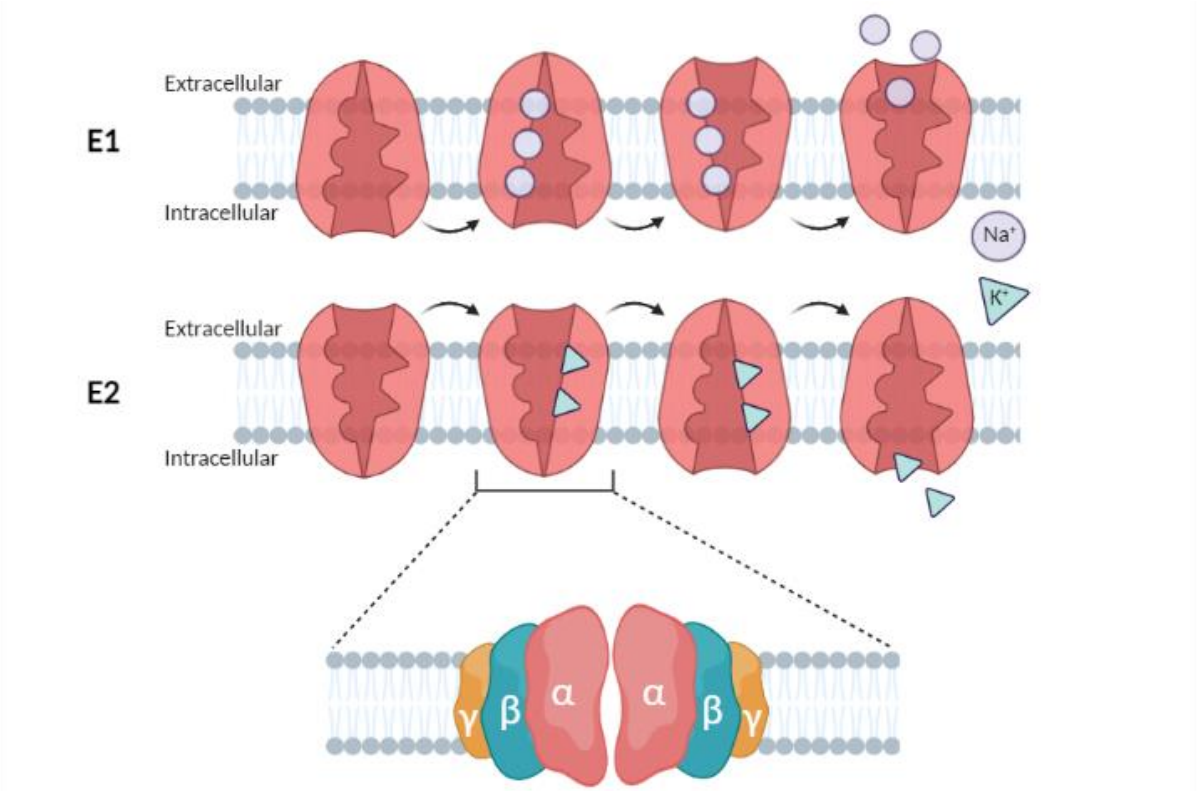

Figure 1. The structure and function of the sodium-potassium pump. The electrogenic pump exchanges three intracellular Na^+ ions in its E1 conformational state for two extracellular K^+ ions in its E2 conformational state. The protein is a tetramer composed of α and β dimer subunits and a third smaller γ subunit. Created using BioRender.com.

The β subunit acts as a chaperone that ensures that the protein is correctly stabilised and orientated in the membrane by acting as an anchor (Hiatt, McDonough and Edelman, 1984). In addition, the β subunit determines some intrinsic transport properties of the pump (Geering, 2001). The γ subunit belongs to the family of FXYD proteins and serves as a modulator of the kinetic properties of the

sodium pump (Garty and Karlish, 2006; Geering, 2006). The α and β subunits can assemble to form a functional pump, but their subunits can also exist on their own (Okamura *et al.*, 2003). Four α subunit isoforms, three β subunit isoforms, and seven FXYD isoforms have been identified thus far in vertebrates and are expressed in a tissue- and development-specific manner.

α1 (α1-NKA) is ubiquitously expressed and is not tissue-specific. α2 (α2-NKA) and α3 (α3-NKA) are expressed in the nervous system, with α2 expressed in glia and α3 exclusively in neurons (McGrail, Phillips and Sweadner, 1991; Cameron *et al.*, 1994). However, α2 is still expressed in neurons at birth and in the early postnatal days in mice before becoming glia-specific later in development (Moseley *et al.*, 2003). α4 has the most restricted expression of any of the isoforms and is currently thought only to be expressed in male germ cells of the testis (Clausen, Nissen and Poulsen, 2011). α4 in spermatozoa is required for sperm motility and hyperactivation and is, interestingly, a highly appealing target for the development of male contraceptive drugs (Syeda *et al.*, 2020).

The inter-species genetic sequences for α1-α3 are highly conserved, suggesting an essential physiological function tied to the structure of the α subunit preserved throughout evolution (Takeyasu, Lemas and Fambrough, 1990) (Table 1). The homology of α1-, α2-, α3- isoforms between humans and rats (*Rattus norvegicus)* is >97%, with the a3 isoform having a massive 99.5% conservation (Clausen, Nissen and Poulsen, 2011). Structural differences between species appear to be largely superficial, occurring on the protein's surface in contact with the extracellular space. In contrast, the residues on the interior of the protein responsible for ion binding are unchanged (Clausen, Hilbers and Poulsen, 2017).

Table 1. *ATP1A3* orthology between human, mouse, zebrafish, *Drosophila melanogaster*, and *C. elegans.* Adapted from Ng, Ogbeta and Clapcote (2021)

Species	Gene symbol	% Protein homology	% DNA homology
Human (*H. sapiens)*	ATP1A3	100	100
Mouse (*M. musculus)*	*Atp1a3*	99.6	90.8
Zebrafish (*D. rerio)*	*atp1a3a*	90.0	81.0
	atp1a3b	91.6	79.5
D. melanogaster	*Atpα*	76.3	71.7
C. elegans	*eat-6*	73.5	67.0

Functionally, the α subunits differ in their sodium affinity and voltage dependence. α1 has a high affinity for sodium, with α2 and α3 having lower affinities for the cation. The high sodium affinity of α1 allows it to act as a 'housekeeping' unit, continuously regulating basal intracellular sodium levels and thus maintaining the cell's resting membrane potential. α3's low sodium affinity makes it a better candidate to compensate for large transients in intracellular sodium, such as those that might occur during periods of high-intensity or prolonged firing in neurons (Azarias *et al.*, 2013). α3's high affinity for ATP allows this isoform to utilise low nucleotide levels near the cell membrane (Blanco and Mercer, 1998). While α2 is only expressed in the astrocytes and oligodendrocytes of the mature nervous system, it still plays an essential role in excitability. Neuronal activation leads to depolarisation of the astrocytic membrane due to increased extracellular K^+. Astrocytic α2 clears this increase in extracellular potassium to prevent further depolarisation due to its low K^+ affinity (Crambert *et al.*, 2000; Larsen *et al.*, 2014).

Like the α subunit isoforms, the β subunit isoforms also have distinct functions and expression profiles. The different isoforms allow the sodium-potassium pump to adapt to various tissues, activity levels, and environments. β2 was first identified in glia, where it is involved in cell-cell contacts and thus was initially coined Adhesion Molecule On Glia, or AMOG (Martin-Vasallo *et al.*, 1989; Gloor *et al.*, 1990). It has the most substantial effect on the kinetic properties of the pump of the three isoforms, with its

expression reducing potassium affinity and increasing extracellular sodium affinity compared to the other isoforms (Larsen *et al.*, 2014; Hilbers *et al.*, 2016). β1 appears to be the predominant β subunit isoform in neurons (McGrail, Phillips and Sweadner, 1991; Watts *et al.*, 1991; Arystarkhova and Sweadner, 1997). β3 expression in the mouse brain has not been studied extensively; however, mRNA of the β3 isoform is highly expressed in the testis while the kidney, spleen, lung and brain show only moderate expression of the isoform (Malik *et al.*, 1996). Overall, no consistent conclusions have been drawn about the exact physiological relevance of the α-β subunit interactions, due primarily to different experimental assays used. Still, a kinetic analysis of the sodium pump activity in rat isozymes showed consistent effects on K^+ affinities in decreasing order from α1 − β1 >α2 − β1 = α2 − β2 >α3 - β1 = α3 − β2 isozymes (Blanco and Mercer, 1998).

The sodium-potassium pump can be modified further by the addition of the FXYD subunit. Most FXYD proteins appear to lower the pump's substrate affinities and potentially modulate pump function (Geering, 2005). FXYD1 is highly expressed in the heart, skeletal muscle, and brain (Chen *et al.*, 1997), with FXYD1 knockout mice showing increased sodium pump activity in the heart (Jia *et al.*, 2005; Bell *et al.*, 2008). FXYD2 is the only protein referred to as the 'γ' subunit, and was the first to be associated with the sodium pump (Forbush, Kaplan and Hoffman, 1978) and, similarly to FXYD1, decreases pump activity with its effects being relieved in knockout mouse models (Jones *et al.*, 2005; Arystarkhova, 2016). It is expressed mainly in the ascending limb of the kidney (Küster *et al.*, 2000; Sweadner and Rael, 2000; Pu *et al.*, 2001).

FXYD3 expression is restricted to smooth muscle, skin and the salivary glands, but its effects on the sodium pump are unclear (Crambert *et al.*, 2005; Bibert *et al.*, 2006; Wujak *et al.*, 2016). FXYD4 is expressed mainly in the collecting duct of the kidney (Béguin *et al.*, 2001; Meyer *et al.*, 2020). FXYD5 is expressed in many tissue types but appears absent in the central nervous system (Lubarski, Karlish and Garty, 2007; Mathias *et al.*, 2008). Both FXYD4 and FXYD5 increase sodium affinity and therefore enhance pump activity.

FXYD6 and FXYD7 are expressed in the neurons and glia (Yamaguchi *et al.*, 2001; Béguin *et al.*, 2002; Delprat, Puel and Geering, 2007; Meyer *et al.*, 2020), and both decrease the enzyme's affinity for extracellular K^+ with mixed effects on the affinity for intracellular Na^+ (Béguin *et al.*, 2002; Meyer *et al.*, 2020).

Neuronal interactome of the sodium-potassium pump

As its role within the cell is so essential, it may not come as a surprise that the sodium-potassium pump does not exist in isolation, nor is its function unaffected by other cellular mechanisms. The sodium-potassium pump forms complexes with multiple other membrane receptors. Both the α1 and α3 subunit isoforms co-immunoprecipitate with postsynaptic density protein 95 (PSD-95) (Blom *et al.*, 2011; Azarias *et al.*, 2013), a membrane protein that is involved in the anchoring of other synaptic proteins. PSD-95 has many binding partners, including N-methyl-D-aspartate (NMDA) receptors – an ionotropic receptor for glutamate, the primary excitatory synaptic transmitter in the mammalian nervous system (Sala *et al.*, 2001; Zhang *et al.*, 2012). A functional complex of both α3 and α1 subunits and NMDA receptors was also found following co-immunoprecipitation in hippocampal neurons. NMDA receptor expression was reduced after applying a low concentration of ouabain, a cardiac glycoside which binds to and inhibits the sodium-potassium pump (Akkuratov *et al.*, 2015). However, other studies have shown contradicting results. Inhibition of the sodium pump has also been found to increase NMDA receptor activation (Reinés, Peña and Rodríguez De Lores Arnaiz, 2001; Reinés *et al.*, 2004). Bersier and colleagues (2008) characterised the effect of the application of endobain E, an endogenous sodium pump inhibitor that shares several properties with ouabain, on NMDA receptor expression. Bersier and colleagues found that two days after administration of endobain E, NMDA receptor subunit expression increased significantly in rats' cerebral cortex and hippocampus. The exact interaction between the sodium-potassium pump and NMDA receptors remains to be fully

understood. Still, these authors suggest the observed differences may be due to differences in the brain region studied or the mode of action of endobain E and ouabain.

The regulation of sodium-potassium pump activity by dopamine is perhaps the best-described membrane interaction of the pump. The α3/PSD-95 complex was found to co-immunoprecipitate with dopamine D1 receptors and D2 receptors recently (Hazelwood *et al.*, 2008; Blom *et al.*, 2012), but much earlier studies have shown that activation of D1 and D2 dopamine receptors inhibit sodium pump activity in cultured neurons (Bertorello and Aperia, 1990). This was later narrowed down to α3-inhibition in neurons and α2-inhibition in glia by dopamine, with the α1 subunit relatively unaffected in striatal cultures (Nishi *et al.*, 1999).

Not only does the sodium pump form complexes with other membrane receptors, but the pump also has an unsurprising amount of crosstalk with many other receptors in the membrane due to its significant effect on intracellular Na^+ concentrations. This crosstalk makes it difficult to differentiate a direct interaction with the sodium pump from an indirect effect via changes in ionic concentrations. Sodium-potassium pump inhibition results in rapid internalisation of AMPA receptors, another ionotropic glutamate receptor that allows the movement of sodium across the membrane. The pump has been found to co-localise and suppress AMPA-mediated synaptic transmission (Zhang *et al.*, 2009). Similarly, inhibition of the pump with ouabain leads to an increased concentration of intracellular Ca^{2+} (Fujino and Fujino, 1982; Deitmer, Eckert and Schlue, 1987; Meyer-Lehnert, Bäcker and Kramer, 2000). This is because inhibition of the pump leads to an increase in intracellular Na^+, which, in turn, activates the Na^+/Ca^{2+} exchanger in reverse mode. The increased Ca^{2+} in the cytoplasm causes even further release of the ion from the intracellular Ca^{2+} depot (Balduini and Costa, 1990; Condrescu *et al.*, 1995; Saghian, Ayrapetyan and Carpenter, 1996; Rakovic *et al.*, 1999). Increases in intracellular Ca^{2+} reduce the inward Cl^- current amplitude caused by acetylcholine (ACh) in the pond snail (Chemeris *et al.*, 1982; Arvanov, Stepanyan and Ayrapetyan, 1992).

While the essential homeostatic role of the sodium pump makes it incredibly interesting to study, it also makes it incredibly difficult to study due to the inability to isolate its effects. In a study investigating the relationship between the sodium-potassium pump and GABA receptors, the authors saw that inhibition of the pump led to increased effects of GABA in Xenopus oocytes (Arvanov and Usherwood, 1991). The authors proposed that, as the sodium pump is essential to the control of cell volume and the application of ouabain produces cell swelling, the increased effects could be due to the enlarged surface area of the membrane making more receptors accessible to exogenously applied agonists. The effect of cell volume on the number of active membrane chemoreceptors has been well studied (Ayrapetyan, 1990). In this sense, blocking the pump may produce an effect on any membrane receptor-mediated activity. Inactivation of the pump also increases intracellular levels of ATP and cAMP, producing knock-on effects for many signalling cascades within the cell (Arvanov, Stepanyan and Ayrapetyan, 1992; Saghian, Ayrapetyan and Carpenter, 1996). Due to these many interactions, while it may bring about its complications such as compensatory upregulation of other proteins, the use of genetic models to diversify the study of sodium-potassium pump function is essential.

Genetic models for studying α-subunit isoform function

The α subunit's tissue- and development-specific expression suggests a unique physiological role for each isoform. A variety of genetic homozygous and heterozygous knockout *Atp1a3* models have been used to elucidate the role of the neuron-specific α3-NKA. Due to the close DNA orthology of the sodium-potassium pump between species, models of dysfunction provide highly valuable information that is potentially applicable across the animal kingdom – even for humans. Most closely related to human *ATP1A3* is mouse *Atp1a3*, and several mouse models have been used to date to study the *in vivo* consequences of α3-NKA mutations.

Moseley and colleagues first described the Atp1a3tm1/Ling model in 2007. This line was generated by introducing a point mutation in embryonic stem cells that resulted in aberrant splicing of the gene. They found that homozygous knockouts of *Atp1a3* die neonatally, which is consistent across all knockout models used. Death is typically caused by a lack of breathing movements after birth. Heterozygous Atp1a3tm1/Ling mice had a 60% reduction in α3-NKA protein levels in the hippocampus, contributing to an overall 16% reduction in NKA activity in the brain. When Atp1a3tm1/Ling mice were exposed to a chronic stress variable, however, mice displayed a further decrease in NKA brain activity to 33%, resulting in several cognitive impairments.

The Atp1a3tm2/Kwk mouse model was produced some years later by Ikeda and colleagues. This line was made similarly to that described by Moseley and colleagues (2007), but instead of a point mutation being introduced, several gene exons were replaced with a loxP-flanked *Atp1a3*-enhance green fluorescent protein which could be subsequently deleted via Cre-mediated recombination (Ikeda *et al.*, 2013). These mice, too, exhibited several cognitive deficits and impaired social behaviours, as well as altered neurotransmission across inhibitory synapses in the cerebellum.

The most widely known *Atp1a3* mouse model is likely the *Myshkin* mouse, harbouring the I810N mutation observed in three human patients affected by Alternating Hemiplegia of Childhood (AHC). AHC is one of the many disorders associated with α3 pump dysfunction discussed later in this general introduction. Heterozygous *Myshkin* mice show a 42% reduction in sodium-potassium pump activity in the brain, consistent with the relatively severe phenotype compared to the two models previously discovered. The *Myshkin* phenotype includes spontaneous seizures, elevated metabolic rate, sleep abnormalities and several motor, cognitive, social, and behavioural deficits (Clapcote *et al.*, 2009; Kirshenbaum *et al.*, 2011, 2013, 2015, 2016). In hippocampal slices from these mice, the CA3-CA1 hippocampal pathway did not exhibit any changes in synaptic activity as described by Ikeda and colleagues under basal conditions but did observe hyperexcitability after high-frequency synaptic input (Clapcote *et al.*, 2009).

The Mashlool mouse model harbours a similar mutation to the *Myshkin* model, D801N. Interestingly, this mutation does not affect expression levels but does reduce enzymatic activity by 54-80% (Heinzen *et al.*, 2012). The CA3-CA1 hippocampal pathway of Mashlool mice also shows hyperexcitable responses to repetitive, high-frequency stimulation (Hunanyan *et al.*, 2015). The Matoub mouse model, which harbours the second most common AHC mutation, E815K, displays similar but more severe deficits to D810N (Helseth *et al.*, 2018).

The Atp1a3D801Y mouse model was similarly made harbouring the D801Y mutation, which affects the aspartic acid position at 801. Mutations at this site have been found in several patients with *ATP1A3*-related disorders. Heterozygous Atp1a3d801Y mice show a 15% reduction in α3-NKA protein expression in the brain (Holm *et al.*, 2016).

While all of these mouse models harbour different mutations, and it is clear that the location of the mutation determines the overall effect on enzyme activity and phenotype severity, there are a few behavioural outcomes that are surprisingly consistent across all models. All *Atp1a3* mouse models show motor abnormalities, particularly hyperexcitability and hyperambulation, accompanied by hindlimb gait abnormalities in several models. These behavioural consistencies suggest that α3 is of functional significance within the motor system of these animals. But, even before these recent mouse models were produced and studied, we have had clues about the role of α3-NKA in motor control for some time.

The Sodium-Potassium Pump in Motor Control

Behaviours as complex but essential as locomotion require flexibility. The ability to adapt quickly to an everchanging and demanding environment may mean the difference between life and death for an animal, whether it is knowing how to meticulously sweep through a landscape in search of food or being able to reflexively initiate an escape response to avoid becoming the food. For the neural circuits underlying these behaviours to be flexible, they need to be highly modulated. When thinking of neuromodulation, one would typically consider the effect of neurotransmitters that target ion channels to tweak and change activity. However, sometimes the activity itself can have a modulatory effect. Membrane proteins like the sodium-potassium pump can detect changes in intracellular ion concentrations that occur because of cell activity and adjust cell excitability as a result.

The role of tonic and dynamic pump currents

As discussed previously, the sodium-potassium pump plays a role in setting membrane excitability in neurons. Through the unequal exchange of three positively charged sodium ions for two positively charged potassium ions, the pump ensures that the membrane potential is slightly hyperpolarised and is therefore electrogenic. This is achieved in both a tonic and dynamic manner depending on which α subunit isoforms are at work.

The α subunit isoforms vary in their affinities for sodium, with the Km (the concentration of substrate required for the enzyme to be 50% saturated) for α1 estimated between 8-17mM and 30-68 mM for α3 (Blanco and Mercer, 1998; Hamada *et al.*, 2003; Dobretsov and Stimers, 2005; Kim *et al.*, 2007). As the basal intracellular sodium concentration in neurons is approximately 10mM (Dobretsov and Stimers, 2005), the α1 isoform is tonically active and perpetually working to maintain the neuron's resting membrane potential. The α3 isoform only becomes active after a period of activity that

increases intercellular sodium and, therefore, has a more dynamic contribution to cell excitability (Fig. 2).

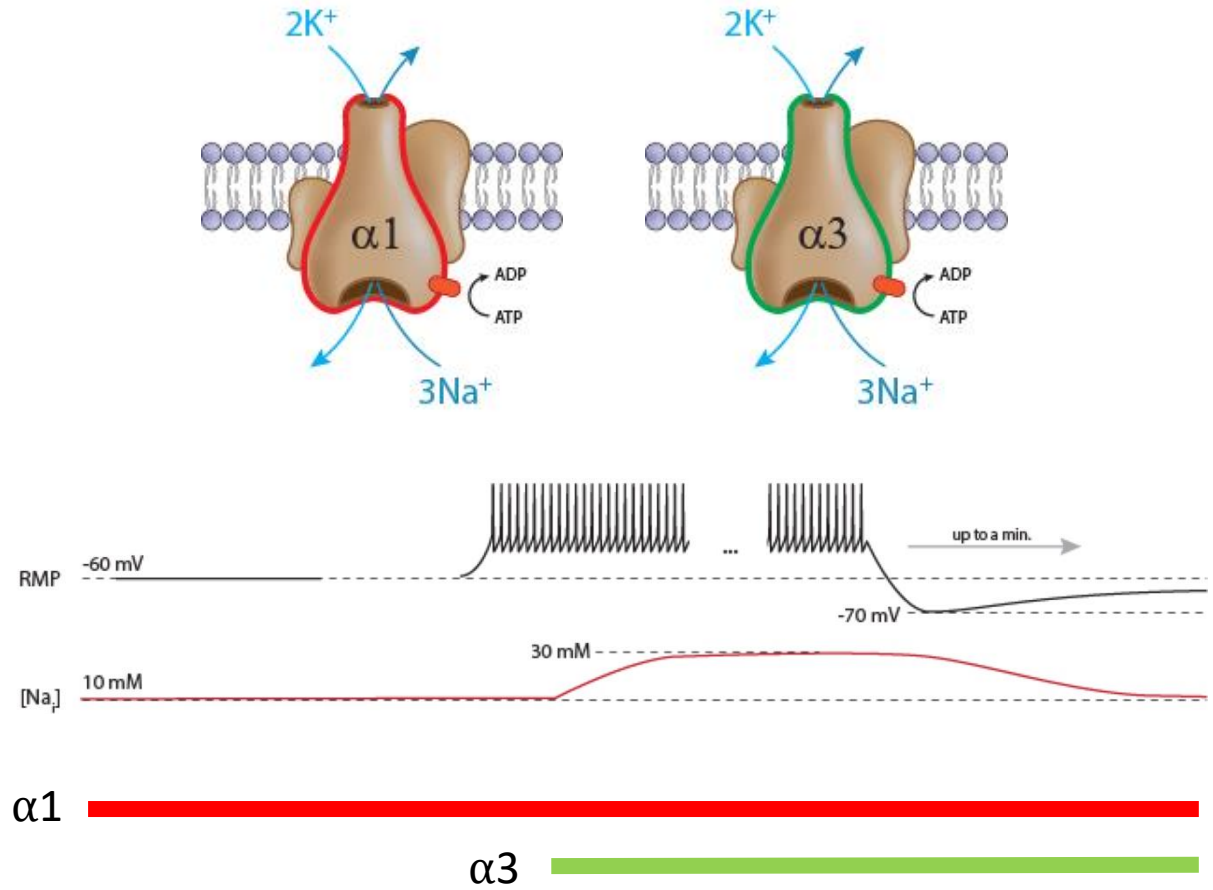

Figure 2. The α1 and α3 subunit isoforms of the sodium-potassium pump have a tonic and dynamic effect on membrane excitability due to their differing affinities for intracellular Na^+. The α1 isoform is tonically active at baseline intracellular Na^+ levels, whilst the α3 isoform only becomes active after a period of neuronal firing leading to an increase in intracellular Na^+ levels. Modified from Miles (2021).

The contribution of the α1 isoform to the maintenance of the resting membrane potential differs across species and cell types (Dobretsov and Stimers, 2005). In many cases, passive diffusion of potassium across the membrane has a more significant impact on resting membrane potential than tonic pump activity. However, a significant role for α1 in setting RMP has been documented in

receptor neurons of the vomeronasal organ (Trotier and Døving, 1996), mesencephalic trigeminal neurons (Kang *et al.*, 2004), and Purkinje cells of the cerebellum (Genet and Kado, 1997).

On the other hand, significant and dynamic changes in intracellular sodium more greatly affect pump activity and thus the pump's influence on neural network output. To date, a pump-mediated hyperpolarising current, produced by the exchange of positively charged ions in a 3:2 ratio described earlier, has been observed across many cell types and model organisms. While it has been documented under many different names, the mechanism for this pump-mediated current seems to be unambiguous, serving as a form of autoinhibition after an extended period of activity. The duration of the pump-mediated hyperpolarisation is typically proportional to the duration and frequency of activity. This activity-dependent pump current has been particularly well described to date in invertebrate systems, typically as an extended post-activity polarisation that is reduced by the application of the sodium pump-blocker ouabain. This pump-mediated current has been observed in leech neurosecretory (Gocht and Heinrich, 2007) and sensory T-cells (Baylor *et al.*, 1969; Catarsi, Scuri and Brunelli, 1993; Scuri, Mozzachiodi and Brunelli, 2002; Scuri *et al.*, 2007), crayfish stretch receptors (Nakajima and Takahashi, 1966; Sokolove and Cooke, 1971), insect mechanoreceptors (French, 1989), and neurosecretory neurons in the snail (Nikolić, Kartelija and Nedeljković, 2008; Nikolić *et al.*, 2012).

In vertebrate systems, a sodium pump-mediated current of the same nature has been described in sensory neurons of the lamprey (Parker, Hill and Grillner, 1996), and the auditory (Kim *et al.*, 2007) and hippocampal pyramidal neurons of the rat (Gulledge *et al.*, 2013).

Dynamic pump currents in central pattern generating networks

To study the roles of proteins such as the sodium-potassium pump in the production of complex behaviours, such as reaching or grabbing, researchers can utilise rhythmic behaviours to simplify the

investigative process. By studying rhythmic movements that produce consistent and repeatable output, such as chewing, breathing, or locomotion, the effect of modulation of these proteins can be more easily extracted. More importantly, these behaviours can often be produced without input from the brain and therefore can be isolated physically with many confounding variables removed.

A central pattern generator can be defined as a 'network of neurons that autonomously generate rhythmic patterns of activity' (Goulding, 2009) and are often the focus of such work. Many models defining the neural architecture of the CPG controlling rhythmic motor behaviours have been produced, arguably beginning with the seminal work of Sir Charles Sherrington. Sherrington first described 'reflex stepping' in cats and dogs (Sherrington, 1906, 1910), setting the foundation for the existence of discrete motor networks in the brain stem and spinal cord. Carrying on the work of his mentor, Thomas Graham Brown showed that rhythmic locomotor output such as walking could be maintained even when all sensory feedback and descending input is removed, proving that not only are these rhythmic motor networks located spinally, but they also do not rely on sensory input and are therefore innate (Graham Brown, 1911). Brown proposed a model of intrinsic rhythmicity, termed the 'half-centre model', which predicts that rhythmic output is achieved via two mutually inhibitory flexor and extensor half-centres (Graham Brown, 1911; Graham Brown, 1914). As motor behaviours such as walking are facilitated by the alternating contraction of flexor and extensor muscles, the flexor half-centre must inhibit the extensor half-centre through its activity and vice versa.

While considered largely theoretical at the time, similar work on invertebrates conducted some 50 years after its proposition lent legitimacy to the Brown half-centre model (reviewed in Mulloney and Smarandache, 2010). It has now been shown across a multitude of species and locomotor behaviours that rhythmic motor output can be generated centrally and does not require sensory input. While it does appear that most CPG networks abide by this concept of reciprocal inhibition between groups of neurons, current research suggests that this model may be too reductive to apply to more complex

movements such as quadruped stepping and alternate models such as the 'Unit Burst Generator' model have been proposed (Grillner, 1981).

The sodium pump current has been shown to regulate invertebrate rhythmic networks such as the leech heartbeat (Tobin and Calabrese, 2005; Calabrese, Norris and Wenning, 2016) and the crawling behaviour of third instar *Drosophila* larvae (Pulver and Griffith, 2010). In the leech, Angstadt and Friesen (1991) propose that the build-up of intracellular sodium after a period of neuronal firing activates the sodium pump. The resulting hyperpolarisation of the membrane potential as the cell exudes sodium is thought to terminate the cell's firing, thereby setting the frequency of the bursting activity of these pacemaker neurons. When the sodium pump is blocked with ouabain, the burst frequency of this rhythmic output increases, presumably because of removal of the sodium pump-mediated current (Tobin and Calabrese, 2005). In *Drosophila*, it was proposed that the sodium pump regulates crawling behaviour generated by endogenously bursting motor neurons by introducing a delay to the first spike (Glanzman, 2010; Pulver and Griffith, 2010).

A similar role for the sodium pump in vertebrates has been suggested to help regulate rhythmic firing in dopaminergic midbrain neurons (Johnson, Seutin and North, 1992; Shen and Johnson, 1998) and cerebellar Purkinje cells (Forrest *et al.*, 2012), both involved in the control of movement.

In terms of spinal CPG circuits, several studies have shown an important role for the sodium pump in respiration (Del Negro *et al.*, 2009; Rubin *et al.*, 2009; Krey *et al.*, 2010; Tsuzawa *et al.*, 2015). However, the role of the sodium-potassium pump in the vertebrate locomotor CPG is relatively undescribed.

The mammalian locomotor system

The selection, initiation, and modulation of different locomotor behaviours involves various regions of the brain, brainstem, and spinal cord. The basic organisation of this locomotor system is well

conserved throughout vertebrate evolution: neuronal systems in the brain select the locomotor behaviour, neuronal systems in the midbrain and lower brainstem initiate the behaviour, and neuronal systems in the spinal cord execute the behaviour (Fig. 3).

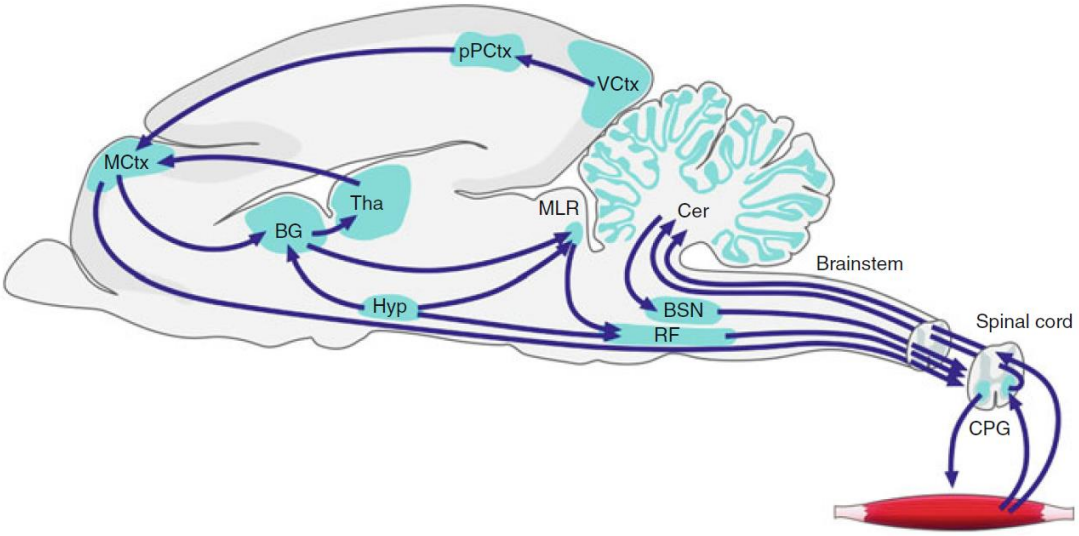

Figure 3. The organisation of the brain and brainstem structures involved in the initiation and control of locomotion in vertebrates. Appropriate locomotor behaviour is selected in the basal ganglia (BG). Neurons from the BG then project the motor cortex (MCtx) via the thalamus (Tha) and the mesencephalic locomotor region (MLR). Locomotion is initiated by the neurons of the MLR that then project to the medial reticular formation (RF) in the brainstem. RF neurons then project to the locomotor central pattern generator in the spinal cord, and locomotion is finally executed by the motor neurons, which project from the spinal cord and innervate the muscles. The cerebellum (Cer), visual cortex (VCtx), and posterior parietal cortex (pPCtx) modulate motor behaviour in response to proprioceptive sensory and visual feedback. Taken from Kiehn and Dougherty (2013).

First, selecting the appropriate motor pattern to allow one to navigate the environment efficiently is essential. A variety of different locomotor behaviours may be necessary, such as slow exploratory movement when searching for food or a fast escape movement when avoiding a predator. Experiments in several animal models have shown that the basal ganglia, a group of subcortical nuclei situated above the midbrain and at the base of the forebrain, is largely responsible for motor pattern

selection (reviewed in Grillner and Robertson, 2015). The basal ganglia receive input from the cortex and thalamus and project output neurons to the midbrain's mesencephalic locomotor region (MLR).

Stimulation of the MLR has been shown to initiate locomotion in resting animals in a frequency-dependent manner, with more intense stimulation increasing the speed of the locomotion until the animal eventually transitions from a walk to a gallop (Shik, Severin and Orlovsky, 1969). Neurons from the MLR project to the reticular formation of the lower brainstem before a final motor command is sent from the reticular formation to the spinal cord. Stimulation of the subthalamic/diencephalic locomotor region also evokes locomotion and, like the MLR, this region projects to neurons in the reticular formation (Milner and Mogenson, 1988). However, the input received by the subthalamic/diencephalic locomotor is not well understood. Similarly, the identity of the reticulospinal neurons that send the final motor command from the brain are not fully described, but there are two likely culprits: a glutamatergic locomotor pathway found in all vertebrates (Douglas *et al.*, 1993; Stein *et al.*, 1997; Jordan *et al.*, 2008), and a serotonergic locomotor pathway observed in experiments in rats (Schmidt and Jordan, 2000; Liu and Jordan, 2005).

While all of this occurs, motor circuits in the brain are constantly monitoring feedback from the spinal cord to adapt ongoing motor activity and maintain the proper position and balance of the body. This function is largely performed by the cerebellum, which receives input from excitatory spinal neurons via the dorsal spinocerebellar tract (DSCT) and the ventral spinocerebellar tract (VSCT).

Gross anatomy of the spinal cord

Once the signal has reached the spinal cord, locomotion can take place. The spinal cord is the part of the central nervous system that controls the muscles of the limbs and the trunk. The cord is a column of tissue that extends from the base of the neck to the tailbone and is divided into four segments based upon the pattern of the spinal nerves that emerge from them: cervical, thoracic, lumbar, and

sacral (Fig. 4). In humans, the spinal nerves of the cervical segment innervate the muscles of the neck, diaphragm, and arms. The thoracic nerves control the intercostal muscles and the muscles of the chest and back. Branches of the thoracic nerves are also involved in the autonomic nervous system. The lumbar nerves innervate the erector muscles of the back, the hips, and legs. The sacral nerves innervate much of the hips, legs, and feet.

A dorsal nerve root and a ventral nerve root emerge from each segment and bundle together to form a spinal nerve. Dorsal nerve roots contain sensory fibres made up of sensory neuron axons, and ventral nerve roots contain motor fibres made up of motor neuron axons (Hawkins, 1869). A feedback loop is created between these nerve roots whereby sensory information from the periphery can enter the spinal cord via the dorsal roots, and motor commands can be sent out to the periphery via the ventral roots. This signal transduction takes place within the main body of the cord which is composed of grey matter and white matter. The white matter surrounds the grey matter along the perimeter of the cord. The dorsally projecting arms of the grey matter are referred to as the dorsal 'horns' and the ventrally projecting arms the ventral 'horns'. The central region between the dorsal and ventral horns is referred to as the intermediate grey matter.

There is a large amount of morphological heterogeneity in the grey matter of the spinal cord. However, there is some intrinsic organisation so that grey matter can be divided into ten regions, or 'laminae', based on the grey matter's cytoarchitecture as seen in transverse sections (Rexed, 1952, 1954). Most notably, lamina IX contains the motor neurons of the grey matter and is located at the base of the ventral horn. Lamina IX contains both the α-motor neurons, which are large cells whose axons innervate the striated muscles and the γ-motor neurons, which are smaller cells that innervate the muscle spindles: the stretch receptors that detect changes in muscle length. The α-motor neurons are organised into three discrete medial and lateral longitudinal columns. The medial motor column extends the entire length of the spinal cord, and its constituent motor neurons innervate the muscles of the trunk, whilst the lateral motor column is isolated to the cervical and lumbar spinal cord and

contains motor neurons that innervate the limbs. The lateral motor column emerged with the first vertebrates to evolve paired appendages: the elasmobranchs (sharks and rays). Before this point in the mammalian lineage, vertebrates, such as the lamprey, which moved via undulation of the axial muscles, possessed only the medial motor column. While the elasmobranchs do still move largely via undulation of the trunk, the pectoral fins can also be used for locomotion (Jung *et al.*, 2018). This suggests that the basic internal anatomy required for limbed locomotion evolved nearly 420 million years ago and has been quite well conserved since as the molecular signatures of distinct neuronal subtypes that make up the CPG circuits of the tetrapod spinal cord are still present in these animals (Catela, Shin and Dasen, 2015; D'Elia and Dasen, 2018; Grillner, 2018; Jung *et al.*, 2018).

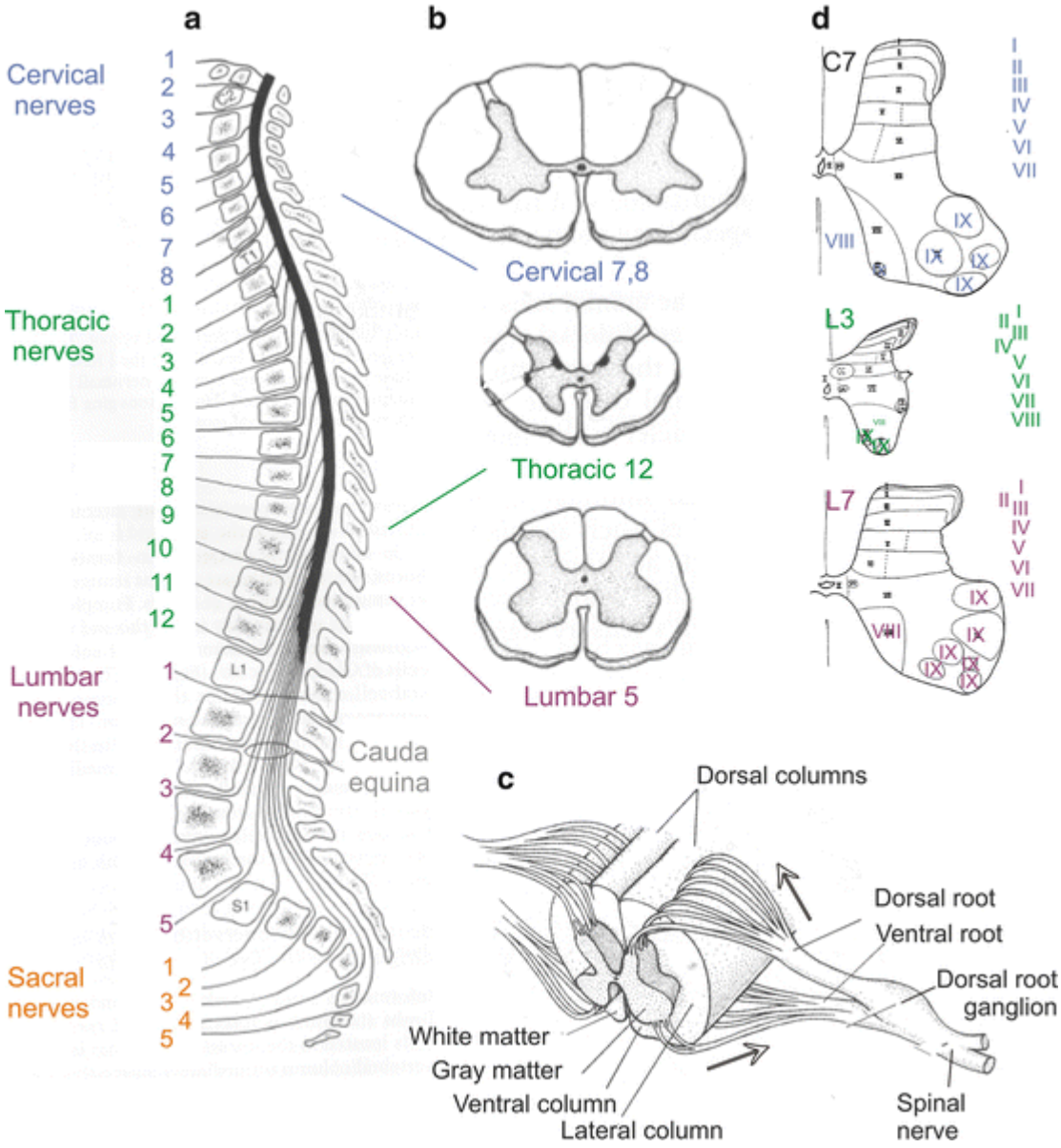

Figure 4. The basic morphology of the human spinal cord. (**a**) Location of the spinal nerves with respect to the spinal vertebrae. (**b**) Examples of the different grey to white matter ratios of different spinal segments. (**c**) Diagram illustrating how sensory information is brought to the spinal cord via the dorsal roots and motor information is sent to the muscles via the ventral roots, joining to form the spinal nerve. (**d**) Rexed laminae of neurons in the grey matter at C7, L3, and L7. Taken from Jankowska (2016).

Development of distinct neuronal subtypes

In walking mammals such as rodents and humans, the spinal CPG is located within cervical and lumbar centres that innervate the limbs (Grillner, 1975). The CPG is comprised of multiple classes of interneurons that modulate motor neuron output (Goulding, 2009). These interneuron classes are functionally diverse and release a variety of modulatory transmitters that help ensure the production of flexible and adaptable motor output (Miles and Sillar, 2011).

The discovery of the genetic programme for embryonic patterning of the spinal cord allowed researchers to pinpoint genetic markers for specific cell subtypes, allowing further scrutiny of the individual cell subtypes involved in the vertebrate central pattern generator (Fig. 5). Neuronal identity in the spinal cord is determined by two morphogen gradients (Lee and Jessell, 1999; Jessell, 2000). The notochord and the floor plate produce the morphogen Sonic hedgehog (Shh) (Jessell, 2000; Shirasaki and Pfaff, 2002), while the opposing epidermis and roof plate produce bone morphogenic proteins (BMPs) (Lee and Jessell, 1999; Jessell, 2000). These two secretion points create a dorsoventral concentration gradient of these two signalling molecules along the transverse spinal cord. Different combinations of Shh and BMP along this gradient activate the expression of varying homeodomain transcription factors. Activation of the homeodomain transcription factors then results in the formation of discrete dorsoventral progenitor domains. Within these domains, different classes of embryonic neurons are generated.

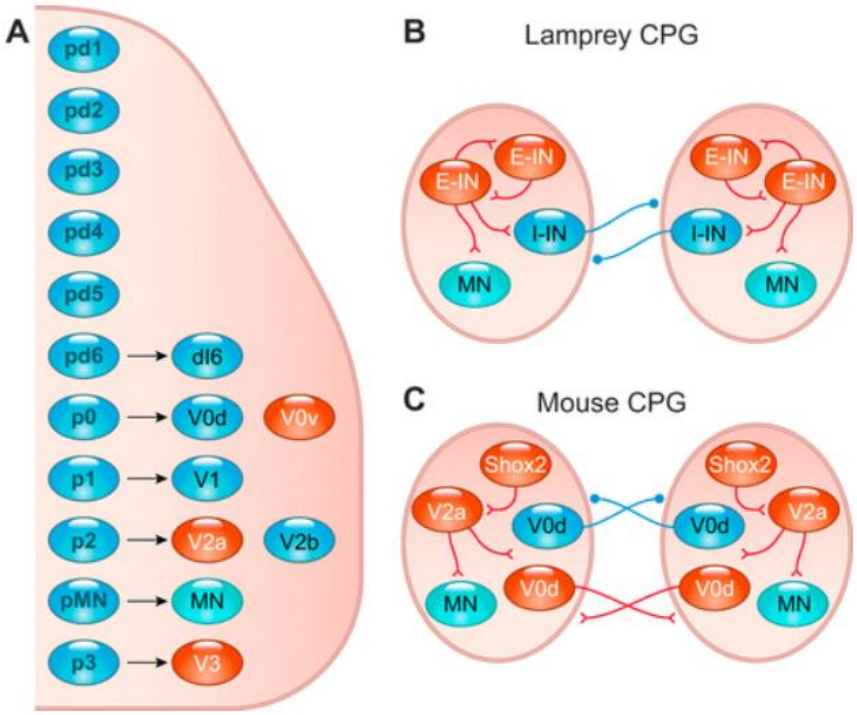

Figure 5. The spinal neurons involved in the control of locomotion. (**A**) Schematic detailing the dorsoventral distribution of progenitor domains (pd) and their resulting neuronal subtypes in the developing mammalian spinal cord. Six dorsal (pd1-pd6) and five ventral (p0-p3 and pMN) progenitor domains give rise to several different interneuron populations and motor neurons. (**B**) The lamprey central pattern generator with the neuron subtype equivalents colour coded as shown in **A**. (**C**) The mouse central pattern generator with the same colour coding at **A** and **B**. Taken from Grillner and Manira (2019).

In the dorsal horn, six progenitor domains generate six classes of dorsal neurons (dI1-dI6) and two classes of dorsal interneurons (Goulding *et al.*, 2002; Gross, Dottori and Goulding, 2002; Müller *et al.*, 2002). In the ventral horn, five progenitor domains give rise to the motor neurons and four classes of interneurons. These interneurons, divided into V0, V1, V2, and V3, are thought to be essential central pattern generating interneurons, as well as the dorsally-located dI6 interneurons which are also thought to contribute to core CPG output in mice (Matise *et al.*, 1997; Saueressig, Burrill and Goulding, 1999; Jessell, 2000; Moran-Rivard *et al.*, 2001; Pierani *et al.*, 2001; Goulding *et al.*, 2002; Shirasaki and

Pfaff, 2002; Al-Mosawie, Wilson and Brownstone, 2007; Lundfald *et al.*, 2007; Peng *et al.*, 2007; Zhang *et al.*, 2008). Each interneuron class exhibits a unique phenotype and transcription-factor expression.

V0 interneurons are commissural neurons expressing transcription factor Dbx1 (Pierani *et al.*, 2001). They can be divided into two subtypes, ventral V0 neurons ($V0_V$) and dorsal V0 neurons ($V0_D$). $V0_V$ neurons also express Evx1 and are glutamatergic, whilst $V0_D$ are GABAergic/glycinergic (Moran-Rivard *et al.*, 2001). Both populations are involved in the coupling of the hindlimbs and thus producing left-right alternation during walking, as isolated spinal cords from $Dbx1^{-/-}$ mice exhibit periods of synchronous hopping-like activity (Lanuza *et al.*, 2004). Although $Dbx1^{-/-}$ mice do show some periods of retained left-right alternation so they cannot be solely responsible (Lanuza *et al.*, 2004). The earlier mentioned dI6 neurons are thought to assist in securing this left-right alteration (Gross, Dottori and Goulding, 2002; Müller *et al.*, 2002; Lanuza *et al.*, 2004).

A small proportion of V0 interneurons expressing transcription factor paired-like homeodomain 2 (Pitx2) have been identified. They can be subdivided into cholinergic ($V0_C$) and glutamatergic ($V0_G$) subtypes (Zagoraiou *et al.*, 2009). These subpopulations are not involved in left-right alternation or flexor-extensor coordination like the other V0 interneurons. Instead, $V0_C$ interneurons modulate the amplitude of motor output (Zagoraiou *et al.*, 2009; Nascimento *et al.*, 2020). The functional role of $V0_G$ interneurons remains undetermined, but they do not appear to contribute to the generation or modulation of motor output (Nascimento *et al.*, 2020).

V3 are excitatory commissural neurons identified by the expression of Sim-1 and play an important role in producing symmetrical output from the spinal cord (Zhang *et al.*, 2008).

V1 interneurons are ipsilaterally projecting inhibitory neurons expressing transcription factor En1 (Matise *et al.*, 1997; Saueressig, Burrill and Goulding, 1999; Wenner, O'Donovan and Matise, 2000; Higashijima *et al.*, 2004; Li *et al.*, 2004). Their role appears to be in setting the speed of locomotion, although there is also evidence for their involvement in flexor-extensor alternation (Gosgnach *et al.*, 2006; Zhang *et al.*, 2014). V2 interneurons can be split into ipsilateral excitatory and inhibitory

subpopulations (Al-Mosawie, Wilson and Brownstone, 2007; Lundfald *et al.*, 2007; Peng *et al.*, 2007). Excitatory V2a neurons are identified by the transcription factor Chx10 and contribute to left-right alternation (Crone *et al.*, 2008; Zhong *et al.*, 2010). Inhibitory V2b neurons express Gata2/3 and contribute to flexor-extensor alternation along with V1 (Zhang *et al.*, 2014).

And finally, the pMN domain results in new-born motor neurons expressing transcription factor Hb9, which can differentiate into visceral or somatic motor neurons which innervate the muscles (Lee and Jessell, 1999; Jessell, 2000).

Neuromodulation of spinal locomotor networks

As discussed, it is essential that motor output be readily adaptable to fit ever-changing environmental requirements. One method by which this output is adapted is via modulation of the locomotor network by several extrinsic and intrinsic modulators. Extrinsic modulators are produced by descending inputs from higher brain centres such as the brainstem and cortex. The extrinsic modulators with the most significant effect on the spinal locomotor CPG are 5-hydroxytryptamine (5-HT or serotonin), noradrenalin (NA), and dopamine (DA). I will discuss briefly the neuromodulatory effects of 5-HT and DA as they will be most pertinent to this thesis.

Spinal 5-HT originates from the raphe nuclei in the brainstem and the parapyramidal region (Lakke, 1997). Many different spinal cell types, including both motor neurons and a number of different classes of interneurons, are targets for 5-HT (Alvarez *et al.*, 1998; Carr, Pearson and Fyffe, 1999; Hammar *et al.*, 2004; Wilson *et al.*, 2005; Al-Mosawie, Wilson and Brownstone, 2007; Noga *et al.*, 2009). 5-HT has been shown to activate spinal locomotion in a number of species. 5-HT affects ongoing locomotor activity by modulating motor neurons and last order interneurons to determine the magnitude and rhythmicity of motor output, as well as timing and co-ordination of said output (Miles and Sillar, 2011).

Spinal DA arises from the hypothalamic A11 region (Skagerberg and Lindvall, 1985). The descending inputs from this region are found throughout the ventral horn of the spinal cord (Zhu *et al.*, 2007). Dopamine is less effective at initiating locomotion than 5-HT (Barbeau and Rossignol, 1991; Kiehn and Kjærulff, 1996; Barrière, Mellen and Cazalets, 2004), but still has a significant neuromodulatory effect. In cats, dopamine increases the amplitude of flexor-related locomotor activity (Barbeau and Rossignol, 1991), whilst in rodents, application of dopamine reduces the frequency and increases the amplitude of locomotor bursts (Whelan, Bonnot and O'Donovan, 2000; Barrière, Mellen and Cazalets, 2004; Gordon and Whelan, 2006). This suggests that dopamine is largely a modulator of motor neurons only in cats but may modulate both motor neurons and interneurons in rodents.

Intrinsic modulators arise from sources within the spinal cord and act locally to modulate neural activity. Examples of these transmitters include glutamate, GABA, acetylcholine, purines, and nitric oxide. These transmitters conventionally act via fast ionotropic receptors but can also activate metabotropic receptors and produce varying neuromodulatory effects on motor output (Miles and Sillar, 2011). For example, GABA is produced from spinal inhibitory interneurons and reduces burst frequency and amplitude of locomotor output (Bertrand, 1999). Acetylcholine is released from interneurons throughout the dorsal and ventral horn (Oguz Kayaalp and Neff, 1980) and can increase neuronal excitability to modulate motor output (Kiehn, Johnson and Raastad, 1996; Jordan *et al.*, 2008).

The role of the sodium-potassium pump current in mammalian motor control

Neuromodulators change the electrical properties of integral neurons within the motor circuits and the synaptic connections between them, producing circuit adaptability. Said changes are typically mediated by the opening and closing of ion channels in the cell membrane. For example, dopamine increases the excitability of neurons within motor circuits by modulating Ca^{2+}-dependent K^+ currents

(Han *et al.*, 2007). However, when membranous ion channels are opened, the cell experiences decreased input resistance, resulting in the shunting of incoming synaptic input. This decrease in synaptic input would decrease the responsiveness and thus the activity of the neurons and the neuronal network. The modulation of membrane pump activity, such as the sodium-potassium pump, is an enticing alternative strategy as pump activity does not alter input resistance and, therefore, maintains the cell's responsiveness after periods of activity. As excitability can be affected for several seconds to tens of seconds, modulation of pump activity also presents a different time scale on which the cells and neuromodulation can function.

Building upon many years of invertebrate research into the role of sodium pump-mediated hyperpolarisations in rhythmic circuits, a recent role for the sodium pump in the dynamic regulation of spinal motor circuits has been presented across multiple animal models (Fig. 6). In *Drosophila melanogaster* larvae, prolonged high-frequency action potential firing of motor neurons in the nerve cord results in an afterhyperpolarisation lasting tens of seconds – far longer than the canonical 'slow' afterhyperpolarisation frequently observed after short bouts of firing (Pulver and Griffith, 2010). A remarkably similar afterhyperpolarisation has also been observed in *Xenopus laevis* tadpole spinal motor neurons (Zhang and Sillar, 2012; Zhang *et al.*, 2015)and neonatal mouse lumbar motor neurons (Picton *et al.*, 2017). These hyperpolarisations are prolonged (lasting at least 20 seconds) and of considerable magnitude (>5mV change from resting potential) and thus have been termed 'ultra-slow' afterhyperpolarisations, or 'usAHPs'. Due to the length of the hyperpolarisation, the underlying mechanism is likely to be NKA-mediated. There are also no changes in conductance before, during, or after the usAHP, suggesting it is likely produced by the activity of a membrane pump as opposed to the opening and closing of ion channels (Fig. 6). And indeed, the usAHP was found to be reduced, if not completely abolished, by the application of the cardiac glycoside ouabain. As sodium-potassium pump function relies on the accumulation of intracellular sodium ions that follows repetitive firing, blocking fast sodium channels with tetrodotoxin (TTX) and thereby preventing action potential generation was also found to reduce or completely abolish the usAHP in these models. There is

currently no known pharmacological activator of the sodium-potassium pump. Still, the pump may be indirectly activated by increasing the concentration of intracellular sodium, which can be achieved via the application of the sodium ionophore monensin. Monensin converted dynamic usAHPs into tonic hyperpolarisations, presumably due to NKA activity remaining high in response to the continuous influx of sodium ions into the cell (Picton *et al.*, 2017). The sodium-potassium pump cannot 'switch off', and thus, the membrane potential cannot depolarise back to its prior resting point.

The remarkable similarities of these phenomena across multiple phylogenetically disparate species suggests an essential physiological role for the usAHP that has been highly conserved throughout evolution. As the sodium-potassium pump is ubiquitously expressed and it is known that the pump mediates the usAHP, it may be surprising to discover that not all spinal cord neurons have been found to exhibit an usAHP. There is currently an emerging hypothesis that the heterogeneous distribution of the usAHP may be due to the heterogeneity of the subunit isoform expression in the sodium pump. With our understanding of the different functional roles of the different α subunit isoforms, we may hypothesise that only cells expressing the α3 subunit isoform, with its low affinity for intracellular sodium and dynamic role, may produce an usAHP. There is evidence to support this theory, as the different α subunit isoforms are differentially sensitive to ouabain, with the α3 isoform being selectively blocked with low drug concentrations (1-3μM). Picton and colleagues (2017) showed that the usAHP is significantly reduced with the application of 1-3μM ouabain. Similarly, the usAHP was found to be abolished entirely with the application of 1-3 μM ouabain in the tadpole (Zhang and Sillar, 2012). Picton and colleagues (2017) characterised the distribution of the usAHP in the neonatal mouse as being present in approximately 40% of motor neurons, 25% of unknown interneurons, and approximately 60% of Pitx2 interneurons. Pitx2 interneurons are a subtype of V0 interneurons that are thought to contribute to locomotor control with activity that is phase-locked to motor neuron output (Zagoraiou *et al.*, 2009). Similar distributions were observed in *Xenopus* tadpoles, with 40% of motor neurons and 30% of interneurons displaying usAHPs (Zhang and Sillar, 2012).

The functional importance of this heterogeneous distribution remains unclear. However, it can be said that there may be an obvious broader explanation as to why all spinal cord neurons do not express the usAHP. Picton and colleagues (2017) suggest that, as many spinal cord neurons form parts of the motor circuits that control movement, it may be catastrophic for there to be a homogeneous distribution of cells capable of producing an usAHP. As the usAHP can be as long as one minute in duration, if all cells were to be capable of undergoing such a long hyperpolarisation, the probability that several critical neurons in the functioning of the circuit may be rendered inactive simultaneously increases. For behaviours such as locomotion, the inability to execute appropriate locomotor actions in situations such as escaping from a predator would be fatal. In this sense, said heterogeneous distribution may thereby act as a safeguard against total circuit failure.

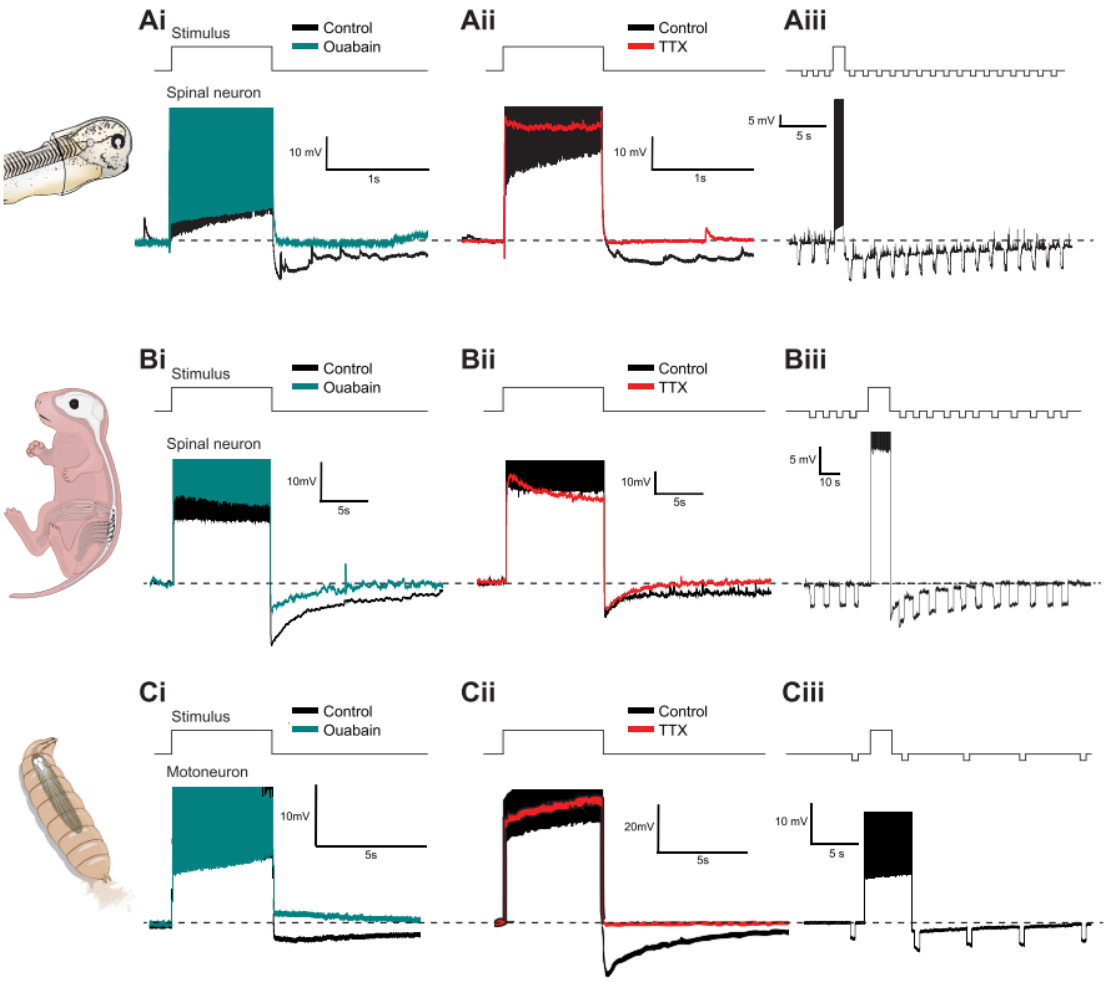

Figure 6. A comparison of the sodium-potassium pump-generated ultra-slow afterhyperpolarisation (usAHP) across animal models. (**Ai**) The usAHP is reduced or abolished with the application of the sodium-pump blocker ouabain. (**Aii**) The usAHP is sodium dependent as it is abolished by the application of Na^+ channel blocker TTX. (**Aiii**) There are no changes in conductance before, during, or after the usAHP, suggesting that it is not caused by the opening and closing of ion channels but instead a membrane pump. (**B**) The experimental outline as described in **A** in the neonatal mouse. (**C**) The experimental outline described in **A** in *Drosophila melanogaster*. Taken from Picton, Zhang and Sillar (2017).

Picton and colleagues further examined the role of the pump and the pump-mediated usAHP in motor network output through a number of preparations and paradigms. First, they utilised the canonical drug-induced fictive locomotor preparation (Fig. 7). In this preparation, a cocktail of drugs made up of DA, 5-HT, and *N*-methyl-D-aspartic acid can be applied to an isolated spinal cord preparation. The

purpose of this cocktail is to mimic descending input from the locomotor regions of the brain and, when applied, the spinal cord will begin to produce robust alternating bursts of ventral root activity that follows the expected rostral-caudal gradient of excitability of the lumbar cord. This 'fictive locomotion' allows insight into the effect of different drugs or environmental conditions at the spinal cord level that may translate into locomotor behaviour that might be seen in a full animal, without the confounding input from higher brain centres. When the sodium-potassium pump blocker ouabain was applied to this preparation (Fig. 7), the frequency of locomotor bursts increased in a dose-dependent manner. If the sodium-potassium pump plays a role in setting the frequency of this rhythm, it is presumably via the production of the usAHP. Suppose the pump is blocked and cannot produce this hyperpolarisation. In that case, more neurons within the motor network are more likely to be depolarised and therefore fire more frequently, translating into an increased frequency of motor neuron output via the ventral roots. The converse is also true: burst frequency decreases when you indirectly increase pump activity in this preparation via monensin application.

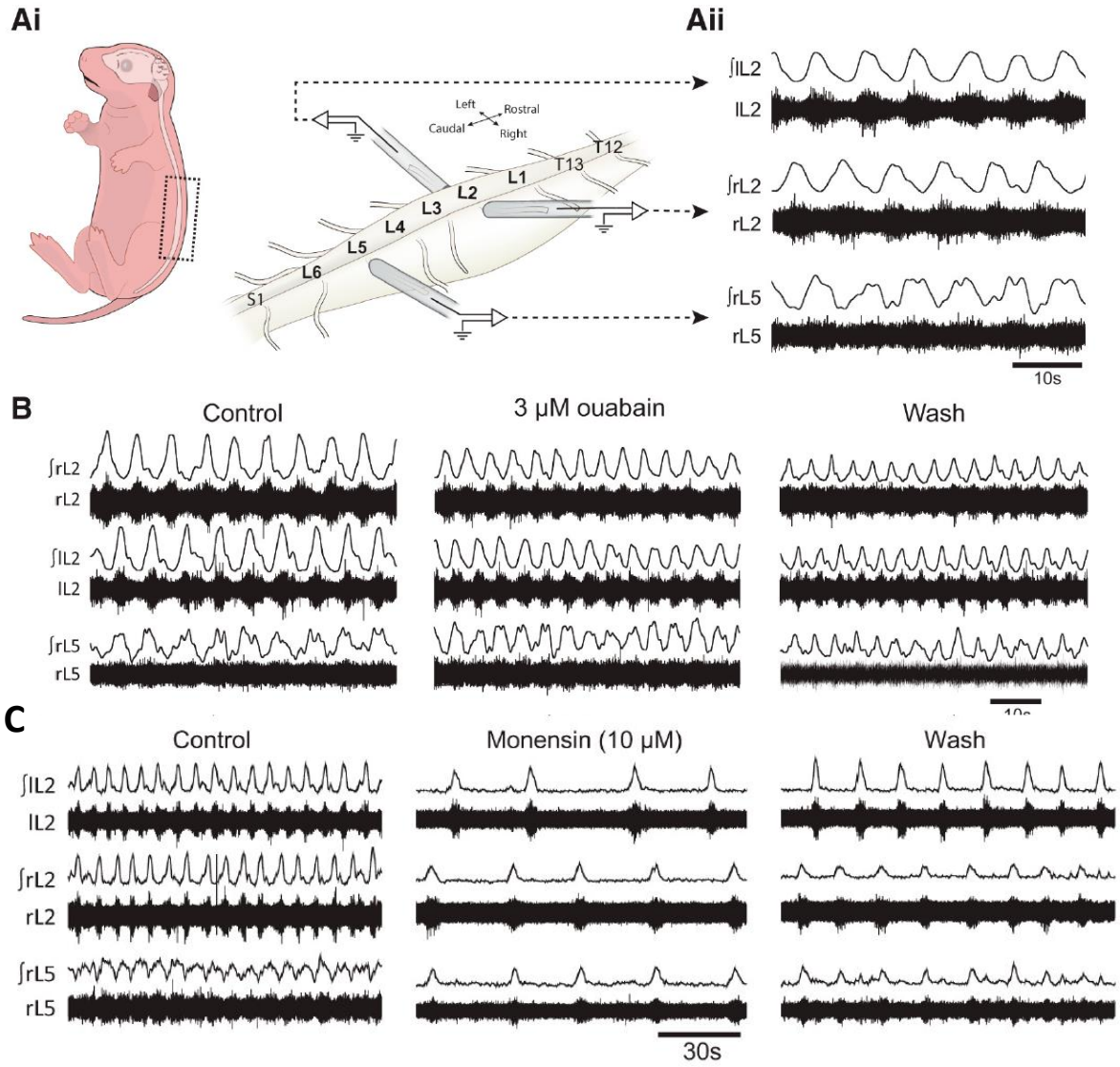

Figure 7. The sodium-potassium pump plays a role in setting the frequency of drug-induced rhythmic bursting. (**Ai**) Fictive locomotor output can be recorded from the ventral lumbar roots of an isolated spinal cord with the application of dopamine, serotonin, and N-methyl-D-aspartic acid. (**Aii**) Rhythmic bursts alternate between the left and right ventral roots and show a rostral-caudal delay associated with alternating flexor-extensor activity. (**B**) Application of the sodium-potassium pump blocker ouabain increases the frequency of these locomotor-like bursts, presumably through the reduction in the size of the usAHP. (**C**) Activation of the sodium-potassium pump via application of the sodium ionophore monensin has the opposite effect, slowing down rhythmic bursting, presumably through an increase in the size of the usAHP. Modified from Picton *et al.* (2017).

To further support this role for the sodium-potassium pump in motor output, Picton and colleagues repeated these experiments using a potentially more physiologically realistic stimulation method as opposed to the locomotor cocktail. In these experiments, sensory stimulation in the form of electrical current pulses was applied to a lumbar dorsal root to evoke brief episodes of locomotor-like activity (Fig. 8). The results were similar, with ouabain increasing the frequency of these sensory-induced locomotor bouts and monensin decreasing the frequency. These data show a role for the sodium-potassium pump in the modulation of motor output, presumably via changes in the usAHP.

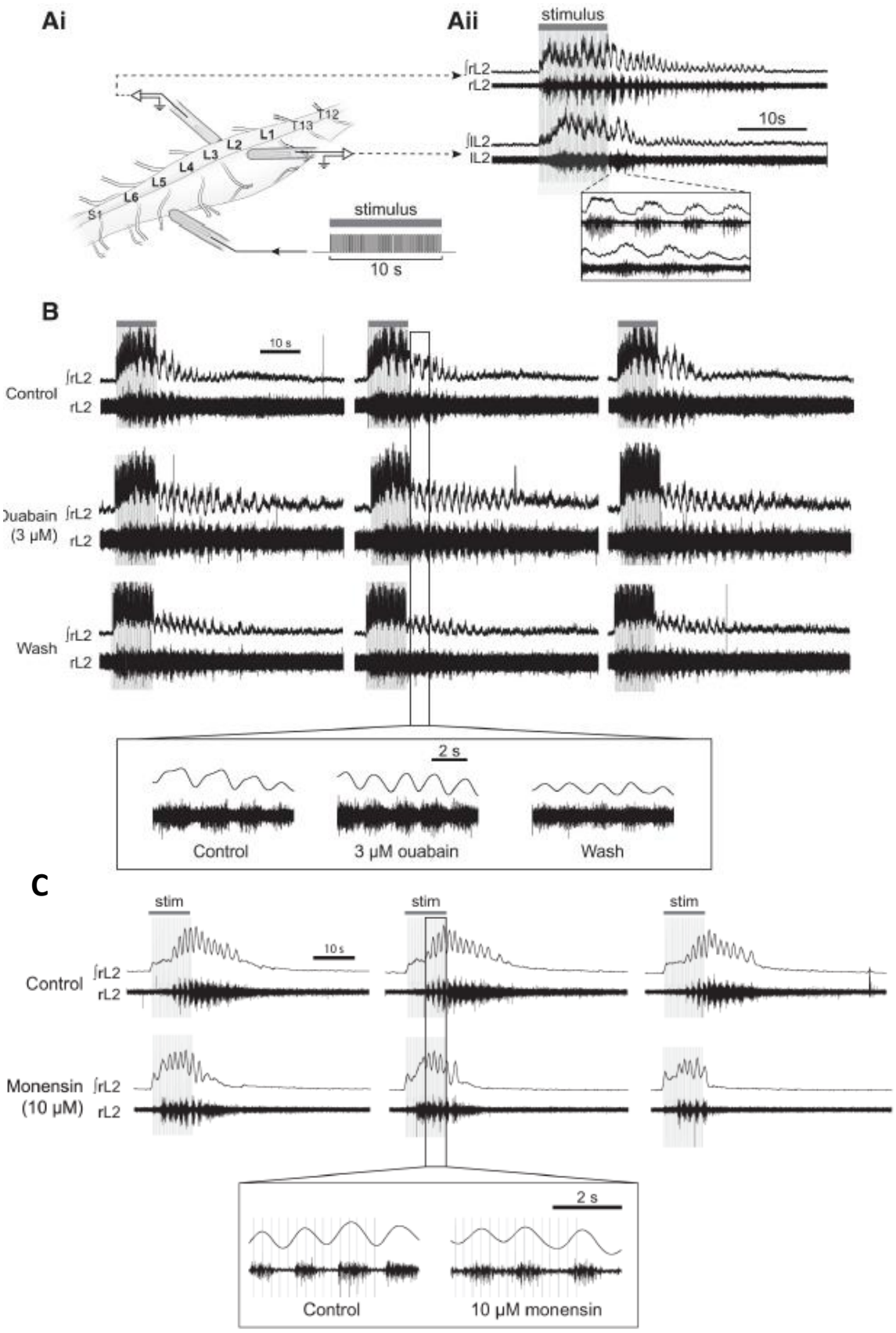
Ai
Aii
stimulus
∫rL2
rL2
∫lL2
lL2
10s
T12
T13
L1
L2
L3
L4
L5
L6
S1
stimulus
10 s
B
10 s
Control
∫rL2
rL2
Ouabain
(3 μM)
Wash
2 s
Control
3 μM ouabain
Wash
C
stim
10 s
Control
Monensin
(10 μM)
2 s
Control
10 μM monensin

Figure 8. The sodium-potassium pump plays a role in setting the frequency of sensory-evoked locomotor-related activity. (Ai) Sensory-evoked locomotor-related activity can be evoked through the application of an electrical stimulus to a dorsal lumbar root. (**Aii**) After the application of the sensory stimulus, left-right alternating locomotor-related activity can be recorded from the ventral lumbar roots. (**B**) Application of the sodium-potassium pump blocker ouabain increases the duration and frequency of the sensory-evoked locomotor-related bursts, presumably through a reduction in the usAHP produced by the pump. (**C**) Activation of the sodium-potassium pump via application of the sodium ionophore monensin has the opposite effect, decreasing both the duration and frequency of the sensory-evoked locomotor-related bursts, presumably through an increase in the size of the usAHP. Modified from Picton *et al.* (2017).

In terms of its physiological role, the sodium-potassium pump may act as a form of 'short-term memory' within the locomotor system of *Xenopus* tadpoles (Zhang and Sillar, 2012) and neonatal mice (Picton *et al.*, 2017). As the usAHP acts as negative feedback for neuronal excitation, it inherently acts as a sort of memory of previous circuit activity. In the tadpole, when the intervals between evoked swim bouts were shorter in duration than the length of the usAHP, the second swim bout was seen to be shorter, slower, and weaker. This function of the sodium-potassium pump and the usAHP as a regulator of network output is further emphasised when the pump is blocked, causing the tadpole to swim almost indefinitely, unable to regulate its network activity. Similar results were also found in neonatal mice, where subsequent bouts of sensory-evoked locomotor-related activity were affected by the interval between episodes being shorter than one minute (Picton et al., 2017) – a relationship that is also lost with the application of ouabain and the subsequent blocking of the sodium-potassium pump.

Picton and colleagues suggest that the usAHP prevents motor fatigue by preventing over-stimulation of the cell via this eloquent explanation of the physiological significance of short-term motor memory:

"The swim durations and inter-episode intervals involved may seem short anthropomorphically (tens of seconds) but need to be scaled to be appreciated from a human perspective and in the broader context of locomotion. If we treat a single tail undulation as equivalent to one human stride, then a typical 2-min episode of 20-Hz swimming (~2,400 swim cycles) could be considered broadly

equivalent to a 5-km sprint for a human (assuming a typical stride length of ~2 m). This distance could comfortably be covered in around 30 min, but imagine resting only for a minute before being stimulated to sprint again while still fatigued; the runner is unlikely to get as far, or locomote at the same speed, as it could from a well-rested start."

There is well-documented evidence for a central mechanism for fatigue (reviewed in Gandevia, 2001), as well as evidence that this central mechanism involves an activity-dependent reduction in motor neuron activity which very well could be produced by the ultra-slow afterhyperpolarisation (Ranieri and Di Lazzaro, 2012; Rossi, Rossi and Ginanneschi, 2012). While a role for the sodium pump in human fatigue has not yet been determined, human motor axons have been shown to display a similar Na^+- and activity-dependent hyperpolarisation as has been described by Pulver, Zhang, and Picton (Vagg *et al.*, 1998; Kiernan, Lin and Burke, 2004). These data strongly support a role for the sodium-potassium pump in fatigue during human locomotion, which proposes interesting avenues of biomedical research as fatigue symptoms and other motor symptoms present in many neurological disorders.

The Sodium-Potassium Pump and Disease

Due to the essential homeostatic role of the sodium-potassium pump, pump dysfunction can have catastrophic pathophysiological consequences.

The catalytic α subunit of the sodium-potassium pump is most susceptible to damage, largely due to much of its structure being exposed to the reducing environment of the cytoplasm as well as its large number of oxidisable groups (Kim and Akera, 1987; Mense, Stark and Apell, 1997). As far as I am aware, there are currently no reported diseases associated with mutations of the β or FXYD subunits.

One organ that relies heavily on the potassium and sodium gradients to function is the heart. The α subunit isoforms expressed in the heart vary from species to species, but all three are expressed in the human heart. Therefore, it is not surprising that a reduction in sodium-potassium pump expression is observed in cases of heart failure (Schwinger *et al.*, 1999; Borlak and Thum, 2003).

Due to the vital importance of potassium and sodium gradient in all organs, perturbation in sodium-potassium pump activity has been implicated in many other pathological conditions, including cancer (Durlacher *et al.*, 2015) and diabetes (Vague *et al.*, 2004). The sodium-potassium pump is even a tempting pharmacological target for diseases not necessarily associated with its dysfunction. Studies of numerous respiratory viruses, including even SARS-CoV-2, have shown that the sodium-potassium pump can be an enticing drug target for treating disease. The pumps have many signalling targets, including Src, necessary for viral replication (Souza e Souza *et al.*, 2021).

However, there is no physiological system more reliant on the sodium-potassium pump than the nervous system, in which pump dysfunction can be found in several disorders.

Neurological disorders involving mutations in α1-NKA and α2-NKA

ATP1A1 mutations have been reported in a range of diseases, including Charcot-Marie-Tooth disease, also known as hereditary motor and sensory neuropathy; one of the most commonly inherited neurological disorders caused by repeated cycles of myelin sheath demyelination and remyelination of the peripheral nerves (Lassuthova *et al.*, 2018; He *et al.*, 2019). Patients with *de novo ATP1A1* mutations present with a varying combination of developmental delay, poor executive functioning, learning and memory impairment, seizures, and disordered sleep (Schlingmann *et al.*, 2018; Stregapede *et al.*, 2020; Lin *et al.*, 2021). *ATP1A1* mutations are also linked to aldosterone-producing adenomas – a form of hypertension (Gomez-Sanchez, Kuppusamy and Gomez-Sanchez, 2015).

Mutations in *ATP1A2* are most commonly associated with Familial Hemiplegic Migraine 2 (FHM2), a rare migraine subtype with aura, motor, and sensory weaknesses (Clausen, Hilbers and Poulsen, 2017; Pelzer *et al.*, 2017). The pathology of FHM2 is likely due to a reduced rate of glutamate and potassium clearance (Capuani *et al.*, 2016) since α2-NKA is expressed in astrocytes only. *ATP1A2* mutations are rarely associated with severe phenotypes, unlike the *ATP1A3* paralog. However, a novel *ATP1A2* mutation has recently been found in two patients presenting with severe stepwise regression, paralysis, epilepsy and persistent motor deficits (Calame *et al.*, 2021). While α2-NKA mutations will only affect astrocytes, the reduced clearance rate of extracellular potassium will lead to activation of the neuronal α3-NKA, and thus, impaired α2-NKA can also impact neuronal functioning.

Neurological disorders involving mutations in the α3-NKA

The involvement of *ATP1A3* gene mutations in rare neurological disorders seen in humans was established relatively recently by de Carvalho Aguiar and colleagues in 2004. Disorders related to *ATP1A3* mutations represent a phenotypic continuum. Different mutations result in a spectrum of

established disorders, all with overlapping symptoms that vary in severity, progression, and age of onset (Sweney, Newcomb and Swoboda, 2015). However, due to this phenotypic spectrum of *ATP1A3* disorders, Sival et al. (2018) have cautioned against drawing overly exact phenotype-genotype relationships.

ATP1A3 mutations are pathological via a reduction in catalytic activity and thereby inability to generate pump-mediated currents in neurons. This occurs via several pathways, including reduced Na^+ or K^+ affinity, over-inhibition of action by K^+, the inability of the protein to undergo a conformational change, or overall reduced protein expression (de Carvalho Aguiar *et al.*, 2004; Heinzen *et al.*, 2012; Kirshenbaum *et al.*, 2013; Toustrup-Jensen *et al.*, 2014; Weigand *et al.*, 2014; Holm *et al.*, 2016; Simmons *et al.*, 2018; Tranebjærg *et al.*, 2018; Roenn *et al.*, 2019).

Mutations that result in the neonatal onset of disease are considered to be the most severe, such as polymicrogyria (PMG) and alternating hemiplegia of childhood (AHC) (Sweadner *et al.*, 2019). As evidence of the novelty of these *ATP1A3*-related disorders, *de novo* familial mutations in *ATP1A3* were only found in patients with a severe form of PMG in 2021 (Miyatake *et al.*, 2021; Smith *et al.*, 2021; Vetro *et al.*, 2021). Patients with PMG experience epilepsy and a global developmental delay. PMG mutations include D801N, the most common mutation in AHC (Panagiotakaki *et al.*, 2015).

AHC is the most common *ATP1A3*-related disorder, with 1 in 1,000,000 (Neville and Ninan, 2007) to 1 in 100,000 children (Hoei-Hansen *et al.*, 2014) affected. AHC is characterised by sudden episodes of paralysis of one half of the body (hemiplegia) or both sides of the body. Other variable clinical features include abnormal eye movements, involuntary twitching or writhing (choreoathetosis), and involuntary muscle contractions that result in slow, repetitive movements or abnormal postures (dystonia) (Bourgeois, Aicardi and Goutières, 1993; Panagiotakaki *et al.*, 2010; Rosewich, Baethmann, *et al.*, 2014). Epileptic seizures also occur in approximately half of AHC patients (Panagiotakaki *et al.*, 2010; Uchitel *et al.*, 2019), and almost all patients show signs of cognitive impairment (Sweney *et al.*,

2009; Panagiotakaki *et al.*, 2010). Hemiplegic episodes are often triggered by physical or psychological stressors (Sweney *et al.*, 2009).

Following on in order of decreasing severity and increasing age of onset, CAPOS syndrome (cerebellar ataxia, areflexia, pes cavus, optic atrophy, and sensorineural hearing loss) is another *ATP1A3*-related disorder that can present typically up to about five years of age. Patients present with fever-induced episodes where the patient cannot coordinate balance or gait (cerebellar ataxia), progressive optic atrophy and sensorineural hearing loss, decreased muscle tone, and loss of deep tendon reflexes (areflexia). Foot deformities (pes cavus) also affect approximately 30% of patients (Duat Rodriguez *et al.*, 2017). Symptom onset begins with one to three fever-induced episodes of ataxia (Duat Rodriguez *et al.*, 2017). All reported cases of CAPOS to date are caused by a single missense mutation, E818K (Demos *et al.*, 2014; Rosewich, Weise, *et al.*, 2014; Heimer *et al.*, 2015; Potic, Nmezi and Padiath, 2015; Maas *et al.*, 2016; Duat Rodriguez *et al.*, 2017; Han *et al.*, 2017; Stenshorne *et al.*, 2019).

The least severe *ATP1A3*-related disorder with the latest age of onset is Rapid-Onset Dystonia-Parkinsonism (RDP). RDP was the first disorder associated with an *ATP1A3* mutation (de Carvalho Aguiar *et al.*, 2004). RDP is characterised by the sudden onset (hours to weeks) of dystonia with parkinsonism features such as tremor, slowed movement (bradykinesia), muscle rigidity, and impaired posture and balance. Symptoms initially appear in the arms or legs in most RDP patients (Haq *et al.*, 2019). Symptom onset most commonly occurs in adolescence and, similarly to AHC and CAPOS, is triggered by a physical or environmental stressor such as heat exhaustion, fever, exercise, or childbirth (Dobyns *et al.*, 1993; Brashear *et al.*, 2007). Despite the parkinsonism features, patients do not show signs of nigral degeneration (Oblak *et al.*, 2014), and dopaminergic medication is ineffective at improving symptoms (Brashear *et al.*, 2007). Currently, RDP neuropathology includes atrophy/neuronal loss in parts of the brain stem and cerebellum involved in regulating movement (Oblak *et al.*, 2014).

The exact mechanism by which the physical or psychological trigger leads to symptom onset in these conditions is currently not well understood, and, sadly, patients appear to be unresponsive to standard drugs for central nervous system disorders such as levodopa, calcium channel blockers, or benzodiazepines (Neville and Ninan, 2007; Brashear *et al.*, 2012).

Beyond these few well-described disorders, *ATP1A3* mutations have been discovered in individuals displaying rare clinical phenotypes, including dystonia, and developmental delays (Prange *et al.*, 2020), as well as individuals experiencing severe infantile seizures (Paciorkowski *et al.*, 2015; Arystarkhova *et al.*, 2019).

ATP1A3 mutations have also been identified in individuals with forms of Autism Spectrum Disorder (ASD) (Chaumette *et al.*, 2018; Takata *et al.*, 2018; Torres *et al.*, 2018) and schizophrenia (Smedemark-Margulies *et al.*, 2016; Chaumette *et al.*, 2018). ASD includes a wide range of neurodevelopmental symptoms not commonly seen in the more canonical *ATP1A3*-related disorders, such as difficulty with social interaction, restricted interests, and repetitive behaviours. Interestingly, the proband carrying the *de novo ATP1A3* mutation first identified in ASD had a record of motor impairment. Schizophrenia is a severe mental disorder associated with hallucinations, delusions, disorganisation of speech and several other cognitive deficits. Schizophrenic patients do sometimes also suffer from movement disorders. Although the link between *ATP1A3* and ASD/schizophrenia requires further study, these cases suggest that *ATP1A3* mutations can not only lead to motor-related symptoms but may also contribute to some neuropsychiatric disorders.

The emerging role of the α3-NKA in neurodegenerative disease

Although not associated with *ATP1A3* mutations directly, recent findings link the α3-subunit to many neurogenerative diseases as it was found that α3-NKA directly interacts with several hallmark pathogenic proteins. These prion-like proteins form aggregations that are trafficked between cells

(Brundin, Melki and Kopito, 2010; Shrivastava *et al.*, 2017; Melki, 2018). Pathogenic proteins such as α-synuclein and amyloid-β are released from one cell and bind to an adjacent cell before being endocytosed into the cytosol, where the protein can amplify further (Brundin, Melki and Kopito, 2010; Melki, 2015, 2017, 2018; Shrivastava *et al.*, 2017; Surmeier *et al.*, 2017). The pathogenic protein interacts with several membrane-associated components during this process (Shrivastava *et al.*, 2017). At the membrane, pathogenic proteins diffuse anomalously and form clusters of aggregated protein. These clusters act as 'diffusion traps' for membrane proteins such as α3-NKA (Renner *et al.*, 2010; Shrivastava *et al.*, 2013, 2015). After exposure of a neuron to α-synuclein, a pathogenic protein associated with Parkinson's Disease, trapping of α3-NKA lead to a clustering of α3-containing pumps across the membrane. This change in the distribution of α3-NKA was associated with a reduced capacity to extrude intracellular sodium levels following a stimulus. The basal intracellular sodium levels before the stimulus, which are set by α1-NKA, were unaffected by exposure to α-synuclein, which suggests the pathogenic protein specifically affects the α3-NKA (Shrivastava *et al.*, 2015).

Interactions have also been discovered between α3-NKA and tau/amyloid-β – two protein aggregates thought to be hallmarks of Alzheimer's Disease. Tau was found to increase α3-NKA turnover (Shrivastava *et al.*, 2019), while amyloid-β exposure reduced the enzyme's activity and increased intracellular Na^+ levels (Ohnishi *et al.*, 2015). Amazingly, when binding to α3-NKA was inhibited, amyloid-β-induced neurotoxicity was found to be reduced in hippocampal cell cultures (Ohnishi *et al.*, 2015). Petrushanko and colleagues (2016) found that β-amyloid bound between the α and β subunits of the sodium-potassium pump in neuroblastoma cells, preventing them from moving towards one another and thus inhibiting the activity of the enzyme. While these studies suggest a role for α3-NKA in Parkinson's and Alzheimer's Disease, how exactly the enzyme contributes to the disease pathology is yet to be determined. While the α3-NKA interactions shown in these studies happen quite early in disease pathogenesis, there is also some evidence for the involvement of α3-NKA in late-stage disease. Reduced immunoreactivity of α3-NKA has been observed in amyloid-β plaques in the hippocampus of transgenic mouse models of Alzheimer's Disease (Dickey *et al.*, 2005). Post-mortem patient studies

have also shown a reduction in α3-NKA mRNA with no change in α1-NKA mRNA in an Alzheimer's patient's brain (Chauhan, Lee and Siegel, 1997).

Dysfunction of α3 subunit-containing sodium pumps is also implicated in disease mechanisms underlying Amyotrophic Lateral Sclerosis (ALS). ALS is a fatal neurodegenerative disease characterised by the death of motor neurons. Of known cases, 10% are familial, whilst 90% are sporadic. Degeneration begins in the motor neurons controlling the muscles of the limbs. It progresses centrally until the motor neurons that control the intercostal and swallowing muscles deteriorate, leading to death via respiratory failure. In some cases, a bulbar onset occurs, which can accelerate the emergence of swallowing issues (Turner *et al.*, 2010). Early symptoms typically include muscle weakness and spasms leading to the inability to control voluntary movement. In patients with limb-onset ALS, initial symptoms typically include awkwardness when walking or running due to the failure to coordinate limb movement, which may cause individuals to stumble during movement.

The disease mechanisms that underlie motor neuron loss in ALS are wide-ranging with considerable overlap. Proposed mechanisms include oxidative stress, mitochondrial dysfunction, neurofilament abnormalities, compromised axonal transport, protein aggregates, non-cell-autonomous death, glutamate-mediated excitotoxicity, and potential RNA processing defects (reviewed in Mejzini *et al.*, 2019). At the cellular level, pathological hallmarks include changes in the excitability of motor neurons and spinal circuits. This is of interest as such changes in excitability resonate with the changes seen when blocking the sodium pump with ouabain, i.e., blocking the pump results in cell hyperexcitability.

More than 50 genes have now been associated with ALS. The most frequently observed pathogenic variants are in *SOD1*, *C9ORF72*, *FUS*, and *TARDBP* (Boylan, 2015). *SOD1* (encoding superoxide dismutase 1) functions by converting superoxide to water and hydrogen peroxide in the body. Loss of *SOD1* activity has been ruled out as a simple cause for the disease; however, misfolding of the protein has been seen to result in a toxic 'gain of function' resulting in cell damage which is not alleviated by alterations in normal *SOD1* activity (Cleveland and Rothstein, 2001; Julien, 2001).

Studies have shown links between *SOD1*-type ALS and dysfunction of the α3 subunit of the sodium pump. Ruegsegger et al. (2016) identified a direct isozyme-specific association between misfolded *SOD1* and α3-NKA, resulting in the impairment of sodium pump activity. The research group showed that mutant *SOD1* expressing motor neurons show changes in excitability from as early as the second postnatal week. Pharmacological inhibition of the α3-NKA worsened the m*SOD1* mouse model disease pathology with changes in the molecular components involved in neuronal transmission observed. Ellis et al. (2003) also observed a decrease in ouabain-sensitive sodium pump activity and an overall decrease in the expression of all α subunit isoforms in the spinal cords of a mutant S*OD1* mouse model. Aggregation of α3-NKA within the cytoplasm of motor neurons has also been observed in mutant *SOD1* mouse models (Martin *et al.*, 2007).

Ruegsegger and colleagues conclude from this pharmacological manipulation, as well as the identified association between m*SOD1* and α3-NKA, and further experimentation showing that altered α3-NKA expression has been observed in the post-mortem spinal cord tissues of patients with both familial and sporadic ALS, that a reduction or complete inhibition of α3-NKA may result in a toxic hyperexcitability which, if prolonged, results in cell hypoexcitability (Devlin *et al.*, 2015). This excitability loss will eventually lead to a collapse of the membrane potential of the motor neurons, contributing to motor neuron death in these disease models.

It is unlikely that such a critical protein is implicated in multiple neurodegenerative diseases simply by chance. These studies suggest aggregation with pathogenic proteins such as those discussed here may lead to redistribution of α3-NKA across the membrane or a reduction of α3-NKA being trafficked successfully to the membrane. These distribution changes throughout the cell may lead to a loss-of-function of the α3-NKA, which very well may contribute to cell death in these diseases.

As can be seen by the variety of diseases discussed in this general introduction, the pathological consequences of α3-NKA dysfunction are far-reaching and manifest themselves in various clinical

symptoms, including motor dysfunction. With much still to understand about the role of the sodium-potassium pump, more research into its functional significance in both health and disease is essential.

Chapter 1: *The role of α3-NKA in healthy and disordered spinal motor networks*

Chapter 1 contributions:

All experiments were conducted by Francesca Sorrell apart from the behavioural characterisation of the T613M mouse model and the sodium imaging experiments, which were conducted by Evgeny Akkuratov, of the Karolinska Institutet.

Summary

Several neurological disorders are associated with mutations in the *ATP1A3* gene that encodes for the α3 subunit isoform of the sodium-potassium pump (α3-NKA). While these disorders typically present with motor symptoms, little consideration has been given to the involvement of spinal motor circuits in the manifestation of these disorders. However, a growing body of research now suggests that the α3-NKA plays an important role in regulating rhythmically active motor networks in the spinal cord via the production of a pump-mediated ultra-slow afterhyperpolarisation. To address this, we have aimed to establish the contribution of spinal motor circuit pathology to *ATP1A3*-related disorders.

In this chapter I, in collaboration with the Aperia Lab at the Karolinska Institut, I utilised a novel mouse model harbouring the T613M mutation of the *Atp1a3* gene. T613M is a common gene mutation found in patients with the disorder Rapid-Onset Dystonia-Parkinsonism (RDP). RDP is characterised by an abrupt onset of Parkinsonian symptoms and limb dystonia in early adulthood brought about by a physical or psychological trigger. Patients will then typically present with parkinsonism and limb dystonia.

We show that animals with the T613M mutation are hyperactive and hyperambulatory. When examining the potential involvement of spinal motor circuit pathology in this behaviour, we observed a complete lack of usAHPs in T613M-affected lumbar neurons, and a reduced capacity for isolated spinal cords to regulate rhythmic motor output in response to large increases of intracellular sodium. We suggest that this deficiency is caused by a reduced capacity for α3-NKA with the T613M mutation to extrude sodium and therefore maintain sodium homeostasis.

Overall, we provide the first characterisation of the T613M mutation of *ATP1A3* commonly found in patients with RDP as well as a novel role for motor neuron pathophysiology in this disorder.

Introduction

The sodium-potassium pump (NKA) is a ubiquitously expressed membrane protein that regulates cell excitability by exchanging three intracellular sodium ions for two extracellular potassium ions - an active process that is responsible for up to 50% of total brain energy consumption (Erecińska and Silver, 1994). Mammalian neurons express two isoforms of the catalytic α subunit, the ubiquitous α1, and the neuron-specific α3. α1-NKA is thought to be tonically active due to its high affinity for Na^+ and therefore largely responsible for setting the resting membrane potential of the cell. α3-NKA, with its relatively low affinity for Na^+, is thought to be more dynamically active and is responsible for returning intracellular [Na^+] to basal levels following a period of suprathreshold neuronal activity.

The sodium-potassium pump is thought to mediate an activity-dependent hyperpolarisation in a number of species and cell types. At the network level, it has been shown that pump-mediated hyperpolarising currents play a significant role in regulating rhythmically active networks (reviewed in the General Introduction). More pertinent to this thesis, the sodium-potassium pump has also been shown to mediate activity-dependent changes in the locomotor networks of a number of species via a pump-mediated hyperpolarising current termed the ultra-slow afterhyperpolarisation (usAHP) (*Drosophila melanogaster* Pulver and Griffith, 2010; *Xenopus laevis* Zhang and Sillar, 2012; *Mus musculus* Picton *et al.*, 2017). Although *Drosophila* do not share the same α-subunit isoforms as vertebrates, pharmacological experiments suggest a role for α3-NKA in the production of the usAHP in the tadpole and the mouse. Picton and colleagues (2017) showed that, when a low concentration of the cardiac glycoside ouabain is applied (for which α3-NKA has a high affinity), locomotor rhythms become faster and short-term motor memory is lost, presumably because of the abolition of the usAHP in the network of neurons underlying the behaviour. The opposite was seen to be true when the pump is activated indirectly by application of the sodium ionophore monensin, with locomotor rhythms slowing and short-term motor memory becoming enhanced. This is physiologically significant as maintenance of short-term motor memory can be seen to act as a fatigue-prevention mechanism

within the network. As fatigue is a common symptom in neurological disease, further research into the functional significance of the α3-NKA in healthy and disordered spinal motor networks is needed.

Several neurological disorders are associated with mutations in the *ATP1A3* gene encoding the α3-subunit isoform of the sodium-potassium pump. The most reported *ATP1A3*-related disorders are Rapid-Onset Dystonia Parkinsonism (RDP) and Alternating Hemiplegia of Childhood (AHC). Whilst RDP was originally characterised by the abrupt onset of dystonia with parkinsonism features and prominent bulbar findings (Brashear *et al.*, 2007), recent findings from a comprehensive study by Haq and colleagues (2019) suggest a more benign manifestation of symptoms may be more common. These studies indicate that dystonia in the arms and legs may be a prominent symptom and raises the question of whether the manifestations of *ATP1A3* mutations may involve pathophysiology of the motor circuits controlling the limbs.

Previous research conducted into *ATP1A3*-related disorders focused largely on the brain centres thought to be involved such as the cerebellum (Fremont *et al.*, 2014). However, to the best of my knowledge, no research has been conducted into potential pathophysiology of spinal motor circuits in these disorders despite the motor symptoms observed in patients. With the growing body of evidence that the α3-NKA and pump-mediated usAHP play a significant role in the regulation of rhythmic motor output from spinal networks, it is worth considering a potential role for motor neurons and the usAHP in the manifestation of *ATP1A3*-related disorders.

Due to the conserved homology of α3-NKA, mouse models can be utilised to gain transferable knowledge on the role of α3-NKA in health and disease. A number of α3-subunit isoform knockdown/knockout mouse models have been produced to aid in the study of the membrane protein (reviewed in Ng *et al.,* 2021). The location of the mutation that causes the knockdown produces varying symptoms in the mice, not dissimilar to what is observed in patients. Consistently, α3-NKA knockdown/knockout mouse models show motor deficits and hyperactivity, lending further support to the role of the isoform in the control of movement. The observed hyperactivity of α3-NKA

knockdown/knockout mice is particularly interesting as it is what one might expect given our knowledge of the pump-mediated usAHP and its importance to the regulation of rhythmic output. If an α3-NKA mutation were to mimic the pharmacological effects of ouabain, we would expect the dysfunction of the sodium-potassium pump to lead to a lack of usAHPs expressed by the motor neurons innervating the limbs. Picton et al. (2017) showed, at the network level, that pharmacological inhibition of the pump leads to an increase in the frequency of locomotor-related rhythmic activity. One would expect this to translate to hyperambulation in the intact animal, which is indeed what is observed in the mutant animal models.

To probe the significance of the α3-NKA in the regulation of locomotor output in health and disease, I utilised a novel α3-NKA knockdown mouse model harbouring the T613M mutation. The T613M mutation of *ATP1A3* is commonly found in patients with RDP (Barbano *et al.*, 2012). In collaboration with the Aperia Lab at the Karolinska Institutet, we characterised the manifestation of the T613M mutation via a series of behavioral, electrophysiological, and molecular studies.

In this chapter, we show that the T613M mutation causes hyperactivity and hyperambulation in mice. We show that the T613M-affected α3-NKA have a reduced capacity to extrude sodium and thus maintain sodium homeostasis. At the single neuron level, we show that lumbar motor neurons do not exhibit usAHPs but are otherwise comparable to wildtype motor neurons in terms of their physiology. At the network level, we show that the reduction in α3-NKA activity caused by the T613M mutation does not affect canonical drug-induced locomotor rhythms, nor sensory-evoked locomotion. T613M mice also retain short-term motor memory in the same capacity as wildtype mice. These results cast doubt on the previously established significance of the α3-NKA in regulating motor output. However, when the sodium ionophore monensin was applied to T613M isolated spinal cords, a motor deficit was revealed. While wildtype preparations showed a consistent decrease in drug-induced fictive locomotor bursting frequency, T613M-affected preparations did not respond to the sudden increase in intracellular sodium consistently, with some preparations showing a modest decrease and some

showing an opposing increase in burst frequency. These results suggest that, when a challenge is presented to the system, T613M-affected motor networks are less able to restore homeostasis than wildtype motor networks.

Our results characterise the effect of the common RDP mutation for the first time as well as providing a potential novel role for motor neuron pathophysiology in the manifestation of *ATP1A3*-related disorders. These data provide definitive evidence for the α3-NKA mediation of the ultra-slow afterhyperpolarisation. More generally, these data lend support to the fundamental role of α3-NKA in regulating motor output but perhaps bring previous pharmacological data into a more nuanced physiological perspective.

Methods

Animal ethics and husbandry

The following experimental procedures were conducted in accordance with the UK Animals (Scientific Procedures) Act 1986, with approval from the Animal Welfare Ethics Committee (AWEC) of the University of St Andrews in line with UK Home Office regulations. Wild type (WT) neonatal mice used in the following experiments were bred on a C57BL/6 background acquired from Charles River Laboratories (Scotland, UK). T613M *ATP1A3*-knockdown mice were acquired from the Karolinska Institute (Solna, Sweden) and crossed with in-house C57BL/6 mice to heterozygosity. Mice were genotyped using 5'-CGTGAACTTCACCACAGACAACCTT-3' and 5'-GTGGAAGGGAGGAGTTGGAGGAGT-3' primers, along with a restriction step using a MIsl restrictase (Thermo Fisher Scientific, Horsham, UK). Mice were housed in individually ventilated cages maintained at 22°C and 56% humidity with a 12h light-dark cycle. All animals had unrestricted access to food and water. Experiments were performed using heterozygous *T613M* mice and age-matched WT mice aged postnatal day (P)1-10. Due to the difficulty of sexing early postnatal mice, all postnatal experiments include both male and female mice.

Behavioural characterisation of T613M knock-in mouse model

Open field test

Spontaneous locomotor activity was recorded during an open field test. The animal was placed in the centre of the Noldus open field test apparatus and its velocity, total distance traveled, and time spent in the centre area was recorded for 10 minutes. For this test, both sexes were used.

Elevated plus-maze

Anxiety was measured via an elevated plus-maze test. The animal was placed in the centre of the Noldus plus-maze apparatus. Two arms of the plus-maze are walled and two arms are open. Total time spent in the open and closed arms was measured. For this test, only males were used.

Forced swim test

Depression-like behaviour was measured via a forced swim test. The animal was placed in a plastic cylinder with warm (25°C) water for six minutes and the total floating time without active movement was calculated. For this test, only males were used.

Passive avoidance

Memory was tested via a passive avoidance test. The animal was placed into the light compartment of an apparatus which contains light and dark compartments separated by a door. After one minute the door was opened. After the animal moved into the dark compartment, the door was closed behind it and an electrical current was passed through the floor of the dark compartment. This protocol was repeated with the same animal the following day, with the latency of entering the dark compartment taken as a measurement of memory. If the animal had not moved between compartments in over nine minutes, the animal was removed and returned to its home cage. For this test, only males were used.

Pole test

Nigrostriatal function was tested via a pole test. The animal was placed on the top of the vertical pole with its head towards the top of the pole. The animal would then turn on the pole and climb down towards the base. The time taken for the animal to turn, and the time taken for the animal to reach the base of the pole was measured. This test contains one training trial (not calculated) and five testing

trials. The data are presented as the mean of these five testing trials. For this test, both genders were used.

Rotarod

Sensorimotor coordination was measured via an accelerated rotarod test. The animal was placed onto an accelerating rod with an initial speed of five rotations per minute (rpm). After 30 seconds the rotation rate was accelerated to 40rpm for three minutes. This test was repeated three times per day over two consecutive days and the mean of latency to fall was calculated. For this test, both genders were used.

Trigger studies

There are three triggers used in this study: immobilization for one-hour, standing in ice-cold water for five minutes, and alcohol intraperitoneal injection at 2.25 g/kg.

Sodium imaging

Recordings were performed on primary hippocampal cell cultures on day 6-21 *in vitro* (DIV). The cells were transfected two days before imaging with plasmids containing either WT or T613M mutant α3-NKA together with plasmids containing mTurquoise2 (used for identifying transfected cells). Cells were loaded at 37°C with the Na^+-sensitive cytosolic ANG2 (Asante NaTRIUM Green 2, excitation 517nm) in Krebs solution: 110mM NaCl, 4mM KCl, 1mM NaH_2PO_4, 25mM $NaHCO_3$, 1.5mM $CaCl_2$, 1.2mM $MgCl_2$, 20mM glucose, 1% BSA and 20mM HEPES at pH 7.4 for 25 minutes and then placed in a heated chamber for rapid exchange of solutions continuously warmed at 37°C. Low-light level fluorescence imaging was performed on inverted Zeiss Axiovert 200 with a 40× (1.4 NA, oil) objective equipped with

an Andor iXon+ 897 EMCCD camera and with filter cubes selected for ANG2 and mTurquoise2. Cells were imaged during perfusion with aCSF (artificial cerebrospinal fluid): 125mM NaCl, 26mM $NaHCO_3$, 4mM KCl, 1.2mM $MgCl_2$, 1.25mM NaH_2PO_4, 2mM $CaCl_2$, 10mM glucose and was continuously bubbled with carbogen (5% CO_2, 95% O_2) resulting in a pH of 7.4. The K^+-free solution (0 $[K^+]_o$) had the same composition, except that the NaCl and KCl concentrations were 129mM and 0mM, respectively. The NMDA solution had the same composition with the addition of 20µM NMDA. At the end of each experiment, neurons were superfused with Na^+ calibration solutions containing stepwise increasing concentrations of Na^+ (0mM and 15mM) in the presence of 3µM gramicidin, 10µM monensin, and 1mM ouabain. Na^+ calibration solutions contained $[Na^+ + K^+]$ = 165mM, 136mM gluconate, 0.81mM $MgSO_4$, 0.78mM KH_2PO_4, 20mM HEPES, 1.3mM $CaCl_2$, pH adjusted to 7.2 with KOH. Images were analysed and quantified with ImageJ software. Calibrated values from soma and dendrites were analysed as a ratio between transfected and non-transfected neurons to account for variation between experiments.

***In vitro* spinal cord preparation**

Neonatal mice were euthanised via cervical dislocation, decapitated, and eviscerated. Animals were secured to the base of a dissecting chamber filled with dissecting artificial cerebrospinal fluid (aCSF) (equilibrated with 95% oxygen, 5% carbon dioxide, ~4°C). A vertebrectomy was performed, removing the vertebrae covering the spinal cord. The cord was then isolated by separating the cord from the spinal roots with microscissors. Once isolated from the body, any remaining dorsal or ventral roots or connective tissue were trimmed away if preparing slices.

To produce spinal cord slices, the isolated cord was then set in 0.5% agar and immersed in a bath containing dissecting aCSF. A vibratome (Leica VT1200) was used to produce 300µm thick transverse slices of the lumbar region of the spinal cord. Lumbar slices were transferred to a chamber containing recovery aCSF (equilibrated with 95% oxygen, 5% carbon dioxide,) at ~34°C and allowed to recover for

30-45 minutes. Once recovered, the slices were transferred to a chamber containing recording aCSF (equilibrated with 95% oxygen, 5% carbon dioxide) at room temperature and allowed to equilibrate for approximately 30 further minutes before recording.

For whole cord physiology experiments, the spinal cords were dissected in recording aCSF as opposed to dissecting aCSF before being transferred to a recording chamber containing circulating oxygenated recording aCSF ready for experimentation.

Electrophysiological recordings

Whole-cell patch clamp recordings of spinal motor neurons

Spinal lumbar slices were placed in a recording chamber containing aCSF perfused at a continuous rate of ~1mL per minute. Whole-cell patch clamp recordings were made from motor neurons of the ventral horn. Motor neurons were identified by morphology, passive properties, and location within the ventral horn. Lumbar motor neurons are in discrete ventromedial and ventrolateral pools and differ from interneurons in whole-cell capacitance and input resistance (Carlin, Jiang and Brownstone, 2000). Borosilicated glass microelectrodes (2.5-5 MΩ) containing intracellular solution were attached to the membrane of the neurons via a high resistance (>1 GΩ) seal. Suction was applied to rupture the patch of membrane within the seal, allowing the intracellular fluid within the glass microelectrode to become continuous with the inside of the cell. Signals were amplified and filtered with a MultiClamp 700B amplifier (Molecular Devices, Sunnyvale, CA, USA) and acquired at >10Hz using a Digidata 1440A A/D board and pClamp software (Molecular Devices, Sunnyvale, CA, USA). All cells used for experiments showed a resting potential between -50 and -80 mV. Firing output was measured in current-clamp mode with a bias current applied to all cells to maintain a consistent resting membrane potential of -60mV between recordings. Firing output was measured either as a single action potential acquired by injecting a 10ms supramaximal current pulse, a series of 1s square step current pulses

ranging from 50pA to 4000pA, or via a 10s square step current pulse/pulse train (30Hz) applied at an amplitude of ~1.5x rheobase.

Ventral root recordings from whole spinal cords *in vitro*

Isolated spinal cords were secured to the base of a recording chamber so that the ventral roots were accessible. The chamber was then continuously perfused with recording aCSF (~20mL/min; equilibrated with 95% oxygen 5% carbon dioxide gas). Plastic suction electrodes were then attached to either the first or the second ventral lumbar ($L_{1/2}$) root on each side of the spinal cord to record flexor-mediated locomotor-related activity. For sensory-evoked activity recordings, a third stimulating suction electrode was attached to the fifth dorsal lumbar (L_5) root. Isolated spinal cords were allowed to recover for at least 45 minutes post-euthanisation before locomotor-related activity was recorded. Drug-induced locomotor-related activity was evoked via bath application of a dopamine (DA; 50uM), serotonin (5-HT; 10uM), and *N*-methyl-D-aspartic acid (NMDA; 5uM). Locomotor drugs were allowed to circulate until a stable locomotor rhythm was established. 'Stable' rhythms were classified as contralateral alternating ventral root bursts that were consistent in frequency, duration, and amplitude for at least 5 minutes, with rhythmic activity being analysed from the 10 minutes following this stabilisation.

For dorsal root stimulation experiments, isolated spinal cords were allowed to recover for at least 45 minutes post-euthanisation before stimulation was applied. A series of 40 current pulses (4 Hz, 50-100 μA) was then delivered to the L_5 dorsal root via the stimulating electrode at varying time intervals using a Master-8 pulse generator and iso-flex pulse stimulator (Master-9, AMPI, Jerusalem, Israel) in order to evoke short episodes of locomotor-like activity (as in Whelan, Bonnot and O'Donovan, 2000). Application of dopamine (50uM) has been found to stabilise sensory-evoked motor output (Picton *et al.,* 2017) and was therefore added to the recording aCSF after initial baseline protocols were

completed. Dopamine was applied for at least 30 minutes before the aforementioned protocols were repeated.

For the short-term motor memory paradigm, dorsal root stimulation was applied as described above at varying time intervals. A stimulation was applied at two-minute intervals to allow full recovery of the usAHP, after which a stimulation was applied at either 30 seconds or 15 seconds post recovery. After activity had returned to baseline a final stimulation was applied two minutes later to complete one short-term motor-memory 'sweep'. Several sweeps were performed at each time interval before and after the application of 50µM dopamine.

For both drug- and sensory-evoked experiments, signals were amplified and filtered (30-3000Hz; A-M Systems Differential AC Amplifier, Model 1700, Sequim, WA, USA) and then acquired at a sampling frequency of 3 kHz using a Digidata 1440A A/D board and AxoScope software (Molecular Devices, Sunnyvale, CA, USA).

Drugs and Solutions

Dissecting aCSF: 25mM NaCl, 188mM sucrose, 1.9mM KCl, 1.2mM NaH_2PO_4, 10mM $MgSO_4$, 1mM CaCl, 26mM $NaHCO_3$, 25mM glucose and 1.5mM kynurenic acid.

Recovery aCSF: 119mM NaCl, 1.9mM KCl, 1.2mM NaH_2PO_4, 10mM $MgSO_4$, 1mM CaCl, 26mM $NaHCO_3$, 20mM glucose and 1.5mM kynurenic acid.

Recording aCSF: 127mM NaCl, 3mM KCl, 2mM $CaCl_2$, 1mM $MgCl_2$, 26mM $NaHCO_3$, 1.25mM NaH_2PO_4, 10mM glucose.

Intracellular solution for patch clamp recordings: 14mM $KMeSO_4$, 10mM NaCl, 1mM CaCl, 10mM HEPES, 1mM EGTA, 3mM Mg-ATP and 45mM Mg-GTP.

Dopamine (DA; 50uM; Sigma-Aldrich, Poole, UK), serotonin (5-HT; 10uM, Sigma-Aldrich, Poole, UK), and N-methyl-D-aspartic acid (NMDA; 5µM; Sigma-Aldrich, Poole, UK), monensin (10uM, Tocris Bioscience, Abingdon, UK).

Data analysis

Whole-cell patch clamp recordings

Whole-cell patch clamp recordings were analysed using Clampfit software (Molecular Devices, Sunnyvale, CA, USA). For the analysis of single action potentials, 10 waveform samples were averaged into a single representative waveform. This representative trace was then used to calculate the firing threshold, amplitude, rise time, half-width, and mAHP measurements for each cell. Frequency-current (f-I) relationships were determined from a series of 1s square current pulses ranging from 50pA to 4000pA. Steady-state firing frequency (Hz) was determined from the last 500ms of the current pulse. Post-discharge activity denotes the activity of the cell after a period of prolonged firing (10s current pulse/train). Post-discharge activity area (mVs) is a combined measure of voltage change and recovery time. The area measurement represents the area under/over resting membrane potential starting at the cessation of firing and ending once resting membrane potential has been restored.

Data are presented as mean ± standard error. In these data, the 'n' value represents the number of cells.

Ventral root recordings

Ventral root data were analysed using Dataview software (v 10.3.0, courtesy of Dr. W. J. Heitler, University of St Andrews) before being imported into Excel and analysed. Rhythmic events were

identified from rectified/integrated traces. Burst frequency and duration were measured from integrated traces while peak-to-peak amplitude was measured from corresponding raw traces. Amplitude was measured as a non-calibrated unit and is therefore presented as an arbitrary unit. Statistical analyses were conducted using GraphPad (Prism 9).

Results

Effects of T613M on animal behaviours

A knock-in mouse model of T613M *ATP1A3* was created using CRISPR/Cas technology. Heterozygous T613M female and male mice were born without any obvious physical abnormalities but weighed less than their wild type (WT) littermates (Fig. 1A). The Mendelian distribution of WT and Het crossing was 151 WT: 132 T613M. There were eight spontaneous deaths among T613M mice and two among WT mice (Fig. 1H). Three T613M animals were found to have mobility deficits and appeared lame. These animals were sacrificed along ethical guidelines.

We applied three triggers (immobilization, cold water stress, and alcohol injection) however no symptom progression was observed in the triggered mice. However, we found two spontaneously triggered (abrupt onset/worsening of RDP-related symptoms) animals.

Several behavioural tests were performed, where T613M mice showed considerably higher levels of locomotor activity compared to WT mice. During the open field behaviour test T613M mice moved with higher speed and took fewer and shorter pauses in locomotor activity than WT mice. The traveled distance was approximately 50% larger than in WT mice (Fig. 1B).

In the elevated plus-maze behaviour test the T613M mice moved with higher velocity and spent twice as much time in open arms and less time in closed arms compared to WT mice (Fig. 1C). During the forced swim behaviour test, WT mice were found in the passive floating state twice as often as T613M mice (Fig. 1D).

As cognitive deficits have been observed in a number of *ATP1A3* mutant mouse models (reviewed in Ng, Ogbeta and Clapcote, 2021), a passive avoidance behaviour test was performed to assess the memory of T613M mice. The passive avoidance behaviour test did not reveal any cognitive differences between T613M and WT mice (Fig. 1E).

To assess nigrostriatal function, a pole test was conducted. There was no difference in turning time between WT and T613M mice, but T613M mice did require more time to return to the base (Fig. 1F). To assess sensorimotor co-ordination, a rotarod test was conducted. There was no difference between WT and T613M mice in the rotarod behaviour test (Fig. 1G).

These results are consistent with previous studies showing an overall higher level of locomotor activity in *ATP1A3* mutant mouse models compared to WT mice. To systematically test the effects of the T613M mutation on locomotor performance we performed a Catwalk gait analysis on WT and T613M mice. T613M mice walked with a higher frequency of stepping characterised by a shorter step cycle duration in fore- and hind-limbs. This was accompanied by a reduction in the stance phase across all limbs (Fig. 1I).

Collectively, the hyperactivity and hyperambulation observed in the T613M mice is compatible with a potential pathophysiological effect of the T613M mutation on the network of motor neurons and interneurons responsible for the production of locomotor output.

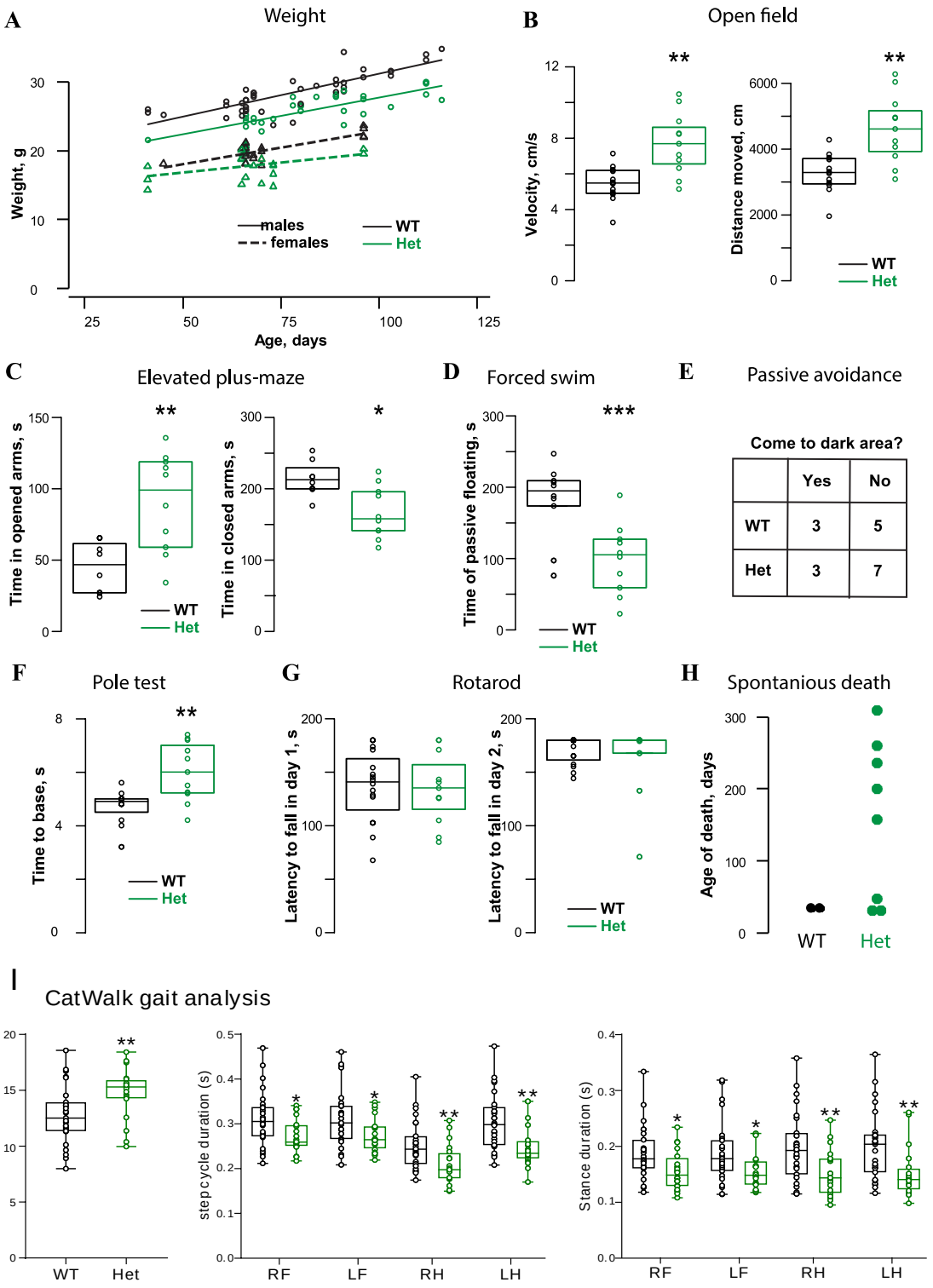
A
Weight
Weight, g
Age, days
males
females
WT
Het
B
Open field
Velocity, cm/s
Distance moved, cm
WT
Het
C
Elevated plus-maze
Time in opened arms, s
Time in closed arms, s
WT
Het
D
Forced swim
Time of passive floating, s
WT
Het
E
Passive avoidance
Come to dark area?
Yes
No
WT 3 5
Het 3 7
F
Pole test
Time to base, s
WT
Het
G
Rotarod
Latency to fall in day 1, s
Latency to fall in day 2, s
WT
Het
H
Spontanious death
Age of death, days
WT
Het
I
CatWalk gait analysis
Cadence (steps/s)
step cycle duration (s)
Stance duration (s)
WT
Het
RF
LF
RH
LH

Figure 1. Behavioural characterisation of the T613M *ATP1A3* knock-in mouse model. (A) Weight analysis for males and females 2-4 months old. *n*=41, *n*=32, *n*=18, *n*=21 for WT and Het males and WT and Het females respectively. (B) Boxplot diagrams of results from the open field test. The left panel presents the velocity of movement and the right panel presents total distance (WT *n*=12, T613M *n*=11). (C) Boxplot diagrams of results from the elevated plus-maze test. The left panel presents time spent in open arms and the right panel presents time spent in closed arms (WT *n*=8, T613M *n*=10). (D) Boxplot diagrams of results from forced swim test showing time of passive floating. (WT *n*=10, T613M *n*=10). (E) Contingency table of results from the passive avoidance test presenting the number of animals which entered the dark compartment (WT *n*=8, T613M *n*=10) (F) Boxplot diagrams of results from the pole test presenting time to travel to the base of the pole (WT *n*=12, T613M *n*=11). (G) Boxplot diagrams of results from the rotarod test. The left panel presents latency to fall time on the first day of the experiment and the right panel presents latency to fall time on the second day of the experiment (WT *n*=16, T613M *n*=11). (H) Dependency of spontaneous death and age of animals (WT *n*=2, T613M *n*=8). (I) Boxplot diagrams of results from Catwalk gait analysis (WT *n*=27, T613M *n*=20). *, $p<0.05$; **, $p<0.01$; ***, $p<0.001$ with Mann-Whitney rank test.

Effect of T613M on the sodium extrusion rate of transfected neurons

To determine the exact manner in which the T613M mutation effects α3-NKA protein function, and how any functional changes may translate to the behavioural changes seen in the intact animals, we conducted a series of sodium imaging experiments to determine the extent to which sodium homeostasis may be affected in T613M-affected neurons.

In this protocol, we expressed WT NKA or T613M mutant NKA tagged with mTurquoise, in hippocampal neurons. The neurons were loaded with the sodium-sensitive dye Asante (Fig. 2A) and continuously perfused with an artificial cerebrospinal fluid (aCSF) solution. To correct for inconsistencies in culture conditions, data are given as the ratio between transfected neurons, visualised by the turquoise signal, and non-transfected neurons on the same coverslip. Basal intracellular sodium concentration was significantly higher in both the soma and dendrites of T613M α3-NKA expressing neurons than in WT α3-NKA expressing neurons (Fig. 2D).

To record the maximum sodium extrusion rate, NKA activity was transiently blocked by brief exposure to a potassium-free solution and the sodium extrusion rate was recorded following a return of a potassium-containing solution (Fig. 2B). Representative recordings are shown in Fig. 2C. The sodium extrusion rate was significantly lower in neurons expressing T613M mutant α3-NKA than in neurons expressing WT α3-NKA both in the soma and in dendrites (Fig. 2E). To mimic the increase in intracellular sodium occurring during high neuronal activity, the neurons were briefly exposed to 20μM NMDA in a magnesium-free solution. The rate of sodium extrusion following NMDA exposure was significantly lower in neurons expressing T613M mutant α3-NKA than in neurons expressing WT α3-NKA (Fig. 2F).

These data provide further validation of our T613M mutant mouse model and provide insight into the molecular dynamics that may underlie physiological differences observed in this model.

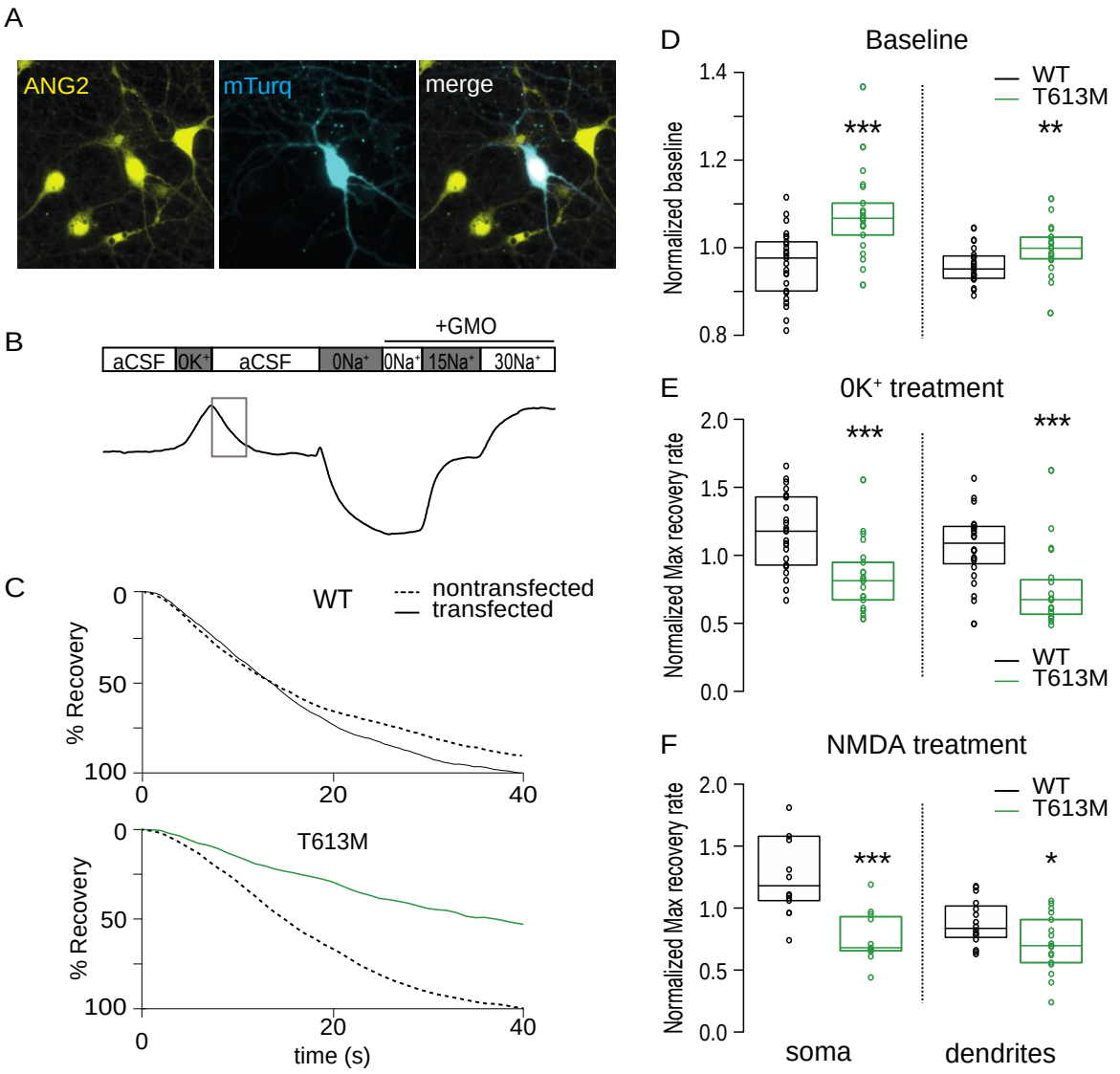

Figure 2. Sodium homeostasis is affected by the T613M mutation of α3-NKA. (A) Representative pictures of hippocampal neurons in culture expressing WT α3-NKA and mTurquoise for identification of transfected cells and cells loaded with ANG2. (B) Typical recording of Na^+ intracellular levels in hippocampal neurons challenged with a change in extracellular K^+ concentration ($0K^+$). A calibration curve was performed at the end of each experiment using increasing concentrations of Na^+ in a solution containing Gramicidin/Monensin/Ouabain (GMO). (C) Representative traces of the recovery after a temporary NKA block using 0mM KCl solution in neurons expressing WT (top, black) and T613M (bottom, green) α3-NKA. (D) Basal intracellular level of sodium in neurons transfected with WT (black) or T613M (green) α3-NKA in soma (left) and dendrites (right). Results are presented as a ratio between transfected neurons and non-transfected neurons from the same experiment. *n*=26, *n*=20, *n*=18, *n*=18 for WT and T613M soma and for WT and T613M dendrites respectively. (E) Ratio of maximum initial pumping rate after $0K^+$ treatment between neurons transfected with WT (black) or T613M (green) α3-NKA and non-transfected neurons in soma and dendrites. *n*=25, *n*=21, *n*=24, *n*=19 for WT and T613M soma and WT and T613M dendrites respectively. (F) Ratio of maximum initial pumping rate after NMDA treatment between neurons transfected with WT (black) or T613M (green) α3-NKA and non-transfected neurons in soma and dendrites. *n*=14, *n*=11, *n*=16, *n*=17 for WT and T613M soma and WT and T613M dendrites respectively. *, $p<0.05$; **, $p<0.01$; ***, $p<0.001$ with Mann-Whitney rank test.

Effects of T613M on motor neuron passive properties

To gain insight into the fundamental role of the α3-NKA in motor control, as well as its role in the pathophysiology of Rapid-Onset Dystonia-Parkinsonism, we investigated any physiological differences between WT and T613M-affected lumbar motor neurons using whole-cell patch-clamp electrophysiology in spinal cord slices. We first compared the passive properties of MNs from WT and T613M mice (Figure 3). Unpaired t-tests showed that the two models did not differ in passive properties such as whole-cell capacitance (pF)(Fig. 3a, WT 110 ± 8.1, T613M 126 ± 6.2, p=0.1095) or input resistance (MΩ)(Fig.3b, WT 75 ± 6.2, T613M 77 ± 4.8, p=0.8620) (WT n=35, T613M n=38). We did, however, observe a hyperpolarised resting membrane potential in T613M-affected motor neurons compared to WT motor neurons (mV)(Fig. 3c, WT -59.11 ± 0.83, T613M -62.09 ± 0.72, p=0.0081, WT n=35, T613M n=38). We suggest that this hyperpolarisation of RMP may be caused by a compensatory upregulation of α1 that is responsible for the maintenance of RMP.

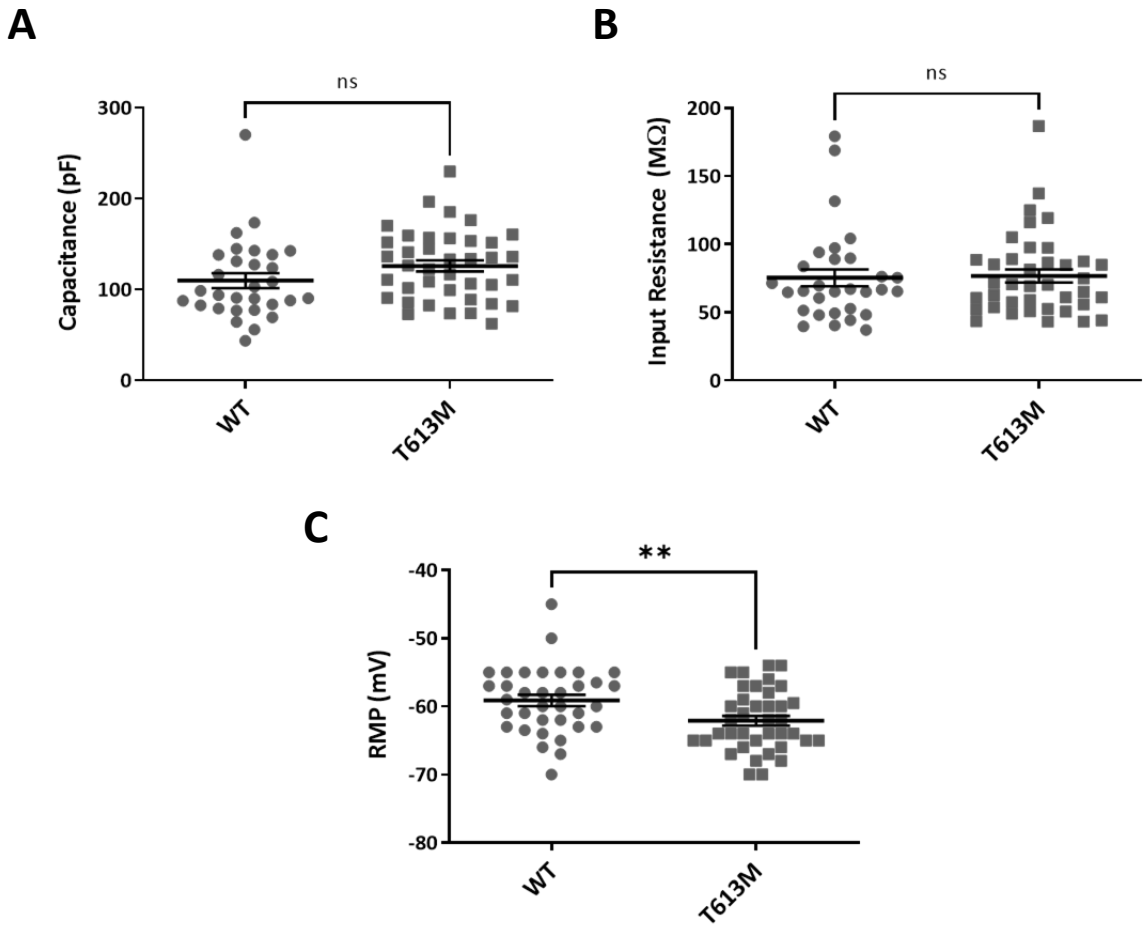

Figure 3. T613M hyperpolarises the resting membrane potential of motor neurons but leaves other passive properties unaffected. (A) Mean capacitance of WT (*n*=35) and T613M (*n*=38) lumbar motor neurons (*p*=0.1095). (B) Mean input resistance of WT (*n*=35) and T613M (*n*=38) lumbar motor neurons (*p*=0.8620). (C) Mean resting membrane potential (RMP) of WT (*n*=35) and T613M (*n*=38) lumbar motor neurons (*p*=0.0081). *, *p*<0.05; **, *p*<0.01; ***, *p*<0.001 with an unpaired t-test.

Effects of T613M on motor neuron action potential properties

Next, we compared the action potential properties of WT and T613M MNs. Unpaired t-tests showed all relevant parameters, including firing threshold (mV) (Fig. 4Ci, WT -45.54 ± 1.352, T613M -45.66 ± 0.9017, *p*=0.9426), amplitude (mV)(Fig. 4Cii, WT 75.27 ± 2.004, T613M 74.27 ± 1.42, *p*=0.6885), rise time (ms)(Fig. 4Ciii, WT 0.96 ± 0.078, T613M 0.92 ± 0.041, *p*=0.6331), and half-width (ms)(Fig. 4Civ, WT 0.903 ± 0.075, T613M 0.93 ± 0.048, *p*=0.8023) to be comparable between the two models (Fig. 4a, WT *n*=11, T613M *n*=34).

We also found that the parameters of the medium afterhyperpolarisation (mAHP) such as amplitude (mV)(Fig. 4Di, WT -6.91 ± 1.03, T613M -7.20 ± 0.39, *p*=0.7979), half-width (ms)(Fig. 4Dii, WT 59.11 ± 8.99, T613M 61.27 ± 3.48, *p*=0.8259), duration (ms)(Fig. 4Diii, WT 218.3 ± 27.42, T613M 218.6 ± 11.44, *p*=0.9911), and area (mVs)(Fig. 4Div, WT -526.5 ± 117.1, T613M -538.8 ± 45.32, *p*=0.9231) were also comparable between WT and T613M-affected motor neurons (Fig. 4b, WT *n*=11, T613M *n*= 34). Due to the α3-subunit isoform's low affinity for sodium, it is unlikely that enough intracellular sodium would accumulate from a single action potential to evoke considerable α3-NKA activity.

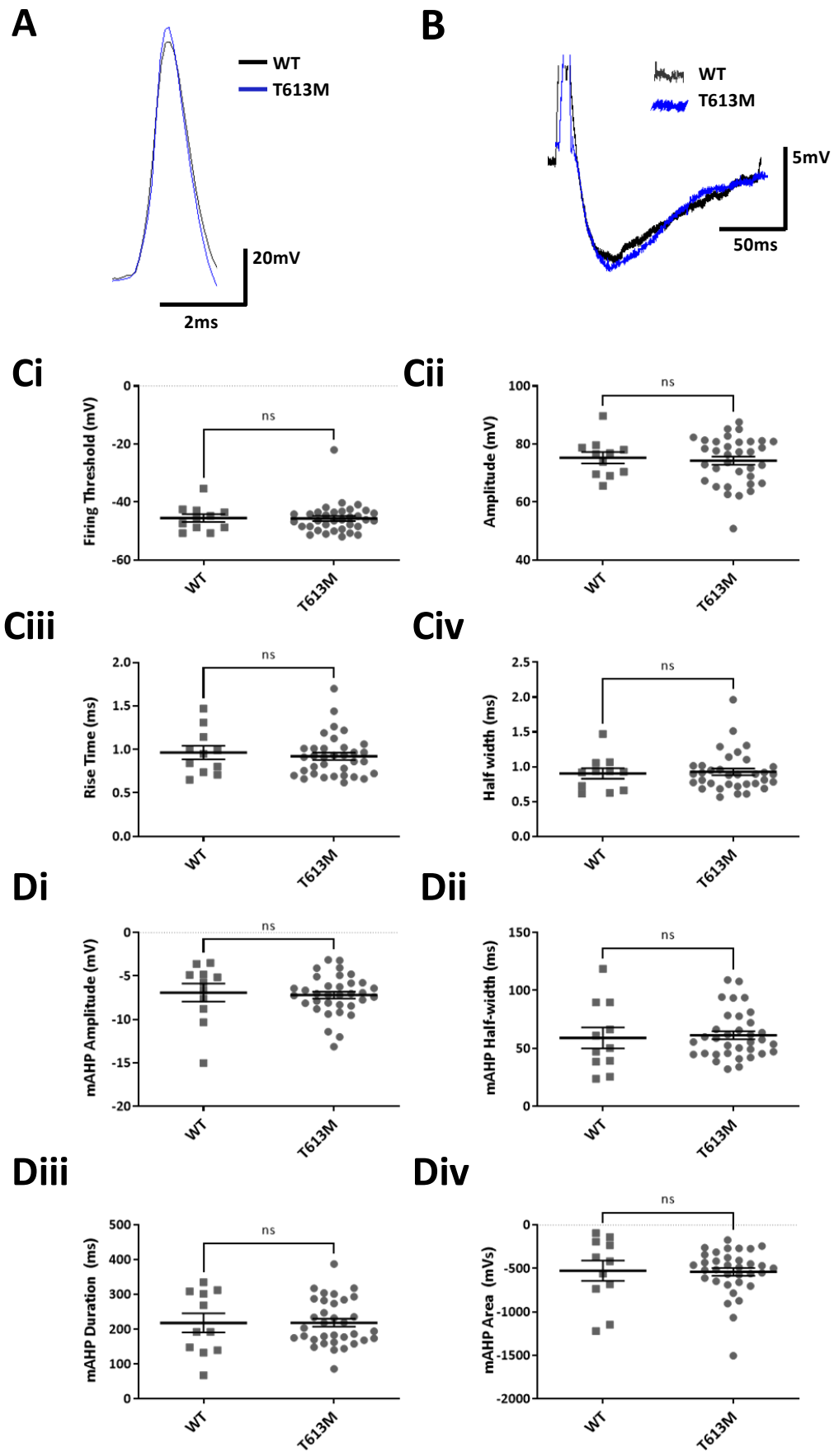
A
WT
T613M
20mV
2ms
B
WT
T613M
5mV
50ms
Ci
Firing Threshold (mV)
ns
WT
T613M
Cii
Amplitude (mV)
ns
WT
T613M
Ciii
Rise Time (ms)
ns
WT
T613M
Civ
Half width (ms)
ns
WT
T613M
Di
mAHP Amplitude (mV)
ns
WT
T613M
Dii
mAHP Half-width (ms)
ns
WT
T613M
Diii
mAHP Duration (ms)
ns
WT
T613M
Div
mAHP Area (mVs)
ns
WT
T613M

Figure 4. T613M does not affect single action potential properties of lumbar motor neurons. (A) Raw traces showing an action potential from a WT motor neuron (black) and T613M motor neuron (blue). (B) Raw traces showing the medium afterhyperpolarisation (mAHP) from a WT motor neuron (black) and a T613M motor neuron (blue). (Ci) Mean firing threshold (mV) of single action potentials from WT motor neurons and T613M motor neurons (p=0.9426). (Cii) Mean amplitude (mV) of single action potentials from WT motor neurons and T613M motor neurons (p=0.6885). (Ciii) Mean rise time (ms) of single action potentials from WT motor neurons and T613M motor neurons (p=0.6331). (Civ) Mean half-width (ms) of single action potentials from WT motor neurons and T613M motor neurons (p=0.8023). (Di) Mean amplitude (mV) of the mAHP from WT motor neurons and T613M motor neurons (p=0.7979). (Dii) Mean half-width (ms) of the mAHP from WT motor neurons and T613M motor neurons (p=0.8259). (Diii) Mean duration (ms) of the mAHP from WT motor neurons and T613M motor neurons (p=0.9911). (Div) Mean area (mVs) of the mAHP from WT motor neurons and T613M motor neurons (p=0.9231). All measurements were taken from 11 WT motor neurons and 34 T613M motor neurons. *, p<0.05; **, p<0.01; ***, p<0.001 with an unpaired t-test.

Effects of T613M on the f-I relationship of motor neurons

We then analysed the frequency-current (f-I) relationship of the WT and T613M MNs (Fig. 5a, Fig. 5b). This protocol is used to determine the relationship between the input stimulus (one second current steps of increasing amplitude) and the response of the cell (frequency of action potentials produced) to infer any differences in the excitability of the cell, as determined by its membrane properties and channel kinetics.

Similarly, unpaired t-tests showed that the f-I parameters such as slope (Fig. 5Ci, WT 0.036 ± 0.0034, T613M 0.35 ± 0.0021, p=0.728), repetitive firing threshold (pA)(Fig. 5Cii, WT 313.3 ± 36.67, T613M 361.3 ± 36.57, p=0.3583), maximum firing frequency (Hz)(Fig. 5Ciii, WT 31.35 ± 1.448, T613M 28.95 ± 1.081, p=0.3807), and minimum firing frequency (Hz)(Fig. 5Civ, WT 10.76 ± 0.72, T613M 9.798 ± 0.82, p=0.1886) were comparable between WT and T613M-affected motor neurons (WT n=30, T613M n=31). We again presume that this lack of difference between WT and T613M-affected motor neurons is due to the short time course of the f-I protocol, as it is unlikely that there would be a large enough increase in intracellular [Na^+] to warrant considerable α3-NKA activation.

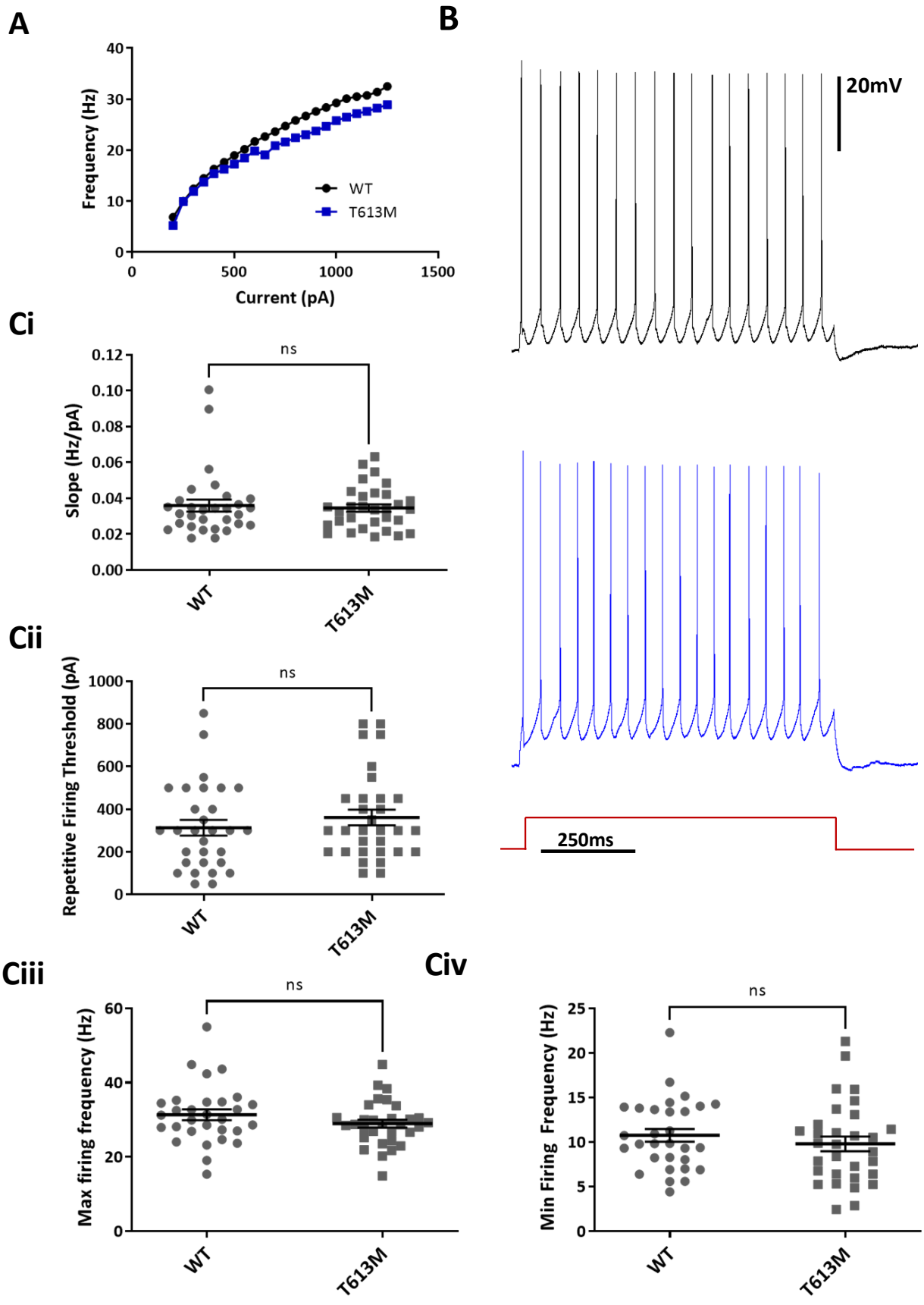
A
B
Frequency (Hz)
Current (pA)
WT
T613M
20mV
250ms
Ci
Slope (Hz/pA)
ns
Cii
Repetitive Firing Threshold (pA)
Ciii
Max firing frequency (Hz)
Civ
Min Firing Frequency (Hz)

Figure 5. T613M does not affect the frequency-current (f-I) relationship of lumbar motor neurons. (A) Representative slope of the f-I from a WT (black) and T613M (blue) motor neuron. (B) Raw traces showing repetitive firing following a 1 second current step used to determine f-I from a WT motor neuron (black) and T613M motor neuron (blue). The red trace shows the shape of the current step applied to elicit spiking. (Ci) Mean f-I slope for WT and T613M motor neurons (p=0.728). (Cii) Mean repetitive firing threshold for WT and T613M motor neurons (p=0.1886). (Ciii) Mean maximum firing frequency for WT and T613M motor neurons (p=0.3807). (Civ) Mean minimum firing frequency for WT and T613M motor neurons (p=0.3583). All measurements were taken from 20 WT motor neurons and 31 T613M motor neurons. *, p<0.05; **, p<0.01; ***, p<0.001 with an unpaired t-test.

Effect of T613M on the post-discharge activity of motor neurons

Although we did not find any differences between the action potential properties or the frequency-current relationship of WT and T613M-affected motor neurons, we precited that the most likely differences would be revealed when looking at the post-discharge activity of these cells as the involvement of the sodium-potassium pump in the production of the ultra-slow afterhyperpolarisation is well documented.

Finally, we investigated the effect of the T613M mutation on post-discharge activity (PDA). PDA refers to the activity of a neuron after a period of prolonged discharge. PDA has three main phenotypes: an afterdepolarisation (ADP) where the membrane potential after discharge is depolarised compared to baseline; a slow-afterhyperpolarisation (sAHP) where the membrane potential is briefly hyperpolarised; or an ultra-slow afterhyperpolarisation where the membrane potential hyperpolarises significantly (>5mV) with a prolonged recovery period (>20s) (Fig. 6A).

We found that the post-discharge activity profile of T613M motor neurons is significantly different from that of WT motor neurons (Fig. 6B). From a random sampling of motor neurons from both WT and T613M-affected lumbar tissue, we found that 20% of WT motor neurons exhibited an usAHP at baseline conditions, 14% exhibited a sAHP, and 66% exhibited an ADP (Fig. 6B, *n*=35). Contrastingly, no usAHPs were observed from T613M-affected motor neurons under baseline conditions, with instead 6% exhibiting a sAHP, and the remaining 94% exhibiting an ADP (Fig. 6B, *n*=35). When probed further, unpaired t-tests showed that the post-discharge area (mVs) of T613M motor neurons was significantly more depolarised than WT motor neurons (Fig. 6Ci, WT 4.020 ± 8.036, T613M 40.01 ± 6.138, p=0.0007, WT n=35, T613M n=35). Regardless of whether the post-discharge activity was hyperpolarised or depolarised, the post-discharge activity of WT and T613M motor neurons exhibited similar recovery times (s)(Fig. 6Ciii, WT 20.7 ± 2.54, T613M 25.73 ± 3.37, p=0.2375, WT n=35, T613M n=35).

Next, we asked whether afterdepolarisations were, on average, larger in T613M motor neurons. We did not find there to be any differences in the post-discharge area (mVs)(Fig. 6Di, WT 29.71 ± 6.086, T613M 43.74 ± 5.84, *p*=0.1133, WT *n*=22, T613M *n*=33), amplitude (Fig. 6Dii, WT 6 ± 0.61, T613M 6.8 ± 0.5, *p*=0.3433, WT *n*=22, T613M *n*=33), or recovery time (Fig. 6Diii, WT 17.16 ± 2.63, T613M 25.92 ± 3.45, *p*=0.0705, WT *n*=22, T613M *n*=22) of motor neurons exhibiting ADPs between WT and T613M motor neurons.

These data provide definitive evidence that the usAHP is largely α3-NKA mediated and suggests that the T613M mutation is enough to create a haploinsufficiency in terms of usAHP production in motor neurons. The usAHP facilitates a period of hypoexcitability that may act to prevent fatigue after high levels of cell activity. Contrastingly, when the cell is depolarised after discharging it is in a more excitable state, with cells displaying ADPs being more likely to fire spontaneously or exhibit plateau potentials and self-sustained firing (Fig. 6E). These data suggest that, while T613M motor neurons may not differ in firing properties over shorter time courses, T613M motor neurons respond differently to prolonged periods of activity that are often necessary for motor neuron function.

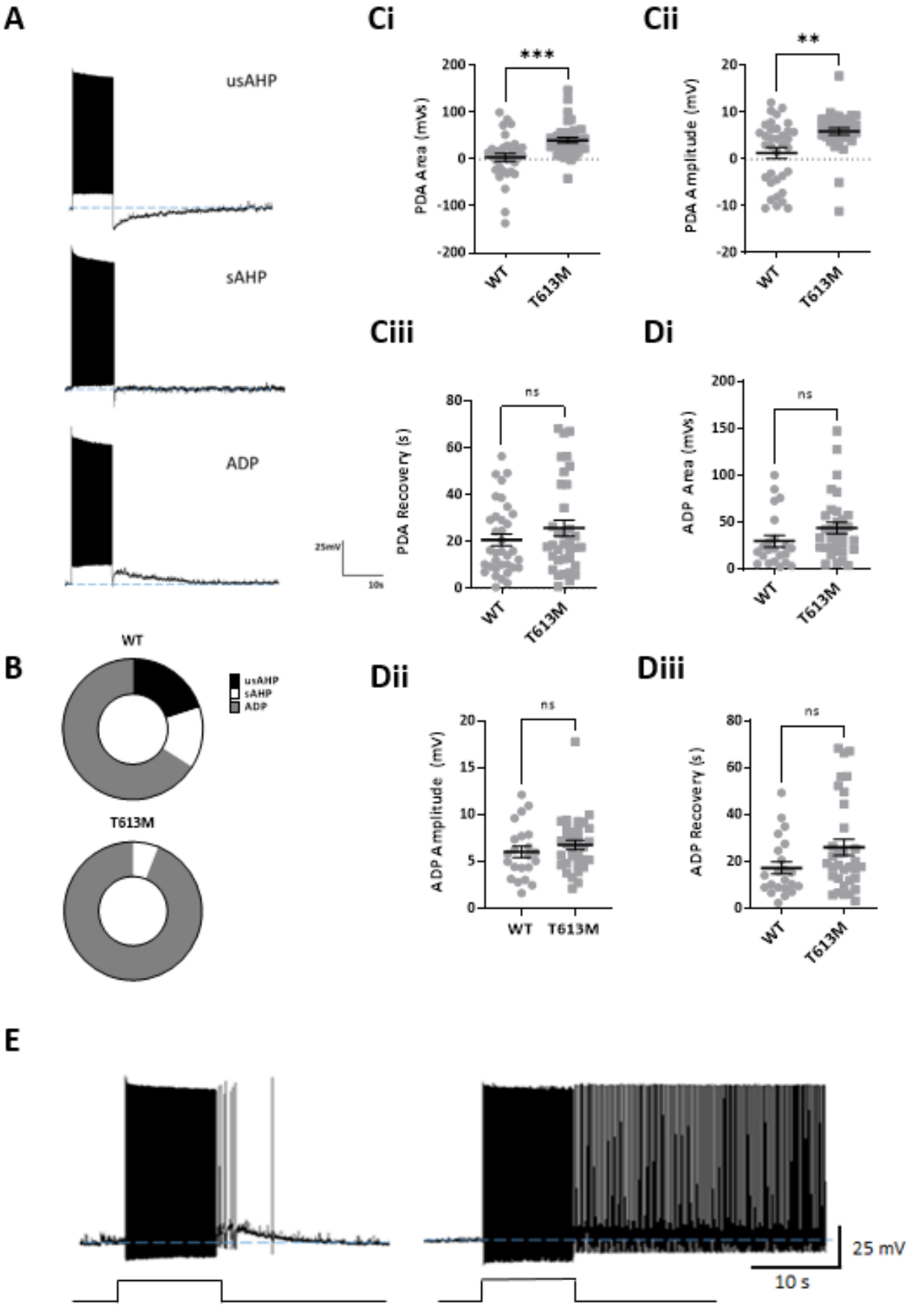
A
usAHP
sAHP
ADP
25mV
10s
Ci
PDA Area (mVs)
***
WT
T613M
Cii
PDA Amplitude (mV)
**
Ciii
PDA Recovery (s)
ns
Di
ADP Area (mVs)
B
WT
T613M
usAHP
sAHP
ADP
Dii
ADP Amplitude (mV)
Diii
ADP Recovery (s)
E
25 mV
10 s

Figure 6. T613M-affected lumbar motor neurons do not exhibit ultra-slow afterhyperpolarisations (usAHPs). (A) Raw electrophysiological traces showing three lumbar motor neurons displaying different post-discharge activities. (B) Proportions of WT and T613M lumbar motor neurons exhibiting usAHPs, sAHPs, and ADPs. Note the complete lack of usAHPs observed in T613M motor neurons. (Ci) Mean post-discharge activity area (mVs) of WT (*n*=35) and T613M (*n*=35) motor neurons (*p*=0.0007). (Cii) Mean post-discharge activity amplitude (mV) of WT (*n*=35) and T613M (*n*=35) motor neurons (*p*=0.0014). (Ciii) Mean post-discharge activity recovery time (ms) of WT (*n*=35) and T613M (*n*=35) motor neurons (*p*=0.2375). (Di) Mean afterdepolarisation (ADP) area (mVs) of WT (*n*=22) and T613M (*n*=33) motor neurons (*p*=0.1133). (Dii) Mean afterdepolarisation (ADP) amplitude (mV) of WT (*n*=22) and T613M (*n*=33) motor neurons (*p*=0.3433). (Diii) Mean afterdepolarisation (ADP) recovery time (s) of WT (*n*=22) and T613M (*n*=33) motor neurons (*p*=0.0705). (E) Raw traces showing increased excitability of MNs exhibiting ADPs such as rebound firing (left) and plateau potentials (right). *, $p<0.05$; **, $p<0.01$; ***, $p<0.001$ with an unpaired t-test.

Effects of T613M on spontaneous spinal motor network output

After revealing that T613M-affected lumbar motor neurons do not exhibit usAHPs, we wanted to investigate how a lack of usAHPs in motor neurons affected spinal network output. Pharmacological experiments using ouabain to block the sodium-potassium pump have shown that the sodium-potassium pump is involved in regulating the frequency of drug-induced and sensory-evoked locomotor-related rhythms, as well as facilitating a form of short-term motor memory within the network (Picton *et al.* 2017).

Utilising an isolated spinal cord preparation, we first looked at spontaneous output from the lumbar ventral roots. When at rest, the spinal cord will produce bouts of spontaneous activity without any sensory or pharmacological stimulation (Fig. 7). As T613M mice and other mice with *ATP1A3* mutations have been found to be hyperactive/hyperambulatory (reviewed in Ng, Ogbeta and Clapcote, 2021), we predicted that we may see an increased level of spontaneous activity from T613M-affected isolated spinal cords. However, no differences in total amount of spontaneous activity (Fig. 7Ci, WT 298.77 ± 50.64, T613M 232.5 ± 39.44, p=0.3034), the frequency of spontaneous bouts (Fig. 7Cii, WT 0.283 ± 0.0218, T613M 0.2646 ± 0.0226, p=0.5637), or the average duration of spontaneous bouts (Fig. 7Ciii, WT 2938 ± 349.1, T613M 2714 ± 497.4, p=0.7158) were observed between T613M and WT preparations (WT n=14, T613M n=17) using unpaired t-tests.

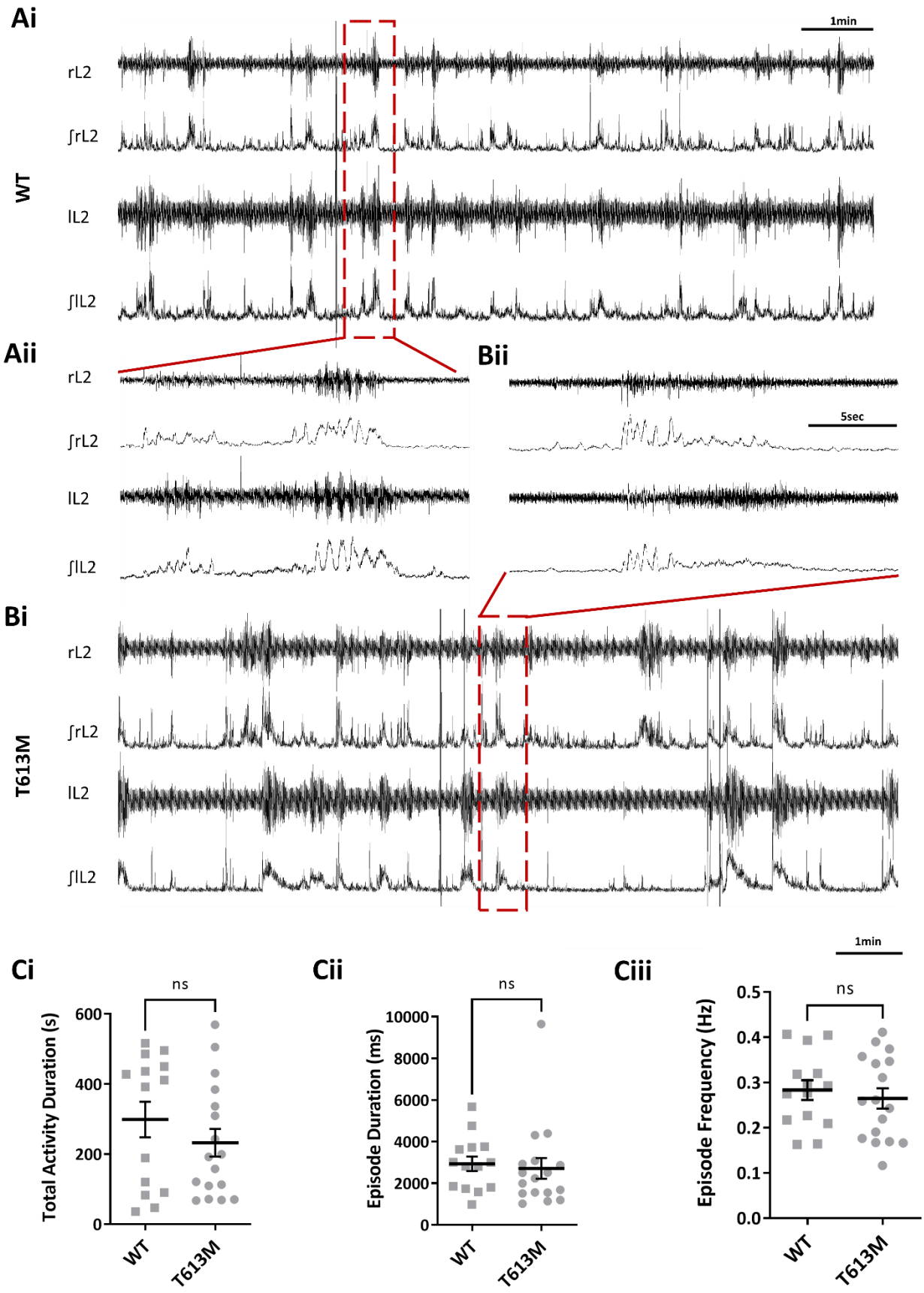
Ai
1min
rL2
∫rL2
WT
lL2
∫lL2
Aii
Bii
rL2
5sec
∫rL2
lL2
∫lL2
Bi
rL2
∫rL2
T613M
lL2
∫lL2
Ci
ns
Total Activity Duration (s)
600
400
200
0
WT
T613M
Cii
ns
Episode Duration (ms)
10000
8000
6000
4000
2000
0
WT
T613M
Ciii
1min
ns
Episode Frequency (Hz)
0.5
0.4
0.3
0.2
0.1
0.0
WT
T613M

Figure 7. T613M does not affect spontaneous motor output from isolated spinal cords. (Ai) Raw and rectified/integrated (∫) traces showing spontaneous motor output from the left and right L_2 ventral roots of a WT spinal cord. (Aii) Output shown in Ai on an expanded time base to exemplify the rhythmic elements of the spontaneous activity. (Bi) Raw and rectified/integrated (∫) traces showing spontaneous motor output from the left and right L_2 ventral roots of a T613M spinal cord. (Bii) Output shown in Bi on an expanded time base to exemplify the rhythmic elements of the spontaneous activity. (Ci) Mean total spontaneous activity duration (s) of WT (*n*=14) and T613M (*n*=17) spinal cords over a 10 minute recording period (*p*=0.3034). (Cii) Mean episode duration of spontaneous activity from WT (*n*=14) and T613M (*n*=17) spinal cords (*p*=0.7269). (Ciii) Mean episode frequency of spontaneous activity from WT (*n*=14) and T613M (*n*=17) spinal cords (*p*=0.5637).

Effects of T613M on sensory-evoked locomotor-related output

Next, we investigated the effects of the T613M mutation on sensory-evoked locomotor-related activity. In these preparations, a stimulating electrode is attached to the fifth lumbar dorsal root and a series of current pulses are applied to elicit a bout of locomotor-related activity (Fig. 8A). Previous research from Picton and colleagues (2017) showed that the frequency of these sensory-evoked locomotor-related bursts and the duration of locomotor-related episodes was increased with the application of the sodium pump-blocker ouabain. They speculate that this is due to the blocking of the α3-NKA with ouabain diminishing the usAHP significantly in spinal neurons. Without the inhibitory influence of the usAHP on spinal neuron activity, the motor network is more depolarised and therefore the burst frequency and episode duration of this output is increased.

We predicted that, due to the T613M mutation reducing the activity of α3-NKA in the network similarly to the effect of ouabain, we would observe a similar effect in these preparations. We did not observe longer episode durations in T613M preparations (Fig. 8Ci, WT 28.54 ± 1.42, T613M 30.66 ± 2.104, p=0.3967) or any difference in the burst duration of sensory-evoked motor output between the WT and T613M preparations (Fig. 8Ciii, WT533 ± 29, T613M 436 ± 56, p=0.1074) (WT n=10, T613M n=5) using unpaired t-tests. However, we did observe a significantly higher burst frequency in T613M preparations, in line with our predictions (Fig. 8Cii, WT 0.94 ± 0.072, T613M 1.2 ± 0.098, p=0.0453).

A

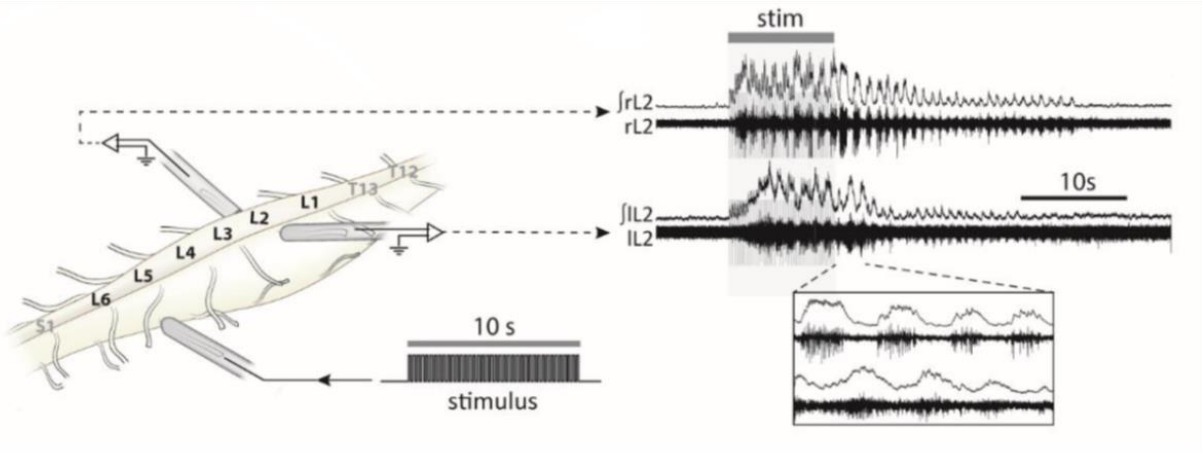

Bi

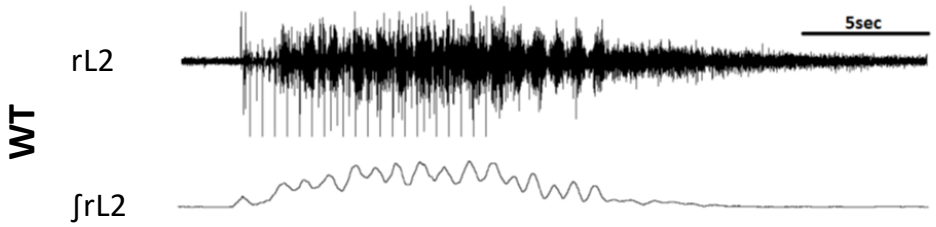

Bii

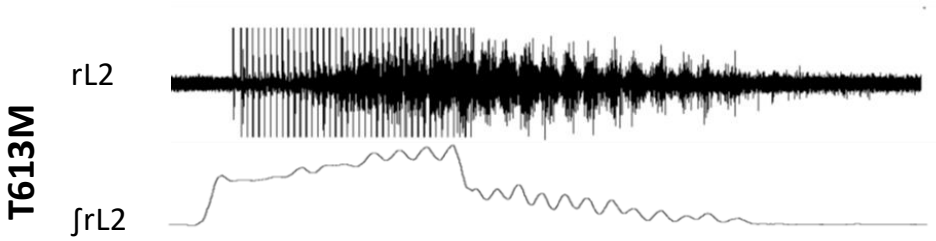

Ci

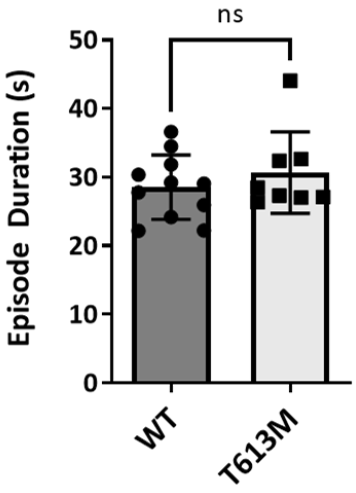

Cii

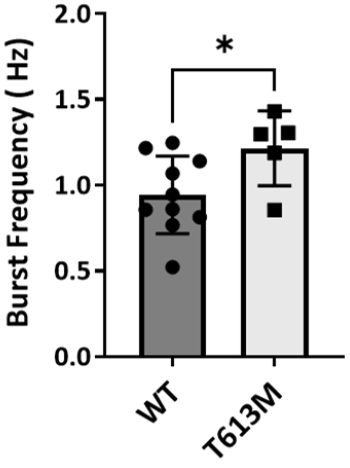

Ciii

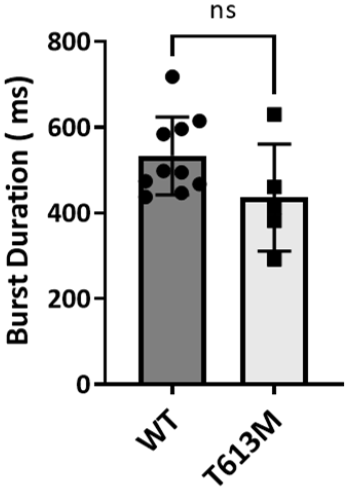

Figure 8. T613M increases the burst-frequency of sensory-evoked locomotor-related output. (A) Schematic illustrating the preparation used for recording sensory-evoked locomotor-related output. Glass suction electrodes are attached to the ventral roots to record motor output, whilst a stimulating electrode is applied to the dorsal root to provide sensory input to the cord to initiate locomotion (see Methods). (Bi) Raw and rectified/integrated (∫) traces showing the locomotor-related output observed from a wildtype (WT) animal after a series of current pulses is applied to the cord via the stimulating electrode. (Bii) Raw and rectified/integrated (∫) traces showing the locomotor-related output observed from a T613M animal after a series of current pulses is applied to the cord via the stimulating electrode. (Ci) Mean episode duration of sensory-evoked locomotor-related output from WT (*n*=11) and T613M (*n*=8) animals (*p*=0.3967). (Cii) Mean burst frequency (Hz) of sensory-evoked locomotor-related output from WT (*n*=11) and T613M (*n*=8) animals (*p*=0.0453). (Ciii) Mean burst duration (ms) of sensory-evoked locomotor-related output from WT (*n*=11) and T613M (*n*=8) animals (*p*=0.1074). *, *p*<0.05 with an unpaired t-test.

Several groups have implicated the usAHP in the facilitation of a form of short-term motor memory (STMM) in locomotor networks, across multiple animal models (Zhang and Sillar, 2012; Picton *et al.*, 2017; Hachoumi *et al.* 2022). When the pump is blocked pharmacologically using ouabain, the STMM observed at baseline is abolished (Picton *et al.* 2017). Here, we utilised the T613M model to further test the involvement of the α3-NKA in short-term motor memory and its potential role in the disease manifestation of the *ATP1A3* mutation. We predicted that short-term motor memory would be absent or at least diminished in the T613M preparations.

Interestingly, this was not the case. We found that there was no considerable difference in STMM between WT and T613M preparations (Fig. 9, Fig. 10). In this paradigm, we applied a series of STMM 'sweeps' which involved an 'initial' stimulation at least two minutes after the previous sweep, an 'interruption' stimulation either 30 or 15 seconds after activity had returned to baseline, and a 'recovered' stimulation two minutes after activity produced from the interruption stimulation had returned to baseline. According to previous work conducted on this short-term motor memory, the episode of activity produced by the 'interruption' stimulation should be shorter in length and the bursts should be less frequent. This is due to a network 'memory' of previous activity in the form of the usAHP. As many of the cell's comprising the underlying motor network will be hyperpolarised after the initial stimulation, the network will be unable to produce output of the same power. However, this should recover if you allow the network to rest longer than the duration of the usAHP: approximately two minutes. The 'recovered' episode should then be comparable to the 'initial' episode. These three stimulations therefore make up one STMM 'sweep'.

A two-way ANOVA was performed to determine the effect of genotype and stimulation interval on the parameters of this STMM. For episode duration, there was found to be no significant interaction between these two variables at the 30 second (Fig. 9Ci, WT n=11, T613M n=10, $F_{(2,36)}$= 0.8477, p=0.4368) or 15 second stimulation interval (Fig. 10Ci, WT n=11, T613M n=10, $F_{(2,36)}$= 1.133, p=0.3333),

nor a main effect of genotype at the 30 second ($F_{(1,18)}$= 0.533, *p*=0.4748)of 15 second stimulation interval ($F_{(1,18)}$= 0.1876, *p*=0.6701).

For intra-episode burst frequency, there was found to be no significant interaction between stimulation interval and genotype at the 30 second interval (Fig. 9Cii, WT *n*=10, T613M *n*=5, $F_{(2,26)}$=1.088, *p*=0.3518) however a main effect of genotype was observed ($F_{(1,13)}$=6.949, *p*=0.0205). At the 15 second stimulation interval, a significant interaction between stimulation interval and genotype was observed (Fig. 10Cii, WT *n*=9, T613M *n*=4, $F_{(2,22)}$=4.730, *p*=0.0196) as well as a main effect of genotype ($F_{(1,11)}$=9.012, *p*=0.012).

For intra-episode burst duration, there was found to be no significant interaction between stimulation interval and genotype at the 30 second interval (Fig. 9Ciii, WT *n*=10, T613M *n*=5, $F_{(2,26)}$=0.6616, *p*=0.5245) nor a main effect of genotype ($F_{(1,13)}$=4.083, *p*=0.0644). At the 15 second stimulation interval, there was found to be a significant interaction between stimulation interval and genotype (Fig. 10Ciii, WT *n*=9, T613M *n*=4, $F_{(2,22)}$=4.306, *p*=0.0264) as well as a main effect of genotype ($F_{(1,11)}$=15.89, *p*=0.0021).

Ultimately, these results show large amounts of variability and are difficult to resolve. The STMM elicited using this paradigm does not appear to be as strong as what has been previously reported (Zhang and Sillar, 2012; Picton *et al.*, 2017) regardless of genetic model used.

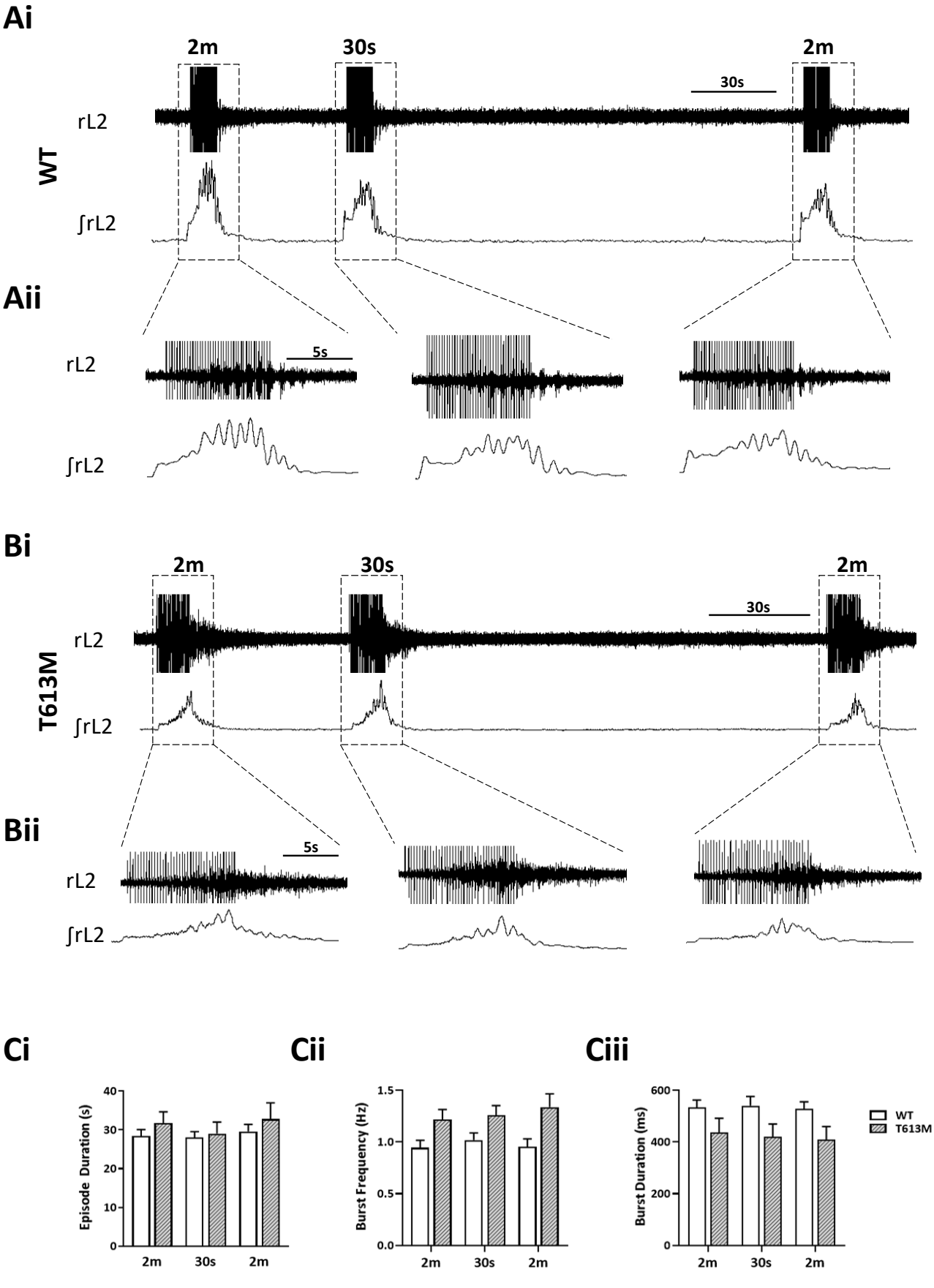
Ai
2m
30s
2m
30s
WT
rL2
∫rL2
Aii
5s
rL2
∫rL2
Bi
2m
30s
2m
30s
T613M
rL2
∫rL2
Bii
5s
rL2
∫rL2
Ci
Episode Duration (s)
40
30
20
10
0
2m
30s
2m
Cii
Burst Frequency (Hz)
1.5
1.0
0.5
0.0
2m
30s
2m
Ciii
Burst Duration (ms)
600
400
200
0
2m
30s
2m
WT
T613M

Figure 9. T613M does not affect short-term motor memory produced by 30 second stimulation intervals. (Ai) Raw and rectified/integrated (∫) traces of the short-term motor memory (STMM) applied to a WT preparation. The initial current pulse was applied at least two minutes after the previous sweep. A second current pulse was then applied 30 seconds after activity had returned to baseline. A final current pulse was then applied two minutes after activity returned to baseline to complete one STMM sweep. (Aii) Expanded time base of the output shown in Ai to highlight the rhythmic locomotor-like output elicited by the stimulation and the respective change in this output between stimulation intervals. (Bi) Raw and rectified/integrated (∫) traces of the short-term motor memory (STMM) applied to a T613M preparation. The initial current pulse was applied at least two minutes after the previous sweep. A second current pulse was then applied 30 seconds after activity had returned to baseline. A final current pulse was then applied two minutes after activity returned to baseline to complete one STMM sweep. (Bii) Expanded time base of the output shown in Bi to highlight the rhythmic locomotor-like output elicited by the stimulation and the respective change in this output between stimulation intervals. (Ci) Mean episode duration of sensory-evoked locomotor-related output at two minute and 30 second stimulation intervals for WT (*n*=11) and T613M (*n*=9) preparations. (Cii) Mean burst frequency of sensory-evoked locomotor-related output at two minute and 30 second stimulation intervals for WT (*n*=10) and T613M (*n*=5) preparations. (Ciii) Mean burst frequency of sensory-evoked locomotor-related output at two minute and 30 second stimulation intervals for WT (*n*=10) and T613M (*n*=5) preparations.

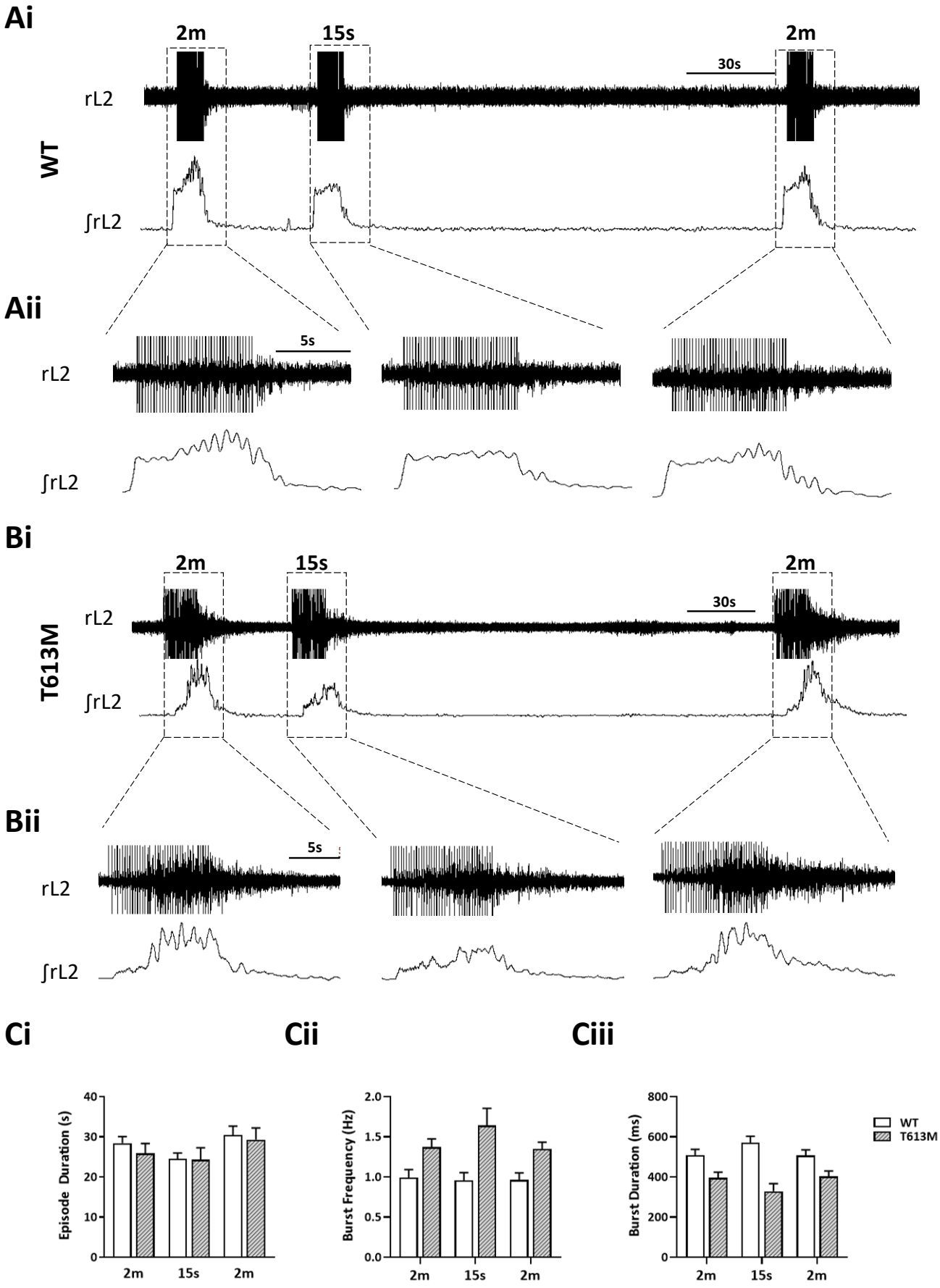
Ai
2m
15s
2m
30s
rL2
WT
∫rL2
Aii
5s
rL2
∫rL2
Bi
2m
15s
2m
30s
rL2
T613M
∫rL2
Bii
5s
rL2
∫rL2
Ci
Cii
Ciii
Episode Duration (s)
40
30
20
10
0
2m
15s
2m
Burst Frequency (Hz)
2.0
1.5
1.0
0.5
0.0
2m
15s
2m
Burst Duration (ms)
800
600
400
200
0
2m
15s
2m
WT
T613M

Figure 10. T613M does not affect short-term motor memory produced by 15 second stimulation intervals. (Ai) Raw and rectified/integrated (∫) traces of the short-term motor memory (STMM) applied to a WT preparation. The initial current pulse was applied at least two minutes after the previous sweep. A second current pulse was then applied 15 seconds after activity had returned to baseline. A final current pulse was then applied two minutes after activity returned to baseline to complete one STMM sweep. (Aii) Expanded time base of the output shown in Ai to highlight the rhythmic locomotor-like output elicited by the stimulation and the respective change in this output between stimulation intervals. (Bi) Raw and rectified/integrated (∫) traces of the short-term motor memory (STMM) applied to a T613M preparation. The initial current pulse was applied at least two minutes after the previous sweep. A second current pulse was then applied 15 seconds after activity had returned to baseline. A final current pulse was then applied two minutes after activity returned to baseline to complete one STMM sweep. (Bii) Expanded time base of the output shown in Bi to highlight the rhythmic locomotor-like output elicited by the stimulation and the respective change in this output between stimulation intervals. (Ci) Mean episode duration of sensory-evoked locomotor-related output at two minute and 15 second stimulation intervals for WT (*n*=11) and T613M (*n*=9) preparations. (Cii) Mean burst frequency of sensory-evoked locomotor-related output at two minute and 15 second stimulation intervals for WT (*n*=9) and T613M (*n*=4) preparations. (Ciii) Mean burst frequency of sensory-evoked locomotor-related output at two minute and 15 second stimulation intervals for WT (*n*=9) and T613M (*n*=4) preparations.

Effects of dopamine administration on motor network activity in T613M mice

Picton and colleagues (2017) found the effects of ouabain on locomotor-related output to be dopamine dependent. They predict that, as dopamine increases the size of the usAHP in motor neurons, the effects of ouabain on dopamine-treated preparations are more pronounced. Dopamine is a well-established modulator of spinal motor network activity (see General Introduction) as well as sodium-potassium pump activity (Hazelwood *et al.*, 2008; Azarias *et al.*, 2013). We therefore also performed an analysis of the influence of dopamine on motor network activity in WT and T613M isolated spinal cord preparations.

First, we examined the dopamine-evoked rhythms generated in both preparations. When dopamine alone is applied to an isolated spinal cord, it produces slow rhythmic bursts of activity (Fig. 11A, 11B). Using unpaired t-tests, we observed that the frequency (Hz) of dopamine-evoked episodes was lower in T613M preparations (0.0099 ± 0.00052, n=5) than in WT preparations (0.02007 ± 0.0037, n=6, p=0.0368) (Fig. 11Ci). Episode duration did not differ between WT and T613M preparations (s)(Fig. 9Cii, WT 16.62 ± 1.676, n=6, T613M 22.51 ± 3.397, n=5, p=0.1351). The episode interval (s) was seen to be considerably longer in T613M (80.09 ± 2.065, n=5) than in WT preparations (39.78 ± 6.704, n=6, p=0.0005) (Fig. 11Ciii).

Intra-episode parameters such as burst frequency (Hz)(Fig. 11Di, WT 0.09395 ± 0.1006, T613M 1.170 ± 0.072, p=0.1073), burst duration (ms)(Fig. 11Dii, WT 499.4 ± 58.19, T613M 444.1 ± 42.35 p=0.4785), and burst interval (ms)(Fig. 11Diii, WT 1187 ± 108.3, T613M 942.2 ± 73.94 p=0.1074) were all found to be comparable between WT and T613M preparations.

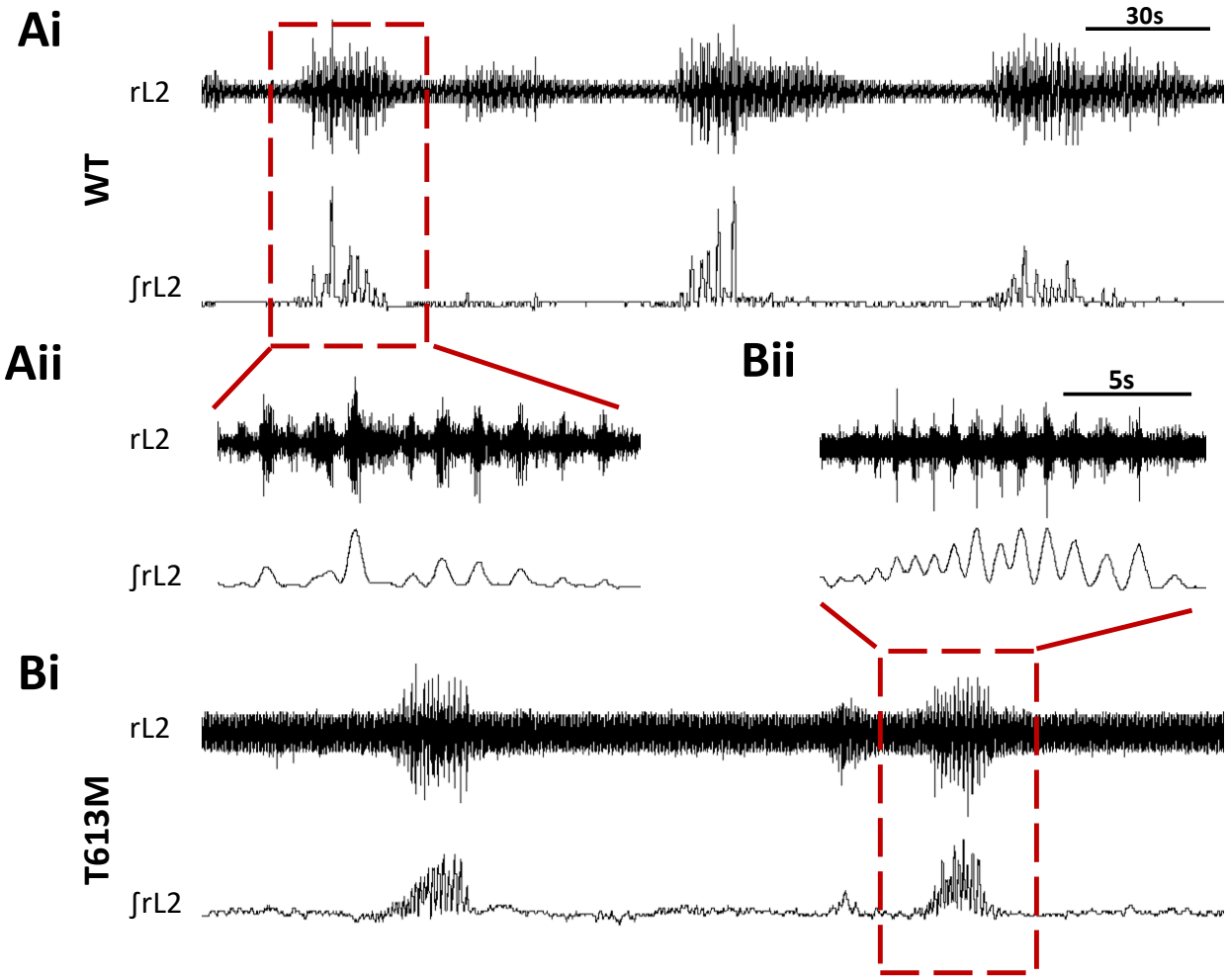
Ai
30s
rL2
WT
∫rL2
Aii
Bii
5s
rL2
∫rL2
Bi
rL2
T613M
∫rL2

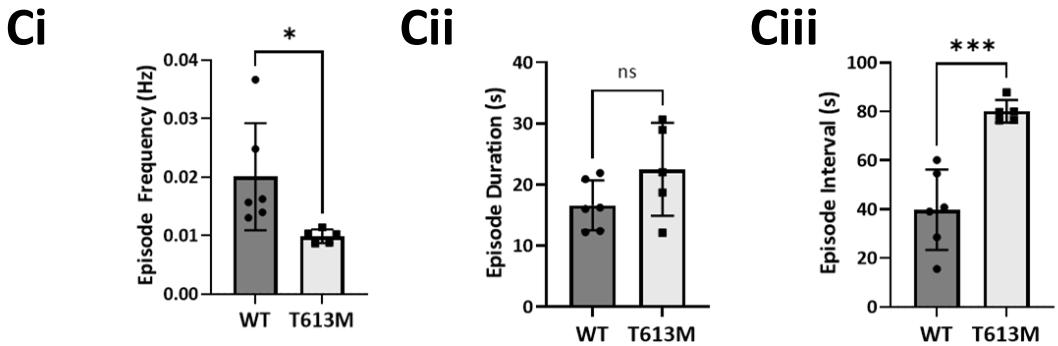
Ci
*
Episode Frequency (Hz)
0.04
0.03
0.02
0.01
0.00
WT
T613M
Cii
ns
Episode Duration (s)
40
30
20
10
0
WT
T613M
Ciii
***
Episode Interval (s)
100
80
60
40
20
0
WT
T613M

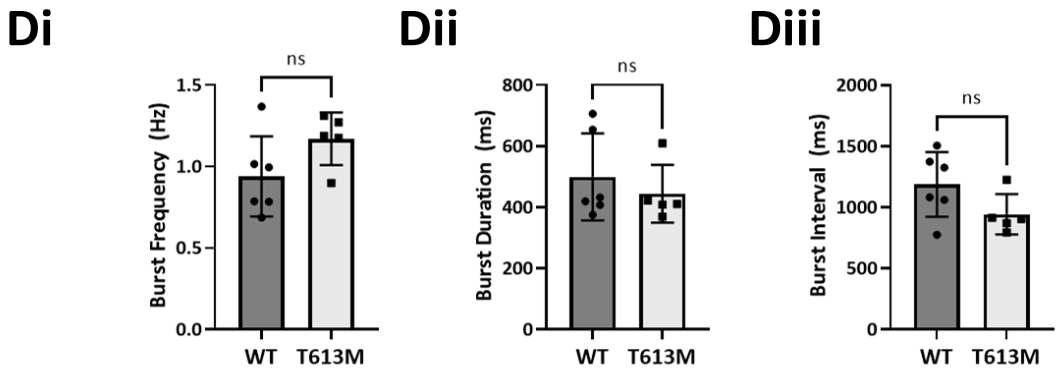
Di
ns
Burst Frequency (Hz)
1.5
1.0
0.5
0.0
WT
T613M
Dii
ns
Burst Duration (ms)
800
600
400
200
0
WT
T613M
Diii
ns
Burst Interval (ms)
2000
1500
1000
500
0
WT
T613M

Figure 11. T613M causes dopamine-evoked rhythms to be slower and less frequent. (Ai) Raw and rectified/integrated (∫) traces showing dopamine-evoked rhythms from a wildtype (WT) preparation. (Aii) Output shown in Ai on an expanded time base to exemplify the rhythmic elements of the dopamine-evoked activity (Bi) Raw and rectified/integrated (∫) traces showing dopamine-evoked rhythms from a T613M preparation. (Bii) Output shown in Bi on an expanded time base to exemplify the rhythmic elements of the dopamine-evoked activity. (Ci) Mean episode frequency of dopamine-evoked rhythms in WT (*n*=6) and T613M (*n*=5) preparations (*p*=0.0368). (Cii) Mean episode duration of dopamine-evoked rhythms in WT (*n*=6) and T613M (*n*=5) preparations (*p*=0.1351). (Ciii) Mean episode interval of dopamine-evoked rhythms in WT (*n*=6) and T613M (*n*=5) preparations (*p*=0.0005). (Di) Mean burst frequency of dopamine-evoked rhythms in WT (*n*=6) and T613M (*n*=5) preparations (*p*=0.1073). (Dii) Mean burst duration of dopamine-evoked rhythms in WT (*n*=6) and T613M (*n*=5) preparations (*p*=0.4785). (Diii) Mean burst interval of dopamine-evoked rhythms in WT (*n*=6) and T613M (*n*=5) preparations (*p*=0.1074). *, *p*<0.05; ***, *p*<0.001 with an unpaired t-test.

Next, we examined the differential effect of dopamine on sensory-evoked locomotor-related output between WT and T613M preparations. Dopamine is utilised in these preparations as it increases the excitability of the network and therefore ensures rhythmic output after a sensory stimulation which may not otherwise be observed using just aCSF (Fig. 12)

When examining the effects of dopamine on sensory-evoked locomotor-related output, we first compared the effects of dopamine on episode duration in general (without consideration of STMM) (Fig.12). A two-way ANOVA was performed to determine the effect of genotype and dopamine on episode duration. There was found to be no significant interaction between genotype and dopamine on episode duration (Fig. 12C, WT n=12, T613M n=11, $F_{(1,34)}$=0.55, p=0.4634) but there was a main effect of dopamine ($F_{(1,34)}$=9.134, p=0.0047) with dopamine making the episode duration significantly longer in both genotypes.

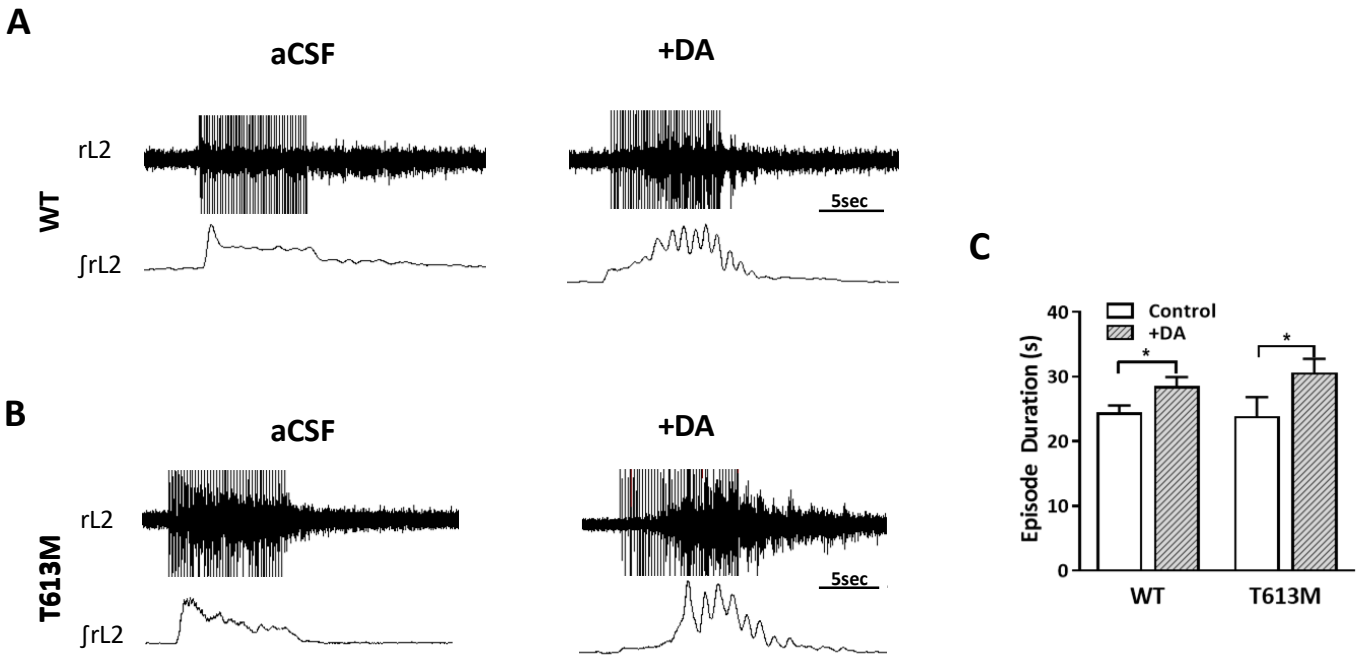

Figure 12. Dopamine does not differentially affect sensory-evoked locomotor-related output in WT and T613M animals. (A) Raw and rectified/integrated (∫) traces showing sensory-evoked locomotor-related output from a WT preparation before and after the application of dopamine (DA, 50µM). (B) Raw and rectified/integrated (∫) traces showing sensory-evoked locomotor-related output from a T613M preparation before and after the application of DA (50µM). (C) Mean episode duration of sensory-evoked locomotor-related activity before and after application of DA in WT and T613M preparations. *, $p<0.05$ with an unpaired t-test.

Next, I examined the effect of dopamine on STMM in both WT and T613M preparations (Fig. 13). As sensory-evoked locomotor-related bursts lack reliable rhythmicity within the episode, only episode duration was used in this comparison. I examined the effect of dopamine and genotype on STMM at both 30 second and 15 second stimulation intervals.

A three-way ANOVA was performed to determine the effect of genotype, dopamine, and stimulation interval on episode duration. With 30 second stimulation intervals, there was found to be no interaction between stimulation interval, dopamine, and genotype on episode duration (Fig.13Cii, WT n=12, T613M n=7, $F_{(2,29)}$=1.396, p=0.2638) and no interaction between stimulation interval and dopamine ($F_{(2,29)}$=0.9978, p=0.1884). With the 15 second stimulation interval, there was also found to be no significant interaction between stimulation interval, dopamine, and genotype on episode duration (Fig. 13Cii, WT n=12, T613M n=7, $F_{(2,29)}$=3.216, p=0.0548) and no interaction between stimulation interval and dopamine ($F_{(1.226,17.78)}$=4.014, p=0.7205).

From this we can conclude that dopamine increases the duration of sensory-evoked locomotor-related episodes but does not affect STMM in WT or T613M preparations.

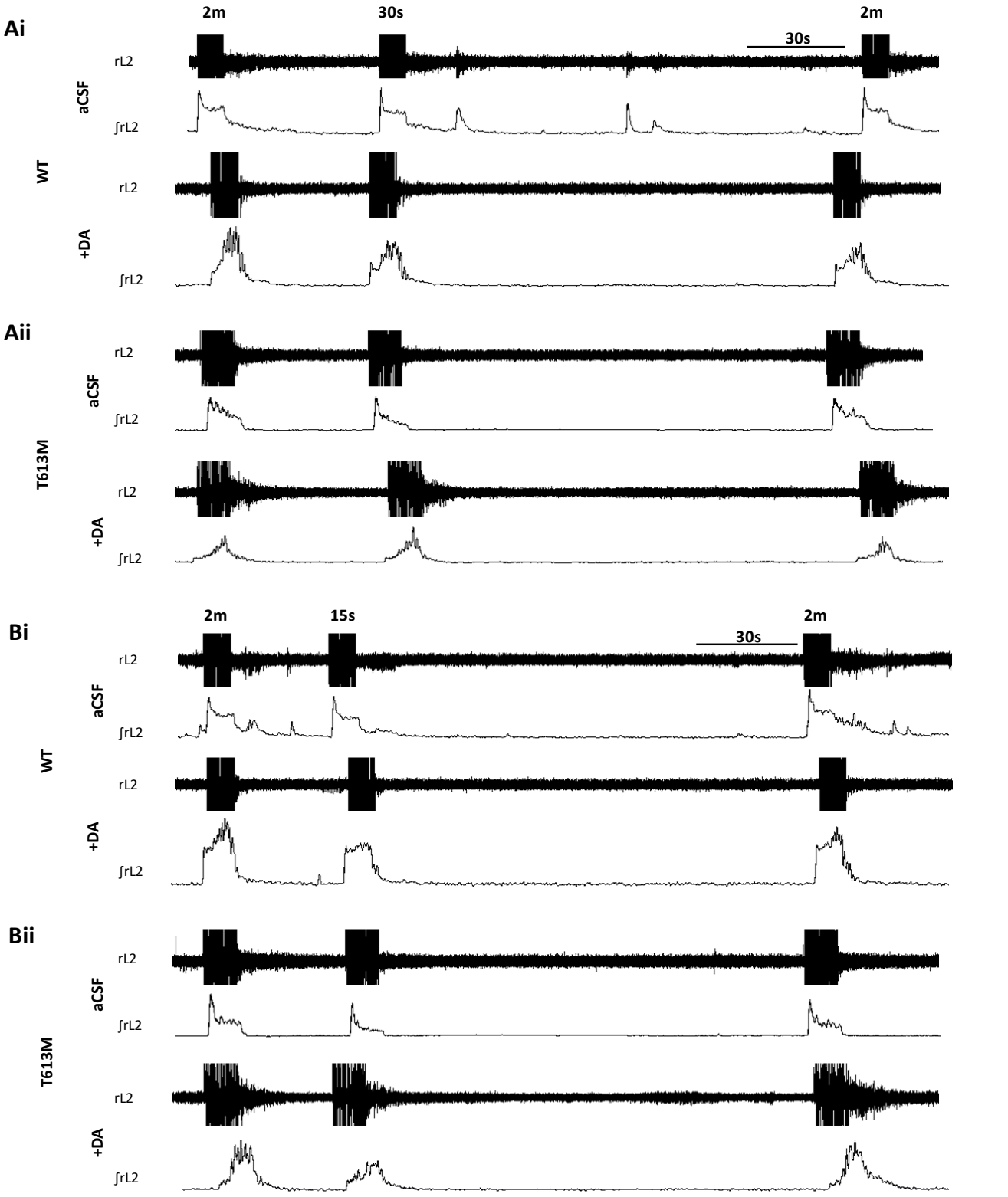
Ai
2m
30s
2m
30s
rL2
aCSF
∫rL2
WT
rL2
+DA
∫rL2
Aii
rL2
aCSF
∫rL2
T613M
rL2
+DA
∫rL2
Bi
2m
15s
2m
30s
rL2
aCSF
∫rL2
WT
rL2
+DA
∫rL2
Bii
rL2
aCSF
∫rL2
T613M
rL2
+DA
∫rL2
Ci
Episode Duration (s)
40
30
20
10
0
2m
30s
2m
Cii
Episode Duration (s)
40
30
20
10
0
2m
15s
2m
WT
WT +DA
T613M
T613M +DA

Figure 13. Dopamine does not differentially affect short-term motor memory in WT and T613M animals. (Ai) Raw and rectified/integrated (∫) traces showing a STMM sweep with a 30 second stimulation interval in a WT preparation before and after application of DA (50 µM). (Aii) Raw and rectified/integrated (∫) traces showing a STMM sweep with a 30 second stimulation interval in a T613M preparation before and after application of DA (50 µM). (Bi) Raw and rectified/integrated (∫) traces showing a STMM sweep with a 15 second stimulation interval in a WT preparation before and after application of DA (50 µM). (Bii) Raw and rectified/integrated (∫) traces showing a STMM sweep with a 15 second stimulation interval in a T613M preparation before and after application of DA (50 µM). (Ci) Mean episode duration of sensory-evoked locomotor-related output at two minute and 30 second stimulation intervals for WT (*n*=12) and T613M (*n*=11) preparations before and after the application of DA (50 µM). (Cii) Mean episode duration of sensory-evoked locomotor-related output at two minute and 15 second stimulation intervals for WT (*n*=12) and T613M (*n*=7) preparations before and after the application of DA (50 µM).

Effects of increased intracellular Na^+ on drug-induced locomotor-related output in T613M mice

Finally, we investigated the effect of the T613M mutation on drug-induced locomotor-related output. In this preparation, the motor network is stimulated via the application of a cocktail of pharmacological agents as opposed to an electrical stimulus to the dorsal root. As reviewed in the General Introduction, discrete central pattern generators in the spinal cord are sufficient to produce locomotor-related output without input from higher brain centres, however the command to initiate locomotion does come from these higher centres. To mimic this descending input in an isolated spinal cord preparation, a combination of dopamine, serotonin, and *N*-methyl-d-aspartic acid is applied to the spinal cord to initiate locomotion.

Pharmacological blockade of the sodium-potassium pump using ouabain has been shown to increase the frequency of drug-induced locomotor-related bursts, similar to the effects observed on sensory-evoked locomotor-related activity (Picton *et al.* 2017). We therefore predicted we would see a similar effect in the T613M animals.

We did not observe any differences in burst parameters such as burst frequency (Fig. 14Ci, WT 0.221 ± 0.032, T613M 0.226 ± 0.0179, p= 0.8881) or burst duration (Fig. 14Cii, WT 1668 ± 74.59, T613M 1736 ± 120.6, p=0.6702) between WT and T613M preparations (WT n=10, T613M n=14) using unpaired t-tests.

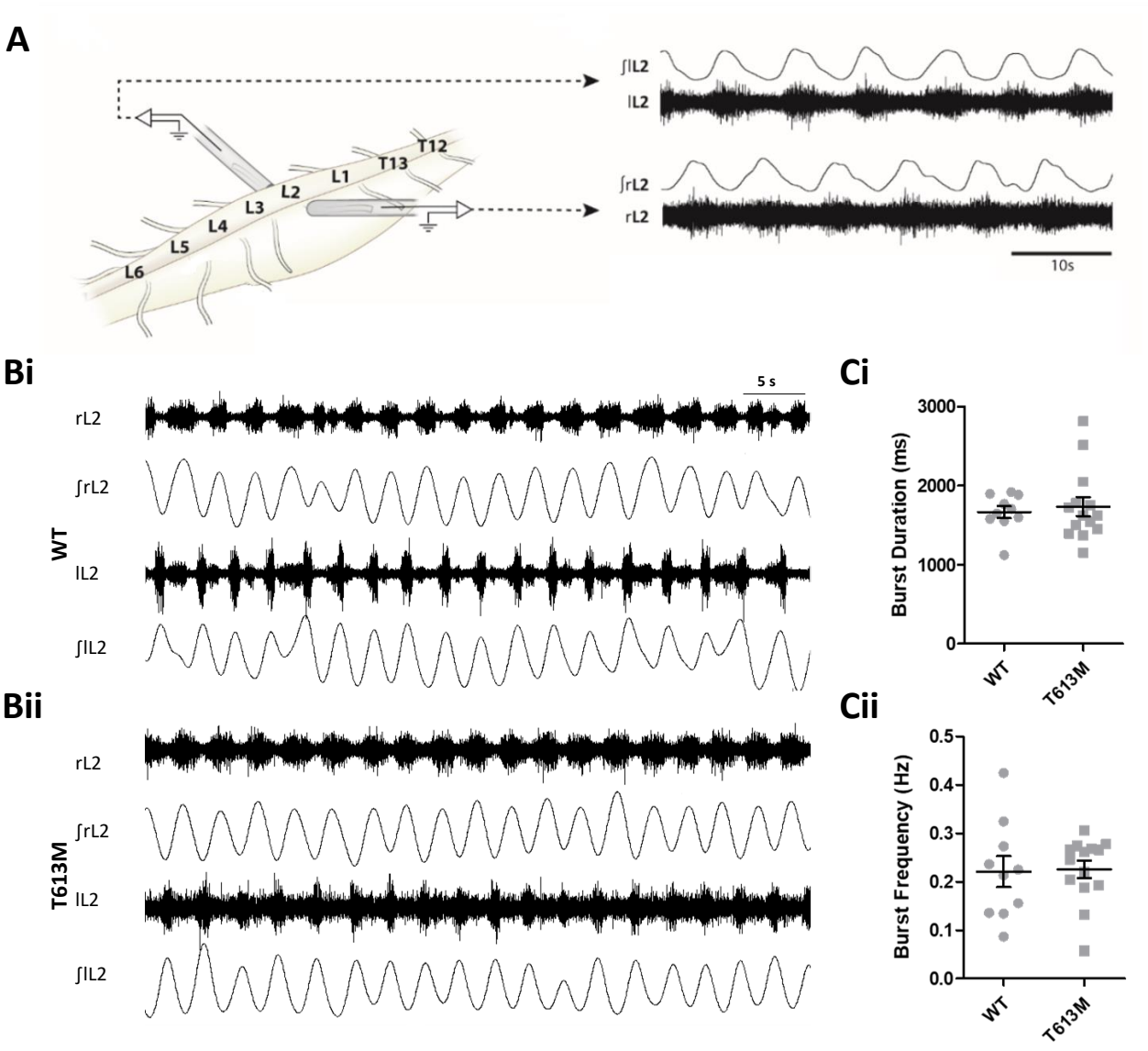

Figure 14. T613M does not affect drug-induced locomotor-related output under baseline conditions. (A) Schematic illustrating an isolated spinal cord preparation with glass suction electrodes placed on the second lumbar ventral roots for the recording of locomotor-like activity. (Modified from Picton *et al.* 2017) (Bi) Raw and rectified/integrated (∫) traces showing drug-induced locomotor-like output from the left and right L_2 ventral roots of a wildtype (WT) preparation. (Bii) Raw and rectified/integrated (∫) traces showing drug-induced locomotor-like output from the left and right L_2 ventral roots of a T613M preparation. (Ci) Mean locomotor-related burst duration of WT and T613M preparations (WT n=10, T613M n=14, p=0.67). (Cii) Mean locomotor-related burst frequency of WT and T613M preparations (WT n=10, T613M n=14, p=0.88).

We questioned whether the motor network was truly being challenged when producing drug-induced locomotor-related rhythms to the point at which a deficit produced by a lack of functioning α3-NKA may be revealed. Unfortunately, while cardiac glycosides like ouabain exist to block pump function, there is no known pharmacological 'activator' of the sodium-potassium pump. Instead, we chose to apply the sodium ionophore monensin which produces an increase in intracellular [Na^+] which will indirectly increase pump function. By applying the monensin to this protocol, we can therefore 'challenge' the sodium-potassium pump.

Previous work by Picton and colleagues (2017) showed that, when monensin was applied to WT drug-induced locomotor preparations, the sodium ionophore had the opposite effect on the locomotor-related rhythm as the sodium-potassium pump blocker ouabain, further supporting that the drug is indirectly activating the pump. Picton and colleagues (2017) observed a slowing of the locomotor-related rhythm with the application of monensin.

We therefore aimed to replicate these experiments using the T613M mutant mouse model to see how the T613M mutation affected the motor network's ability to cope with large increases in intracellular [Na^+] (Fig. 15). According to the results of unpaired t-tests, we were able to replicate the results shown by Picton and colleagues, observing a reduced burst frequency in WT drug-induced locomotor-related rhythms after the application of monensin (Fig. 15Bi, Baseline 0.1737 ± 0.021, Monensin 0.1036 ± 0.013, n=10, p=0.0005). This relationship, however, was not as strong in the T613M preparations (Fig. 15Bi, Baseline 0.128 ± 0.024, Monensin 0.1098 ± 0.027, n=9, p=0.1933). We also observed a small but significant increase in the burst duration in WT preparations (Fig. 15Bii, Baseline 1496 ± 114, Monensin 1994 ± 216.2, n=10, p=0.0305) which was also not observed in the T613M preparations (Fig. 15Bii, Baseline 1601 ± 147.8, Monensin 1621 ± 162.4, n=9, p=0.9012). No change was observed in burst amplitude after the application of monensin in WT (Fig. 15Biii, Baseline 350.7 ± 30.47, Monensin 342.7 ± 34.6, n=10, p=0.5207) or T613M preparations (Fig. 15Biii, Baseline, 298.7 ± 40.92, Monensin 299 ± 50.19, n=9, p=0.9793).

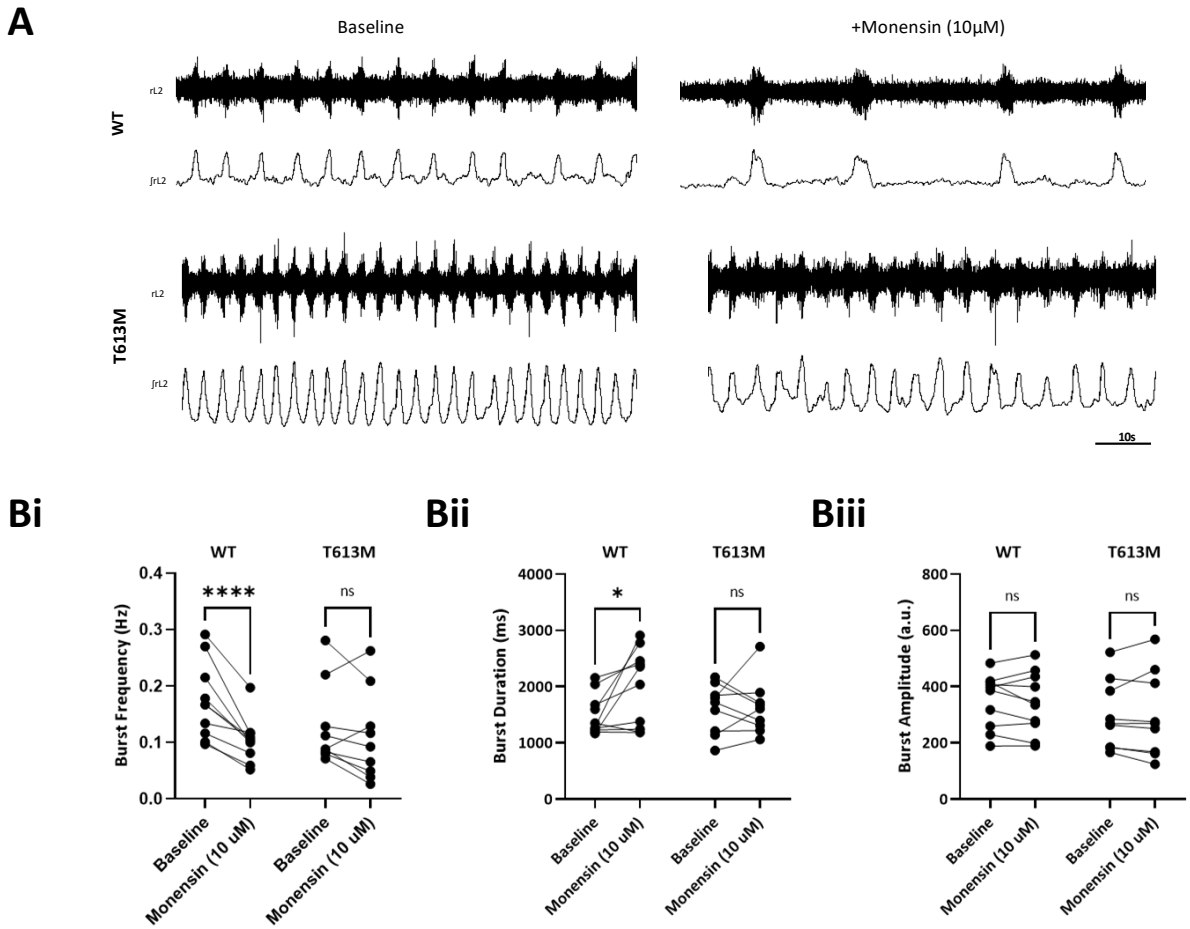

Figure 15. T613M reduces the ability of the spinal motor network to regulate activity after large increases in intracellular [Na^+]. (A) Raw and rectified/integrated (∫) traces showing drug-induced locomotor-like output from the right L_2 ventral roots of a wildtype (WT) preparation and T613M preparation at baseline and after application of the sodium ionophore monensin (10µM). (Bi) Mean locomotor-related burst frequency before and after application of monensin of WT preparations (n=10, p=0.0005) and T613M preparations (n=9, p=0.1933). (Bii) Mean locomotor-related burst duration before and after application of monensin for WT preparations (n=10, p=0.0305) and T613M preparations (n=9, p=0.901). (Biii) Mean locomotor-related burst amplitude before and after application of monensin for WT preparations (n=10, p=0.5207) and T613M preparations (n=9, p=0.9793). *, p<0.05; **, p<0.01, ***, p<0.001 with a paired t-test.

Discussion

In this chapter, we utilised a novel *ATP1A3* mutant mouse model harbouring the T613M mutation commonly seen in patients with Rapid-Onset Dystonia Parkinsonism (Barbano *et al.*, 2012) to gain insight into the role of α3-NKA in healthy and disordered spinal motor networks.

In collaboration with Evgeny Akkuratov and colleagues at the Karolinska Institutet, we showed that the T613M mutant mouse is hyperactive and hyperambulatory. Higher levels of activity were observed in T613M mice in an open field, with T613M mice travelling 50% greater distance than their wildtype counterparts. T613M mice also moved at a higher velocity than wildtype mice with a higher frequency of stepping observed (Fig. 1). This hyperactivity combined with the hyperambulation observed falls in line with what has been observed in many other mutant *ATP1A3* mouse models (reviewed in Ng, Ogbeta and Clapcote, 2021). Although originally characterised as quite a severe phenotype, further research into larger cohorts of RDP patients suggest that many cases could be much less severe with only mild motor deficits observed in the limbs (Brashear *et al.*, 2007; Haq *et al.*, 2019), very alike what we observed here with our T613M mouse model.

Perhaps what is most interesting about the behavioural studies conducted on the T613M mouse model and other mouse models harbouring *ATP1A3* mutations is the consistent hyperactivity observed in these animals. Given what we know about the role of the usAHP in the spinal cord from studies completed by Zhang and colleagues (2012) and Picton and colleagues (2017), one might expect that if the usAHP is α3-NKA mediated, then any mutation that effects α3-NKA function will affect the production of the usAHP. We know that when the α3-NKA is blocked pharmacologically with ouabain, the usAHP is diminished in motor neurons and the locomotor-related output recorded from isolated spinal cords that is linked to stepping increases in frequency. We would predict that this increase in burst frequency of the locomotor-related output would translate to increased rate of movement in the intact animal which is indeed what we have observed here. This lends support to the role of the α3-NKA mediated usAHP in regulating rhythmic output of the lumbar spinal cord. Interestingly, it also

raises the question of the involvement of potential spinal pathology in the manifestation of RDP and other *ATP1A3*-related disorders.

In collaboration with Evgeny and colleagues, we also conducted sodium imaging experiments to determine whether the T613M mutation affected the α3-NKA's ability to extrude sodium and therefore maintain sodium homeostasis. We found that T613M-affected neurons had higher basal sodium concentrations in the soma and dendrites than WT neurons and showed significantly lower sodium extrusion rate (Fig. 2). This shows that the T613M mutation does significantly affect neuron function by reducing the capacity for sodium homeostasis to be reached after periods of suprathreshold neuronal activity.

To begin our examination of the involvement of the α3-NKA in the regulation of motor output and any potential spinal motor pathology in RDP, we began with a physiological analysis of lumbar motor neurons from T613M mice. We found that WT and T613M-affected motor neurons did not differ in terms of passive properties such as input resistance or capacitance, but T613M-affected motor neurons did have a significantly more hyperpolarised resting membrane potential than WT motor neurons (Fig. 3). This could be due to a compensatory upregulation in α1-NKA, the sodium-potassium pump isoform thought to contribute to the resting membrane potential, in response to the α3-NKA knockdown mutation in this animal. Compensatory upregulations of unaltered α-subunit isoforms has been observed in other *ATP1A3* genetic models, with Moseley and colleagues (2007) observing a 35% increase in α1-NKA expression in the brain of their heterozygous α3-NKA knock-down mouse model. Potential compensatory upregulation of other membrane proteins should therefore be kept in consideration when interpreting the results of experiments using the T613M model. This is a disadvantage of using this genetic model to study α3-NKA function instead of pharmacological manipulation, however future experiments could utilise in situ hybridisation on T613M-affected

lumbar spinal tissue to determine if there is any compensatory upregulation of α1-NKA or WT α3-NKA in these animals. A Cre-loxP conditional knockout genetic model with viral vector/exogenous inducer-mediated Cre expression could also be utilised to overcome the challenge of compensatory upregulation.

We found that T613M-affected and WT motor neurons were comparable in terms of their single-action potential properties (Fig. 4), and the parameters of their frequency-current relationship: a measure of neuronal excitability in response to a brief stimulation (Fig. 5). Intracellular concentrations of sodium and potassium have been shown to respond to increased levels of neuronal activity on relatively slow timescales (Cressman *et al.*, 2009; Hübel, Schöll and Dahlem, 2014; Contreras *et al.*, 2021), with increases in intracellular sodium concentrations observed on the order of 3—10 seconds in mammalian pyramidal neurons (Gulledge *et al.*, 2013). With this in mind, a lack of effect of T613M is not entirely surprising, as the stimuli applied to neurons as part of these protocols are over particularly short time courses (one second or less), and the amount of intracellular sodium accumulating from these levels of neuronal firing would be unlikely to activate a significant number of α3-NKA in these cells and thus would be unlikely to reveal any physiological deficit that the T613M mutation may cause.

Next, we characterised the post-discharge activity of T613M-affected motor neurons (Fig. 5). Due to the proposed role for α3-NKA in the production of a large hyperpolarisation after prolonged periods of suprathreshold neuronal activity, we expected any physiological deficits caused by the T613M mutation to present themselves post-discharge. We found that approximately 20% of motor neurons showed an usAHP at baseline with 14% showing a slow afterhyperpolarisation (sAHP), and the remaining 66% showing an afterdepolarisation (ADP). T613M-affected motor neurons did not produce usAHPs, with instead 4% of neurons surveyed exhibiting an sAHP and the remaining 94% exhibiting an

ADP. These data suggest that the T613M mutation, although only affecting half of the α3-NKA expressed in these heterozygous animals, produces a haploinsufficiency in terms of usAHP production in lumbar motor neurons. These data provide the first definitive evidence for the essential role of the α3-NKA in mediating the usAHP observed in motor neurons and neurons more generally.

What is also interesting is that, even though the α3-NKA is not thought to be involved in the production of sAHPs or ADPs, the proportions of these post-discharge activity phenotypes also differ in T613M-affected neurons. One might expect that those neurons that would have otherwise had an usAHP would instead simply produce an sAHP without the hyperpolarising input of the α3-NKA. But instead, even fewer T613M-affected neurons are hyperpolarised, with almost all motor neurons surveyed showing ADPs. If the membrane potential of the cell is depolarised after firing, less input is required to elicit future activity, as can be seen by the examples of rebound firing and plateau potentials produced because of an ADP in Fig. 5. In this sense, T613M does not only render the motor neuron incapable of producing an usAHP but increases the excitability of the neuron in general post-discharge. The ADP therefore has the exact opposite functional significance of the usAHP, which is thought to act as a fatigue-prevention mechanism. T613M-affected motor neurons may be more likely to be active, producing cumulative effects on network output which may translate into behavioural phenotypes such as fatigue or dystonia. The lack of usAHPs and increased occurrence of ADPs in these motor neurons may therefore produce cumulative network effects that contribute to the manifestation of RDP symptoms. We would predict these changes in post-discharge activity profile to also occur in the interneurons that comprise the central pattern generators of the spinal cord. Further investigation into the post-discharge activity profiles of spinal interneurons in WT and T613M-affected animals would help to determine their contribution to any cumulative effects on network output.

To further investigate the fundamental role of the α3-NKA in motor output now that we know that T613M-affected motor neurons do not produce usAHPs, we conducted a series of experiments using

isolated spinal cords to examine motor network output. After we observed hyperactive behaviour in the intact animal, we first investigated whether there was any increase in spontaneous output from the isolated spinal cord of T613M mutant mice (Fig. 6). We did not find this to be the case, however we questioned whether, without a stimulus, there would be enough network activity to activate the dynamic α3-NKA.

We next examined sensory-evoked motor output in WT and T613M animals (Fig. 7). A series of current pulses were applied to the dorsal root of an isolated spinal cord preparation and the activity of the ventral roots was recorded. We found that T613M preparations did not differ in the episode duration from the sensory stimulus but did exhibit higher intra-episode burst frequency. When the α3-NKA is pharmacologically blocked with ouabain, episode duration was found to increase as well as burst frequency in WT preparations (Picton *et al.* 2017). Similar effects on swim bout duration have been observed with bath application of ouabain in *Xenopus* tadpoles (Zhang and Sillar, 2012). This discrepancy may be due to the T613M model acting as a 'half-block' of α3-NKA function as the animals are heterozygous for the mutation. The effect of the T613M mutation may therefore be expected to be more nuanced than that observed with pharmacological inhibition of α3-NKA. However, the observed increase in burst frequency in T613M-affected preparations does support a role for α3-NKA in the regulation of locomotor-related output.

Zhang and colleagues (2012, 2015) and Picton and colleagues (2017) showed that the inter-episode interval determines the duration and frequency of locomotor-related output. In summary, they predict that a short-term motor-memory of previous network activity is produced by the ultra-slow afterhyperpolarisation. If the network is stimulated within the length of the usAHP (>20s), consecutive bouts of locomotor-related output will be shorter in duration and intra-episode bursts will be less frequent. It is speculated that this may act as a fatigue-prevention mechanism within the network. As the usAHP is α3-NKA mediated, blocking the α3-NKA with ouabain diminishes the short-term motor

memory, with consecutive bouts of locomotor-related output being of comparable duration and burst frequency regardless of inter-episode interval. As this appears to be an important physiological function of the usAHP, we examined whether short-term motor-memory was intact in T613M preparations (Fig. 7, 8). We applied the short-term motor-memory paradigm to these preparations using 30 second and 15 second stimulation intervals. The results, however, were conflicting and difficult to meaningfully interpret.

Short-term motor-memory appeared to be less robust than previously reported with our preparations. Episode duration and burst frequency were not reliably shorter in WT preparations when the inter-episode interval was reduced, making any differences observed between WT and T613M preparations difficult to interpret.

Any differences between the data presented here and that presented by previous groups (Zhang and Sillar, 2012; Zhang *et al.*, 2015; Picton *et al.*, 2017) may be due to slightly different protocols used to elicit STMM. In our paradigm, we applied discrete STMM 'sweeps'. Current pulses were applied two minutes after the previous sweep, 30 or 15 seconds after activity returned to baseline, and then two minutes after the shorter interval when the network was considered to be 'recovered'. The averages of 3-5 sweeps were then used in our analysis. Picton and colleagues, however, continually stimulated the preparation every 100 seconds, which would occasionally be interrupted at 30 or 15 second episode intervals. There is a possibility that the continual stimulation resulted in a sort of 'entrainment' of the network that made the effect of the shortened inter-episode interval more pronounced. Entrainment of spinal central pattern generators has been documented in response to mechano-sensory feedback in the lamprey spinal cord (Grillner, McClellan and Perret, 1981; McClellan and Sigvardt, 1988) and in response to ventral root stimulation in disinhibited spinal cord preparations of the neonatal mouse (Bonnot *et al.*, 2009; Nagaraja, 2020).

Ultimately, STMM did not appear to be completely absent in T613M mice, which does call into question the involvement of the α3-NKA mediated usAHP in the production of STMM. An interesting

increase in burst frequency with 15 second stimulation intervals was observed in the T613M preparations, which may allude to a reduced capacity for the T613M-affected network to extrude the accumulated intracellular sodium from the first episode. Further experiments using alternate paradigms for eliciting STMM, such as the 'entrainment' paradigm used previously, will be required to draw more confident conclusions on the role of the α3-NKA in STMM, and any changes in STMM related to movement disorders such as RDP.

Previous work by Picton and colleagues (2017) found the effect of ouabain on locomotor-related output to be dopamine dependent. They show that dopamine enhances the size of the usAHP, making the effects of the pharmacological block more prominent. These results are physiologically relevant as dopamine is an important modulator of motor circuits (see General Introduction) which is released into the spinal cord during locomotion in mammals (Gerin, Becquet and Privat, 1995). In fact, it is important to consider the effects of known spinal neuromodulators on α3-NKA and α3-NKA mediated conductances as the α3-NKA is a well-studied target of modulation. Dopamine, acting upon Protein Kinase A (PKA) as part of the cAMP-PKA signalling pathway, has been shown to modulate the responsiveness of a neuron to changes in intracellular sodium concentrations via phosphorylation/dephosphorylation of the α3-NKA (Azarias *et al.*, 2013). D1 and D2 receptors have also been shown to form a complex with α3-NKA, enabling direct reciprocal modulation (Hazelwood *et al.*, 2008). Furthermore, intense motor activity results in increased dopamine release which is thought to contribute to central fatigue (Meeusen *et al.*, 2012). With all this in mind, we thought to further examine the relationship between dopamine, the usAHP, and the α3-NKA using our T613M mouse model.

First, we examined the dopamine-evoked motor rhythms of WT and T613M preparations. Bath application of dopamine alone produces a slow, synchronous rhythm (Sharples and Whelan, 2017). When examining the dopamine-evoked rhythms in WT and T613M preparations, we found that

dopamine-evoked rhythms of T613M preparations were less frequent with larger inter-episode intervals (Fig. 9). This could imply that the usAHP plays a role in regulating dopamine-evoked rhythms.

In all other rhythmic motor activity examined in this chapter, reduced α3-NKA function in presumed to reduce the usAHP and therefore put the network into a more excitable state. Logically, this would translate into an increase in the activity of the network. However, the opposite is observed with dopamine-evoked rhythms. While this may be difficult to rationalise, a recent computational study conducted by Sharples and colleagues (2022) suggests that this would indeed be in the case with slightly reduced α3-NKA function, as opposed to a full pharmacological block with ouabain.

Alternatively, the slower and less frequent dopamine-evoked rhythms could suggest that T613M-affected spinal cords respond differentially to the application of dopamine, potentially due to formation of faulty receptor complexes. It is possible that other motor output paradigms used here may be differentially affected by the presence of dopamine between WT and T613M preparations. We therefore examined the effect of dopamine on sensory-evoked locomotor-related output and short-term motor memory in WT and T613M preparations.

In many preparations, rhythmic output was not observed in response to sensory stimulation without the presence of dopamine (Fig. 10). This may be due to the network being in a lower excitation state than that needed to produce rhythmic output (as described in Sharples and Whelan, 2017). As a result of this, when comparing the effects of dopamine on sensory-evoked output between WT and T613M preparations we could only analyse episode duration. Application of dopamine was found to increase the duration of sensory-evoked locomotor-related episodes in both WT and T613M preparations to a similar extent. Dopamine also did not appear to differentially effect the STMM of WT and T613M preparations (Fig. 11).

Finally, we utilised the canonical drug-induced locomotor preparation to examine any potential differences in motor output between WT and T613M preparations. Application of ouabain was found to increase the frequency of locomotor-related bursts in this preparation by Picton and colleagues (2017), however we saw no differences in the burst frequency or burst duration of the drug-induced locomotor-related rhythms between WT and T613M preparations (Fig. 12). This was surprising given data from previous studies. We questioned, since the T613M model is heterozygous, whether baseline activity levels produced by the application of the locomotor cocktail were perhaps not accumulating enough intracellular sodium to provide a challenge to the α3-NKA. Given that T613M animals are heterozygous and still express 50% WT α3-NKA, there may be enough functional α3-NKA present to cope with lower levels of activity and therefore a deficit would not be revealed. Unfortunately, there is no known pharmacological activator of the α3-NKA, so the sodium ionophore monensin was utilised to activate the α3-NKA indirectly through an increase in intracellular sodium. Previous work by Picton and colleagues (2017) showed a slowing of the drug-induced locomotor-related rhythm after application of monensin: the opposite effect of blocking the α3-NKA with ouabain. As with the effect of ouabain, they postulate that this is due to modulation of the usAHP. With more α3-NKA active, more cells will be hyperpolarised and therefore the locomotor-related rhythm would slow. Interestingly, after the application of monensin a difference between WT and T613M preparations was revealed (Fig. 13). WT preparations showed a consistent slowing of the drug-induced locomotor-related rhythm, whilst this relationship was greatly weakened in the T613M preparations. In some T613M preparations, the locomotor-related rhythm increased in frequency, which is what we may expect if the network is not able to extrude the increased intracellular sodium accumulated by the application of monensin and thus becomes more depolarised. It is possible, therefore, that by challenging the network we have unveiled a deficit caused by the T613M mutation. As we know from our sodium imaging data, T613M-affected neurons are less effective as extruding sodium and therefore maintaining sodium homeostasis.

While the single-cell physiological data shows a clear effect of the T613M mutation on post-discharge activity in lumbar motor neurons, the isolated spinal cord data tells a slightly more nuanced story. It proves difficult to compare the use of a heterozygous knock-down model with pharmacological data. The data from the drug-induced locomotor preparations suggest that perhaps a 'challenge' is required to reveal the deficits caused by the T613M mutation. In future research, this should be considered. Particularly with the sensory-evoked locomotor preparations, either an increase in the intensity of sensory input or the application of monensin should be utilised to determine whether a clearer effect of the mutation on sensory-evoked locomotor-related output and short-term motor memory can be seen.

In summary, in this chapter I have provided a characterisation of a novel T613M model for RDP. Our behavioural studies show motor deficits in line with patient studies and other *ATP1A3* mutant models. We propose a potential mechanism for the hyperactivity observed in our behavioural studies through an observed loss of the usAHP in lumbar motor neurons and a reduced capacity of the spinal motor network to respond to rapid increases in intracellular sodium brought about by the application of monensin. Our data suggests a novel role for motor neurons in the pathophysiology α3-NKA of Rapid-Onset Dystonia-Parkinsonism, where pathology has largely been thought to be centred in the higher brain centres contributing to the control of movement such as the cerebellum (Fremont *et al.*, 2014). As *ATP1A3*-related disorders exist on a phenotypic spectrum, and hyperactivity and motor deficits have been observed in animals models for other *ATP1A3*-related disorders such as Alternating Hemiplegia of Childhood (AHC) (reviewed in Ng, Ogbeta and Clapcote, 2021), it is possible that the results we have found here may be applied to other *ATP1A3*-related disorders such as AHC, and beyond into movement disorders in general.

While these implications for disease are exciting, these data do bring into question the more fundamental role of the usAHP in motor regulation. Although the use of a heterozygous genetic model to study the functional significance of the α3-NKA is a caveat, it was surprising to not be able to replicate the results of pharmacological experiments more closely, particularly those involving short-term motor memory. What is perhaps most interesting is the lack of obvious network effects given that no usAHPs were observed in the lumbar motor neurons. If the usAHP plays such an important physiological role in regulating rhythmic output, one might expect catastrophic effects on the network when almost all motor neurons exhibit ADPs instead. This suggests that, either it is not the motor neurons that are contributing to this regulatory role and perhaps instead the interneurons that comprise the central pattern generators of the spinal cord, or that the usAHP itself is not as critical as we once thought. This further speaks to the need to investigate the post-discharge activity of spinal interneurons in WT and T613M-affected animals.

Picton and colleagues (2017) suggest the heterogeneity of usAHP expression in motor neurons to be purposeful, as complete inhibition of the motor neurons after a period of high neuronal activity would render an animal paralysed – a fatal outcome when attempting to escape a predator. However, if the usAHP is functionally significant in this way then surely other post-discharge activity phenotypes such as sAHPs and ADPs are as well. These data highlight how little we know about the functional significance of post-discharge activity more generally on motor output, and why we see such a variety of phenotypes in a single cell type. I will attempt to address these questions and more in Chapter 2: *Characterising post-discharge activity in motor neurons*.

Chapter 2: *Characterising post-discharge activity in motor neurons*

Chapter 2 contributions:

All experiments were conducted by Francesca Sorrell besides the data presented in Figures 5-7 which were collected in collaboration with Gina Gnanasampanthan. Whole-cell patch-clamp data using muscarine were collected by Dr. Simon Sharples. Francesca Sorrell designed all experiments, interpreted all data, and constructed all figures.

Summary

In Chapter 1, we utilised an α3-NKA knock-down mouse model to investigate the functional significance of the α3-NKA in the regulation of motor output in health and disease. We found that lumbar motor neurons of α3-NKA knock-down mice do not exhibit usAHPs, however the loss of this α3-NKA mediated conductance translated into only minor network-level changes. This suggests that the influence of a neuron's post-discharge activity on motor output may be more complex than initially thought.

In this chapter, we aim to more generally characterise the post-discharge activity of motor neurons so that we may gain inference on not only the role of the usAHP, but also other post-discharge polarisations, on network-level output. We show that post-discharge activity can be broadly categorised into three subtypes: afterdepolarisations (ADPs), slow afterhyperpolarisations (sAHPs), and ultra-slow afterhyperpolarisations (usAHPs), and that these subtypes are consistent regardless of stimulus intensity.

We show that usAHPs are more commonly observed in the second postnatal week and suggest that this may be due to an upregulation of α3-NKA in lumbar motor neurons alongside the development of weight-bearing locomotion. While the heterogenous distribution of usAHPs amongst populations of motor neurons was previously thought to be due to mosaicism of α3-NKA expression, we show that all lumbar motor neurons express α3-NKA. As an alternative to this hypothesis, we present data that suggests that neurons expressing low levels of α3-NKA may have weak NKA-mediated currents that are masked by competing conductances. We conclude that a neuron's post-discharge activity at baseline conditions is more likely to be determined by the complement of ion channels/membrane pumps expressed than the complete absence of said constructs in certain cells. Finally, we show that the post-discharge activity of a neuron can be modulated by extrinsic and intrinsic modulators such as 5-HT and muscarine to enhance or unmask certain post-discharge activity subtypes.

Introduction

In Chapter 1 of this thesis, we utilised an α3-NKA knock-down mouse model (T613M) to study the functional significance of the α3-NKA in the production of the usAHP and the regulation of motor output in both healthy and disordered spinal cords. We found that T613M mice did not produce usAHPs, providing definitive evidence that this hyperpolarising current is α3-NKA mediated. However, the complete lack of usAHPs in lumbar motor neurons translated to only minor effects on network-level output. Given the implied importance of the usAHP in the regulation of motor output from previous studies (Pulver and Griffith, 2010; Zhang and Sillar, 2012; Zhang *et al.*, 2015; Picton *et al.*, 2017) one might expect the complete lack of the α3-NKA mediated conductance to have catastrophic effects on network output, suggesting that the role of the usAHP (at least in motor neurons) is not as significant as we may have once thought.

Interestingly, T613M motor neurons did not exhibit slow AHPs in the absence of usAHPs, as one might expect given that the slow AHP is known to be Ca^{2+}-activated potassium channel mediated and does not involve the sodium-potassium pump (Kato *et al.*, 2006; Turner *et al.*, 2016; Tiwari *et al.*, 2018). Instead, almost all T613M motor neurons were found to be depolarised post-discharge. This suggests that the α3-NKA may not only play a role in the production of the usAHP but may contribute to the production of post-discharge activity in general.

The first focus of this chapter was to characterise this post-discharge activity more generally to determine the significance of not only the usAHP, but other post-discharge polarisations, on motor output. We found that post-discharge activity can be broadly categorised into three subtypes: afterdepolarisations (ADPs), slow afterhyperpolarisations (sAHPs), and ultra-slow afterhyperpolarisations (usAHPs). The polarisation (i.e., whether the post-discharge activity is depolarised or hyperpolarised relative to the resting membrane potential) of a given neuron's post-discharge activity is not input-dependent. Increased input to the neuron may increase the amplitude

of the post-discharge activity but will not convert an afterdepolarisation into an afterhyperpolarisation and vice versa. We sampled a significantly larger cohort of motor neurons than described in Chapter in an attempt to develop a more thorough understanding of the expression profile of these three post-discharge subtypes in lumbar motor neurons. We found the proportions to be similar but not identical: of the 166 motor neurons from wildtype mice surveyed, 96 displayed an afterdepolarisation (58%), 45 showed a slow afterhyperpolarisation (27%), and 25 showed an ultra-slow afterhyperpolarisation (15%).

Secondly, we wanted to investigate the factors that determine a given neuron's post-discharge activity at baseline conditions. We found that the expression profile of the post-discharge activity subtypes changes across the first two weeks of postnatal development. In the first postnatal week, the majority of motor neurons exhibited ADPs but a transition into the majority of motor neurons exhibiting AHPs occurred in the second postnatal week, with the exhibition of usAHPs peaking at the 8^{th} postnatal day. We show that this increase in usAHP prevalence coincides with an increased expression of α3-NKA in lumbar motor neurons at the beginning of the second postnatal week. This increase also aligns with the emergence of weight-bearing locomotion in these animals.

Picton and colleagues (2017) suggest that the heterogeneity of usAHP exhibition in lumbar motor neurons is purposeful, as a homogenous expression of such a prolonged hyperpolarisation may be catastrophic for the neural network. If all motor neurons were to, by chance, be hyperpolarised at once then there may not be enough net neural output from the spinal cord to generate a muscle contraction. In a life-or-death situation, like escaping from a predator, network failure in this manner would have fatal consequences. Picton and colleagues (2017) propose that expression of α3-NKA may be mosaic within the lumbar spinal cord. Cells expressing α3-NKA would generate an usAHP after a period of prolonged firing, and cells that do not express α3-NKA would not. However, genetic

knockdown of the α3-NKA caused almost all motor neurons sampled to exhibit ADPs which may suggest that the α3-NKA plays a role in determining the post-discharge activity of all neurons. We show that all lumbar motor neurons express some degree of α3-NKA, suggesting that mosaicism of α3-NKA expression is not the root determinant of post-discharge activity subtype.

We propose that instead, motor neurons expressing lower levels of α3-NKA may have weaker α3-NKA mediated currents such as the usAHP which could be masked by competing conductances. We show that, when pharmacological blockers of the ion channels and membrane pumps thought to mediate the different post-discharge activity subtypes are applied, a neuron's post-discharge activity can often be converted from an ADP to an AHP and vice versa. This implies that the post-discharge activity of a given neuron under baseline conditions is determined more by the complement of ion channels/membrane pumps expressed by the cell as opposed to any mosaicism of expression.

This flexibility of post-discharge activity subtype is further emphasised by the degree to which post-discharge activity can be modulated. The amplitude of the usAHP has been shown to be increased by dopamine (Picton *et al.*, 2017) and decreased by nitric oxide (Hachoumi *et al.*, 2022) in motor neurons. In this chapter, we show that another monoaminergic neurotransmitter 5-HT, as well as the cholinergic neurotransmitter muscarine, can not only enhance the size of the usAHP similarly to dopamine but can convert post-discharge activity from afterdepolarisations to afterhyperpolarisations.

These data allow a more holistic view of post-discharge activity as opposed to the discrete roles of the usAHP, sAHP, and sADP. Instead, post-discharge activity can be thought of as a phenotypic spectrum that allows motor neurons to be highly flexible to the ever-changing demands on the system.

Methods

Animal ethics and husbandry

The following experimental procedures were conducted in accordance with the UK Animals (Scientific Procedures) Act 1986, with approval from the Animal Welfare Ethics Committee (AWEC) of the University of St Andrews in line with UK Home Office regulations. Wild type (WT) neonatal mice used in the following experiments were bred on a C57BL/6 background acquired from Charles River Laboratories (Scotland, UK). Mice were housed in individually ventilated cages maintained at 22°C and 56% humidity with a 12h light-dark cycle. All animals had unrestricted access to food and water. Experiments were conducted on neonatal mice at postnatal day (P) 2-14.

In vitro spinal cord preparation

Neonatal mice were euthanised via cervical dislocation, decapitated, and eviscerated. Animals were secured to the base of a dissecting chamber filled with dissecting artificial cerebrospinal fluid (aCSF) (equilibrated with 95% oxygen, 5% carbon dioxide, ~4°C). A vertebrectomy was performed, removing the vertebrae covering the spinal cord. The cord was then isolated by separating the cord from the spinal roots with microscissors. Once isolated from the body, any remaining dorsal or ventral roots or connective tissue were trimmed away.

To produce spinal cord slices, the isolated cord was then set in 0.5% agar and immersed in a bath containing dissecting aCSF. A vibratome (Leica VT1200) was used to produce 300µm transverse slices of the lumbar region of the spinal cord. Lumbar slices were transferred to a chamber containing recovery aCSF (equilibrated with 95% oxygen, 5% carbon dioxide,) at ~34°C and allowed to recover for 30-45 minutes. Once recovered, the slices were transferred to a chamber containing recording aCSF (equilibrated with 95% oxygen, 5% carbon dioxide) at room temperature and allowed to equilibrate for approximately 30 further minutes before recording.

Electrophysiological recordings

Whole-cell patch clamp recordings of spinal motor neurons

Spinal lumbar slices were placed in a recording chamber containing aCSF perfused at a continuous rate of ~1 mL per minute. Whole-cell patch clamp recordings were made from motor neurons of the ventral horn. Motor neurons were identified by morphology, passive properties, and location within the ventral horn. Lumbar motor neurons are in discrete ventromedial and ventrolateral pools and differ from interneurons in whole-cell capacitance and input resistance (Carlin, Jiang and Brownstone, 2000). Borosilicated glass microelectrodes (2.5-5 MΩ) containing intracellular solution were attached to the membrane of the neurons via a high resistance (>1 GΩ) seal. Suction was applied to rupture the patch of membrane within the seal, allowing the intracellular fluid within the glass microelectrode to become continuous with the inside of the cell. Signals were amplified and filtered with a MultiClamp 700B amplifier (Molecular Devices, Sunnyvale, CA, USA) and acquired at >10Hz using a Digidata 1440A A/D board and pClamp software (Molecular Devices, Sunnyvale, CA, USA). All cells used for experiments showed a resting potential between -50 and -80 mV. Firing output was measured in current-clamp mode with a bias current applied to all cells to maintain a consistent resting membrane potential of -60mV between recordings. Firing output was measured either as a single action potential acquired by injecting a 10ms supramaximal current pulse, a series of 1s square step current pulses ranging from 50pA to 4000pA, or via a 10s square step current pulse/pulse train (30Hz) applied at an amplitude of ~1.5x rheobase.

Drugs and Solutions

Dissecting aCSF: 25mM NaCl, 188mM sucrose, 1.9mM KCl, 1.2mM NaH_2PO_4, 10mM $MgSO_4$, 1mM CaCl, 26mM $NaHCO_3$, 25mM glucose and 1.5mM kynurenic acid.

Recovery aCSF: 119mM NaCl, 1.9mM KCl, 1.2mM NaH_2PO_4, 10mM $MgSO_4$, 1mM CaCl, 26mM $NaHCO_3$, 20mM glucose and 1.5mM kynurenic acid.

Recording aCSF: 127mM NaCl, 3mM KCl, 2mM $CaCl_2$, 1mM $MgCl_2$, 26mM $NaHCO_3$, 1.25mM NaH_2PO_4, 10mM glucose.

Intracellular solution for patch clamp recordings: 14mM $KMeSO_4$, 10mM NaCl, 1mM CaCl, 10mM HEPES, 1mM EGTA, 3mM Mg-ATP and 45mM Mg-GTP.

Serotonin (5-HT; 10µM, Sigma-Aldrich, Poole, UK), Cadmium chloride (CdCl; 100µM, Sigma-Aldrich, Poole, UK), Apamin (100nM, Sigma-Aldrich, Poole, UK), Ouabain (3µM, Tocris Bioscience, Abindgon, UK).

Histology

Tissue preparation

Spinal cords were isolated using the same technique as described above before being submerged in 4% paraformaldehyde for 16-18 hours at 4°C. Cords were then placed in 30% sucrose solution at 4°C for 6 hours before being transferred to a 1:1 solution of 30% sucrose solution and Optimal Cutting Temperature (OCT) embedding compound for a further 30 minutes. Cords were then embedded in OCT and stored at -80°C. Cords were sectioned using a Leica CM1860 cryostat (20µm thickness) and mounted on Superfrost Plus (VWR) microscopy slides.

Tissue immunohistochemistry

Mounted tissue was washed three times with PBS before a blocking/permeabilisation solution was applied (3% Bovine serum albumin (BSA), 0.2% Triton X) and allowed to incubate for two hours at room temperature. The blocking/permeabilisation was removed and replaced with a primary antibody

solution consisting of 1.5% BSA, 0.1% Triton X and the following antibodies: Rabbit Anti-Alpha 3 Na^+/K^+ ATPase (Alomone, 1:250) and Goat Anti-Choline Acetyltransferase (Millipore, 1:200) and allowed to incubate at 4°C for 24 hours. The tissue was then washed 10 times for a total of 50 minutes in PBS before being incubated for 2 hours at room temperature in a secondary antibody solution consisting of 0.1% Triton X and the following antibodies: Donkey Anti-Rabbit Alexa 647 (Abcam, 1:500) and Donkey Anti-Goat Alexa 488 (Invitrogen, 1:500). Tissue was then washed a further 10 times for a total of 50 minutes before being briefly incubated for 10 minutes with DAPI (dH_20; Sigma-Aldrich, 1:1000) and washed once more in dH_20. Slides were then mounted using Vectashield Vibrance (Vector) mounting medium and a coverslip was applied. Control stainings for Donkey Anti-Rabbit Alexa 647 (Abcam, 1:500) and Donkey Anti-Goat Alexa 488 (Invitrogen, 1:500) were found to be devoid of labelling.

Fluorescence microscopy

Single focal plane images of motor neuron pools were captured at x63 magnification using a Zeiss Apotome 2 Structured Illumination microscope.

Data analysis

Whole-cell patch clamp recordings

Whole-cell patch clamp recordings were analysed using Clampfit (Molecular Devices, Sunnyvale, CA, USA). For the analysis of single action potentials, 10 waveform samples were averaged into a single representative waveform. This representative trace was then used to calculate the firing threshold, amplitude, rise time, half-width, and mAHP measurements for each cell. Frequency-current (f-I) relationships were determined from a series of 1s square current pulses ranging from 50pA to 4000pA.

Steady-state firing frequency (Hz) was determined from the last 500ms of the current pulse. Post-discharge activity denotes the activity of the cell after a period of prolonged firing (10s current step/pulse train). Post-discharge activity area (mVs) is a combined measure of voltage change and recovery time. The area measurement represents the area under/over resting membrane potential starting at the cessation of firing and ending once resting membrane potential has been restored.

Data are presented as mean ± standard error. In these data, the 'n' value represents the number of cells. All statistical comparisons were conducted using GraphPad (Prism 9).

Image analysis

Image analysis was conducted using FIJI (Schindelin *et al.*, 2012). Regions of Interest (ROI) maps were drawn around ChAT-positive motor neurons. ChAT fluorescence was used for the identification of motor neurons only and therefore was not quantified. The mean fluorescence intensity of the Rabbit Anti-Alpha 3 Na^+/K^+ ATPase antibody was measured for each ChAT-positive cell. Mean fluorescence intensity was averaged for all motor neurons in each animal to compare α3-NKA expression specifically in motor neurons. For comparisons between lateral and medial motor pools, pools were identified visually. To measure field intensity in the ventral horn more generally, ROIs were disregarded, and the mean fluorescence intensity of the entire image was measured. All statistical comparisons were conducted using GraphPad (Prism 9).

Results

The post-discharge activity of lumbar spinal motor neurons

First, we wanted to make a general characterisation of post-discharge activity in lumbar motor neurons. We found that post-discharge activity can be broadly categorised into three distinct subtypes: ultra-slow afterhyperpolarisations (usAHPs) characterised by a significant hyperpolarisation of the membrane potential from baseline (>5mV) and a significant recovery period (>20s); slow afterhyperpolarisations (sAHPs) characterised by a rapid hyperpolarisation of the membrane potential but a quick recovery period; and afterdepolarisations (ADPs) characterised by any depolarisation of the membrane potential for any length of recovery time after discharge (Fig. 1). All motor neurons surveyed showed one of these three subtypes of post-discharge activity under baseline conditions.

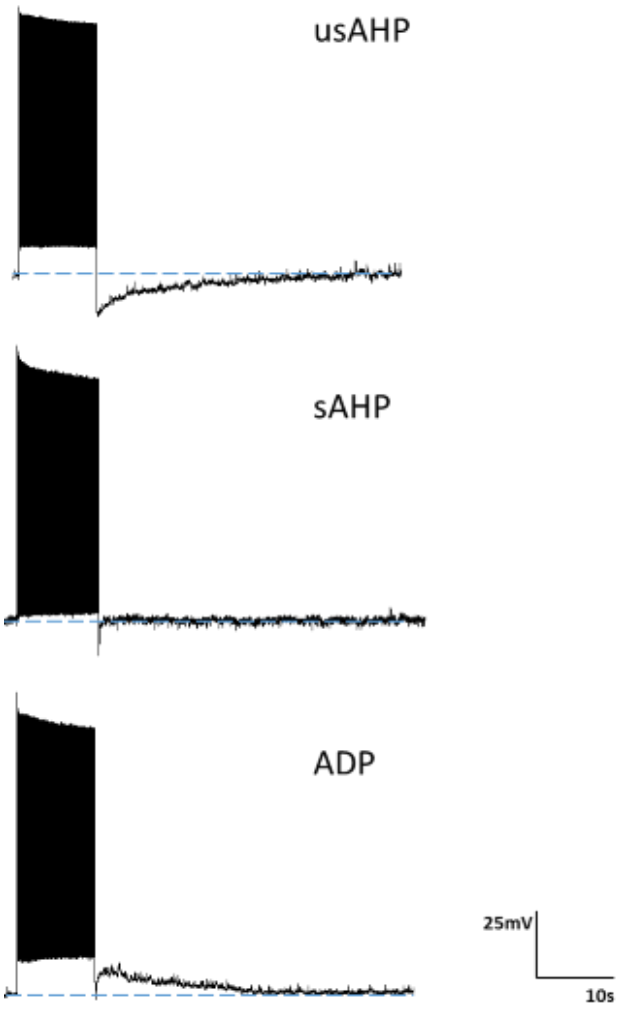

Figure 1. The post-discharge activity of lumbar spinal motor neurons can be divided into three broad subtypes. Raw electrophysiological traces showing three lumbar motor neurons displaying different post-discharge activities. After a period of prolonged firing (10 seconds) lumbar motor neurons will display one of three post-discharge subtypes: an ultra-slow afterhyperpolarisation (usAHP) characterised by a change in membrane potential >5mV and a recovery time (time to return to resting membrane potential) of >20s, a slow afterhyperpolarisation (sAHP) characterised by a hyperpolarisation of the membrane potential of any magnitude and any recovery time, and an afterdepolarisation (ADP) characterised by a depolarisation of the membrane potential of any magnitude and any recovery time. Blue dotted line denotes the resting membrane potential of the cell (approximately -60mV).

As we know from previous studies that the usAHP is an activity-dependent hyperpolarisation, we questioned whether sAHPs and ADPs were also input-dependent. We applied a frequency-duration protocol to a motor neuron exhibiting an AHP at baseline conditions and a motor neuron exhibiting an ADP at baseline conditions (Fig. 2). To each motor neuron we applied a suprathreshold current pulse train at several frequency intervals (5Hz, 10Hz, 20Hz, and 40Hz) and step durations (5s, 10s, 15s, and 20s). We found that the post-discharge activity subtype of the motor neurons remained consistent regardless of the stimulus intensity applied. For the motor neuron exhibiting an ADP, the post-discharge ADP only increased in size with increasing firing frequency and stimulation duration. For the motor neuron exhibiting the AHP, the cell showed an sAHP at lower-intensity stimulations and an usAHP at high frequency stimulations. From this we can assume that afterdepolarisations and afterhyperpolarisations are discrete behaviours that are not input-dependent i.e., no amount of physiologically realistic stimulus will convert an afterdepolarisation into an afterhyperpolarisation and vice versa. Both afterdepolarisations and afterhyperpolarisations, however, do increase in amplitude and recovery time with increasing stimulus intensity, presumably through the recruitment of new ion channels or membrane pumps.

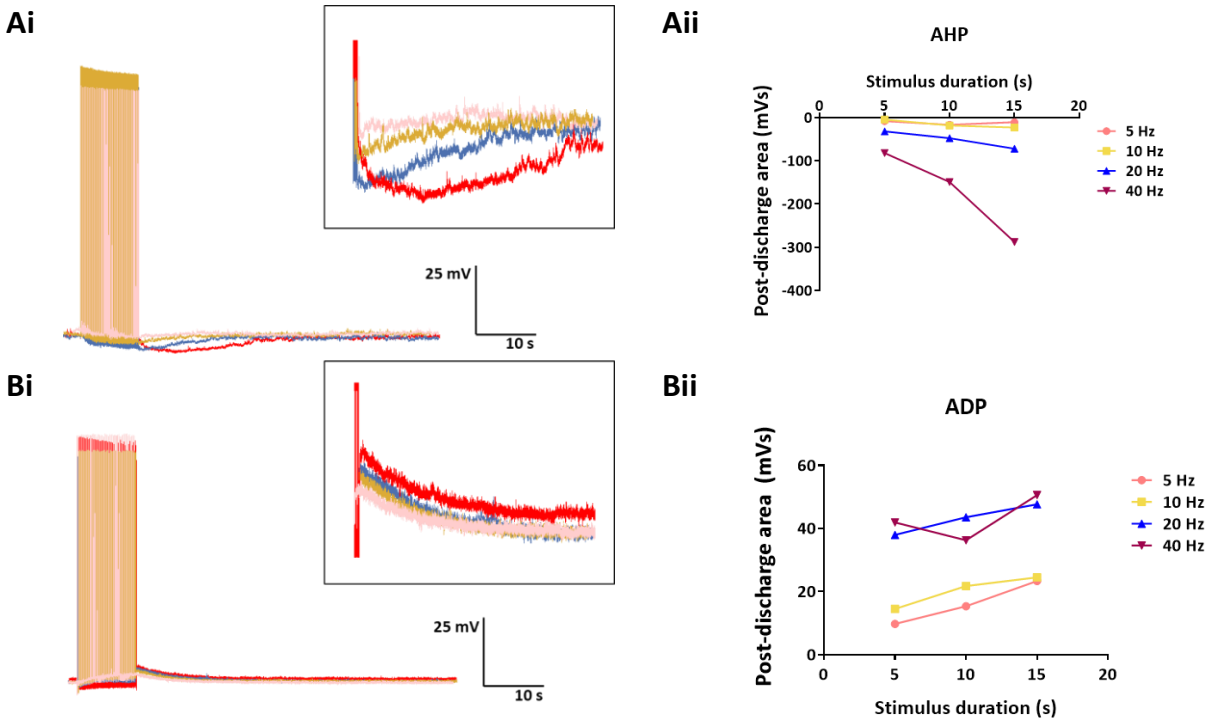

Figure 2. The polarisation of an individual motor neuron's post-discharge activity remains consistent regardless of stimulus intensity. (Ai) Raw traces from a motor neuron displaying an afterhyperpolarisation (AHP) post-discharge. The area (mVs) of the AHP is increased by increasing frequency (5-40Hz) 10 second depolarising pulse train stimuli. (Aii) Summary of the post-discharge area (mVs) of the same cell across a range of frequency (5-40Hz) and duration (5-15s) stimuli. The size of the post-discharge activity area is increased with increasing frequency and duration of stimuli, but the subtype is consistent. (Bi) Raw traces from a motor neuron displaying an afterdepolarisation (ADP) post-discharge. The area (mVs) of the ADP is increased similarly as in (Ai). (Bii) Summary of the post-discharge area (mVs) of the same cell across the same range of stimuli applied in (Aii). Similarly, while the post-discharge activity area grows, the subtype does not change in response to varying stimuli.

Next, we surveyed a large amount of lumbar motor neurons to determine the distribution of each of these three post-discharge subtypes within the cell population (Fig. 3). Of the 166 motor neurons surveyed, 96 displayed an afterdepolarisation (58%), 45 showed a slow afterhyperpolarisation (27%), and 25 showed an ultra-slow afterhyperpolarisation (15%). The distribution of non-usAHP post-discharge activity subtypes among motor neurons has not been documented previously. The proportion of motor neurons exhibiting an usAHP was lower than that reported by Picton and colleagues (2017), who observed approximately 40% of lumbar motor neurons exhibiting an usAHP, as well as being lower than the population sampled in Chapter 1: *The role of α3-NKA in healthy and disordered spinal motor networks*. This suggests that the expression profile of post-discharge activity is highly diverse depending on the population sampled.

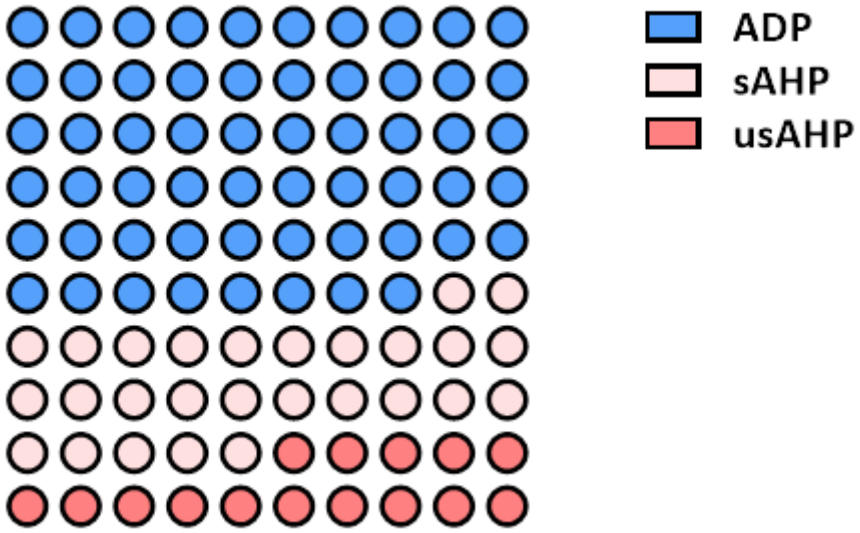

Figure 3. The expression profile of post-discharge activity across a general population of lumbar motor neurons. The post-discharge activity of a random sampling of 166 lumbar motor neurons in postnatal mice, 96 displayed an afterdepolarisation (ADP), 45 showed a slow afterhyperpolarisation (sAHP), and 25 showed an ultra-slow afterhyperpolarisation (usAHP).

A developmental role for the ultra-slow afterhyperpolarisation

The first two postnatal weeks are a crucial period in the development of spinal motor networks (Altman and Sudarshan, 1975; Brocard, Vinay and Clarac, 1999), with animals being almost sessile in the first postnatal week until weightbearing behaviour emerges at the beginning of the second postnatal week. By week three, diverse gaits begin to emerge, and locomotor maturity is essentially reached (Fig. 4A). We therefore wanted to probe into any developmental changes in post-discharge activity profiles during this critical period. We predicted that changes in post-discharge activity may facilitate the development and ongoing modulation of motor output.

When further analysing the whole-cell patch-clamp recordings presented in Figure 3, we discovered that the post-discharge profiles of lumbar motor neurons did change significantly between the first and second postnatal weeks (Fig. 4B). Up until postnatal day 7, most motor neurons exhibited ADPs, with very few showing sAHPs, and almost no usAHPs observed (P2 *n*=12, P3 *n*=16, P4 *n*=27, P5 *n*=33, P6 *n*=13). Around the beginning of the second postnatal week, we see a distinct switch in post-discharge activity from being largely depolarised to largely hyperpolarised with usAHP exhibition peaking around the 8th postnatal day (Fig. 4B, P7 *n*=34, P8 *n*=10, P9 *n*=9, P10 *n*=8). This change in post-discharge activity coincides with the emergence of weightbearing in these animals (Fig. 4C). We therefore predict that, as motor neurons mature to accommodate the development of weight bearing movement, so does this post-discharge activity.

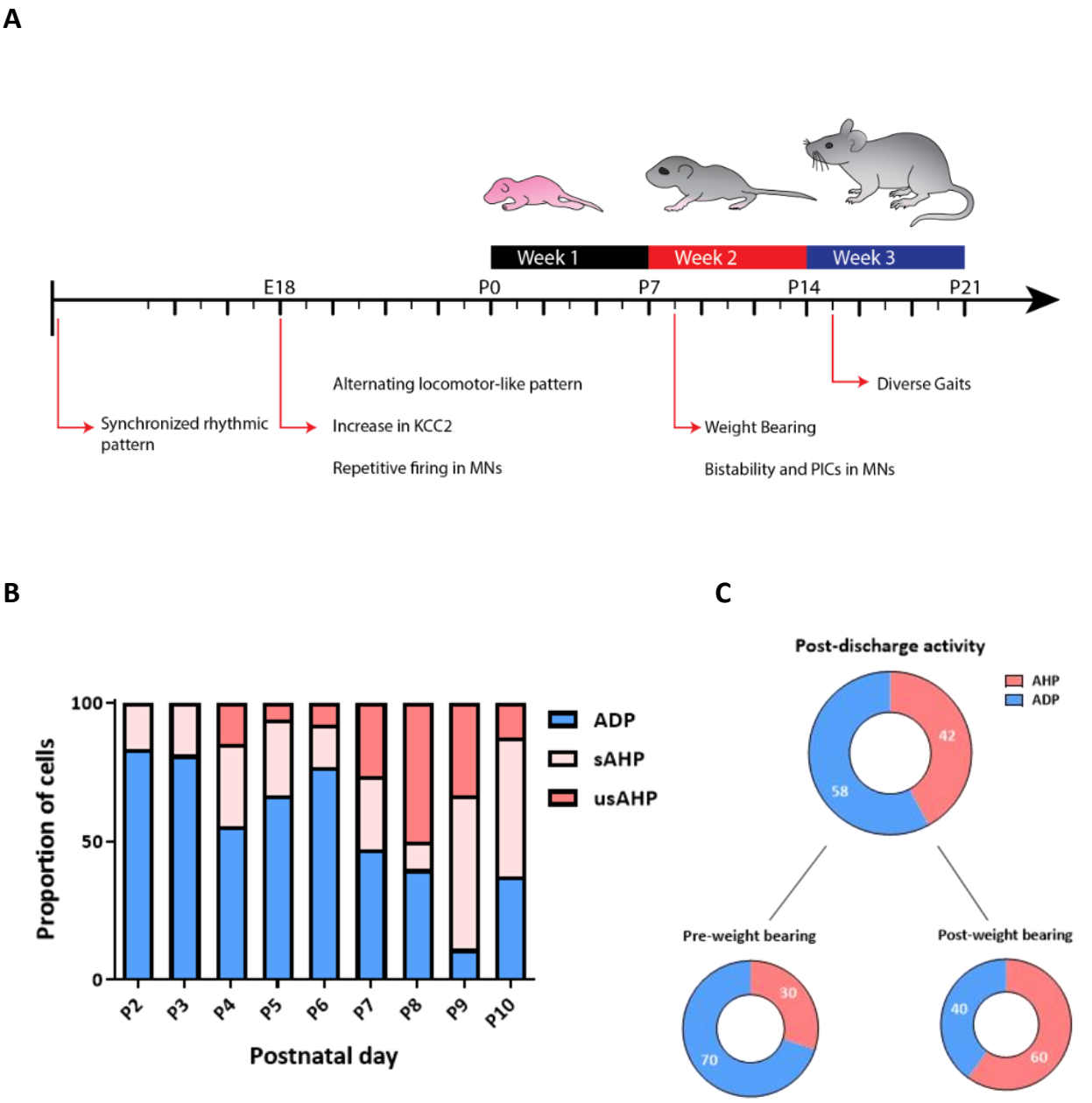

Figure 4. The expression profile of post-discharge activity changes around the emergence of weight-bearing locomotion. (A) Infographic showing postnatal development of the mouse and accompanying motor network changes. Adapted from Jean-Xavier *et al.*, 2018. (B) Day-by-day expression profile for post-discharge activity across postnatal days 2 to 10 (*n*=166; P2 *n*=12, P3 *n*=16, P4 *n*=27, P5 *n*=33, P6 *n*=13). A given cell's post-discharge activity is typically depolarised up until P7, where a larger proportion of motor neurons begin to display sAHPs or usAHPs. (C) Proportions of afterdepolarisations and afterhyperpolarisations for general cell population, pre-weight bearing and post-weight bearing (*n*=166). Weight bearing locomotion emerges at the beginning of the second postnatal week.

Expression of the α3 subunit isoform across early development

We then asked what is changing about these cells during this period that could account for the increased observation of usAHPs in the second postnatal week. As we know that the usAHP is sodium pump-mediated, we postulated that there may be an increase in α3-NKA protein expression during this time which results in a stronger pump current.

We prepared lumbar spinal slices from neonatal mice at P4, P8, and P12 and co-stained for the motor neuron marker ChAT (choline acetyltransferase) and *Atp1a3* (α3-NKA) (Fig. 5). As all electrophysiological recordings were made from motor neurons, we first quantified the α3-NKA expression on ChAT-positive cells only. In line with traditional immunohistochemical analysis, we analysed the data grouped by experimental animal. A one-way ANOVA showed no significant effect of age on α3-NKA mean fluorescence intensity (Fig. 5Bi, $F_{(2,6)}$= 4.642, *p*=0.6074). We observed a non-significant increase in mean α3-NKA fluorescence intensity at P8 (*n*=3, 7.206 ± 0.4022) which decreased again at P12 (*n*=3, 5.504 ± 0.5906). α3-NKA fluorescence intensity was similar between P4 (*n*=3, 5.664 ± 0.2448) and P12. When the data is analysed grouped by cell, as it is with electrophysiological recordings, this trend is further emphasised. α3-NKA fluorescence intensity is significantly higher at P8 (Fig. 5Bii, $F_{(2,681)}$= 51.55, *p*=<0.0001). This may of course simply be a result of increased statistical power accompanying an increase in sample size (P4 *n*=248, P8 *n*=207, P12 *n*=229). However, even with such an increase in power, the mean α3-NKA fluorescence intensity does not differ between P4 and P12 (*p*=0.3766).

Next, we examined whether α3-NKA fluorescence intensity may be generally higher in all ventral horn neurons, not just motor neurons, by quantifying the field intensity of α3-NKA fluorescence between the age groups (Fig. 5Biii). A one-way ANOVA found there to be no significant differences in α3-NKA field intensity between ages P4, P8, and P12 although the data did trend in line with the α3-NKA fluorescence intensity of motor neurons observed in Fig. 5Bi ($F_{(2,6)}$= 4.742, *p*=0.0582).

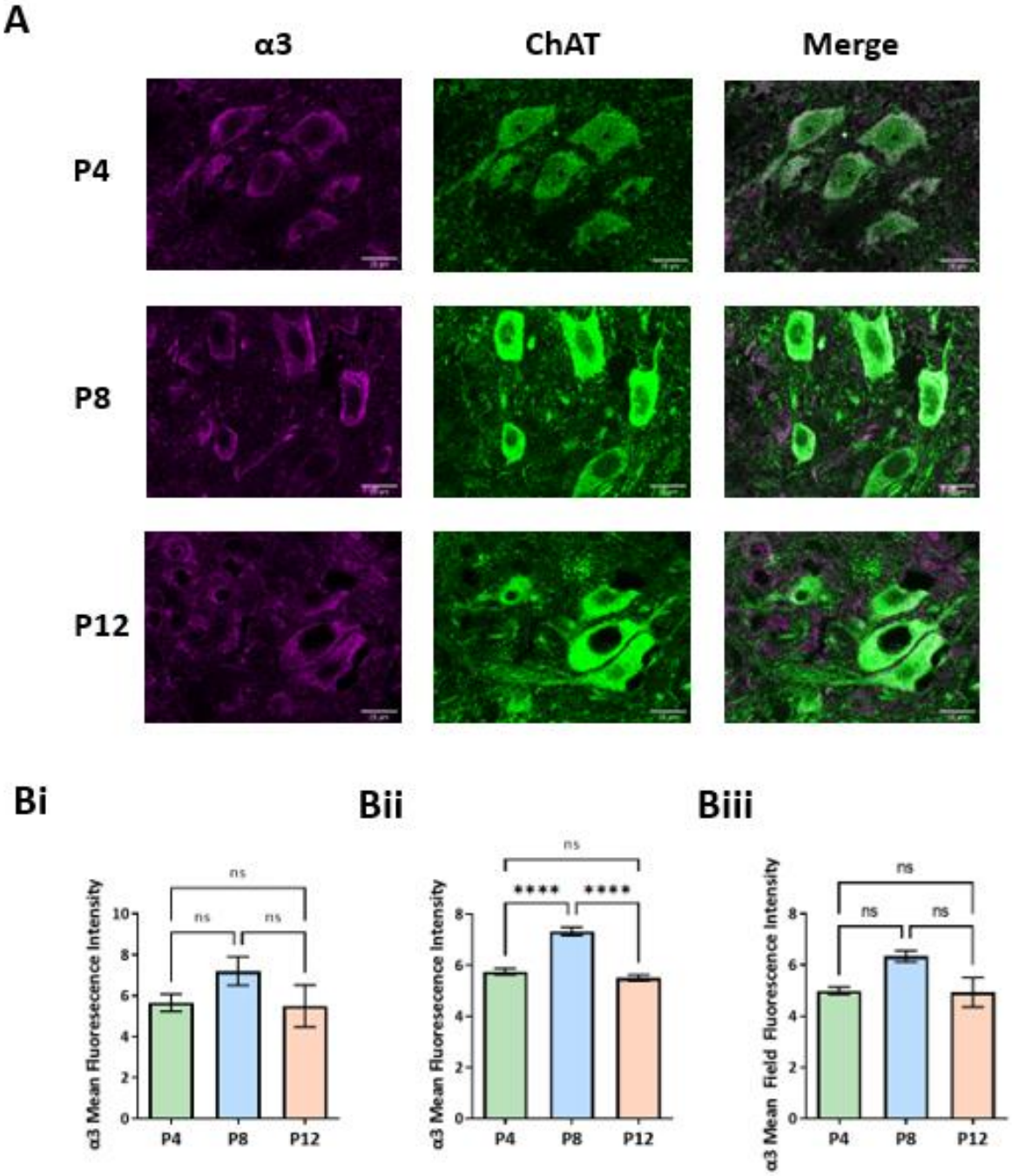

Figure 5. Developmental changes in α3-NKA expression in lumbar motor neurons across the first two postnatal weeks. (A) Example images showing α3-NKA expression in ChAT-positive lumbar motor neurons from animals aged 4, 8, and 12 days postnatally. The scale bar denotes 20µm (Bi) Mean α3-NKA fluorescence intensity of ChAT-positive motor neurons only across development, grouped by experimental animal (P4 *n*=3, P8 *n*=3, P12 *n*=3, *p*= 0.605). (Bii) Mean α3-NKA fluorescence intensity of ChAT-positive motor neurons only across development, grouped by cell (P4 *n*=248, P8 *n*=207, P12 *n*=229, *p*=<0.0001). (Bii) Mean α3-NKA fluorescence field intensity grouped by animal (P4 *n*=3, P8 *n*=3, P12 *n*=3, *p*=0.0582). ****, *p*≤0.0005 with a one-way ANOVA.

Expression of the α3 subunit isoform across the lumbar spinal cord

To delve further into elucidating the factors that determine a cell's post-discharge activity under baseline conditions, we examined α3-NKA expression more generally in the lumbar spinal cord.

Picton and colleagues (2017) postulated that there may be a degree of mosaicism to α3-NKA expression among ventral horn neurons which would account for why the usAHP is only observed in a subpopulation of sampled cells. If α3-NKA expression was mosaic, neurons that express α3-NKA would exhibit an usAHP and those that do not would exhibit an ADP or sAHP.

We found this to likely not be the case, as all ChAT-positive cells analysed did show some degree of α3-NKA fluorescence (Fig. 6A). A complete lack of α3-NKA is therefore unlikely to explain why some cells exhibit a usAHP and some do not. While the distribution in Fig.6A is not completely uniform, it does appear that most motor neurons express roughly the same amount of α3-NKA, with only small cell counts at the extremes. This raises the question – what does then account for this differing α3-NKA expression across age and cell population?

One possibility that we considered is that α3-NKA expression may be linked to cell size (Fig. 6B). We compared the relative frequency distribution (Fig. 6Bi) and cumulative frequency distribution (Fig. 6Bii) of motor neuron area (μM^2) of P4, P8, and P12 animals and found motor neuron size to be comparable between P4 and P8 animals, and slightly larger in P12 animals. The relative frequency distribution of P4 and P8 animals showed two peaks at approximately 300 and 500 μM^2 (Fig. 6Bi). We examined whether this represented two distinct subpopulations of motor neurons in the first postnatal week that may have differential expression of α3-NKA that may account for some of the diversity we have observed. We therefore separated these two populations and compared their respective α3-NKA mean fluorescence intensity.

A one-way ANOVA showed that, in motor neurons with an area of <400μM^2, the α3-NKA mean fluorescence intensity at P4 (*n*=125, 5.606 ± 0.1659) was significantly lower than P8 (*n*=89, 7.967 ± 0.28) but did not differ from P12 (*n*=61, 5.607 ± 0.24), similar to what we observed in the general population (Fig. 6Ci, $F_{(2,272)}$= 36.28, *p*=<0.0001).

Next, we examined the α3-NKA mean fluorescence intensity of motor neurons with an area of >400μM^2. The results were comparable with the subgroup of motor neurons of <400μM^2, with a one-way ANOVA showing that the α3-NKA mean fluorescence intensity at P4 (*n*=123, 5.914 ± 0.19) was significantly lower than P8 (*n*=118, 6.852 ± 0.18) but did not differ from P12 (*n*=168, 5.477 ± 0.13), similar to what we observed in the whole population (Fig. 6Cii, $F_{(2,406)}$= 18.57, *p*=<0.0001). From these results we determined it was therefore unlikely that these two subpopulations of motor neurons differ in α3-NKA expression on the basis of size.

Finally, we examined if α3-NKA expression was related to size more generally at these three developmental ages. We plotted α3-NKA mean fluorescence intensity against motor neuron area (μM^2) for each age group. We found that α3-NKA mean fluorescence intensity did not correlate with motor neuron area at ages P4 (Fig. 6Di, *n*=248, *r*=0.83, *p*=0.1911) and P12 (Fig. 6Diii, *n*=229, *r*=0.13, *p*=0.0521), but there was a significant correlation between these two variables for P8 animals (Fig. 6Dii, *n*=207, *r*=-0.29, *p*=<0.0001). As our P12 results are close to significance, there is a possibility that smaller motor neurons have been under-sampled at the age. If this is the case, this would be represented in the relative frequency distribution of cell size presented in Fig. 6Bi, where only P12 lacks the distinct 'double-peak' observed at P4 and P8.

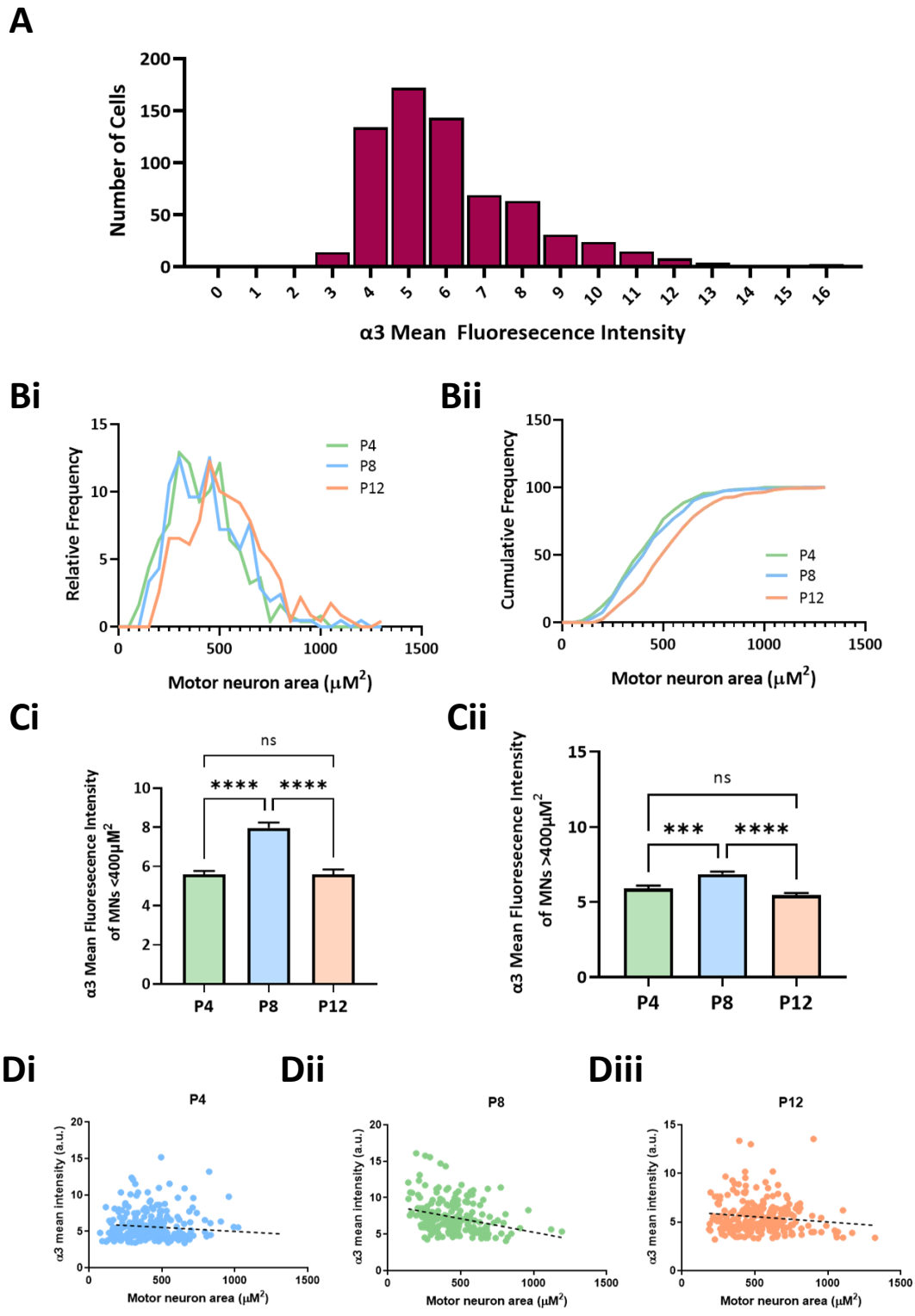
A
Number of Cells
α3 Mean Fluoresecence Intensity
Bi
Relative Frequency
P4
P8
P12
Motor neuron area (μM²)
Bii
Cumulative Frequency
Motor neuron area (μM²)
Ci
α3 Mean Fluoresecence Intensity of MNs <400μM²
ns
****
Cii
α3 Mean Fluoresecence Intensity of MNs >400μM²
***
Di
Dii
Diii
α3 mean intensity (a.u.)

Figure 6. Differences in α3-NKA expression across development as a function of motor neuron size. (A) Frequency histogram of α3-NKA mean fluorescence intensity of ChAT-positive lumbar motor neurons. Note that all motor neurons express some quantifiable amount of α3-NKA. (Bi) Relative frequency distribution of lumbar motor neurons by size at ages 4, 8, and 12 days postnatally. (Bii) Cumulative frequency distribution of lumbar motor neurons by size at ages 4, 8, and 12 days postnatally. (Ci) Mean of α3-NKA fluorescence intensity of ChAT-positive neurons <400μM^2 grouped by cell (P4 *n*=125, P8 *n*=89, P12 *n*=61, *p*=<0.0001). (Cii) Mean of α3-NKA fluorescence intensity of ChAT-positive neurons >400μM^2 grouped by cell (P4 *n*=123, P8 *n*=118, P12 *n*=168, *p*=<0.0001). (Di) Scatterplot showing α3-NKA mean fluorescence intensity against motor neuron size for P4 motor neurons (*n*=248, *r*=0.833). (Dii) Scatterplot showing α3-NKA mean fluorescence intensity against motor neuron size for P8 motor neurons (*n*=207, *r*=-0.288). (Diii) Scatterplot showing α3-NKA mean fluorescence intensity against motor neuron size for P12 motor neurons (*n*=229, *r*=-0.1285). ***, *p*<0.001; ****, *p*≤0.0005 with one-way ANOVA.

Lastly, we considered whether there may be expression differences between the two motor columns of the lumbar spinal cord: the lateral motor column and the medial motor column, whose constituent motor neurons innervate the muscles of the hind limbs and the muscles of the trunk, respectively. A two-way ANOVA was performed to determine the effect of cell location and age on α3-NKA fluorescence intensity, revealing no significant interaction between the effects of these two variables (Fig. 7A, 10B, $F_{(2,12)}$= 0.1669, *p*=0.8482), nor a main effect of cell location ($F_{(1,6)}$= 1.871, *p*=0.1964).

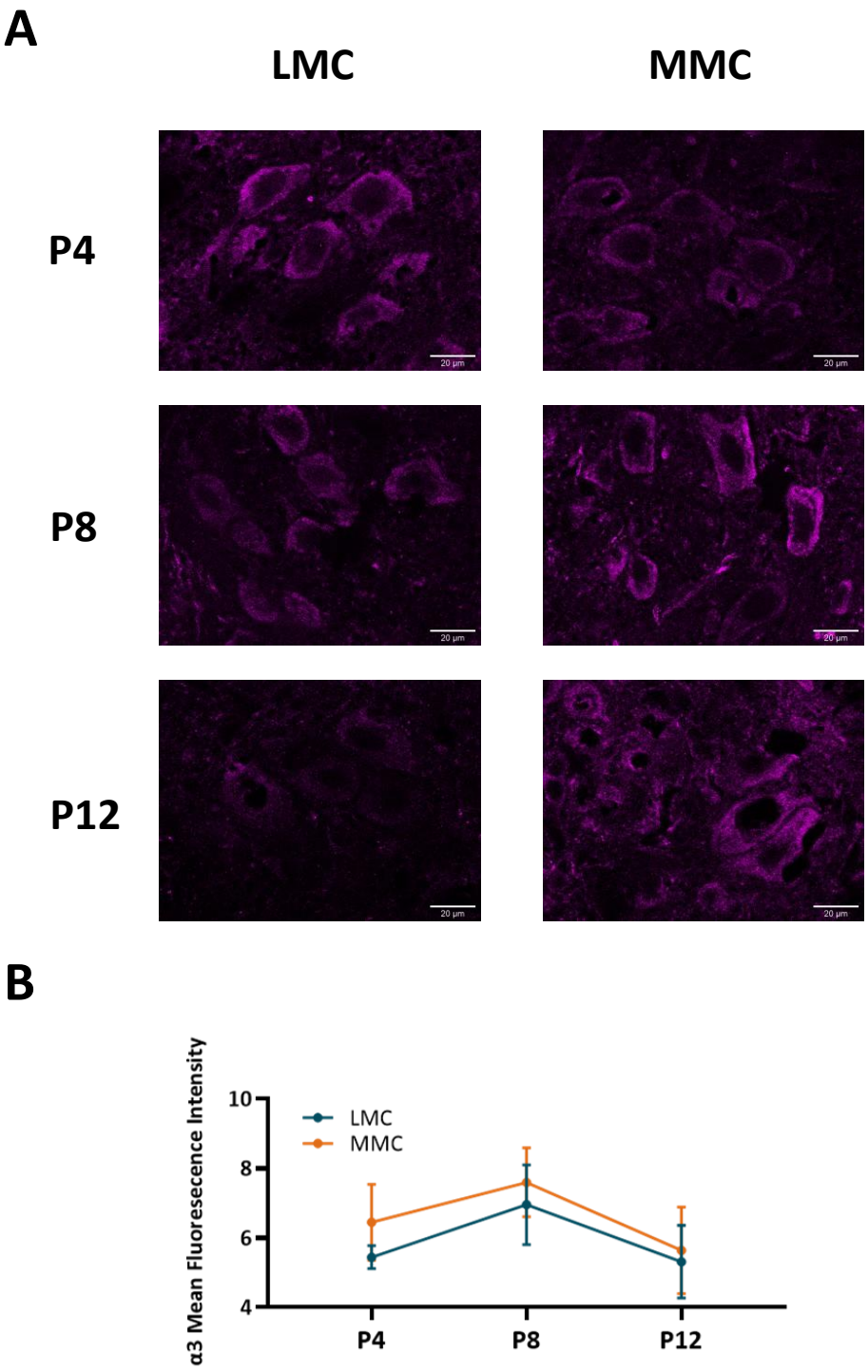

Figure 7. Differences in α3-NKA expression between lateral and medial motor column motor neurons. (A) Example images showing α3-NKA expression in a sample of lateral motor column neurons (LMC) or medial motor column neurons (MMC) at ages 4, 8, and 12 days postnatally. The scale bar denotes 20µm (B) Mean α3-NKA fluorescence intensity of ChAT-positive LMC or MMC neurons at ages 4, 8, and 12 days postnatally and grouped by animal (P4 *n*=3, P8 *n*=3, P12 *n*=3, *p*=0.1964).

Post-discharge activity is determined by competing conductances

Since our immunohistochemical data suggests that α3-NKA expression is not mosaic in motor neurons, we had to further examine why some cells would exhibit usAHPs at baseline conditions whilst others may not. We questioned whether, particularly for neurons where α3-NKA expression is present but comparatively low, a weak pump current may be 'masked' by other conductances present post-discharge. Whilst the ion channels and membrane pumps contributing to post-discharge activity are still being described, we chose three known mediators: high-voltage-activated Ca^{2+} channels that are known to contribute to the production of the post-discharge ADP (Bouhadfane *et al.*, 2013), Ca^{2+}-activated potassium channels that are known to contribute to the production of the sAHP (Kato *et al.*, 2006; Turner *et al.*, 2016; Tiwari *et al.*, 2018), and the sodium-potassium pump that is known to contribute to the production of the usAHP (Genet and Kado, 1997; Zhang and Sillar, 2012; Gulledge *et al.*, 2013; Turner *et al.*, 2016; Picton *et al.*, 2017). We applied pharmacological blockers for each of these ion channels/membrane pumps to motor neurons exhibiting a spectrum of post-discharge activities to determine whether competing conductances were determining the post-discharge activity of a given neuron at baseline conditions.

First, we examined the effect of blockade of high-voltage-activated Ca^{2+} channels using cadmium chloride ($CdCl_2$) on post-discharge activity (Fig. 8). Examination of the frequency-current relationship before and after the application of $CdCl_2$ confirmed there was an effect of the drug as excitability increased (Fig. 8A). Due to this excitability increase, a pulse train stimulus was used to control for the changes in firing frequency between baseline and drug conditions. A repeated-measures ANOVA showed that $CdCl_2$ had a significant suppressing effect on post-discharge activity across all neurons (Fig. 8B, n=18, Baseline -4.88 ± 13.93, $CdCl_2$ -73.05 ± 25.66, Wash -62.30 ± 23.80, $F_{(0.7427, 10.03)}$= 12.33, p=0.0083). When examining strictly neurons exhibiting an ADP at baseline conditions, $CdCl_2$ significantly diminished the area of ADPs and converted some ADPs into AHPs (mVs) (Fig. 8Ci, n=11,

Baseline 30.05 ± 7.805, $CdCl_2$ 0.4055 ± 3.747, Wash 10.68 ± 5.670, $F_{(1.183, 8.281)}$=9.788, *p*=0.0114). When examining strictly neurons exhibiting an AHP at baseline conditions, $CdCl_2$ significantly enhanced the area of the AHP (mVs) (Fig.8Cii, *n*=7, Baseline -59.11 ± 20.80, $CdCl_2$ -188.5 ± 33.58, Wash -123.1 ± 20.71, $F_{(1.257, 6.912)}$=14.92, *p*=0.005).

A

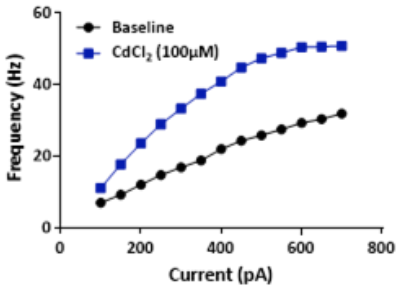
Baseline
CdCl2 (100µM)
Frequency (Hz)
Current (pA)

B

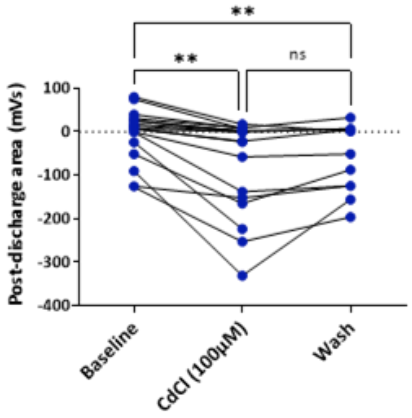
**
**
ns
Post-discharge area (mVs)
Baseline
CdCl (100µM)
Wash

Ci

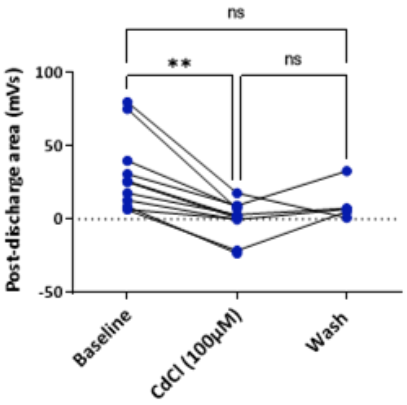
ns
**
ns
Post-discharge area (mVs)
Baseline
CdCl (100µM)
Wash

Cii

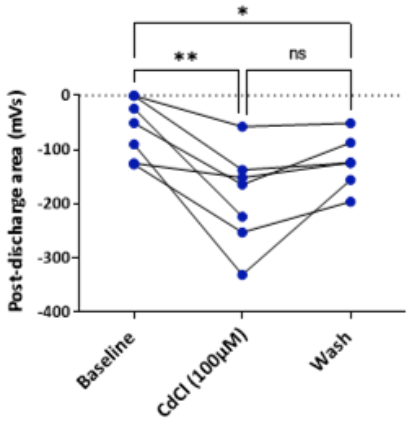
*
**
ns
Post-discharge area (mVs)
Baseline
CdCl (100µM)
Wash

D

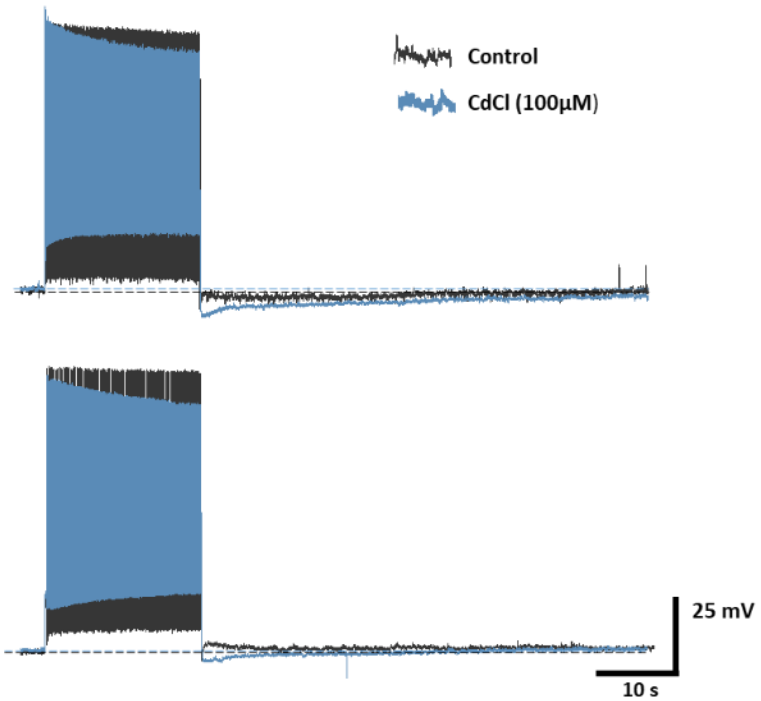
Control
CdCl (100µM)
25 mV
10 s

Figure 8. Blockade of high voltage activated Ca^{2+} channels supress post-discharge activity. (A) Representative frequency-current relationship for baseline conditions and after application of cadmium chloride ($CdCl_2$, 100µM). (B) $CdCl_2$ affects post-discharge activity by enhancing the amplitude of afterhyperpolarisations (AHPs) and reducing the amplitude of afterdepolarisations (ADPs), as well as converting ADPs to AHPs (n=18, p=0.0083). (Ci) Application of $CdCl_2$ diminishes ADP size and causes cells previously exhibiting ADPs at baseline conditions to instead exhibit AHPs (n=11, p=0.0114) (Cii) Application of $CdCl_2$ increases the size of the hyperpolarisation in cells already exhibiting AHPs (n=7, p=0.005). (D) Raw traces showing the effect of $CdCl_2$ on the post-discharge activity of a cell exhibiting an AHP at baseline and a cell exhibiting an ADP at baseline. The black dotted line denotes the resting membrane potential of the cell (approximately -60mV). *, p<0.05; **, p<0.01 with a repeated-measures ANOVA.

Next, we examined the effect of blockade of Ca^{2+}-activated potassium channels that are known to contribute to the production of the sAHP on post-discharge activity (Fig. 9). Examination of the frequency-current relationship before and after the application of apamin confirmed there was an effect of the drug as excitability increased (Fig. 9A). Due to this excitability increase, a pulse train stimulus was used to control for the changes in firing frequency between baseline and drug conditions. A paired t-test showed that apamin had varying effects on post-discharge activity (Fig. 9B, *n*=7, Baseline -44 ± 47, Apamin (100nM) 0.84 ±8.4, Wash -45 ± 44, *p*=0.3492). When examining strictly neurons that exhibited an ADP at baseline conditions, apamin was found to have mixed effects (Fig. 9Ci, *n*=4, Baseline 28 ± 11, Apamin 11 ± 6.5, Wash 17 ± 16, *p*=0.3715) with some neurons showing an increase in the amplitude of the ADP and some neurons showing a decrease. When examining strictly neurons that exhibited an AHP at baseline conditions, apamin was found to decrease the amplitude of the AHP though non-significantly (Fig. 9Cii, *n*=3, Baseline -140 ± 83, Apamin -13 ± 15, Wash -127 ± 85, *p*=0.2719). Interestingly, in some neurons where the amplitude of the ADP was increased by the application of apamin, spontaneous rebound firing was observed (Fig. 9E).

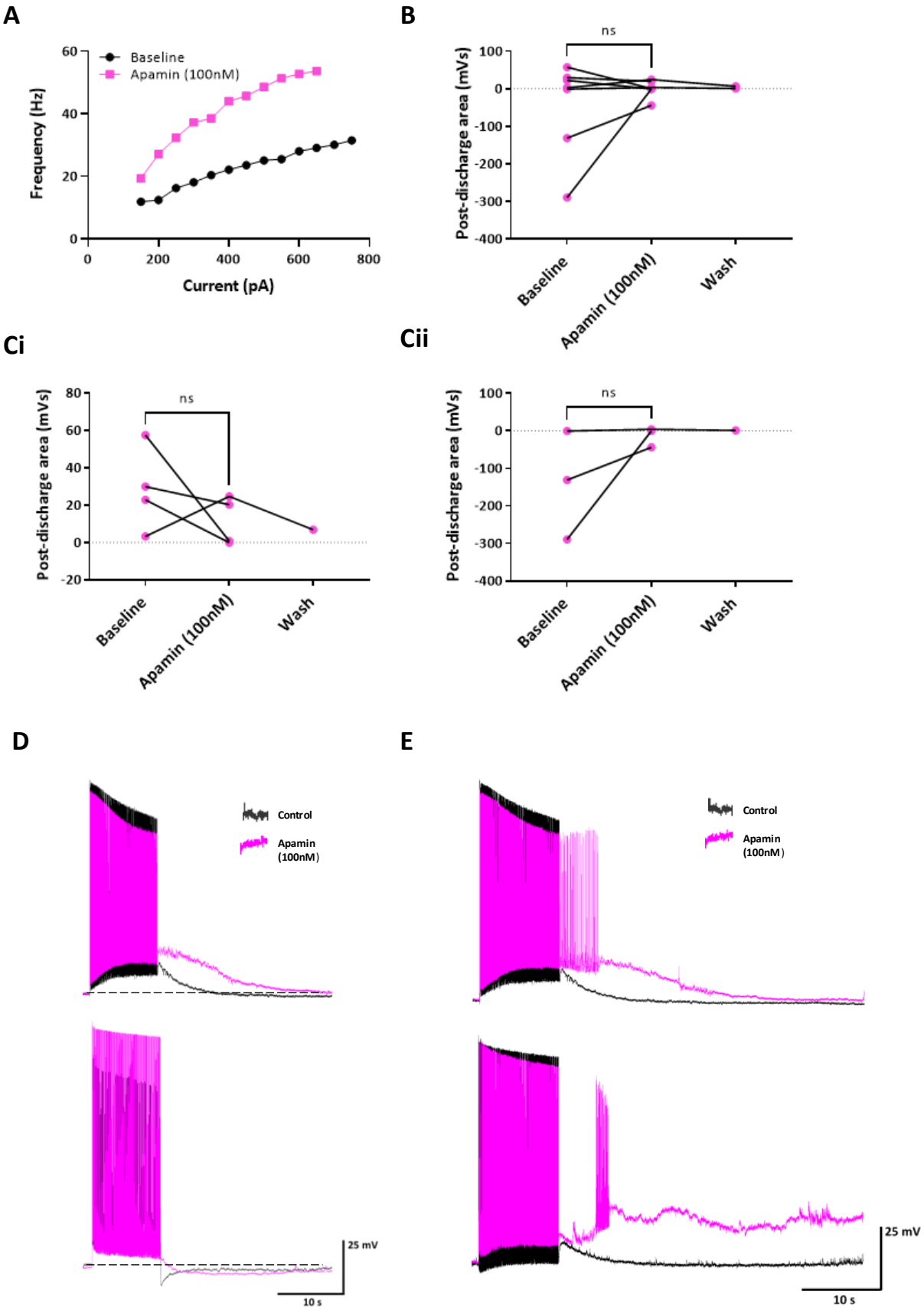
A
Baseline
Apamin (100nM)
Frequency (Hz)
Current (pA)
B
ns
Post-discharge area (mVs)
Baseline
Apamin (100nM)
Wash
Ci
ns
Post-discharge area (mVs)
Baseline
Apamin (100nM)
Wash
Cii
ns
Post-discharge area (mVs)
Baseline
Apamin (100nM)
Wash
D
Control
Apamin (100nM)
25 mV
10 s
E
Control
Apamin (100nM)
25 mV
10 s

Figure 9. The effect of blocking calcium-activated potassium channels on post-discharge activity. (A) Representative frequency-current relationship for baseline conditions and after application of apamin (100nM). (B) Apamin affects post-discharge activity by decreasing the amplitude of afterhyperpolarisations (AHPs) and increasing the amplitude of afterdepolarisations (ADPs) in most motor neurons (n=7, p=0.3492). (Ci) Application of apamin has mixed effects on motor neurons exhibiting ADPs at baseline conditions (n=4, p=0.3715) (Cii) Application of apamin decreases the size of the hyperpolarisation in cells already exhibiting AHPs (n=3, p=0.2719). (D) Raw traces showing the effect of apamin on the post-discharge activity of a cell exhibiting an ADP at baseline and a cell exhibiting an AHP at baseline. (E) Raw traces showing the induction of spontaneous rebound firing post-discharge after the application of apamin in cells exhibiting ADPs at baseline conditions. The black dotted line denotes the resting membrane potential of the cell (approximately -60mV).

Finally, we examined the effect of blockade of the sodium-potassium pumps that are known to contribute to the production of the usAHP on post-discharge activity (Fig. 10). Examination of the frequency-current relationship before and after the application of ouabain showed no notable changes in excitability, however a pulse train stimulus was still used to conform with previous pharmacological experiments (Fig. 10A). A repeated-measures ANOVA showed that ouabain had mixed effects on post-discharge activity (Fig. 10B, n=10, Baseline 1.572 ± 12.26, Ouabain (3μM) 19.91 ± 6.106, Wash 21.25 ± 5.36, $F_{(1.183,\ 7.689)}$=2.169, p=0.1816). When examining strictly neurons that exhibited an ADP at baseline conditions, ouabain had mixed effects on post-discharge activity (Fig. 10Ci, n=7, Baseline 22.02 ± 4.971, Ouabain 26.88 ± 6.565, Wash 21.25 ± 5.36, $F_{(1.71,\ 8.552)}$=0.3591, p=0.677) increasing the amplitude of the ADP in some neurons whilst decreasing the amplitude of the ADP in others. When examining strictly neurons that exhibited an AHP at baseline conditions, ouabain had a consistently depolarising, though non-significant, effect on post-discharge activity (Fig. 10Cii, n=3, Baseline -46.13 ± 21.35, Ouabain, 3.653 ± 8.298, Wash -49.78 ± 17.28, p=0.1023), decreasing the amplitude of the AHP in some neurons and converting a smaller AHP to an ADP in one neuron.

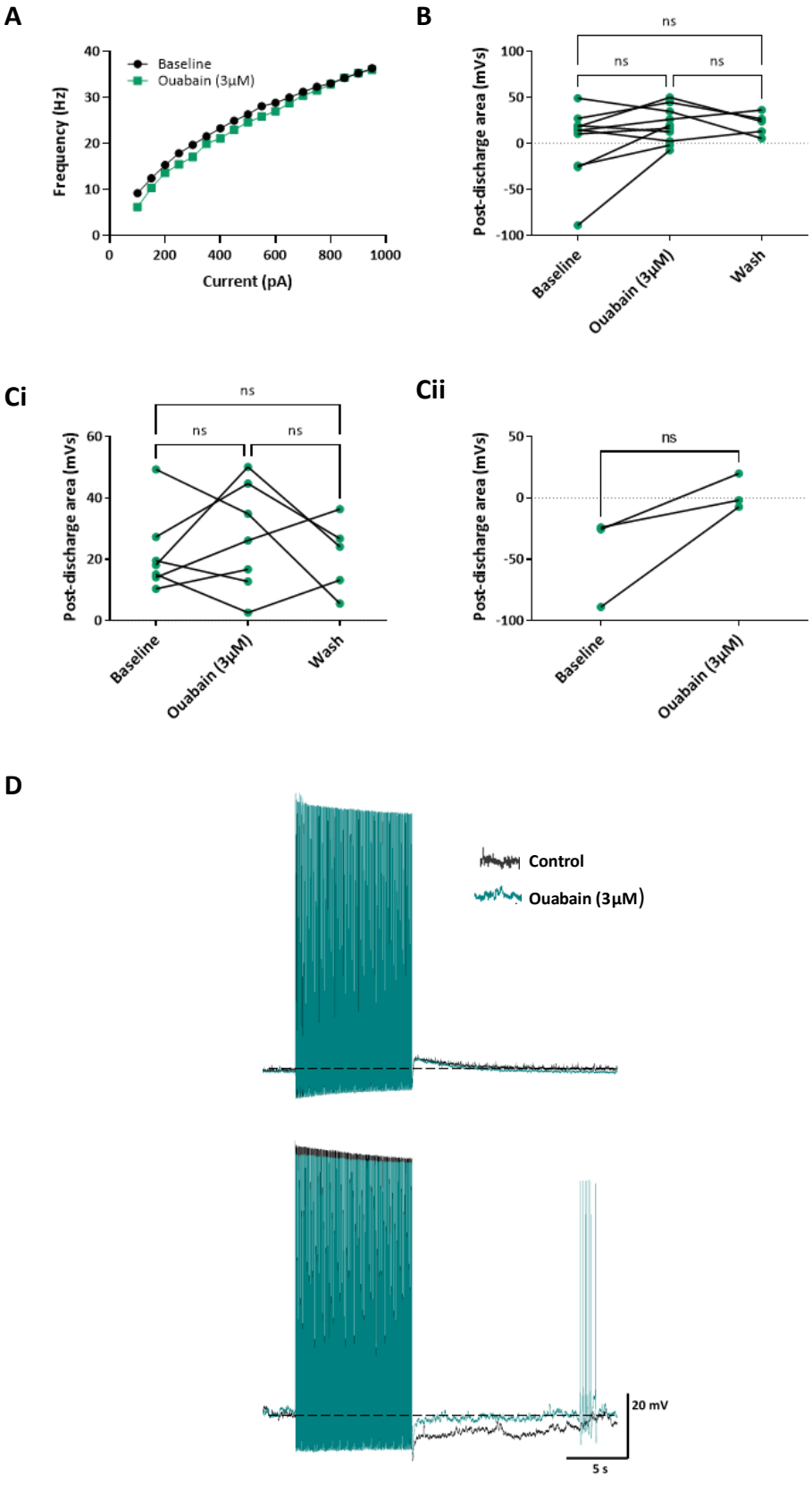
A
Baseline
Ouabain (3µM)
Frequency (Hz)
Current (pA)
B
ns
ns
ns
Post-discharge area (mVs)
Baseline
Ouabain (3µM)
Wash
Ci
ns
ns
ns
Post-discharge area (mVs)
Baseline
Ouabain (3µM)
Wash
Cii
ns
Post-discharge area (mVs)
Baseline
Ouabain (3µM)
D
Control
Ouabain (3µM)
20 mV
5 s

Figure 10. The effect of blocking sodium-potassium pumps on post-discharge activity. (A) Representative frequency-current relationship for baseline conditions and after application of ouabain (3μM). (B) Ouabain affects post-discharge activity by enhancing the amplitude of afterdepolarisations (ADPs) and reducing the amplitude of afterhyperpolarisations (AHPs), as well as converting AHPs to ADPs (n=10, p=0.1816). (Ci) Application of ouabain has mixed effects on cells already exhibiting ADPs, increasing the size of the ADP in some cells whilst decreasing the size of the ADP in others (n=7, p=0.677) (Cii) Application of ouabain diminishes the size of the hyperpolarisation in cells already exhibiting AHPs and causes some cells already exhibiting AHPs to instead exhibit ADPs (n=3, p=0.1023). (D) Raw traces showing the effect of ouabain on the post-discharge activity of a cell exhibiting an ADP at baseline and a cell exhibiting an AHP at baseline. The black dotted line denotes the resting membrane potential of the cell (approximately -60mV).

Modulation of post-discharge activity

The sodium-potassium pump is a well-established target of modulation. Here, we examined the effects of serotonin (5-HT) (Fig. 11), a monoamine and key neuromodulator during early postnatal development (Schmidt and Jordan, 2000; Dunbar, Tran and Whelan, 2010), and muscarine (Fig. 12), a well-studied modulator of sensory and motor networks (Kiehn, Johnson and Raastad, 1996; Jiang, Carlin and Brownstone, 1999; Miles *et al.*, 2007), on the post-discharge activity of lumbar motor neurons.

Examination of the frequency-current relationship before and after the application of 5-HT confirmed there was an effect of the drug as excitability increased (Fig. 11A). Due to this excitability increase, a pulse train stimulus was used to control for the changes in firing frequency between baseline and drug conditions. We found that 5-HT had a hyperpolarising effect on post-discharge activity area (Fig. 11B, n=16, Baseline -29.82 ± 15.11, 5-HT (10µM) -77.27 ± 19.11, Wash -37.10 ± 18.25, $F_{(1.103,15.44)}$= 8.8689, p=0.084). To determine which underlying channels or membrane pumps 5-HT may be acting upon, we separated cells into those exhibiting ADPs at baseline conditions and those exhibiting AHPs at baseline conditions. 5-HT had a mixed effect on the post-discharge area of cells exhibiting ADPs at baseline (Fig. 11Ci, n=6, Baseline 13.76 ± 3.769, 5-HT (10µM) -54.86 ± 27.66, Wash 20.19 ± 13.52, $F_{(1.054,6.854)}$= 4.755, p=0.0653), however notably 5-HT did convert ADPs into usAHPs in two of the six cells. 5-HT was found to have a significant hyperpolarising effect on the post-discharge activity of cells exhibiting AHPs at baseline (Fig. 11Cii, n=10, Baseline -55.97 ± 20.05, 5-HT (10µM) -90.72 ± 25.67, Wash -60.02 ± 21.09, $F_{(1.390,12.51)}$=5.783, p=0.0243).

A

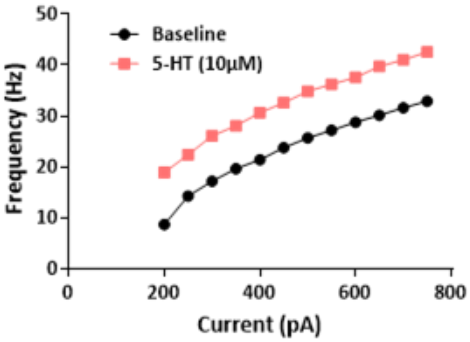
Baseline
5-HT (10µM)
Frequency (Hz)
Current (pA)

B

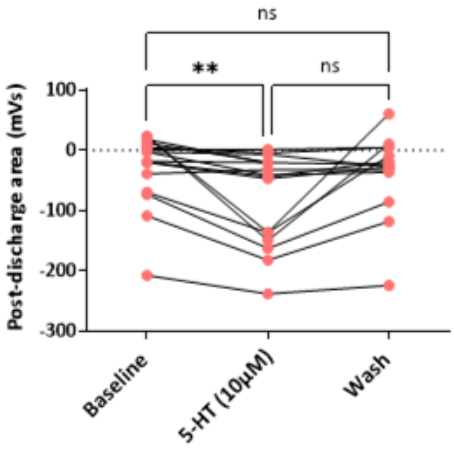
ns
**
ns
Post-discharge area (mVs)
Baseline
5-HT (10µM)
Wash

Ci

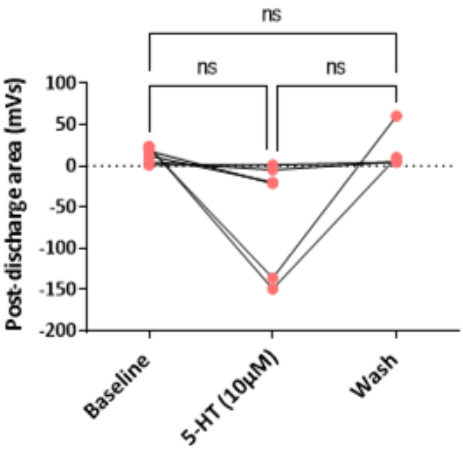
ns
ns
ns
Post-discharge area (mVs)
Baseline
5-HT (10µM)
Wash

Cii

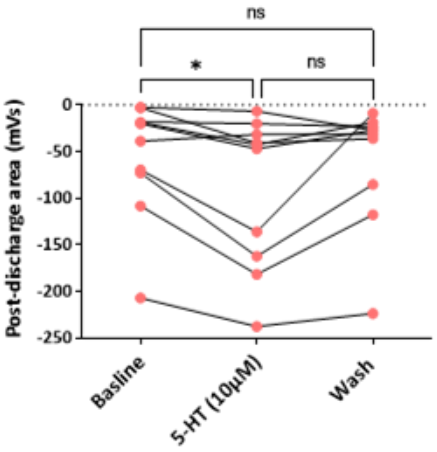
ns
*
ns
Post-discharge area (mVs)
Basline
5-HT (10µM)
Wash

D

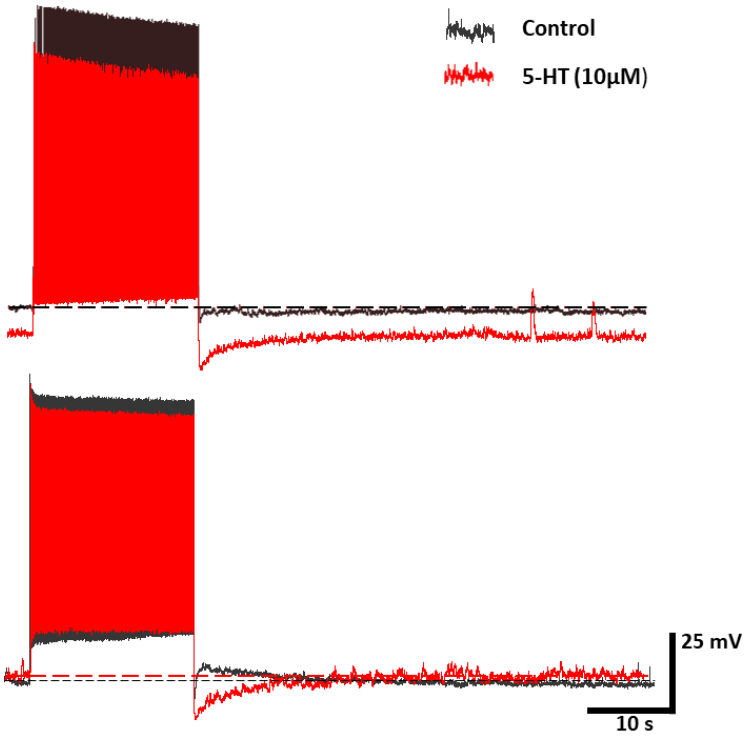
Control
5-HT (10µM)
25 mV
10 s

Figure 11. Post-discharge activity is subject to serotonergic modulation. (A) Representative frequency-current relationship for baseline conditions and after application of 5-HT (10μM). (B) Application of 5-HT hyperpolarises post-discharge activity by enhancing AHPs and converting ADPs to AHPs (n=16, p=0.0084). (Ci) Application of 5-HT tends to convert ADPs to AHPs (n=6, p=0.0653). (Cii) Application of 5-HT increases the size of the hyperpolarisation in cells already exhibiting AHPs (n=10, p=0.0243). (D) Raw traces showing the effect of 5-HT on the post-discharge activity of a cell exhibiting an AHP under baseline conditions and a cell exhibiting an ADP under baseline conditions. The black dotted line denotes the resting membrane potential of the cell (approximately -60mV). *, p<0.05; **, p<0.01 with a repeated-measures ANOVA.

Examination of the frequency-current relationship before and after the application of muscarine confirmed there was an effect of the drug as excitability decreased (Fig. 12A). Due to this excitability decrease, a pulse train stimulus was used to control for the changes in firing frequency between baseline and drug conditions. We found that muscarine also had a significant hyperpolarising effect on post-discharge activity area (Fig. 12B, n=16, Baseline -1.447 ± 10.05, Muscarine (20µM) -41.43 ± 10.07, Wash 11.47 ± 6.302, $F_{(1.937,22.27)}$=16.75, p=<0.0001). To determine which underlying channels or membrane pumps muscarine may be acting upon, we separated cells into those exhibiting ADPs and baseline conditions and those exhibiting AHPs at baseline conditions. We found muscarine to have a significant hyperpolarising effect on the post-discharge activity area of cells exhibiting ADPs at baseline conditions (Fig. 12Ci, n=11, Baseline 23.29 ± 3.34, Muscarine (20µM) -24.30 ± 10.02, Wash 16.45 ± 6.29, $F_{(1.307,10.46)}$=13.76, p=0.0024) as well as cells exhibiting AHPs at baseline conditions (Fig. 12Cii, n=5, Baseline -55.88 ± 8.508, Muscarine (20µM) -79.13 ± 12.20, Wash -5.949 ± 14.44, $F_{(0.7612,1.903)}$=29.30, p=0.0356).

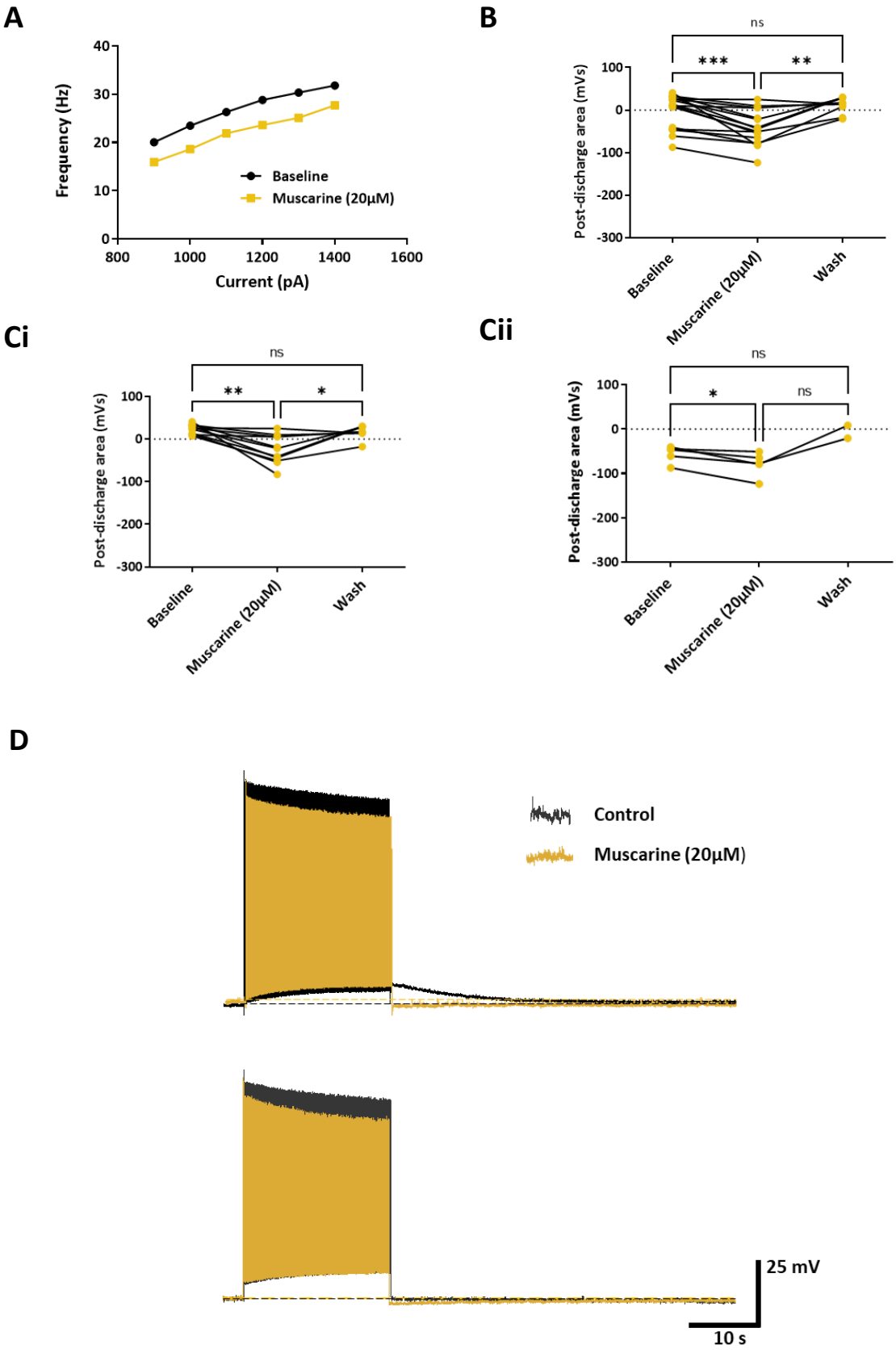
A
Frequency (Hz)
Current (pA)
Baseline
Muscarine (20µM)
B
Post-discharge area (mVs)
ns
***
**
Baseline
Muscarine (20µM)
Wash
Ci
Post-discharge area (mVs)
ns
**
*
Baseline
Muscarine (20µM)
Wash
Cii
Post-discharge area (mVs)
ns
*
ns
Baseline
Muscarine (20µM)
Wash
D
Control
Muscarine (20µM)
25 mV
10 s

Figure 12. Post-discharge activity is subject to muscarinic modulation. (A) Representative frequency-current relationship for baseline conditions and after application of muscarine (20μM). (B) Application of muscarine affects post-discharge activity by enhancing AHPs, diminishing the size of ADPs, and converting ADPs to AHPs (n=16, p=<0.0001). (Ci) Application of muscarine causes cells previously exhibiting ADPs to express AHPs (n=11, p=0.0024). (Cii) Application of muscarine increases the size of the hyperpolarisation in cells already exhibiting AHPs under baseline conditions (n=5, p=0.0356). (D) Raw traces showing the effect of muscarine on the post-discharge activity of a cell exhibiting an ADP under baseline conditions and a cell exhibiting an AHP under baseline conditions. The black dotted line denotes the resting membrane potential of the cell (approximately -60mV). *, p<0.05; **, p<0.01; ***, p<0.001 with a repeated-measures ANOVA.

Discussion

In this chapter, we aimed to more generally characterise the post-discharge activity of spinal motor neurons so that we may gain further understanding of not only the role of the usAHP, but also the role of other post-discharge polarisations in motor output.

First, we determined that a neuron's post-discharge activity can be broadly categorised into three subtypes: afterdepolarisations (ADPs), slow afterhyperpolarisations (sAHPs), and ultra-slow afterhyperpolarisations (usAHPs) (Fig. 1). We found post-discharge afterdepolarisations and afterhyperpolarisations to be consistent regardless of stimulus intensity i.e., increasing the intensity of the stimulus may increase the size of the activity (or may convert a sAHP into an usAHP) but no amount of stimulus input could convert an afterdepolarisation to an afterhyperpolarisation and vice versa (Fig. 2).

Next, we wanted to determine the expression profile of the three post-discharge subtypes in a large sample of lumbar motor neurons. We found that, of the 166 motor neurons surveyed, 96 displayed an afterdepolarisation (58%), 45 showed a slow afterhyperpolarisation (27%), and 25 showed an ultra-slow afterhyperpolarisation (15%) (Fig. 3). Whilst the prevalence of the usAHP in this population of neurons has been described previously (Picton *et al.*, 2017), to the best of my knowledge the prevalence of ADPs and sAHPs observed at baseline conditions has never been determined. The prevalence of the usAHP in this sample (Fig. 3) is significantly lower than that observed by Picton and colleagues (2017) who documented 40% of lumbar motor neurons exhibiting the usAHP. However, as we can see from our breakdown of post-discharge activity across development (Fig. 4), there can be considerable changes in the likelihood of observing certain post-discharge activity subtypes on even a day-by-day basis. We found that there was a shift in the dominance of depolarised post-discharge activity to hyperpolarised post-discharge activity at the start of the second postnatal week. In particular, the frequency of usAHP observation peaked on the 8th postnatal day. It is unlikely that Picton and colleagues (2017) would have been knowledgeable or considerate of this, and therefore it

is possible that this higher prevalence is due to a biased selection of late postnatal week one or early postnatal week two animals used for experiments.

To determine if there was an anatomical correlate to this change in post-discharge activity profile at the beginning of the second postnatal week, we completed an immunohistochemical staining of α3-NKA across the first two postnatal weeks of development (Fig. 5). We found that α3-NKA expression did increase between postnatal day 4 and day 8, in line with our electrophysiological data. We suggest that this upregulation of α3-NKA may account for the increased prevalence of usAHPs observed in these cells at the end of the first postnatal week/beginning of the second postnatal week. These first two weeks are a critical period for spinal motor circuit development, with weight-bearing locomotion beginning to emerge at the beginning of the second postnatal week (Brocard, Vinay and Clarac, 1999; Jean-Xavier *et al.*, 2018). There may be a significance to this. It has been suggested that the functional role of the usAHP is that of a fatigue-prevention mechanism (Picton, Zhang and Sillar, 2017) which may be particularly pertinent in cells that must sustain high levels of activity such as motor neurons. However, lumbar motor neurons which innervate the hindlimbs would not be likely to experience these high levels of activity when the muscles of the hindlimbs are not being used. One might suppose, then, that around the emergence of weightbearing, lumbar motor neurons may begin to experience increasingly higher loads of intracellular sodium due to novel levels of activity and therefore may upregulate expression of α3-NKA to compensate. This may be why we observed an increase in α3-NKA expression and usAHP prevalence at this age. These data lend support to previous work showing that α3-NKA expression is higher in the adult mouse brain when compared to neonatal mice (Sundaram *et al.*, 2019) however a full analysis of α3-NKA expression in the spinal cord across development has yet to be completed. α3-NKA expression appeared to decrease again between days 8 and 12 to levels of expression comparable with postnatal day 4, which is much more difficult to explain with this narrative. However, a more general analysis of our α3-NKA staining may provide insight.

As an explanation for why only a subset of motor neurons display usAHPs at baseline conditions when the usAHP is thought to play such an important physiological role as a fatigue-prevention mechanism, Picton and colleagues (2017) suggest that the heterogenous distribution of usAHPs amongst populations of cells may actually be purposeful. Motor neurons comprise part of a central pattern generating network responsible for the production of purposeful movement. If every neuron in this network were to be largely hyperpolarised in unison, it would render the network silent and the animal paralysed. In a life-or-death situation, such as escaping a predator, the consequences of a total network failure such as this would be fatal. This explanation provides an interesting 'why' but not 'how' only a subset of neurons exhibits an usAHP at baseline conditions. They propose that α3-NKA expression is mosaic in the lumbar spinal cord, in that some neurons will express α3-NKA whilst some neurons will lack it completely. Those that do express the sodium-potassium pump isoform will produce an usAHP in response to prolonged periods of activity while those that do not, will not. However, our data collected from T613M mutant mice that have a knock-down of α3-NKA activity suggested this may not be the case. In T613M-effected preparations, the proportion of motor neurons that did not exhibit an usAHP did not exhibit a sAHP but instead an ADP. From our previous understanding, the α3-NKA has no known involvement in the production of sAHPs or ADPs so this was surprising and suggested that the α3-NKA may not only mediate the usAHP but may play a role in determining the post-discharge activity of a neuron more generally. If this were the case, it is unlikely that α3-NKA is completely absent from the membrane of certain neurons.

When we looked at α3-NKA expression in motor neurons more generally, we found that this was indeed the case. All ChAT-positive lumbar motor neurons had some degree of α3-NKA fluorescence (Fig. 6), confirming that mosaicism of α3-NKA expression cannot explain the heterogeneity of usAHP exhibition in these neurons. Whilst not normally distributed, most motor neurons did have roughly the same degree of α3-NKA expression with smaller cell counts at the particularly high and particularly

low ends. We then questioned what may account for these differences in expression. We examined cell size as a potential determinant of α3-NKA expression. We found that cell size was comparable between postnatal days 4 and 8 and slightly larger at day 12. When analysing the relative frequency distribution, we found there to be two 'peaks' in frequency at approximately 300 μM^2 and 500 μM^2 for postnatal days 4 and 8 that could potentially represent two subpopulations of neurons which may differ in α3-NKA fluorescence. We therefore separated these two populations for analysis but did not find any differences in α3-NKA expression. Finally, we plotted α3-NKA mean fluorescence intensity against motor neuron area (μM^2) for each age group. We found that α3-NKA mean fluorescence intensity did not correlate with motor neuron area at ages P4 and P12, but there was a significant correlation between these two variables for P8 animals, with larger motor neurons having less α3-NKA and smaller motor neurons having more. As our P12 results are close to significance, there is a possibility that smaller motor neurons have been under-sampled at this age. If this is the case, this would also be represented in the relative frequency distribution of cell size presented, where only P12 lacks the distinct 'double-peak' observed at P4 and P8.

If we may disregard the measured decrease in α3-NKA between postnatal days 8 and 12, then the negative correlation between α3-NKA fluorescence and motor neuron size would align physiologically with the functional diversification of motor neuron subtypes that occurs during this period of development (Sharples and Miles, 2021). There are three types of somatic motor neurons: alpha motor neurons, beta motor neurons, and gamma motor neurons. Alpha motor neurons innervate extrafusal muscle fibres, forming a 'motor unit' (Liddell and Sherrington, 1925). Motor units can be divided into three subtypes based upon their twitch kinetics: slow, fast fatiguing, and fast fatigue resistant. The motor neurons that comprise these different subtypes exist on a size continuum, with 'slow' motor neurons being smaller and 'fast' motor neurons being larger (Burke *et al.*, 1982). Sharples and Miles (2021) show that the electrophysiological properties that differentiate these subtypes and thereby ensure the orderly recruitment of motor units diversify in the second postnatal week. We could therefore be observing part of this diversification at the beginning of the second postnatal week,

where ‘fast’ motor neurons express less α3-NKA, and ‘slow’ motor neurons express more α3-NKA. The diversity in usAHP exhibition could therefore be due to motor neuron subtype, with ‘fast’ motor neurons less likely to display an usAHP at baseline conditions than ‘slow’.

Another alternative explanation is that we may be sampling from different somatic motor neuron subtypes. Besides the alpha motor neurons which innervate the extrafusal muscle fibres, there are also gamma motor neurons which innervate the intrafusal muscle fibres of the muscle spindle, and beta motor neurons which innervate both the extrafusal and intrafusal muscle fibres (Manuel and Zytnicki, 2012). Alpha motor neurons have significantly larger cell bodies than gamma motor neurons, but the two subtypes are otherwise impossible to differentiate morphologically (Eccles, Eccles and Lundberg, 1957; Burke *et al.*, 1977). Although alpha motor neurons make up the majority, gamma motor neurons still comprise about a third of all motor pools so it is a certainty that these data will contain a mix of alpha and gamma motor neurons. Edwards and colleagues (2013) show that α1-NKA and α3-NKA are differentially expressed in alpha and gamma motor neurons respectively, with α3-NKA being completely absent from the membranes of alpha motor neurons. Obviously, this is not conclusive with the data presented here, however it could suggest that neurons expressing lower amount of α3-NKA could represent alpha motor neurons in our cohort. It may also explain the electrophysiological data presented in Fig. 4, as smaller motor neurons are more robust in older tissue preparations and therefore more likely to be sampled.

Methodological differences such as the age of experimental animals used, as well as the primary antibodies used may be responsible for the differences in data presented here and by Edwards and colleagues (2013). Edwards and colleagues’ (2013) research challenges generally accepted knowledge about the ubiquity of α1-NKA expression, claiming that α1-NKA is expressed only in alpha motor neurons, whilst research conducted in other central nervous system structures have shown that α1-NKA and α3-NKA are very commonly co-expressed (Azarias *et al.*, 2013). Future experiments should utilise the plethora of molecular markers now available for the identification of fast and slow alpha

motor neurons (reviewed in Blum *et al.*, 2021), as well as molecular markers for gamma motor neurons, such as nuclear hormone receptor Err3 (Friese *et al.*, 2009), the GDNF receptor Gfrα1 (Shneider *et al.*, 2009), or serotonin receptor 1d (5Ht1d) (Enjin *et al.*, 2012), to determine any differing α3-NKA expression between motor neuron subtypes and across development. It would also be of interest to determine the post-discharge activity profile of other neuronal subtypes, such as the many classes of interneurons involved in central pattern generation (see General Introduction). usAHP prevalence has been found to be higher in a subset of cholinergic central canal interneurons identified by the expression of transcription factor Pitx2 (Picton *et al.*, 2017), so there may be large degrees of heterogeneity of post-discharge activity between different interneuron subtypes that may help unveil their role in motor control.

Regardless of the factors that determine the α3-NKA expression of a given neuron, we still are unsure of what exactly determines a given neuron's post-discharge activity at baseline conditions. As our immunohistochemical data shows that all motor neurons express some degree of α3-NKA, we can assume it is not due to mosaicism of ion channel/membrane pump expression. Since our T613M data suggests that the α3-NKA may mediate the usAHP but also play in a role in the production of post-discharge activity more generally, we wondered whether all neurons could produce a usAHP, however in cells with presumably less α3-NKA protein expression and therefore weaker α3-NKA mediated currents, the usAHP may be 'masked' by other competing conductances. Whilst the structures that mediate the different post-discharge activity subtypes are still being described, we do have some knowledge that high-voltage-activated Ca^{2+} channels contribute to the production of the post-discharge ADP (Bouhadfane *et al.*, 2013), Ca^{2+}-activated potassium channels contribute to the production of the sAHP (Kato *et al.*, 2006; Turner *et al.*, 2016; Tiwari *et al.*, 2018), and sodium-potassium pumps contribute to the production of the usAHP (Genet and Kado, 1997; Zhang and Sillar, 2012; Gulledge *et al.*, 2013; Turner *et al.*, 2016; Picton *et al.*, 2017). We applied cadmium chloride,

apamin, and ouabain to cells displaying different post-discharge activity subtypes at baseline conditions to determine how high-voltage-activated Ca^{2+} channel, Ca^{2+}-activated potassium channel, and sodium-potassium pump conductances contributed to post-discharge activity, respectively. While not a perfect relationship, we did find that the post-discharge polarisation of a given neuron can be moved one way or the other through the blockade of the channels or membrane pumps known to mediate either the depolarising or hyperpolarising post-discharge currents.

We found that blockade of the high-voltage-activated Ca^{2+} channels that mediate the ADP leads to a reduction in the size of the ADP and converted some ADPs into large AHPs (Fig. 8). Blockade of the Ca^{2+}-activated potassium channels that mediate the sAHP and sodium-potassium pumps which mediate the usAHP had mixed effects on ADPs but reliably reduced the size of post-discharge hyperpolarisations, converting some AHPs into ADPs (Fig. 9, Fig. 10).

The variable response of ADPs to the application of apamin is likely due to the existence of 'sAHP-dependent' and 'sAHP-independent' ADPs. Many neurons will be depolarised immediately after the cessation of firing, with membrane potential slowly returning to the baseline, as can be seen in Fig. 9D. However, some cells exhibit a fast-hyperpolarising element at the cessation of firing, where the membrane potential will rapidly hyperpolarise for only a matter of milliseconds before rebounding back past resting membrane potential to produce an ADP, as can be seen in the ADP example in Fig. 1. It could be that these 'sAHP-dependent' ADPs are a rebound effect of a sAHP. When apamin is applied, this fast-hyperpolarising element that is Ca^{2+}-activated potassium channel mediated is abolished and the post-discharge activity is converted into an almost flat line. In these cells, the amplitude of the ADP is then 'decreased' although we would expect the removal of a hyperpolarising current to increase its size. It could be that the brief hyperpolarisation produced by the activation of Ca^{2+}-activated potassium channels in turn activates hyperpolarisation-activated cyclic nucleotide-gated (HCN) channels (Solomon and Nerbonne, 1993; Bayliss *et al.*, 1994; Ludwig *et al.*, 1998; Santoro *et al.*, 1998). This hyperpolarisation-activated current (I_h), is a mixed Na^+/K^+ current that would result

in the depolarisation of the membrane potential. A mechanism of this nature may also be involved for the neurons where application of ouabain also had an unexpectedly hyperpolarising effect on some ADPs.

These data show a direct interaction between post-discharge AHPs and ADPs, further supporting the idea that they are not discrete behaviours but instead exist as part of a spectrum that is ultimately controlled by the relative contribution of multiple conductances, including that of high-voltage-activated Ca^{2+} channels, Ca^{2+}-activated potassium channels, sodium-potassium pumps and likely many more. Since the conclusion of these experiments, multiple studies have been published that support this notion.

In *Xenopus* tadpoles, there is an entire subclass of excitatory descending interneurons essential to the production of locomotion that, at first, appeared to completely lack the ability to produce usAHPs (Zhang and Sillar, 2012). However, it was found that in these neurons the usAHPs were being masked by an opposing current, the hyperpolarisation-activated cation current, I_h. Blockade of voltage-dependent HCN channels which mediate this current resulted in the unmasking of the usAHP in these cells (Picton, Sillar and Zhang, 2018). However, when the usAHP was unmasked in these cells they became 'too' hyperpolarised and lacked post-inhibitory rebound firing. As a result, suprathreshold input failed to evoke swimming behaviour entirely at shorter inter-episode intervals.

These data provide insight into the functional significance of non-usAHP post-discharge activity subtypes in the production of locomotion. For example, previous research has implicated the ADP in the production of plateau potentials (Bouhadfane *et al.*, 2013), suggesting an important functional role for this post-discharge activity subtype in direct opposition to the auto-inhibitory role of the usAHP. In spinal motor neurons, "plateau potentials" are a period of prolonged depolarisation of the membrane potential that leads to self-sustained firing (Perrier and Hounsgaard, 2000; Brownstone, 2006). They are triggered by brief excitations and terminated by inhibitory inputs that produces a "bistability" of the membrane potential (Hultborn, Wigström and Wängberg, 1975; Schwindt and Crill,

1980; Hounsgaard *et al.*, 1984). Plateau potentials and self-sustained firing of motor neurons is thought to be of great importance for the maintenance of posture (Hounsgaard *et al.*, 1988), which is essential for locomotion.

As well as the involvement of HCN channels, thermosensitive Trpm5 channels have also been recently implicated in the production of afterdepolarisations and plateau potentials (Bos *et al.*, 2021). Taken together with the data presented in this chapter, it appears that post-discharge activity is highly flexible to accommodate the ever-changing needs of an adaptable system. Future research should investigate the contribution of these channels to post-discharge activity more generally, as well as persistent sodium currents (I_{NaP}) and calcium-activated non-selective cation currents (I_{CaN}) which have both been implicated in the production of the slow afterdepolarisation (Bouhadfane *et al.*, 2013).

Lastly, we wanted to gain knowledge about the modulatory capacity of post-discharge activity. Previous work has shown that dopamine can increase the amplitude of usAHPs (Picton *et al.*, 2017), the neuropeptide myomodulin and monoamine serotonin have been found to decrease sodium pump-mediated AHPs through inhibition of the sodium-potassium pump in the heart interneurons and tactile sensory neurons of the leech respectively (Catarsi, Scuri and Brunelli, 1993; Tobin and Calabrese, 2005), and nitric oxide was found to decrease the amplitude of the usAHP and sodium-potassium pump activity in mammalian spinal neurons (Ellis, Rabe and Sweadner, 2003) and amphibian spinal neurons (Hachoumi *et al.*, 2022) . However, less is known about the modulation of post-discharge activity more generally.

We examined the effects of two modulators: serotonin (5-HT) and muscarine on post-discharge activity. Serotonin is a well-established modulator of motor circuits (Miles and Sillar, 2011) and is of particular interest as it is released into the spinal cord after high levels of motor activity and thought to play a role in central fatigue, similar to dopamine (Meeusen *et al.*, 2012), as well as being a key modulator during the developmental period examined in these experiments (Schmidt and Jordan,

2000; Dunbar, Tran and Whelan, 2010). Serotonin was found to have a hyperpolarising effect on the post-discharge activity of all cells and caused come ADPs to converted into usAHPs (Fig. 11). It is likely that, similarly to dopamine, serotonin is acting upon the PKA or PKC pathway to indirectly activate the α3-NKA. In *Xenopus* tadpoles, the effects of serotonin on the amplitude of the usAHP have been found to be receptor-subtype dependent, with 5-HT_7 receptor agonists increasing the size of the usAHP whilst 5-HT_{2A} receptor agonists had a suppressive effect on the usAHP (Hachoumi *et al.*, 2022). These opposing effects of the 5-HT receptor subtypes could account for some of the variability we see in our own preparations when using 5-HT and thereby globally activating all receptor subtypes at once, as the post-discharge activity of some cells was highly modulated by 5-HT while some displayed only minor changes. Further research into the influence of the modulator and its receptor subtypes in the mammalian spinal cord should be encouraged.

Next, we examined the effect of muscarine, a well-studied intrinsic modulator of the sensory and motor networks of the spinal cord via activation of muscarinic acetylcholine receptors (Kiehn, Johnson and Raastad, 1996; Jiang, Carlin and Brownstone, 1999; Miles *et al.*, 2007). Although there are 5 muscarinic receptor subtypes (M1-M5) in the central nervous system, only M2 and M3 receptors appear to modulate these networks. Both receptor subtypes act via G-coupled proteins to either decrease cAMP or activate phospholipase C and increase intracellular Ca^{2+} (Kurihara *et al.*, 1993; Scarr, 2012; Jordan *et al.*, 2014). We found that, similarly to serotonin, muscarine had a hyperpolarising effect on post-discharge activity and could convert some ADPs into usAHPs (Fig. 12). Similarly to 5-HT, M2 and M3 receptor activation has been found to have contrasting modulatory effects on locomotor-related output, likely due to opposing cellular mechanisms of action, with M2 receptor activation inducing an outward current, decreasing rheobase and synaptic inputs, and shortening action potential duration while M3 receptor activation induced an inward current, increased rheobase and synaptic inputs, and lengthened action potential duration (Nascimento, Spindler and Miles, 2019). Like 5-HT, the differences in the magnitude of the modulatory effect we see between cells could be due to the global activation of M2 and M3 receptors when using muscarine.

Bimodal modulation of the usAHP via application of 5-HT and nitric oxide was found to modulate short-term motor memory in *Xenopus* tadpoles (Hachoumi *et al.*, 2022), therefore it is likely that the modulators examined here would produce cumulative effects on spinal motor network output. Future experiments should examine the effects of these modulators and any differential effects of activating their respective receptor subtypes on spinal network output in mammalian preparations. Future work should also examine the effects of bath application of cadmium chloride and apamin, the high-voltage-activated Ca^{2+} channel and Ca^{2+}-activated potassium channel blockers we examined earlier in this chapter on spinal network output in mammalian preparations. We have shown that cadmium chloride hyperpolarises the post-discharge activity of lumbar motor neurons which is the opposite known effect of ouabain. It would be interesting to observe whether cadmium chloride decreases the frequency of fictive locomotor rhythms in whole cord preparations as ouabain is known to increase the frequency through the suppression of the usAHP.

In conclusion, the data presented here suggest that the functional significance of post-discharge activity is infinitely more complicated and fascinating than previously thought. We present the idea of post-discharge activity as a highly flexible, highly modulated system that allows a spectrum of cellular behaviours to be utilised, such as bistability/plateau potentials or autoinhibition, by the network to produce adaptable motor output.

Concluding Remarks

The sodium-potassium pump (NKA) is a ubiquitously expressed membrane protein that regulates cell excitability by exchanging three intracellular sodium ions for two extracellular potassium ions - an active process that is responsible for up to 50% of total brain energy consumption (Erecińska and Silver, 1994). Mammalian neurons express two isoforms of the catalytic α subunit, the ubiquitous α1, and the neuron-specific α3. α1-NKA is thought to be tonically active due to its high affinity for Na^+ and therefore largely responsible for setting the resting membrane potential of the cell. α3-NKA, with its relatively low affinity for Na^+, is thought to be more dynamically active and is responsible for returning intracellular [Na^+] to basal levels following a period of suprathreshold neuronal activity.

The sodium-potassium pump has been shown to mediate activity-dependent changes in the locomotor networks of a number of species via a pump-mediated hyperpolarising current termed the ultra-slow afterhyperpolarisation (usAHP) (*Drosophila melanogaster* Pulver and Griffith, 2010; *Xenopus laevis* Zhang and Sillar, 2012; *Mus musculus* Picton *et al.*, 2017). Although *Drosophila* do not share the same α-subunit isoforms as vertebrates, pharmacological experiments suggest a role for α3-NKA in the production of the usAHP in the tadpole and the mouse.

Mutations in the α3-NKA encoding protein *ATP1A3* result in a phenotypic spectrum of neurological disorders, all with overlapping symptoms that vary in severity, progression, and age of onset (Sweney, Newcomb and Swoboda, 2015). Most of these disorders such as Alternating Hemiplegia of Childhood (AHC), Rapid-Onset Dystonia Parkinsonism (RDP) involve motor deficits. RDP was the first disorder associated with an *ATP1A3* mutation (de Carvalho Aguiar *et al.*, 2004). RDP is characterised by the sudden onset (hours to weeks) of dystonia with parkinsonism features such as tremor, slowed movement (bradykinesia), muscle rigidity, and impaired posture and balance. Symptoms initially appear in the arms or legs in most RDP patients (Haq *et al.*, 2019). Symptom onset most commonly occurs in adolescence and, similarly to AHC and CAPOS, is triggered by a physical or environmental

stressor such as heat exhaustion, fever, exercise, or childbirth (Dobyns *et al.*, 1993; Brashear *et al.*, 2007). Despite the parkinsonism features, patients do not show signs of nigral degeneration (Oblak *et al.*, 2014), and dopaminergic medication is ineffective at improving symptoms (Brashear *et al.*, 2007).

The α3-NKA has also been shown to be involved in Autism Spectrum Disorder (ASD) (Chaumette *et al.*, 2018; Takata *et al.*, 2018; Torres *et al.*, 2018) and schizophrenia (Smedemark-Margulies *et al.*, 2016; Chaumette *et al.*, 2018), as well as having an emerging role in neurodegenerative diseases such as Parkinson's Disease (Renner *et al.*, 2010; Shrivastava *et al.*, 2013, 2015), Alzheimer's Disease (Chauhan, Lee and Siegel, 1997; Dickey *et al.*, 2005; Ohnishi *et al.*, 2015; Petrushanko *et al.*, 2016; Shrivastava *et al.*, 2019), and Amyotrophic Lateral Sclerosis (ALS) (Ellis, Rabe and Sweadner, 2003; Martin *et al.*, 2007; Ruegsegger *et al.*, 2016), as α3-NKA directly interacts with several of the hallmark pathogenic proteins of these diseases.

Due to the conserved homology of α3-NKA, mouse models can be utilised to gain transferable knowledge on the role of α3-NKA in health and disease in humans. A number of α3-NKA knockdown/knockout mouse models have been produced to aid in the study of the membrane protein (reviewed in Ng *et al.,* 2021). The location of the mutation that causes the knockdown produces varying symptoms in the mice, not dissimilar to what is observed in patients. Consistently, α3-NKA knockdown/knockout mouse models show motor deficits and hyperactivity, lending further support to the role of the isoform in the control of movement.

In the first chapter of this thesis, we provide a comprehensive behavioural, cellular, and molecular characterisation of a novel mouse model harbouring the T613M mutation of the *Atp1a3* gene. T613M is a common gene mutation found in patients with the movement disorder Rapid-Onset Dystonia Parkinsonism (RDP). We show that animals with the T613M mutation are hyperactive and hyperambulatory. When examining the potential involvement of spinal motor circuit pathology in this behaviour, we observed a complete lack of usAHPs in T613M-affected lumbar neurons, and a reduced

capacity for isolated spinal cords to regulate rhythmic motor output in response to large increases of intracellular sodium. We suggest that this deficiency is caused by a reduced capacity for α3-NKA with the T613M mutation to extrude sodium and therefore maintain sodium homeostasis.

While we found that lumbar motor neurons of α3-NKA knock-down mice do not exhibit usAHPs, the loss of this α3-NKA mediated current translated into only minor network-level changes. This suggests that the influence of a neuron's post-discharge activity on motor output may be more complex than initially thought. We also found that almost all T613M-affected motor neurons exhibited afterdepolarisations post-discharge, with only a small handful of cells exhibiting a sAHP which we may have expected with the removal of the hyperpolarising α3-NKA mediated current. The α3-NKA is not thought to mediate the sAHP or ADP, which suggests that α3-NKA may not only be mediating the usAHP but may be playing a role in modulating a given cell's post-discharge activity more generally.

In the second chapter of this thesis, we more generally characterise the post-discharge activity of motor neurons so that we may gain inference on not only the role of the usAHP, but also other post-discharge polarisations, on network-level output. We show that post-discharge activity can be broadly categorised into three subtypes: afterdepolarisations (ADPs), slow afterhyperpolarisations (sAHPs), and ultra-slow afterhyperpolarisations (usAHPs), and that these subtypes are consistent regardless of stimulus intensity.

We show that usAHPs are more commonly observed in the second postnatal week and suggest that this may be due to an upregulation of α3-NKA in lumbar motor neurons alongside the development of weight-bearing locomotion. While the heterogenous distribution of usAHPs amongst populations of motor neurons was previously thought to be due to mosaicism of α3-NKA expression, we show that all lumbar motor neurons express α3-NKA. As an alternative to this hypothesis, we present data that suggests that neurons expressing low levels of α3-NKA may have weak NKA-mediated currents that are masked by competing conductances. We conclude that a neuron's post-discharge activity at

baseline conditions is more likely to be determined by the complement of ion channels/membrane pumps expressed than the complete absence of said constructs in certain cells. Finally, we show that the post-discharge activity of a neuron can be modulated by extrinsic and intrinsic modulators such as 5-HT and muscarine to enhance or unmask certain post-discharge activity subtypes.

Taken together, our results characterise the effect of the T613M mutation commonly seen in RDP patients for the first time, as well as providing a potential novel role for motor neuron pathophysiology in the manifestation of *ATP1A3*-related disorders. Disease models of other *ATP1A3*-related disorders, such as the most common *ATP1A3*-related disorder Alternating Hemiplegia of Childhood, show similar motor deficits as the ones we show here with our T613M model. As the *ATP1A3* homology is so well conserved between rodents and humans, it is likely that the α3-NKA plays a similar functional role in humans and therefore in disease. It is entirely possible that other *ATP1A3*-related disorders could also involve spinal motor circuit pathology via the loss of the ultra-slow hyperpolarisation, and the data we have gathered here could be translated to movement disorders more generally and beyond to neurodegenerative disease. With the refinement of induced pluripotent stem cell technology, it would be interesting to see how T613M-affected motor neurons produced from the fibroblasts of RDP patients differ from controls in terms of usAHP production.

Along with the potential translational value, our data provides insight into the more fundamental role of the α3-NKA in motor control. We provide definitive evidence for the α3-NKA mediation of the ultra-slow afterhyperpolarisation. More generally, our data lend support to the fundamental role of α3-NKA in regulating motor output but perhaps bring previous pharmacological data into a more nuanced physiological perspective.

Altogether, we show that the functional significance of post-discharge activity is infinitely more complicated and fascinating than previously thought. By showing that the post-discharge activity of a cell is determined by a complement of competing conductances that can be easily modulated, we

present the idea of post-discharge activity as a highly flexible system that allows a spectrum of cellular behaviours, such as bistability/plateau potentials or autoinhibition, to be utilised by the network to produce adaptable motor output that may be perturbed in disease.

References

Akkuratov, E. E. *et al.* (2015) 'Functional Interaction Between Na/K-ATPase and NMDA Receptor in Cerebellar Neurons', *Molecular Neurobiology*, 52(3), pp. 1726–1734. doi: 10.1007/S12035-014-8975-3.

Al-Mosawie, A., Wilson, J. M. and Brownstone, R. M. (2007) 'Heterogeneity of V2-derived interneurons in the adult mouse spinal cord', *The European Journal of Neuroscience*, 26(11), pp. 3003–3015. doi: 10.1111/J.1460-9568.2007.05907.X.

Altman, J. and Sudarshan, K. (1975) 'Postnatal development of locomotion in the laboratory rat', *Animal Behaviour*. Academic Press, 23(PART 4), pp. 896–920. doi: 10.1016/0003-3472(75)90114-1.

Alvarez, F. J. *et al.* (1998) 'Distribution of 5-hydroxytryptamine-immunoreactive boutons on alpha-motoneurons in the lumbar spinal cord of adult cats.', *The Journal of Comparative Neurology*, 393(1), pp. 69–83. Available at: http://www.ncbi.nlm.nih.gov/pubmed/9520102 (Accessed: 23 May 2018).

Angstadt, J. D. and Friesen, W. O. (1991) 'Synchronized oscillatory activity in leech neurons induced by calcium channel blockers', *Journal of Neurophysiology*, 66(6), pp. 1858–1873. doi: 10.1152/JN.1991.66.6.1858.

Arvanov, V. L., Stepanyan, A. S. and Ayrapetyan, S. N. (1992) 'The effects of cAMP, Ca2+, and phorbol esters on ouabain-induced depression of acetylcholine responses in Helix neurons', *Cellular and Molecular Neurobiology*, 12(2), pp. 153–161. doi: 10.1007/BF00713369.

Arvanov, V. and Usherwood, P. N. R. (1991) 'Effect of ouabain on volume and chemosensitivity of Xenopus oocytes injected with rat brain mRNA', *Neuroscience Letters*, 125(1), pp. 9–11. doi: 10.1016/0304-3940(91)90116-B.

Arystarkhova, E. (2016) 'Beneficial Renal and Pancreatic Phenotypes in a Mouse Deficient in FXYD2 Regulatory Subunit of Na,K-ATPase', *Frontiers in Physiology*, 7, p. 88. doi: 10.3389/FPHYS.2016.00088.

Arystarkhova, E. *et al.* (2019) 'Factors in the disease severity of ATP1A3 mutations: Impairment, misfolding, and allele competition', *Neurobiology of Disease*. Academic Press Inc., 132. doi: 10.1016/j.nbd.2019.104577.

Arystarkhova, E. and Sweadner, K. J. (1997) 'Tissue-specific Expression of the Na,K-ATPase β3 Subunit: THE PRESENCE OF β3 IN LUNG AND LIVER ADDRESSES THE PROBLEM OF THE MISSING SUBUNIT *', *Journal of Biological Chemistry*, 272(36), pp. 22405–22408. doi: 10.1074/JBC.272.36.22405.

Ayrapetyan, S. (1990) 'A New Theory of Metabolic Regulation of Membrane Functional Activity', (January 1990), pp. 24–31.

Azarias, G. *et al.* (2013) 'A specific and essential role for Na,K-ATPase α3 in neurons co-expressing α1 and α3', *Journal of Biological Chemistry*, 288(4), pp. 2734–2743. doi: 10.1074/jbc.M112.425785.

Balduini, W. and Costa, L. G. (1990) 'Characterization of ouabain-induced phosphoinositide hydrolysis in brain slices of the neonatal rat', *Neurochemical Research*, 15(10), pp. 1023–1029. doi: 10.1007/BF00965749.

Barbano, R. L. *et al.* (2012) 'New triggers and non-motor findings in a family with rapid-onset dystonia-parkinsonism', *Parkinsonism and Related Disorders*, 18(6), pp. 737–741. doi: 10.1016/j.parkreldis.2012.03.020.

Barbeau, H. and Rossignol, S. (1991) 'Initiation and modulation of the locomotor pattern in the adult chronic spinal cat by noradrenergic, serotonergic and dopaminergic drugs', *Brain Research*, 546(2), pp. 250–260. doi: 10.1016/0006-8993(91)91489-N.

Barrière, G., Mellen, N. and Cazalets, J. R. (2004) 'Neuromodulation of the locomotor network by dopamine in the isolated spinal cord of newborn rat', *European Journal of Neuroscience*, 19(5), pp. 1325–1335. doi: 10.1111/j.1460-9568.2004.03210.x.

Bayliss, D. A. *et al.* (1994) 'Characteristics and postnatal development of a hyperpolarization-activated inward current in rat hypoglossal motoneurons in vitro', *Journal of Neurophysiology*, 71(1), pp. 119–128. doi: 10.1152/jn.1994.71.1.119.

Baylor, D. A. *et al.* (1969) 'After-effects of nerve impulses on signalling in the central nervous system of the leech', *The Journal of Physiology*, 203(3), pp. 571–589. doi: 10.1113/JPHYSIOL.1969.SP008880.

Béguin, P. *et al.* (2001) 'CHIF, a member of the FXYD protein family, is a regulator of Na,K-ATPase distinct from the γ-subunit', *The EMBO Journal*, 20(15), pp. 3993–4002. doi: 10.1093/EMBOJ/20.15.3993.

Béguin, P. *et al.* (2002) 'FXYD7 is a brain-specific regulator of Na,K-ATPase α1–β isozymes', *The EMBO Journal*, 21(13), pp. 3264–3273. doi: 10.1093/EMBOJ/CDF330.

Bell, J. R. *et al.* (2008) 'Characterization of the phospholemman knockout mouse heart: Depressed left ventricular function with increased Na-K-ATPase activity', *American Journal of Physiology - Heart and Circulatory Physiology*, 294(2), pp. 613–621. doi: 10.1152/AJPHEART.01332.2007.

Bersier, M. G., Peña, C. and Rodríguez De Lores Arnaiz, G. (2008) 'The expression of NMDA receptor subunits in cerebral cortex and hippocampus is differentially increased by administration of endobain E, a Na+, K+-ATPase inhibitor', *Neurochemical Research*, 33(1), pp. 66–72. doi: 10.1007/S11064-007-9412-Z.

Bertorello, A. and Aperia, A. (1990) 'Inhibition of proximal tubule Na(+)-K(+)-ATPase activity requires simultaneous activation of DA1 and DA2 receptors', *The American Journal of Physiology*, 259(6 Pt 2). doi: 10.1152/AJPRENAL.1990.259.6.F924.

Bertrand, S. and Cazalets, J. (1999) 'Presynaptic GABAergic control of the locomotor drive in the isolated spinal cord of neonatal rats', *The European Journal of Neuroscience*, 11(2), pp. 583–592. doi: 10.1046/J.1460-9568.1999.00473.X.

Bibert, S. *et al.* (2006) 'Structural and Functional Properties of Two Human FXYD3 (Mat-8) Isoforms', *Journal of Biological Chemistry*, 281(51), pp. 39142–39151. doi: 10.1074/JBC.M605221200.

Blanco, G. and Mercer, R. W. (1998) 'Isozymes of the Na-K-ATPase: Heterogeneity in structure, diversity in function', *American Journal of Physiology - Renal Physiology*. doi: 10.1152/ajprenal.1998.275.5.f633.

Blom, H. *et al.* (2011) 'Spatial distribution of Na+-K+-ATPase in dendritic spines dissected by nanoscale superresolution STED microscopy', *BMC Neuroscience*, 12(1), p. 16. doi: 10.1186/1471-2202-12-16.

Blom, H. *et al.* (2012) 'Nearest neighbor analysis of dopamine D1 receptors and Na+-K+-ATPases in dendritic spines dissected by STED microscopy', *Microscopy Research and Technique*, 75(2), pp. 220–228. doi: 10.1002/JEMT.21046.

Blum, J. A. *et al.* (2021) 'Single-cell transcriptomic analysis of the adult mouse spinal cord reveals molecular diversity of autonomic and skeletal motor neurons', *Nature Neuroscience*, 24(4), pp. 572–583. doi: 10.1038/s41593-020-00795-0.

Boldyrev, A. A. (1993) 'Functional activity of Na+, K+-pump in normal and pathological tissues', *Molecular and Chemical Neuropathology*, 19(1–2), pp. 83–93. doi: 10.1007/BF03160170.

Bonnot, A. *et al.* (2009) 'Excitatory actions of ventral root stimulation during network activity

generated by the disinhibited neonatal mouse spinal cord', *Journal of Neurophysiology*, 101(6), pp. 2995–3011. doi: 10.1152/JN.90740.2008.

Borlak, J. and Thum, T. (2003) 'Hallmarks of ion channel gene expression in end-stage heart failure', *The FASEB Journal*, 17(12), pp. 1592–1608. doi: 10.1096/FJ.02-0889COM.

Bos, R. *et al.* (2021) 'Trpm5 channels encode bistability of spinal motoneurons and ensure motor control of hindlimbs in mice', *Nature Communications*, 12(1), pp. 1–18. doi: 10.1038/s41467-021-27113-x.

Bouhadfane, M. *et al.* (2013) 'Sodium-Mediated Plateau Potentials in Lumbar Motoneurons of Neonatal Rats', *Journal of Neuroscience*, 33(39), pp. 15626–15641. doi: 10.1523/JNEUROSCI.1483-13.2013.

Bourgeois, M., Aicardi, J. and Goutières, F. (1993) 'Alternating hemiplegia of childhood', *The Journal of Pediatrics*, 122(5), pp. 673–679. doi: 10.1016/S0022-3476(06)80003-X.

Boylan, K. (2015) 'Familial Amyotrophic Lateral Sclerosis', *Neurologic Clinics*, 33(4), pp. 807–830. doi: 10.1016/J.NCL.2015.07.001.

Brashear, A. *et al.* (2007) 'The phenotypic spectrum of rapid-onset dystonia-parkinsonism (RDP) and mutations in the ATP1A3 gene', *Brain*, 130(3), pp. 828–835. doi: 10.1093/brain/awl340.

Brashear, Allison *et al.* (2007) 'The phenotypic spectrum of rapid-onset dystonia–parkinsonism (RDP) and mutations in the ATP1A3 gene', *Brain*, 130(3), pp. 828–835. doi: 10.1093/BRAIN/AWL340.

Brashear, A. *et al.* (2012) 'Psychiatric disorders in rapid-onset dystonia-parkinsonism', *Neurology*, 79(11), pp. 1168–1173. doi: 10.1212/WNL.0b013e3182698d6c.

Brocard, F., Vinay, L. and Clarac, F. (1999) 'Development of hindlimb postural control during the first postnatal week in the rat', *Developmental Brain Research*, 117(1), pp. 81–89. doi: 10.1016/S0165-3806(99)00101-7.

Brown, T. G. (1914) 'On the nature of the fundamental activity of the nervous centres; together with an analysis of the conditioning of rhythmic activity in progression, and a theory of the evolution of function in the nervous system', *The Journal of Physiology*, 48(1), p. 18. doi: 10.1113/JPHYSIOL.1914.SP001646.

Brownstone, R. M. (2006) 'Beginning at the end: Repetitive firing properties in the final common pathway', *Progress in Neurobiology*, 78(3–5), pp. 156–172. doi: 10.1016/J.PNEUROBIO.2006.04.002.

Brundin, P., Melki, R. and Kopito, R. (2010) 'Prion-like transmission of protein aggregates in neurodegenerative diseases', *Nature Reviews Molecular Cell Biology*, 11(4), pp. 301–307. doi: 10.1038/nrm2873.

Burke, R. E. *et al.* (1977) 'Anatomy of medial gastrocnemius and soleus motor nuclei in cat spinal cord', *Journal of Neurophysiology*, 40(3), pp. 667–680. doi: 10.1152/JN.1977.40.3.667.

Burke, R. E. *et al.* (1982) 'An HRP study of the relation between cell size and motor unit type in cat ankle extensor motoneurons', *Journal of Comparative Neurology*, 209(1), pp. 17–28. doi: 10.1002/CNE.902090103.

Cain, C. C., Sipe, D. M. and Murphy, R. F. (1989) 'Regulation of endocytic pH by the Na+,K+-ATPase in living cells', *Proceedings of the National Academy of Sciences of the United States of America*, 86(2), pp. 544–548. doi: 10.1073/pnas.86.2.544.

Calabrese, R. L., Norris, B. J. and Wenning, A. (2016) 'The neural control of heartbeat in invertebrates', *Current Opinion in Neurobiologyi*, 41, p. 68. doi: 10.1016/J.CONB.2016.08.004.

Calame, D. G. *et al.* (2021) 'A novel ATP1A2 variant associated with severe stepwise regression, hemiplegia, epilepsy and movement disorders in two unrelated patients', *European Journal of Paediatric Neurology*, 31, pp. 21–26. doi: 10.1016/j.ejpn.2021.01.004.

Cameron, R. *et al.* (1994) 'Neurons and astroglia express distinct subsets of Na,K-ATPase α and β subunits', *Molecular Brain Research*, 21(3–4), pp. 333–343. doi: 10.1016/0169-328X(94)90264-X.

Capuani, C. *et al.* (2016) 'Defective glutamate and K+ clearance by cortical astrocytes in familial hemiplegic migraine type 2', *EMBO Molecular Medicine*, 8(8), pp. 967–986. doi: 10.15252/EMMM.201505944.

Carlin, K. P., Jiang, Z. and Brownstone, R. M. (2000) 'Characterization of calcium currents in functionally mature mouse spinal motoneurons', *The European Journal of Neuroscience*, 12(5), pp. 1624–1634. doi: 10.1046/J.1460-9568.2000.00050.X.

Carr, P. A., Pearson, J. C. and Fyffe, R. E. W. (1999) 'Distribution of 5-hydroxytryptamine-immunoreactive boutons on immunohistochemically-identified Renshaw cells in cat and rat lumbar spinal cord', *Brain Research*, 823(1–2), pp. 198–201. doi: 10.1016/S0006-8993(98)01210-4.

de Carvalho Aguiar, P. *et al.* (2004) 'Mutations in the Na+/K+-ATPase α3 Gene ATP1A3 Are Associated with Rapid-Onset Dystonia Parkinsonism', *Neuron*, 43(2), pp. 169–175. doi: 10.1016/j.neuron.2004.06.028.

Catarsi, S., Scuri, R. and Brunelli, M. (1993) 'Cyclic AMP mediates inhibition of the Na(+)-K+ electrogenic pump by serotonin in tactile sensory neurones of the leech.', *The Journal of Physiology*, 462(1), pp. 229–242. doi: 10.1113/JPHYSIOL.1993.SP019552.

Catela, C., Shin, M. M. and Dasen, J. S. (2015) 'Assembly and Function of Spinal Circuits for Motor Control', *Annual Review of Cell and Developmental Biology*, 31, pp. 669–698. doi: 10.1146/ANNUREV-CELLBIO-100814-125155.

Chauhan, N. B., Lee, J. M. and Siegel, G. J. (1997) 'Na,K-ATPase mRNA levels and plaque load in Alzheimer's disease', *Journal of Molecular Neuroscience*, 9(3), pp. 151–166. doi: 10.1007/BF02800498.

Chaumette, B. *et al.* (2018) 'Missense variants in ATP1A3 and FXYD gene family are associated with childhood-onset schizophrenia', *Molecular Psychiatry*, 25(4), pp. 821–830. doi: 10.1038/s41380-018-0103-8.

Chemeris, N. K. *et al.* (1982) 'Inhibition of acetylcholine responses by intracellular calcium in Lymnaea stagnalis neurones', *The Journal of Physiology*, 323(1), pp. 1–19. doi: 10.1113/JPHYSIOL.1982.SP014058.

Chen, L. S. K. *et al.* (1997) 'Characterization of the human and rat phospholemman (PLM) cDNAs and localization of the human PLM gene to chromosome 19q13.1', *Genomics*, 41(3), pp. 435–443. doi: 10.1006/GENO.1997.4665.

Clapcote, S. J. *et al.* (2009) 'Mutation I810N in the α3 isoform of Na+,K +-ATPase causes impairments in the sodium pump and hyperexcitability in the CNS', *Proceedings of the National Academy of Sciences of the United States of America*, 106(33), pp. 14085–14090. doi: 10.1073/pnas.0904817106.

Clausen, M. J., Nissen, P. and Poulsen, H. (2011) 'The pumps that fuel a sperm's journey', in *Biochemical Society Transactions*, pp. 741–745. doi: 10.1042/BST0390741.

Clausen, M. V., Hilbers, F. and Poulsen, H. (2017) 'The structure and function of the Na,K-ATPase isoforms in health and disease', *Frontiers in Physiology*. doi: 10.3389/fphys.2017.00371.

Cleveland, D. W. and Rothstein, J. D. (2001) 'From Charcot to Lou Gehrig: deciphering selective

motor neuron death in ALS', *Nature Reviews Neuroscience*, 2(11), pp. 806–819. doi: 10.1038/35097565.

Condrescu, M. *et al.* (1995) 'ATP-dependent regulation of sodium-calcium exchange in Chinese hamster ovary cells transfected with the bovine cardiac sodium-calcium exchanger', *The Journal of Biological Chemistry*, 270(16), pp. 9137–9146. doi: 10.1074/JBC.270.16.9137.

Contreras, S. A. *et al.* (2021) 'Activity-mediated accumulation of potassium induces a switch in firing pattern and neuronal excitability type', *PLOS Computational Biology*, 17(5), p. e1008510. doi: 10.1371/JOURNAL.PCBI.1008510.

Cooper, G. M. (2000) 'The Origin and Evolution of Cells', in *The Cell: A Molecular Approach*. 2nd edn. Sunderland, MA: Sinauer Associates. Available at: https://www.ncbi.nlm.nih.gov/books/NBK9841/ (Accessed: 19 September 2022).

Crambert, G. *et al.* (2000) 'Transport and Pharmacological Properties of Nine Different Human Na,K-ATPase Isozymes *', *Journal of Biological Chemistry*, 275(3), pp. 1976–1986. doi: 10.1074/JBC.275.3.1976.

Crambert, G. *et al.* (2005) 'FXYD3 (Mat-8), a new regulator of Na,K-ATPase', *Molecular Biology of the Cell*, 16(5), pp. 2363–2371. doi: 10.1091/MBC.E04-10-0878.

Cressman, J. R. *et al.* (2009) 'The influence of sodium and potassium dynamics on excitability, seizures, and the stability of persistent states: I. Single neuron dynamics', *Journal of Computational Neuroscience*, 26(2), pp. 159–170. doi: 10.1007/S10827-008-0132-4.

Crone, S. A. *et al.* (2008) 'Genetic Ablation of V2a Ipsilateral Interneurons Disrupts Left-Right Locomotor Coordination in Mammalian Spinal Cord', *Neuron*, 60(1), pp. 70–83. doi: 10.1016/J.NEURON.2008.08.009.

D'Elia, K. P. and Dasen, J. S. (2018) 'Development, functional organization, and evolution of vertebrate axial motor circuits', *Neural Development*, 13(1), pp. 1–12. doi: 10.1186/S13064-018-0108-7.

Deitmer, J. W., Eckert, R. and Schlue, W. R. (1987) 'Changes in the intracellular free calcium concentration of Aplysia and leech neurones measured with calcium-sensitive microelectrodes', *Canadian Journal of Physiology and Pharmacology*, 65(5), pp. 934–939. doi: 10.1139/Y87-149.

Delprat, B., Puel, J. L. and Geering, K. (2007) 'Dynamic expression of FXYD6 in the inner ear suggests a role of the protein in endolymph homeostasis and neuronal activity', *Developmental Dynamics*, 236(9), pp. 2534–2540. doi: 10.1002/DVDY.21269.

Demos, M. K. *et al.* (2014) 'A novel recurrent mutation in ATP1A3 causes CAPOS syndrome', *Orphanet Journal of Rare Diseases*, 9(1), p. 15. doi: 10.1186/1750-1172-9-15.

Devlin, A. C. *et al.* (2015) 'Human iPSC-derived motoneurons harbouring TARDBP or C9ORF72 ALS mutations are dysfunctional despite maintaining viability', *Nature Communications*, 6(1), pp. 1–12. doi: 10.1038/ncomms6999.

Dickey, C. A. *et al.* (2005) 'Dysregulation of Na+/K+ ATPase by amyloid in APP+PS1 transgenic mice', *BMC Neuroscience*, 6(1), pp. 1–11. doi: 10.1186/1471-2202-6-7.

Dobretsov, M. and Stimers, J. R. (2005) *Neuronal function and alpha3 isoform of the Na/K-ATPase*, *Frontiers in Bioscience*.

Dobyns, W. B. *et al.* (1993) 'Rapid-onset dystonia-parkinsonism', *Neurology*, 43(12), pp. 2596–2596. doi: 10.1212/WNL.43.12.2596.

Douglas, J. R. *et al.* (1993) 'The effects of intrathecal administration of excitatory amino acid agonists and antagonists on the initiation of locomotion in the adult cat', *The Journal of Neuroscience*, 13(3), pp. 990–1000. doi: 10.1523/JNEUROSCI.13-03-00990.1993.

Duat Rodriguez, A. *et al.* (2017) 'Early Diagnosis of CAPOS Syndrome Before Acute-Onset Ataxia—Review of the Literature and a New Family', *Pediatric Neurology*, 71, pp. 60–64. doi: 10.1016/J.PEDIATRNEUROL.2017.01.009.

Dunbar, M. J., Tran, M. A. and Whelan, P. J. (2010) 'Endogenous extracellular serotonin modulates the spinal locomotor network of the neonatal mouse', *The Journal of Physiology*, 588(1), pp. 139–156. doi: 10.1113/jphysiol.2009.177378.

Durlacher, C. T. *et al.* (2015) 'Targeting Na+/K+-translocating adenosine triphosphatase in cancer treatment', *Clinical and Experimental Pharmacology and Physiology*, 42(5), pp. 427–443. doi: 10.1111/1440-1681.12385.

Eccles, J. C., Eccles, R. M. and Lundberg, A. (1957) 'The convergence of monosynaptic excitatory afferents on to many different species of alpha motoneurones', *The Journal of Physiology*, 137(1), pp. 22–50. doi: 10.1113/JPHYSIOL.1957.SP005794.

Edwards, I. J. *et al.* (2013) 'NA+/K+ ATPase α1 and α 3 isoforms are differentially expressed in α - and γ-motoneurons', *Journal of Neuroscience*, 33(24), pp. 9913–9919. doi: 10.1523/JNEUROSCI.5584-12.2013.

Ellis, D. Z., Rabe, J. and Sweadner, K. J. (2003) 'Global loss of Na,K-ATPase and its nitric oxide-mediated regulation in a transgenic mouse model of amyotrophic lateral sclerosis.', *The Journal of Neuroscience*, 23(1), pp. 43–51. Available at: http://www.ncbi.nlm.nih.gov/pubmed/12514200 (Accessed: 23 May 2018).

Enjin, A. *et al.* (2012) 'Sensorimotor function is modulated by the serotonin receptor 1d, a novel marker for gamma motor neurons', *Molecular and Cellular Neuroscience*, 49(3), pp. 322–332. doi: 10.1016/J.MCN.2012.01.003.

Erecińska, M. and Silver, I. A. (1994) 'Ions and energy in mammalian brain', *Progress in Neurobiology*, 43(1), pp. 37–71. doi: 10.1016/0301-0082(94)90015-9.

Farley, R. A. *et al.* (1984) 'The amino acid sequence of a fluorescein-labeled peptide from the active site of (Na,K)-ATPase.', *The Journal of Biological Chemistry*, 259(15), pp. 9532–5. Available at: http://www.ncbi.nlm.nih.gov/pubmed/6086638 (Accessed: 22 May 2018).

Forbush, B., Kaplan, J. H. and Hoffman, J. F. (1978) 'Characterization of a New Photoaffinity Derivative of Ouabain: Labeling of the Large Polypeptide and of a Proteolipid Component of the Na,K-ATPase', *American Chemical Society*, 17, pp. 3667–3676. Available at: https://pubs.acs.org/sharingguidelines (Accessed: 10 January 2022).

Forrest, M. D. *et al.* (2012) 'The Sodium-Potassium Pump Controls the Intrinsic Firing of the Cerebellar Purkinje Neuron', *PLOS ONE*, 7(12), p. e51169. doi: 10.1371/JOURNAL.PONE.0051169.

Fremont, R. *et al.* (2014) 'Abnormal High-Frequency Burst Firing of Cerebellar Neurons in Rapid-Onset Dystonia-Parkinsonism', *Journal of Neuroscience*, 34(35), pp. 11723–11732. doi: 10.1523/JNEUROSCI.1409-14.2014.

French, A. S. (1989) 'Ouabain selectively affects the slow component of sensory adaptation in an insect mechanoreceptor', *Brain Research*, 504(1), pp. 112–114. doi: 10.1016/0006-8993(89)91604-1.

Friese, A. *et al.* (2009) 'Gamma and alpha motor neurons distinguished by expression of transcription factor Err3', *Proceedings of the National Academy of Sciences of the United States of America*,

106(32), pp. 13588–13593. doi: 10.1073/PNAS.0906809106.

Fuchs, R., Schmid, S. and Mellman, I. (1989) 'A possible role for Na+,K+-ATPase in regulating ATP-dependent endosome acidification', *Proceedings of the National Academy of Sciences of the United States of America*, 86(2), pp. 539–543. doi: 10.1073/pnas.86.2.539.

Fujino, S. and Fujino, M. (1982) 'Ouabain potentiation and Ca release from sarcoplasmic reticulum in cardiac and skeletal muscle cells', *Canadian Journal of Physiology and Pharmacology*, 60(4), pp. 542–555. doi: 10.1139/Y82-074.

Gandevia, S. C. (2001) 'Spinal and supraspinal factors in human muscle fatigue', *Physiological Reviews*, 81(4), pp. 1725–1789. doi: 10.1152/PHYSREV.2001.81.4.1725.

Garty, H. and Karlish, S. J. D. (2006) 'ROLE OF FXYD PROTEINS IN ION TRANSPORT', *Annual Review of Physiology*, 68, pp. 431–59. doi: 10.1146/annurev.physiol.68.040104.131852.

Geering, K. (2001) 'The Functional Role of β Subunits in Oligomeric P-Type ATPases', *Journal of Bioenergetics and Biomembranes*, 33(5), pp. 425–438. doi: 10.1023/A:1010623724749.

Geering, K. (2005) 'Function of FXYD proteins, regulators of Na, K-ATPase', *Journal of Bioenergetics and Biomembranes*, 37(6), pp. 387–392. doi: 10.1007/S10863-005-9476-X.

Geering, K. (2006) 'FXYD proteins: new regulators of Na-K-ATPase', *American Journal of Physiology-Renal Physiology*, 290(2), pp. F241–F250. doi: 10.1152/ajprenal.00126.2005.

Genet, S. and Kado, R. T. (1997) 'Hyperpolarizing current of the Na/K ATPase contributes to the membrane polarization of the Purkinje cell in rat cerebellum', *European Journal of Physiology*, 434(5), pp. 559–567. doi: 10.1007/S004240050436.

Gerin, C., Becquet, D. and Privat, A. (1995) 'Direct evidence for the link between monoaminergic descending pathways and motor activity. I. A study with microdialysis probes implanted in the ventral funiculus of the spinal cord', *Brain Research*, 704(2), pp. 191–201. doi: 10.1016/0006-8993(95)01111-0.

Glanzman, D. L. (2010) 'Ion pumps get more glamorous', *Nature Neuroscience*, 13(1), pp. 4–5. doi: 10.1038/NN0110-4.

Gloor, S. *et al.* (1990) 'The adhesion molecule on glia (AMOG) is a homologue of the beta subunit of the Na,K-ATPase.', *Journal of Cell Biology*, 110(1), pp. 165–174. doi: 10.1083/JCB.110.1.165.

Gocht, D. and Heinrich, R. (2007) 'Postactivation inhibition of spontaneously active neurosecretory neurons in the medicinal leech', *Journal of Comparative Physiology A*, 193(3), pp. 347–361. doi: 10.1007/S00359-006-0190-X.

Gomez-Sanchez, C. E., Kuppusamy, M. and Gomez-Sanchez, E. P. (2015) 'Somatic mutations of the ATP1A1 gene and aldosterone-producing adenomas', *Molecular and Cellular Endocrinology*, 408, pp. 213–219. doi: 10.1016/J.MCE.2014.12.004.

Gordon, I. T. and Whelan, P. J. (2006) 'Monoaminergic Control of Cauda-Equina-Evoked Locomotion in the Neonatal Mouse Spinal Cord', *Journal of Neurophysiology*, 96, pp. 3122–3129. doi: 10.1152/jn.00606.2006.

Gosgnach, S. *et al.* (2006) 'V1 spinal neurons regulate the speed of vertebrate locomotor outputs', *Nature*, 440(7081), pp. 215–219. doi: 10.1038/NATURE04545.

Goulding, M. *et al.* (2002) 'The formation of sensorimotor circuits', *Current Opinion in Neurobiology*, 12(5), pp. 508–515. doi: 10.1016/S0959-4388(02)00371-9.

Goulding, M. (2009) ‘Circuits controlling vertebrate locomotion: Moving in a new direction’, *Nature Reviews Neuroscience*, pp. 507–518. doi: 10.1038/nrn2608.

Graham Brown, T. (1911) ‘The intrinsic factors in the act of progression in the mammal’, *Proceedings of the Royal Society of London. Series B*, 84(572), pp. 308–319. doi: 10.1098/RSPB.1911.0077.

Grillner, S. (1975) ‘Locomotion in vertebrates: central mechanisms and reflex interaction’, *Physiological Reviews*, 55(2), pp. 247–304. doi: 10.1152/PHYSREV.1975.55.2.247.

Grillner, S. (1981) ‘Control of Locomotion in Bipeds, Tetrapods, and Fish’, *Comprehensive Physiology*, pp. 1179–1236. doi: 10.1002/CPHY.CP010226.

Grillner, S. (2018) ‘Evolution: Vertebrate Limb Control over 420 Million Years’, *Current Biology*, 28(4), pp. R162–R164. doi: 10.1016/J.CUB.2017.12.040.

Grillner, S. and Manira, A. El (2019) ‘Current Principles of Motor Control, with Special Reference to Vertebrate Locomotion’, *Physiological Reviews*, 100(1), pp. 271–320. doi: 10.1152/PHYSREV.00015.2019.

Grillner, S., McClellan, A. and Perret, C. (1981) ‘Entrainment of the spinal pattern generators for swimming by mechano-sensitive elements in the lamprey spinal cord in vitro’, *Brain Research*, 217(2), pp. 380–386. doi: 10.1016/0006-8993(81)90015-9.

Grillner, S. and Robertson, B. (2015) ‘The basal ganglia downstream control of brainstem motor centres-an evolutionarily conserved strategy’, *Current Opinion in Neurobiology*, 33, pp. 47–52. doi: 10.1016/J.CONB.2015.01.019.

Gross, M. K., Dottori, M. and Goulding, M. (2002) ‘Lbx1 Specifies Somatosensory Association Interneurons in the Dorsal Spinal Cord’, *Neuron*, 34(4), pp. 535–549. doi: 10.1016/S0896-6273(02)00690-6.

Gulledge, A. T. *et al.* (2013) ‘A Sodium-Pump-Mediated Afterhyperpolarization in Pyramidal Neurons’, *Journal of Neuroscience*, 33(32), pp. 13025–13041. doi: 10.1523/JNEUROSCI.0220-13.2013.

Hachoumi, L. *et al.* (2022) ‘Bimodal modulation of short-term motor memory via dynamic sodium pumps in a vertebrate spinal cord’, *Current Biology*, 32(5), pp. 1038-1048.e2. doi: 10.1016/J.CUB.2022.01.012.

Hamada, K. *et al.* (2003) ‘Properties of the Na+/K+ pump current in small neurons from adult rat dorsal root ganglia’, *British Journal of Pharmacology*, 138(8), p. 1517. doi: 10.1038/SJ.BJP.0705170.

Hammar, I. *et al.* (2004) ‘The actions of monoamines and distribution of noradrenergic and serotoninergic contacts on different subpopulations of commissural interneurons in the cat spinal cord’, *The European Journal of Neuroscience*, 19(5), pp. 1305–1316. doi: 10.1111/J.1460-9568.2004.03239.X.

Han, K. H. *et al.* (2017) ‘ATP1A3 mutations can cause progressive auditory neuropathy: a new gene of auditory synaptopathy’, *Scientific Reports*, 7(1), pp. 1–11. doi: 10.1038/s41598-017-16676-9.

Han, P. *et al.* (2007) ‘Dopaminergic Modulation of Spinal Neuronal Excitability’, *Journal of Neuroscience*, 27(48), pp. 13192–13204. doi: 10.1523/JNEUROSCI.1279-07.2007.

Haq, I. U. *et al.* (2019) ‘Revising rapid-onset dystonia–parkinsonism: Broadening indications for ATP1A3 testing’, *Movement Disorders*. John Wiley & Sons, Ltd, 34(10), pp. 1528–1536. doi: 10.1002/MDS.27801.

Hawkins, C. H. (1869) ‘Sir Charles Bell And M. Magendie On The Functions Of The Spinal Nerves’,

Medical Journal, 1(419), pp. 21–23. Available at: https://about.jstor.org/terms (Accessed: 18 January 2022).

Hazelwood, L. A. *et al.* (2008) 'Reciprocal modulation of function between the D1 and D2 dopamine receptors and the Na+,K+-ATPase', *The Journal of Biological Chemistry*, 283(52), pp. 36441–36453. doi: 10.1074/JBC.M805520200.

He, J. *et al.* (2019) 'ATP1A1 mutations cause intermediate Charcot-Marie-Tooth disease', *Human Mutation*, 40(12), pp. 2334–2343. doi: 10.1002/HUMU.23886.

Heimer, G. *et al.* (2015) 'CAOS—Episodic Cerebellar Ataxia, Areflexia, Optic Atrophy, and Sensorineural Hearing Loss: A Third Allelic Disorder of the ATP1A3 Gene', *Journal of Child Neurology*, 30(13), pp. 1749–1756. doi: 10.1177/0883073815579708.

Heinzen, E. L. *et al.* (2012) 'De novo mutations in ATP1A3 cause alternating hemiplegia of childhood', *Nature Genetics*, 44(9), pp. 1030–1034. doi: 10.1038/ng.2358.

Helseth, A. R. *et al.* (2018) 'Novel E815K knock-in mouse model of alternating hemiplegia of childhood', *Neurobiology of Disease*, 119, pp. 100–112. doi: 10.1016/J.NBD.2018.07.028.

Hiatt, A., McDonough, A. A. and Edelman, I. S. (1984) 'Assembly of the (Na+/K+)-adenosine triphosphatase. Post-translational membrane integration of the alpha subunit.', *The Journal of Biological Chemistry*, 259(4), pp. 2629–35. Available at: http://www.ncbi.nlm.nih.gov/pubmed/6199349 (Accessed: 22 May 2018).

Higashijima, S.-I. *et al.* (2004) 'Engrailed-1 Expression Marks a Primitive Class of Inhibitory Spinal Interneuron', *The Journal of Neuroscience*. doi: 10.1523/JNEUROSCI.5342-03.2004.

Hilbers, F. *et al.* (2016) 'Tuning of the Na,K-ATPase by the beta subunit', *Scientific Reports*, 6(1), pp. 1–11. doi: 10.1038/srep20442.

Hoei-Hansen, C. E. *et al.* (2014) 'Alternating hemiplegia of childhood in Denmark: Clinical manifestations and ATP1A3 mutation status', *European Journal of Paediatric Neurology*, 18(1), pp. 50–54. doi: 10.1016/J.EJPN.2013.08.007.

Holm, R. *et al.* (2016) 'Neurological disease mutations of α3 Na+,K+-ATPase: Structural and functional perspectives and rescue of compromised function', *Biochimica et Biophysica Acta (BBA) - Bioenergetics*, 1857(11), pp. 1807–1828. doi: 10.1016/J.BBABIO.2016.08.009.

Holm, T. H. *et al.* (2016) 'Cognitive deficits caused by a disease-mutation in the α3 Na+/K+-ATPase isoform', *Scientific Reports*, 6(1), pp. 1–15. doi: 10.1038/srep31972.

Hounsgaard, J. *et al.* (1984) 'Intrinsic membrane properties causing a bistable behaviour of α-motoneurones', *Experimental Brain Research*, 55(2), pp. 391–394. doi: 10.1007/BF00237290.

Hounsgaard, J. *et al.* (1988) 'Bistability of alpha-motoneurones in the decerebrate cat and in the acute spinal cat after intravenous 5-hydroxytryptophan.', *The Journal of Physiology*. Wiley-Blackwell, 405, pp. 345–67. Available at: http://www.ncbi.nlm.nih.gov/pubmed/3267153 (Accessed: 23 May 2018).

Hübel, N., Schöll, E. and Dahlem, M. A. (2014) 'Bistable Dynamics Underlying Excitability of Ion Homeostasis in Neuron Models', *PLOS Computational Biology*, 10(5), p. e1003551. doi: 10.1371/JOURNAL.PCBI.1003551.

Hultborn, H., Wigström, H. and Wängberg, B. (1975) 'Prolonged activation of soleus motoneurones following a conditioning train in soleus Ia afferents — A case for a reverberating loop?', *Neuroscience Letters*, 1(3), pp. 147–152. doi: 10.1016/0304-3940(75)90030-0.

Hunanyan, A. S. *et al.* (2015) 'Knock-in mouse model of alternating hemiplegia of childhood: Behavioral and electrophysiologic characterization', *Epilepsia*, 56(1), pp. 82–93. doi: 10.1111/EPI.12878.

Ikeda, K. *et al.* (2013) 'Enhanced inhibitory neurotransmission in the cerebellar cortex of Atp1a3-deficient heterozygous mice', *The Journal of Physiology*, 591(13), pp. 3433–3449. doi: 10.1113/JPHYSIOL.2012.247817.

Jankowska, E. (2016) 'Spinal Interneurons', *Neuroscience in the 21st Century: From Basic to Clinical, Second Edition*. Springer, New York, NY, pp. 1189–1224. doi: 10.1007/978-1-4939-3474-4_34.

Jean-Xavier, C. *et al.* (2018) 'Retracing your footsteps: Developmental insights to spinal network plasticity following injury', *Journal of Neurophysiology*, 119(2), pp. 521–536. doi: 10.1152/JN.00575.2017.

Jessell, T. M. (2000) 'Neuronal specification in the spinal cord: inductive signals and transcriptional codes', *Nature Reviews Genetics*, 1(1), pp. 20–29. doi: 10.1038/35049541.

Jia, L. G. *et al.* (2005) 'Hypertrophy, increased ejection fraction, and reduced Na-K-ATPase activity in phospholemman-deficient mice', *American Journal of Physiology - Heart and Circulatory Physiology*, 288(4 57-4), pp. 1982–1988. doi: 10.1152/AJPHEART.00142.2004.

Jiang, Z., Carlin, K. P. and Brownstone, R. M. (1999) 'An in vitro functionally mature mouse spinal cord preparation for the study of spinal motor networks.', *Brain Research*, 816(2), pp. 493–9. Available at: http://www.ncbi.nlm.nih.gov/pubmed/9878874 (Accessed: 29 May 2018).

Johnson, S. W., Seutin, V. and North, R. A. (1992) 'Burst Firing in Dopamine Neurons Induced by N-Methyl-D-aspartate: Role of Electrogenic Sodium Pump', *Science*, 258(5082), pp. 665–667. doi: 10.1126/SCIENCE.1329209.

Jones, D. H. *et al.* (2005) 'Na,K-ATPase from mice lacking the gamma subunit (FXYD2) exhibits altered Na+ affinity and decreased thermal stability', *The Journal of Biological Chemistry*, 280(19), pp. 19003–19011. doi: 10.1074/JBC.M500697200.

Jordan, L. M. *et al.* (2008) 'Descending command systems for the initiation of locomotion in mammals', *Brain Research Reviews*. Elsevier, 57(1), pp. 183–191. doi: 10.1016/J.BRAINRESREV.2007.07.019.

Jordan, L. M. *et al.* (2014) 'Cholinergic mechanisms in spinal locomotion — Potential target for rehabilitation approaches', *Frontiers in Neural Circuits*, 8, p. 132. doi: 10.3389/FNCIR.2014.00132/BIBTEX.

Julien, J. P. (2001) 'Amyotrophic lateral sclerosis: unfolding the toxicity of the misfolded.', *Cell*, 104(4), pp. 581–91. Available at: http://www.ncbi.nlm.nih.gov/pubmed/11239414 (Accessed: 23 May 2018).

Jung, H. *et al.* (2018) 'The Ancient Origins of Neural Substrates for Land Walking', *Cell*, 172(4), pp. 667-682.e15. doi: 10.1016/J.CELL.2018.01.013.

Kang, Y. *et al.* (2004) 'Bidirectional Interactions between H-Channels and Na+–K+ Pumps in Mesencephalic Trigeminal Neurons', *The Journal of Neuroscience*, 24(14), p. 3694. doi: 10.1523/JNEUROSCI.5641-03.2004.

Kato, M. *et al.* (2006) 'The SK channel blocker apamin inhibits slow afterhyperpolarization currents in rat gonadotropin-releasing hormone neurones', *The Journal of Physiology*, 574(Pt 2), p. 431. doi: 10.1113/JPHYSIOL.2006.110155.

Kiehn, O. and Dougherty, K. (2013) 'Locomotion: Circuits and Physiology', *Neuroscience in the 21st*

Century: From Basic to Clinical. Springer, New York, NY, pp. 1209–1236. doi: 10.1007/978-1-4614-1997-6_42.

Kiehn, O., Johnson, B. R. and Raastad, M. (1996) 'Plateau properties in mammalian spinal interneurons during transmitter-induced locomotor activity', *Neuroscience*, 75(1), pp. 263–273. doi: 10.1016/0306-4522(96)00250-3.

Kiehn, O. and Kjærulff, O. (1996) 'Spatiotemporal characteristics of 5-HT and dopamine-induced rhythmic hindlimb activity in the in vitro neonatal rat', *Journal of Neurophysiology*, 75(4), pp. 1472–1482. doi: 10.1152/JN.1996.75.4.1472.

Kiernan, M. C., Lin, C. S. Y. and Burke, D. (2004) 'Differences in activity-dependent hyperpolarization in human sensory and motor axons', *The Journal of Physiology*, 558(Pt 1), p. 341. doi: 10.1113/JPHYSIOL.2004.063966.

Kim, J. H. *et al.* (2007) 'Presynaptic Ca2+ buffers control the strength of a fast post-tetanic hyperpolarization mediated by the α3 Na+/K +-ATPase', *Nature Neuroscience*, 10(2), pp. 196–205. doi: 10.1038/nn1839.

Kim, M. S. and Akera, T. (1987) 'O2 free radicals: cause of ischemia-reperfusion injury to cardiac Na+-K+-ATPase', *American Journal of Physiology*, 252(2), pp. H252–H257. doi: 10.1152/ajpheart.1987.252.2.H252.

Kirshenbaum, G. S. *et al.* (2011) 'Mania-like behavior induced by genetic dysfunction of the neuron-specific Na+,K+-ATPase α3 sodium pump', *Proceedings of the National Academy of Sciences of the United States of America*, 108(44), pp. 18144–18149. doi: 10.1073/pnas.1108416108.

Kirshenbaum, G. S. *et al.* (2013) 'Alternating Hemiplegia of Childhood-Related Neural and Behavioural Phenotypes in Na+,K+-ATPase α3 Missense Mutant Mice', *PLOS ONE*, 8(3), p. e60141. doi: 10.1371/JOURNAL.PONE.0060141.

Kirshenbaum, G. S. *et al.* (2015) 'Characterization of cognitive deficits in mice with an alternating hemiplegia-linked mutation.', *Behavioral Neuroscience*. US: American Psychological Association, 129(6), p. 822. doi: 10.1037/BNE0000097.

Kirshenbaum, G. S. *et al.* (2016) 'Deficits in social behavioral tests in a mouse model of alternating hemiplegia of childhood', *Journal of Neurogenetics*, 30(1), pp. 42–49. doi: 10.1080/01677063.2016.1182525.

Krey, R. A. *et al.* (2010) 'Outward currents contributing to inspiratory burst termination in prebötzinger complex neurons of neonatal mice studied in vitro', *Frontiers in Neural Circuits*, 4(NOV), p. 124. doi: 10.3389/FNCIR.2010.00124/BIBTEX.

Krogh, A. (1945) 'The active and passive exchanges of inorganic ions through the surfaces of living cells and through living membranes generally', *Proceedings of the Royal Society of London*, 133(140). Available at: https://royalsocietypublishing.org/ (Accessed: 13 April 2021).

Kurihara, T. *et al.* (1993) 'Muscarinic excitatory and inhibitory mechanisms involved in afferent fibre-evoked depolarization of motoneurones in the neonatal rat spinal cord', *British Journal of Pharmacology*, 110(1), pp. 61–70. doi: 10.1111/J.1476-5381.1993.TB13772.X.

Küster, B. *et al.* (2000) 'A new variant of the gamma subunit of renal Na,K-ATPase. Identification by mass spectrometry, antibody binding, and expression in cultured cells', *The Journal of Biological Chemistry*, 275(24), pp. 18441–18446. doi: 10.1074/JBC.M001411200.

Lakke, E. A. (1997) 'The projections to the spinal cord of the rat during development: a timetable of descent.', *Advances in Anatomy, Embryology, and Cell Biology*, 135. doi: 10.1007/978-3-642-60601-

4.

Lanuza, G. M. *et al.* (2004) 'Genetic identification of spinal interneurons that coordinate left-right locomotor activity necessary for walking movements', *Neuron*, 42(3), pp. 375–386. doi: 10.1016/S0896-6273(04)00249-1.

Larsen, B. R. *et al.* (2014) 'Contributions of the Na+/K+-ATPase, NKCC1, and Kir4.1 to hippocampal K+ clearance and volume responses', *Glia*, 62(4), pp. 608–622. doi: 10.1002/GLIA.22629.

Lassuthova, P. *et al.* (2018) 'Mutations in ATP1A1 Cause Dominant Charcot-Marie-Tooth Type 2', *American Journal of Human Genetics*, 102(3), pp. 505–514. doi: 10.1016/J.AJHG.2018.01.023.

Lee, K. J. and Jessell, T. M. (1999) 'The specification of dorsal cell fates in the vertebrate central nervous system', *Annual Review of Neuroscience*, 22, pp. 261–294. doi: 10.1146/ANNUREV.NEURO.22.1.261.

Li, W. C. *et al.* (2004) 'Primitive Roles for Inhibitory Interneurons in Developing Frog Spinal Cord', *Journal of Neuroscience*, 24(25), pp. 5840–5848. doi: 10.1523/JNEUROSCI.1633-04.2004.

Liddell, E. and Sherrington, C. (1925) 'Further observations on myotatic reflexes', *Proceedings of the Royal Society B*, 97(683), pp. 267–283. doi: 10.1098/RSPB.1925.0002.

Lin, Z. *et al.* (2021) 'ATP1A1 de novo Mutation-Related Disorders: Clinical and Genetic Features', *Frontiers in Pediatrics*, 9, p. 657256. doi: 10.3389/FPED.2021.657256.

Liu, J. and Jordan, L. M. (2005) 'Stimulation of the Parapyramidal Region of the Neonatal Rat Brain Stem Produces Locomotor-Like Activity Involving Spinal 5-HT7 and 5-HT2A Receptors', *Journal of Neurophysiology*, 94(2), pp. 1392–1404. doi: 10.1152/jn.00136.2005.

Lubarski, I., Karlish, S. J. D. and Garty, H. (2007) 'Structural and functional interactions between FXYD5 and the Na +-K+-ATPase', *American Journal of Physiology - Renal Physiology*, 293(6), pp. 1818–1826. doi: 10.1152/AJPRENAL.00367.2007.

Ludwig, A. *et al.* (1998) 'A family of hyperpolarization-activated mammalian cation channels', *Nature*, 393(6685), pp. 587–591. doi: 10.1038/31255.

Lundfald, L. *et al.* (2007) 'Phenotype of V2-derived interneurons and their relationship to the axon guidance molecule EphA4 in the developing mouse spinal cord', *The European Journal of Neuroscience*, 26(11), pp. 2989–3002. doi: 10.1111/J.1460-9568.2007.05906.X.

Maas, R. P. P. W. M. *et al.* (2016) 'The Genetic Homogeneity of CAPOS Syndrome: Four New Patients With the c.2452G>A (p.Glu818Lys) Mutation in the ATP1A3 Gene', *Pediatric Neurology*, 59, pp. 71-75.e1. doi: 10.1016/J.PEDIATRNEUROL.2016.02.010.

Malik, N. *et al.* (1996) 'Identification of the Mammalian Na,K-ATPase β3 Subunit *', *Journal of Biological Chemistry*, 271(37), pp. 22754–22758. doi: 10.1074/JBC.271.37.22754.

Manuel, M. and Zytnicki, D. (2012) 'Alpha, Beta, and Gamma Motoneurons: Functional Diversity in the Motor System's Final Pathway', *Journal of Integrative Neuroscience*, 10(3), pp. 243–276. doi: 10.1142/S0219635211002786.

Martin-Vasallo, P. *et al.* (1989) 'Identification of a putative isoform of the Na,K-ATPase beta subunit. Primary structure and tissue-specific expression.', *The Journal of Biological Chemistry*, 264(8), pp. 4613–8. Available at: http://www.ncbi.nlm.nih.gov/pubmed/2538450 (Accessed: 22 May 2018).

Martin, L. J. *et al.* (2007) 'Motor neuron degeneration in amyotrophic lateral sclerosis mutant superoxide dismutase-1 transgenic mice: Mechanisms of mitochondriopathy and cell death', *The Journal of Comparative Neurology*, 500(1), pp. 20–46. doi: 10.1002/cne.21160.

Mathias, S. D. *et al.* (2008) 'Impact of chronic Immune Thrombocytopenic Purpura (ITP) on health-related quality of life: A conceptual model starting with the patient perspective', *Health and Quality of Life Outcomes*, 6(1), pp. 1–14. doi: 10.1186/1477-7525-6-13/TABLES/3.

Matise, M. P. *et al.* (1997) 'Expression Patterns of Developmental Control Genes in Normal andEngrailed-1 Mutant Mouse Spinal Cord Reveal Early Diversity in Developing Interneurons', *Journal of Neuroscience*, 17(20), pp. 7805–7816. doi: 10.1523/JNEUROSCI.17-20-07805.1997.

McClellan, A. D. and Sigvardt, K. A. (1988) 'Features of entrainment of spinal pattern generators for locomotor activity in the lamprey spinal cord', *Journal of Neuroscience*, 8(1), pp. 133–145. doi: 10.1523/JNEUROSCI.08-01-00133.1988.

McGrail, K. M., Phillips, J. M. and Sweadner, K. J. (1991) 'Immunofluorescent localization of three Na,K-ATPase isozymes in the rat central nervous system: both neurons and glia can express more than one Na,K-ATPase.', *The Journal of Neuroscience*, 11(2), pp. 381–91. doi: 10.1523/JNEUROSCI.11-02-00381.1991.

Meeusen, R. *et al.* (2012) 'Central Fatigue', *Sports Medicine*, 36(10), pp. 881–909. doi: 10.2165/00007256-200636100-00006.

Mejzini, R. *et al.* (2019) 'ALS Genetics, Mechanisms, and Therapeutics: Where Are We Now?', *Frontiers in Neuroscience*, 13, p. 1310. doi: 10.3389/FNINS.2019.01310/BIBTEX.

Melki, R. (2015) 'Role of Different Alpha-Synuclein Strains in Synucleinopathies, Similarities with other Neurodegenerative Diseases', *Journal of Parkinson's Disease*, 5(2), pp. 217–227. doi: 10.3233/JPD-150543.

Melki, R. (2017) 'The multitude of therapeutic targets in neurodegenerative proteinopathies', *Disease-Modifying Targets in Neurodegenerative Disorders: Paving the Way for Disease-Modifying Therapies*, pp. 1–20. doi: 10.1016/B978-0-12-805120-7.00001-4.

Melki, R. (2018) 'How the shapes of seeds can influence pathology', *Neurobiology of Disease*, 109, pp. 201–208. doi: 10.1016/J.NBD.2017.03.011.

Mense, M., Stark, G. and Apell, H.-J. (1997) 'Effects of Free Radicals on Partial Reactions of the Na,K-ATPase', *Journal of Membrane Biology*, 156(1), pp. 63–71. doi: 10.1007/s002329900188.

Meyer-Lehnert, H., Bäcker, A. and Kramer, H. J. (2000) 'Inhibitors of Na-K-ATPase in human urine: effects of ouabain-like factors and of vanadium-diascorbate on calcium mobilization in rat vascular smooth muscle cells: comparison with the effects of ouabain, angiotensin II, and arginine-vasopressin', *American journal of Hypertension*, 13(4 Pt 1), pp. 364–369. doi: 10.1016/S0895-7061(99)00197-1.

Meyer, D. J. *et al.* (2020) 'FXYD protein isoforms differentially modulate human Na/K pump function', *Journal of General Physiology*. doi: 10.1085/jgp.202012660.

Miles, G. B. *et al.* (2007) 'Spinal cholinergic interneurons regulate the excitability of motoneurons during locomotion', *Proceedings of the National Academy of Sciences of the United States of America*, 104(7), pp. 2448–2453. doi: 10.1073/PNAS.0611134104.

Miles, G. B. and Sillar, K. T. (2011) 'Neuromodulation of Vertebrate Locomotor Control Networks', *Physiology*, 26(6). Available at: http://physiologyonline.physiology.org/content/26/6/393 (Accessed: 29 April 2017).

Milner, K. L. and Mogenson, G. J. (1988) 'Electrical and chemical activation of the mesencephalic and subthalamic locomotor regions in freely moving rats', *Brain Research*, 452(1–2), pp. 273–285. doi: 10.1016/0006-8993(88)90031-5.

Miyatake, S. *et al.* (2021) 'De novo ATP1A3 variants cause polymicrogyria', *Science Advances*, 7(13). doi: 10.1126/SCIADV.ABD2368/SUPPL_FILE/ABD2368_SM.PDF.

Moran-Rivard, L. *et al.* (2001) 'Evx1 Is a Postmitotic Determinant of V0 Interneuron Identity in the Spinal Cord', *Neuron*, 29(2), pp. 385–399. doi: 10.1016/S0896-6273(01)00213-6.

Moseley, A. E. *et al.* (2003) 'The Na,K-ATPase α2 isoform is expressed in neurons, and its absence disrupts neuronal activity in newborn mice', *Journal of Biological Chemistry*, 278(7), pp. 5317–5324. doi: 10.1074/jbc.M211315200.

Moseley, A. E. *et al.* (2007) 'Deficiency in Na,K-ATPase α isoform genes alters spatial learning, motor activity, and anxiety in mice', *Journal of Neuroscience*, 27(3), pp. 616–626. doi: 10.1523/JNEUROSCI.4464-06.2007.

Müller, T. *et al.* (2002) 'The homeodomain factor lbx1 distinguishes two major programs of neuronal differentiation in the dorsal spinal cord', *Neuron*, 34(4), pp. 551–562. doi: 10.1016/S0896-6273(02)00689-X.

Mulloney, B. and Smarandache, C. (2010) 'Fifty years of CPGs: Two neuroethological papers that shaped the course of neuroscience', *Frontiers in Behavioral Neuroscience*, 4(JUL), p. 45. doi: 10.3389/FNBEH.2010.00045/BIBTEX.

Nagaraja, C. (2020) 'Ventral root evoked entrainment of disinhibited bursts across early postnatal development in mice', *IBRO Reports*, 9, pp. 310–318. doi: 10.1016/J.IBROR.2020.10.005.

Nakajima, S. and Takahashi, K. (1966) 'Post-tetanic hyperpolarization and electrogenic Na pump in stretch receptor neurone of crayfish', *The Journal of Physiology*, 187(1), p. 105. doi: 10.1113/JPHYSIOL.1966.SP008078.

Nascimento, F. *et al.* (2020) 'Synaptic mechanisms underlying modulation of locomotor-related motoneuron output by premotor cholinergic interneurons', *eLife*, 9. doi: 10.7554/ELIFE.54170.

Nascimento, F., Spindler, L. R. B. and Miles, G. B. (2019) 'Balanced cholinergic modulation of spinal locomotor circuits via M2 and M3 muscarinic receptors', *Scientific Reports*, 9(1), pp. 1–16. doi: 10.1038/s41598-019-50452-1.

Del Negro, C. A. *et al.* (2009) 'Asymmetric control of inspiratory and expiratory phases by excitability in the respiratory network of neonatal mice in vitro', *The Journal of Physiology*, 587(Pt 6), p. 1217. doi: 10.1113/JPHYSIOL.2008.164079.

Neville, B. and Ninan, M. (2007) 'The treatment and management of alternating hemiplegia of childhood', *Developmental Medicine & Child Neurology*, 49(10), pp. 777–780. doi: 10.1111/j.1469-8749.2007.00777.x.

Ng, H. W. Y., Ogbeta, J. A. and Clapcote, S. J. (2021) 'Genetically altered animal models for ATP1A3-related disorders', *Disease Models & Mechanisms*, 14(10). doi: 10.1242/DMM.048938.

Nikolić, L. *et al.* (2012) 'Involvement of Na+/K+ pump in fine modulation of bursting activity of the snail Br neuron by 10 mT static magnetic field', *Journal of Comparative Physiology A*, 198(7), pp. 525–540. doi: 10.1007/S00359-012-0727-0.

Nikolić, L., Kartelija, G. and Nedeljković, M. (2008) 'Effect of static magnetic fields on bioelectric properties of the Br and N1 neurons of snail Helix pomatia', *Comparative Biology and Physiology A*, 151(4), pp. 657–663. doi: 10.1016/J.CBPA.2008.08.006.

Nishi, A. *et al.* (1999) 'Regulation of Na+,K+-ATPase isoforms in rat neostriatum by dopamine and protein kinase C', *Journal of Neurochemistry*, 73(4), pp. 1492–1501. doi: 10.1046/J.1471-4159.1999.0731492.X.

Noga, B. R. *et al.* (2009) 'Locomotor-Activated Neurons of the Cat. I. Serotonergic Innervation and Co-Localization of 5-HT7, 5-HT2A, and 5-HT1A Receptors in the Thoraco-Lumbar Spinal Cord', *Journal of Neurophysiology*, 102(3), p. 1560. doi: 10.1152/JN.91179.2008.

Oblak, A. L. *et al.* (2014) 'Rapid-onset dystonia-parkinsonism associated with the I758S mutation of the ATP1A3 gene: A neuropathologic and neuroanatomical study of four siblings', *Acta Neuropathologica*, 128(1), pp. 81–98. doi: 10.1007/S00401-014-1279-X/FIGURES/9.

Oguz Kayaalp, S. and Neff, N. H. (1980) 'Regional distribution of cholinergic muscarinic receptors in spinal cord', *Brain Research*, 196(2), pp. 429–436. doi: 10.1016/0006-8993(80)90406-0.

Ohnishi, T. *et al.* (2015) 'Na, K-ATPase α3 is a death target of Alzheimer patient amyloid-β assembly', *Proceedings of the National Academy of Sciences of the United States of America*, 112(32), pp. E4465–E4474. doi: 10.1073/PNAS.1421182112/VIDEO-3.

Okamura, H. *et al.* (2003) 'P-type ATPases in Caenorhabditis and Drosophila: Implications for evolution of the P-type ATPase subunit families with special reference to the Na,K-ATPase and H,K-ATPase subgroup', *Journal of Membrane Biology*, 191(1), pp. 13–24. doi: 10.1007/s00232-002-1041-5.

Paciorkowski, A. R. *et al.* (2015) 'Novel mutations in ATP1A3 associated with catastrophic early life epilepsy, episodic prolonged apnea, and postnatal microcephaly.', *Epilepsia*, 56(3), pp. 422–30. doi: 10.1111/epi.12914.

Panagiotakaki, E. *et al.* (2010) 'Evidence of a non-progressive course of alternating hemiplegia of childhood: study of a large cohort of children and adults', *Brain*, 133(12), pp. 3598–3610. doi: 10.1093/BRAIN/AWQ295.

Panagiotakaki, E. *et al.* (2015) 'Clinical profile of patients with ATP1A3 mutations in Alternating Hemiplegia of Childhood - A study of 155 patients', *Orphanet Journal of Rare Diseases*, 10(1), pp. 1–13. doi: 10.1186/S13023-015-0335-5/TABLES/1.

Parker, D., Hill, R. and Grillner, S. (1996) 'Electrogenic pump and a Ca(2+)- dependent K+ conductance contribute to a posttetanic hyperpolarization in lamprey sensory neurons', *Journal of Neurophysiology*, 76(1), pp. 540–553. doi: 10.1152/JN.1996.76.1.540.

Pelzer, N. *et al.* (2017) 'Recurrent coma and fever in familial hemiplegic migraine type 2. A prospective 15-year follow-up of a large family with a novel ATP1A2 mutation', *Cephalalgia*, 37(8), pp. 737–755. doi: 10.1177/0333102416651284.

Peng, C. Y. *et al.* (2007) 'Notch and MAML Signaling Drives Scl-Dependent Interneuron Diversity in the Spinal Cord', *Neuron*, 53(6), pp. 813–827. doi: 10.1016/J.NEURON.2007.02.019.

Perrier, J. F. and Hounsgaard, J. (2000) 'Development and regulation of response properties in spinal cord motoneurons', *Brain Research Bulletin*, 53(5), pp. 529–535. doi: 10.1016/S0361-9230(00)00386-5.

Petrushanko, I. Y. *et al.* (2016) 'Direct interaction of beta-amyloid with Na,K-ATPase as a putative regulator of the enzyme function', *Scientific Reports*, 6(1), pp. 1–10. doi: 10.1038/srep27738.

Picton, L. D. *et al.* (2017) 'Sodium Pumps Mediate Activity-Dependent Changes in Mammalian Motor Networks', *Journal of Neuroscience*, 37(4), pp. 906–921. doi: 10.1523/JNEUROSCI.2005-16.2016.

Picton, L. D., Sillar, K. T. and Zhang, H. Y. (2018) 'Control of Xenopus Tadpole Locomotion via Selective Expression of Ih in Excitatory Interneurons', *Current Biology*, 28(24), pp. 3911-3923.e2. doi: 10.1016/J.CUB.2018.10.048.

Picton, L. D., Zhang, H. and Sillar, K. T. (2017) 'Sodium pump regulation of locomotor control circuits',

Journal of Neurophysiology, 118(2), pp. 1070–1081. doi: 10.1152/jn.00066.2017.

Pierani, A. *et al.* (2001) 'Control of Interneuron Fate in the Developing Spinal Cord by the Progenitor Homeodomain Protein Dbx1', *Neuron*, 29(2), pp. 367–384. doi: 10.1016/S0896-6273(01)00212-4.

Potic, A., Nmezi, B. and Padiath, Q. S. (2015) 'CAPOS syndrome and hemiplegic migraine in a novel pedigree with the specific ATP1A3 mutation', *Journal of the Neurological Sciences*, 358(1), pp. 453–456. doi: 10.1016/J.JNS.2015.10.002.

Prange, L. *et al.* (2020) 'D-DEMØ, a distinct phenotype caused by ATP1A3 mutations', *Neurology: Genetics*, 6(5). doi: 10.1212/NXG.0000000000000466/VIDEO-2.

Pu, H. X. *et al.* (2001) 'Functional Role and Immunocytochemical Localization of the γa and γb Forms of the Na,K-ATPase γ Subunit *', *Journal of Biological Chemistry*, 276(23), pp. 20370–20378. doi: 10.1074/JBC.M010836200.

Pulver, S. R. and Griffith, L. C. (2010) 'Spike integration and cellular memory in a rhythmic network from Na + /K + pump current dynamics', *Nature Neuroscience*, 13(1), pp. 53–59. doi: 10.1038/nn.2444.

Rakovic, S. *et al.* (1999) 'An antagonist of cADP-ribose inhibits arrhythmogenic oscillations of intracellular Ca2+ in heart cells', *The Journal of Biological Chemistry*, 274(25), pp. 17820–17827. doi: 10.1074/JBC.274.25.17820.

Ranieri, F. and Di Lazzaro, V. (2012) 'The role of motor neuron drive in muscle fatigue', *Neuromuscular Disorders*, 22 Suppl 3(SUPPL. 3). doi: 10.1016/J.NMD.2012.10.006.

Reinés, A. *et al.* (2004) 'The effect of endogenous modulator endobain E on NMDA receptor is interfered by Zn2+ but is independent of modulation by spermidine', *Neurochemical Research*, 29(4), pp. 819–825. doi: 10.1023/B:NERE.0000018856.99773.71.

Reinés, A., Peña, C. and Rodríguez De Lores Arnaiz, G. (2001) '[3H]dizocilpine binding to N-methyl-D-aspartate (NMDA) receptor is modulated by an endogenous Na+, K+-ATPase inhibitor. Comparison with ouabain', *Neurochemistry International*, 39(4), pp. 301–310. doi: 10.1016/S0197-0186(01)00034-1.

Renner, M. *et al.* (2010) 'Deleterious Effects of Amyloid β Oligomers Acting as an Extracellular Scaffold for mGluR5', *Neuron*, 66(5), pp. 739–754. doi: 10.1016/J.NEURON.2010.04.029.

Rexed, B. (1952) 'The cytoarchitectonic organization of the spinal cord in the cat', *Journal of Comparative Neurology*. John Wiley & Sons, Ltd, 96(3), pp. 415–495. doi: 10.1002/CNE.900960303.

Rexed, B. (1954) 'A cytoarchitectonic atlas of the spinal cord in the cat', *The Journal of Comparative Neurology*, 100(2), pp. 297–379. doi: 10.1002/CNE.901000205.

Roenn, C. P. *et al.* (2019) 'Functional consequences of the CAPOS mutation E818K of Na+,K+-ATPase', *Journal of Biological Chemistry*, 294(1), pp. 269–280. doi: 10.1074/JBC.RA118.004591.

Rosewich, H., Baethmann, M., *et al.* (2014) 'A novel ATP1A3 mutation with unique clinical presentation', *Journal of the Neurological Sciences*, 341(1), pp. 133–135. doi: 10.1016/J.JNS.2014.03.034.

Rosewich, H., Weise, D., *et al.* (2014) 'Phenotypic overlap of alternating hemiplegia of childhood and CAPOS syndrome', *Neurology*, 83(9), pp. 861–863. doi: 10.1212/WNL.0000000000000735.

Rossi, A., Rossi, S. and Ginanneschi, F. (2012) 'Activity-dependent changes in intrinsic excitability of human spinal motoneurones produced by natural activity', *Journal of Neurophysiology*, 108(9), pp. 2473–2480. doi: 10.1152/JN.00477.2012.

Rubin, J. E. *et al.* (2009) 'Calcium-activated nonspecific cation current and synaptic depression promote network-dependent burst oscillations', *Proceedings of the National Academy of Sciences of the United States of America*, 106(8), p. 2939. doi: 10.1073/PNAS.0808776106.

Ruegsegger, C. *et al.* (2016) 'Aberrant association of misfolded SOD1 with Na+/K+ATPase-α3 impairs its activity and contributes to motor neuron vulnerability in ALS', *Acta Neuropathologica*, 131(3), pp. 427–451. doi: 10.1007/s00401-015-1510-4.

Saghian, A. A., Ayrapetyan, S. N. and Carpenter, D. O. (1996) 'Low concentrations of ouabain stimulate Na/Ca exchange in neurons', *Cellular and Molecular Neurobiology*, 16(4), pp. 489–498. doi: 10.1007/BF02150229.

Sala, C. *et al.* (2001) 'Regulation of dendritic spine morphology and synaptic function by Shank and Homer', *Neuron*, 31(1), pp. 115–130. doi: 10.1016/S0896-6273(01)00339-7.

Santoro, B. *et al.* (1998) 'Identification of a Gene Encoding a Hyperpolarization-Activated Pacemaker Channel of Brain', *Cell*, 93(5), pp. 717–729. doi: 10.1016/S0092-8674(00)81434-8.

Saueressig, H., Burrill, J. and Goulding, M. (1999) 'Engrailed-1 and netrin-1 regulate axon pathfinding by association interneurons that project to motor neurons', *Development*, 126(19), pp. 4201–4212. doi: 10.1242/DEV.126.19.4201.

Scarr, E. (2012) 'Muscarinic Receptors: Their Roles in Disorders of the Central Nervous System and Potential as Therapeutic Targets', *CNS Neuroscience & Therapeutics*, 18(5), pp. 369–379. doi: 10.1111/J.1755-5949.2011.00249.X.

Schindelin, J. *et al.* (2012) 'Fiji: an open-source platform for biological-image analysis', *Nature Methods*, 9(7), pp. 676–682. doi: 10.1038/nmeth.2019.

Schlingmann, K. P. *et al.* (2018) 'Germline De Novo Mutations in ATP1A1 Cause Renal Hypomagnesemia, Refractory Seizures, and Intellectual Disability', *American Journal of Human Genetics*, 103(5), pp. 808–816. doi: 10.1016/J.AJHG.2018.10.004.

Schmidt, B. J. and Jordan, L. M. (2000) 'The role of serotonin in reflex modulation and locomotor rhythm production in the mammalian spinal cord', *Brain Research Bulletin*, 53(5), pp. 689–710. doi: 10.1016/S0361-9230(00)00402-0.

Schwindt, P. C. and Crill, W. E. (1980) 'Properties of a persistent inward current in normal and TEA-injected motoneurons', *Journal of Neurophysiology*, 43(6), pp. 1700–1724. doi: 10.1152/JN.1980.43.6.1700.

Schwinger, R. H. G. *et al.* (1999) 'Reduced Sodium Pump α1, α3, and β1-Isoform Protein Levels and Na+,K+-ATPase Activity but Unchanged Na+-Ca2+ Exchanger Protein Levels in Human Heart Failure', *Circulation*, 99(16), pp. 2105–2112. doi: 10.1161/01.CIR.99.16.2105.

Scuri, R. *et al.* (2007) 'Inhibition of Na+/K+ ATPase potentiates synaptic transmission in tactile sensory neurons of the leech', *The European Journal of Neuroscience*, 25(1), pp. 159–167. doi: 10.1111/J.1460-9568.2006.05257.X.

Scuri, R., Mozzachiodi, R. and Brunelli, M. (2002) 'Activity-Dependent Increase of the AHP Amplitude in T Sensory Neurons of the Leech', *Journal of Neurophysiology*, 88, pp. 2490–2500. doi: 10.1152/jn.01027.2001.

Sharples, S. A. *et al.* (2022) 'Contributions of h- and Na+/K+ Pump Currents to the Generation of Episodic and Continuous Rhythmic Activities', *Frontiers in Cellular Neuroscience*, 15, p. 579. doi: 10.3389/FNCEL.2021.715427/BIBTEX.

Sharples, S. A. and Miles, G. B. (2021) 'Maturation of persistent and hyperpolarization-activated

inward currents shapes the differential activation of motoneuron subtypes during postnatal development', *eLife*, 10. doi: 10.7554/ELIFE.71385.

Sharples, S. A. and Whelan, P. J. (2017) 'Modulation of Rhythmic Activity in Mammalian Spinal Networks Is Dependent on Excitability State', *eNeuro*, 4(1). doi: 10.1523/ENEURO.0368-16.2017.

Shen, K. Z. and Johnson, S. W. (1998) 'Sodium pump evokes high density pump currents in rat midbrain dopamine neurons', *The Journal of Physiology*, 512(2), pp. 449–457. doi: 10.1111/J.1469-7793.1998.449BE.X.

Sherrington, C. S. (1906) 'Observations on the scratch-reflex in the spinal dog', *The Journal of Physiology*, 34(1–2), p. 1. doi: 10.1113/JPHYSIOL.1906.SP001139.

Sherrington, C. S. (1910) 'Flexion-reflex of the limb, crossed extension-reflex, and reflex stepping and standing', *The Journal of Physiology*, 40(1–2), p. 28. doi: 10.1113/JPHYSIOL.1910.SP001362.

Shik, M. L., Severin, F. V. and Orlovsky, G. N. (1969) 'Control of walking and running by means of electrical stimulation of the mesencephalon.', *Electroencephalography and Clinical Neurophysiology*. Edited by G. Balint et al., 26(5), p. 549. doi: 10.2/JQUERY.MIN.JS.

Shirasaki, R. and Pfaff, S. L. (2002) 'Transcriptional codes and the control of neuronal identity', *Annual Review of Neuroscience*, 25, pp. 251–281. doi: 10.1146/ANNUREV.NEURO.25.112701.142916.

Shneider, N. A. *et al.* (2009) 'Gamma motor neurons express distinct genetic markers at birth and require muscle spindle-derived GDNF for postnatal survival', *Neural Development*, 4(1), pp. 1–22. doi: 10.1186/1749-8104-4-42/FIGURES/7.

Shrivastava, A. N. *et al.* (2013) 'β-amyloid and ATP-induced diffusional trapping of astrocyte and neuronal metabotropic glutamate type-5 receptors', *Glia*, 61(10), pp. 1673–1686. doi: 10.1002/GLIA.22548.

Shrivastava, A. N. *et al.* (2015) 'α-synuclein assemblies sequester neuronal α3-Na+/K+-ATPase and impair Na+ gradient', *The EMBO Journal*, 34(19), pp. 2408–2423. doi: 10.15252/EMBJ.201591397.

Shrivastava, A. N. *et al.* (2017) 'Physico-Pathologic Mechanisms Involved in Neurodegeneration: Misfolded Protein-Plasma Membrane Interactions', *Neuron*, 95(1), pp. 33–50. doi: 10.1016/J.NEURON.2017.05.026.

Shrivastava, A. N. *et al.* (2019) 'Clustering of Tau fibrils impairs the synaptic composition of α3-Na+/K+-ATPase and AMPA receptors', *The EMBO Journal*, 38(3), p. e99871. doi: 10.15252/EMBJ.201899871.

Simmons, C. Q. *et al.* (2018) 'Direct evidence of impaired neuronal Na/K-ATPase pump function in alternating hemiplegia of childhood', *Neurobiology of Disease*, 115, pp. 29–38. doi: 10.1016/j.nbd.2018.03.009.

Sival, D. A. *et al.* (2018) 'Fever-Induced Paroxysmal Weakness and Encephalopathy (FIPWE)—Part of a Phenotypic Continuum in Patients With ATP1A3 Mutations?', *Pediatric Neurology*, 81, pp. 57–58. doi: 10.1016/J.PEDIATRNEUROL.2017.12.009.

Skagerberg, G. and Lindvall, O. (1985) 'Organization of diencephalic dopamine neurones projecting to the spinal cord in the rat', *Brain Research*, 342(2), pp. 340–351. doi: 10.1016/0006-8993(85)91134-5.

Smedemark-Margulies, N. *et al.* (2016) 'A novel de novo mutation in ATP1A3 and childhood-onset schizophrenia', *Molecular Case Studies*, 2(5), p. a001008. doi: 10.1101/MCS.A001008.

Smith, R. S. *et al.* (2021) 'Early role for a Na+,K+-ATPase (ATP1A3) in brain development', *Proceedings of the National Academy of Sciences of the United States of America*, 118(25). doi: 10.1073/PNAS.2023333118.

Sokolove, P. G. and Cooke, I. M. (1971) 'Inhibition of Impulse Activity in a Sensory Neuron by an Electrogenic Pump', *Journal of General Physiology*, 57(2), pp. 125–163. doi: 10.1085/JGP.57.2.125.

Solomon, J. S. and Nerbonne, J. M. (1993) 'Hyperpolarization-activated currents in isolated superior colliculus-projecting neurons from rat visual cortex.', *The Journal of Physiology*, 462(1), pp. 393–420. doi: 10.1113/JPHYSIOL.1993.SP019561.

Souza e Souza, K. *et al.* (2021) 'Na +/K +-ATPase as a Target of Cardiac Glycosides for the Treatment of SARS-CoV-2 Infection', *Frontiers in Pharmacology*, 12. doi: 10.3389/FPHAR.2021.624704.

Stein, S. G. *et al.* (1997) *Neurons, Networks, and Motor Behavior*. The MIT Press.

Stenshorne, I. *et al.* (2019) 'Fever-related ataxia: A case report of CAPOS syndrome', *Cerebellum and Ataxias*, 6(1), pp. 1–5. doi: 10.1186/S40673-019-0096-3.

Stregapede, F. *et al.* (2020) 'Hereditary spastic paraplegia is a novel phenotype for germline de novo ATP1A1 mutation', *Clinical Genetics*, 97(3), pp. 521–526. doi: 10.1111/CGE.13668.

Sundaram, S. M. *et al.* (2019) 'Differential expression patterns of sodium potassium ATPase alpha and beta subunit isoforms in mouse brain during postnatal development', *Neurochemistry International*, 128, pp. 163–174. doi: 10.1016/j.neuint.2019.04.009.

Surmeier, J. *et al.* (2017) 'Prying into the Prion Hypothesis for Parkinson's Disease', *Journal of Neuroscience*, 37(41), pp. 9808–9818. doi: 10.1523/JNEUROSCI.1788-16.2017.

Sweadner, K. J. *et al.* (2019) 'Genotype-structure-phenotype relationships diverge in paralogs ATP1A1, ATP1A2, and ATP1A3', *Neurology Genetics*, 5(1), p. 303. doi: 10.1212/NXG.0000000000000303.

Sweadner, K. J. and Rael, E. (2000) 'The FXYD Gene Family of Small Ion Transport Regulators or Channels: cDNA Sequence, Protein Signature Sequence, and Expression', *Genomics*, 68(1), pp. 41–56. doi: 10.1006/GENO.2000.6274.

Sweney, M. T. *et al.* (2009) 'Alternating Hemiplegia of Childhood: Early Characteristics and Evolution of a Neurodevelopmental Syndrome', *Pediatrics*, 123(3), pp. e534–e541. doi: 10.1542/PEDS.2008-2027.

Sweney, M. T., Newcomb, T. M. and Swoboda, K. J. (2015) 'The Expanding Spectrum of Neurological Phenotypes in Children With ATP1A3 Mutations, Alternating Hemiplegia of Childhood, Rapid-onset Dystonia-Parkinsonism, CAPOS and Beyond', *Pediatric Neurology*. Elsevier, 52(1), pp. 56–64. doi: 10.1016/J.PEDIATRNEUROL.2014.09.015.

Syeda, S. S. *et al.* (2020) 'The Na+ and K+ transport system of sperm (ATP1A4) is essential for male fertility and an attractive target for male contraception†', *Biology of Reproduction*, 103(2), pp. 343–356. doi: 10.1093/BIOLRE/IOAA093.

Takata, A. *et al.* (2018) 'Integrative Analyses of De Novo Mutations Provide Deeper Biological Insights into Autism Spectrum Disorder', *Cell Reports*, 22(3), pp. 734–747. doi: 10.1016/J.CELREP.2017.12.074.

Takeyasu, K., Lemas, V. and Fambrough, D. M. (1990) 'Stability of Na(+)-K(+)-ATPase alpha-subunit isoforms in evolution', *American Journal of Physiology*, 259(4), pp. C619–C630. doi: 10.1152/ajpcell.1990.259.4.C619.

Tiwari, M. N. *et al.* (2018) 'Differential contributions of Ca2+-activated K+ channels and Na+/K+-ATPases to the generation of the slow afterhyperpolarization in CA1 pyramidal cells', *Hippocampus*, 28(5), pp. 338–357. doi: 10.1002/hipo.22836.

Tobin, A. E. and Calabrese, R. L. (2005) 'Myomodulin increases Ih and inhibits the Na/K pump to modulate bursting in leech heart interneurons', *Journal of Neurophysiology*, 94(6), pp. 3938–3950. doi: 10.1152/JN.00340.2005.

Torres, A. *et al.* (2018) 'De novo ATP1A3 and compound heterozygous NLRP3 mutations in a child with autism spectrum disorder, episodic fatigue and somnolence, and muckle-wells syndrome', *Molecular Genetics and Metabolism Reports*, 16, pp. 23–29. doi: 10.1016/J.YMGMR.2018.06.001.

Toustrup-Jensen, M. S. *et al.* (2014) 'Relationship between Intracellular Na+ Concentration and Reduced Na+ Affinity in Na+,K+-ATPase Mutants causing Neurological Disease', *Journal of Biological Chemistry*, 289(6), pp. 3186–3197. doi: 10.1074/jbc.M113.543272.

Tranebjærg, L. *et al.* (2018) 'The CAPOS mutation in ATP1A3 alters Na/K-ATPase function and results in auditory neuropathy which has implications for management', *Human Genetics*, 137(2), pp. 111–127. doi: 10.1007/S00439-017-1862-Z.

Trotier, D. and Døving, K. B. (1996) 'Direct influence of the sodium pump on the membrane potential of vomeronasal chemoreceptor neurones in frog', *The Journal of Physiology*, 490 (Pt 3(Pt 3), pp. 611–621. doi: 10.1113/JPHYSIOL.1996.SP021171.

Tsuzawa, K. *et al.* (2015) 'Effects of ouabain on respiratory rhythm generation in brainstem-spinal cord preparation from newborn rats and in decerebrate and arterially perfused in situ preparation from juvenile rats', *Neuroscience*, 286(1), pp. 404–411. doi: 10.1016/J.NEUROSCIENCE.2014.12.006.

Turner, M. R. *et al.* (2010) 'The diagnostic pathway and prognosis in bulbar-onset amyotrophic lateral sclerosis', *Journal of the Neurological Sciences*, 294(1–2), pp. 81–85. doi: 10.1016/J.JNS.2010.03.028.

Turner, R. W. *et al.* (2016) 'Assessing the role of IKCa channels in generating the sAHP of CA1 hippocampal pyramidal cells', *Channels*. Taylor and Francis Inc., 10(4), pp. 313–319. doi: 10.1080/19336950.2016.1161988.

Uchitel, J. *et al.* (2019) 'The epileptology of alternating hemiplegia of childhood', *Neurology*, 93(13), pp. e1248–e1259. doi: 10.1212/WNL.0000000000008159.

Vagg, R. *et al.* (1998) 'Activity-dependent hyperpolarization of human motor axons produced by natural activity', *The Journal of Physiology*, 507(Pt 3), p. 919. doi: 10.1111/J.1469-7793.1998.919BS.X.

Vague, P. *et al.* (2004) 'C-peptide, Na+, K+-ATPase, and Diabetes', *Experimental Diabesity Research*, 5(1), pp. 37–50. doi: 10.1080/15438600490424514.

Vetro, A. *et al.* (2021) 'ATP1A2- and ATP1A3-associated early profound epileptic encephalopathy and polymicrogyria', *Brain*, 144(5), pp. 1435–1450. doi: 10.1093/BRAIN/AWAB052.

Walderhaug, M. 0 *et al.* (1985) 'Structural Relatedness of Three Ion-Transport Adenosine Triphosphatases around Their Active Sites of Phosphorylation*', *Journal of Biological Chemistry*, 260(6), pp. 3852–3859. Available at: https://pdfs.semanticscholar.org/e0a7/24c64c31909f64ecdc76541ed45af4ae6987.pdf (Accessed: 22 May 2018).

Watts, A. G. *et al.* (1991) 'Cell-specific expression of mRNAs encoding Na+,K(+)-ATPase alpha- and beta-subunit isoforms within the rat central nervous system.', *Proceedings of the National Academy*

of Sciences, 88(16), pp. 7425–7429. doi: 10.1073/PNAS.88.16.7425.

Weigand, K. M. *et al.* (2014) 'Alternating Hemiplegia of Childhood mutations have a differential effect on Na+,K+-ATPase activity and ouabain binding', *Biochimica et Biophysica Acta (BBA) - Molecular Basis of Disease*, 1842(7), pp. 1010–1016. doi: 10.1016/J.BBADIS.2014.03.002.

Wenner, P., O'Donovan, M. J. and Matise, M. P. (2000) 'Topographical and Physiological Characterization of Interneurons That Express Engrailed-1 in the Embryonic Chick Spinal Cord', *Journal of Neurophysiology*, 84, pp. 2651–2657.

Whelan, P., Bonnot, A. and O'Donovan, M. J. (2000) 'Properties of rhythmic activity generated by the isolated spinal cord of the neonatal mouse', *Journal of Neurophysiology*, 84(6), pp. 2821–2833. doi: 10.1152/JN.2000.84.6.2821.

Wilson, J. M. *et al.* (2005) 'Conditional Rhythmicity of Ventral Spinal Interneurons Defined by Expression of the Hb9 Homeodomain Protein', *Journal of Neuroscience*, 25(24), pp. 5710–5719. doi: 10.1523/JNEUROSCI.0274-05.2005.

Wujak, Ł. A. *et al.* (2016) 'FXYD1 negatively regulates Na+/K+-ATPase activity in lung alveolar epithelial cells', *Respiratory Physiology & Neurobiology*, 220, pp. 54–61. doi: 10.1016/J.RESP.2015.09.008.

Yamaguchi, F. *et al.* (2001) 'Molecular cloning and characterization of a novel phospholemman-like protein from rat hippocampus', *Molecular Brain Research*, 86(1–2), pp. 189–192. doi: 10.1016/S0169-328X(00)00213-8.

Zagoraiou, L. *et al.* (2009) 'A Cluster of Cholinergic Premotor Interneurons Modulates Mouse Locomotor Activity', *Neuron*, 64(5), pp. 645–662. doi: 10.1016/j.neuron.2009.10.017.

Zhang, D. *et al.* (2009) 'Na,K-ATPase Activity Regulates AMPA Receptor Turnover through Proteasome-Mediated Proteolysis', *Journal of Neuroscience*, 29(14), pp. 4498–4511. doi: 10.1523/JNEUROSCI.6094-08.2009.

Zhang, H. Y. *et al.* (2015) 'Mechanisms underlying the activity-dependent regulation of locomotor network performance by the Na+ pump', *Scientific Reports*, 5(1), pp. 1–14. doi: 10.1038/srep16188.

Zhang, H. Y. and Sillar, K. T. (2012) 'Short-term memory of motor network performance via activity-dependent potentiation of Na +/K + pump function', *Current Biology*, 22(6), pp. 526–531. doi: 10.1016/J.CUB.2012.01.058/ATTACHMENT/030CD4C2-A817-465A-8172-96F4FF8E7B1C/MMC1.PDF.

Zhang, J. *et al.* (2014) 'V1 and V2b interneurons secure the alternating flexor-extensor motor activity mice require for limbed locomotion', *Neuron*, 82(1), pp. 138–150. doi: 10.1016/J.NEURON.2014.02.013.

Zhang, L. *et al.* (2012) 'Na+/K+-ATPase inhibition upregulates NMDA-evoked currents in rat hippocampal CA1 pyramidal neurons', *Fundamental & Clinical Pharmacology*, 26(4), pp. 503–512. doi: 10.1111/J.1472-8206.2011.00947.X.

Zhang, Y. *et al.* (2008) 'V3 spinal neurons establish a robust and balanced locomotor rhythm during walking', *Neuron*, 60(1), p. 84. doi: 10.1016/J.NEURON.2008.09.027.

Zhong, G. *et al.* (2010) 'Electrophysiological Characterization of V2a Interneurons and Their Locomotor-Related Activity in the Neonatal Mouse Spinal Cord', *Journal of Neuroscience*, 30(1), pp. 170–182. doi: 10.1523/JNEUROSCI.4849-09.2010.

Zhu, H. *et al.* (2007) 'Expression and distribution of all dopamine receptor subtypes (D(1)-D(5)) in the mouse lumbar spinal cord: a real-time polymerase chain reaction and non-autoradiographic in situ hybridization study', *Neuroscience*, 149(4), pp. 885–897. doi:

10.1016/J.NEUROSCIENCE.2007.07.052.